Manipulation of Metabotropic and AMPA Glutamate Receptors in the Brain

©Amy G. M. Lam, B.Sc. Hons (University of London)

A thesis submitted for the Degree of Doctor of Philosophy

to the Faculty of Medicine, University of Glasgow

Wellcome Surgical Institute & Hugh Fraser Neuroscience Laboratories,

University of Glasgow,

Garscube Estate, Bearsden Road, Glasgow G61 1QH

March 1999

Declaration

I declare that this thesis comprises my own original work and has not been accepted in any previous application for a degree. The work, of which it is a record, has been carried out by myself, except as acknowledged and indicated in the thesis. All sources of information have been specifically referenced.

Amy Lam

Acknowledgements

LIST OF CONTENTS

CHAPTER 3   MAPPING BRAIN FUNCTION WITH GROUP II SELECTIVE
METABOTROPIC GLUTAMATE RECEPTOR AGONISTS

CHAPTER 4   FUNCTIONAL MAPPING FOLLOWING LIMBIC SYSTEM

MANIPULATION

CHAPTER 5   THE EFFECTS OF THE SELECTIVE GROUP II METABOTROPIC

GLUTAMATE RECEPTOR AGONIST LY354740 IN A RAT MODEL OF

PERMANENT ISCHAEMIA

CHAPTER 8   DISCUSSION

References

Appendices

LIST OF FIGURES

LIST OF TABLES

LIST OF PUBLICATIONS

PAPERS

Lam, A.G.M., Campbell, J.M., Bennett, N., Payne, A.P., Davies, R.W., Sutcliffe, R.G. & McCulloch, J. (1998). Local cerebral glucose utilisation in the AS/AGU mutant rat. *European Journal of Neuroscience*, **10**, 1963-1967.

Lam, A.G.M., Soriano, M.A., Monn, J.A., Schoepp, D.D., Lodge, D. & McCulloch, J. (1998). Effects of the selective metabotropic glutamate agonist LY354740 in a rat model of permanent ischaemia. *Neuroscience Letters*, **254**, 121-123.

Lam, A.G.M., Monn, J.A., Schoepp, D.D., Lodge, D. & McCulloch, J. Group II selective metabotropic glutamate receptor agonists and local cerebral glucose utilisation in the rat. *Journal of Cerebral Blood Flow and Metabolism*. (In press).

Kingston, A.E., O'Neill, M.J., **Lam, A.,** Bales, K.R., Monn, J.A. & Schoepp, D.D. Neuroprotective actions of novel and highly potent group II mGluR agonists: LY354740 and LY389795 in cortical neurons. *European Journal of Pharmacology*. (In press).

Riedel, G., Micheau, J., de Hoz, L., Roloff, E.v.L., Bridge, H., **Lam, A.G.M.,** McCulloch, J. & Morris, R.G.M. Temporary neural inactivation reveals hippocampal participation in several memory processes. *Nature Neuroscience*. (Submitted).

Lam, A.G.M., Riedel, G., Micheau, J., Morris, R.G.M. & McCulloch, J. Reversible hippocampal inactivation: an autoradiographic study. (In preparation).

ABSTRACTS

Lam, A.G.M., Lodge, D. and McCulloch, J. (1997). Effects of the selective group II metabotropic glutamate receptor agonist LY354740 on energy metabolism in the rat brain. *Society for Neuroscience Abstracts*, **23**, 790.2.

Lam, A.G.M., Lodge, D., Monn, J.A., Schoepp, D.D. and McCulloch, J. (1997). The effects of the selective group II metabotropic glutamate receptor agonist LY354740 on local cerebral glucose metabolism in the rat brain. *British Journal of Pharmacology Proceedings Supplement*, **123**, 206P.

Lam, A.G.M., Lodge, D., Monn, J.A., Schoepp, D.D. and McCulloch, J. (1998). Effects of the selective group II metabotropic glutamate receptor agonist LY379268 on energy metabolism in the rat brain. *Society for Neuroscience Abstracts*, **24**, 232.4.

Lam, A.G.M., Monn, J.A., Schoepp, D.D., Lodge, D. & McCulloch, J. The effects of novel group II selective metabotropic glutamate receptor agonists in the rat brain. *Journal of Cerebral Blood Flow and Metabolism*. (In press).

Lam, A.G.M., Riedel, G., Micheau, J., Morris, R.G.M. and McCulloch, J. Reversible hippocampal inactivation and functional mapping in the rat brain. *Journal of Cerebral Blood Flow and Metabolism*. (In press).

Riedel, G., Micheau, J., **Lam, A.,** de Hoz, L., Roloff, E.v.L., Bridge, H., McCulloch, J. & Morris, R.G.M. Hippocampal involvement in multiple memory processes in rats. *British Neuroscience Association.* (In press).

Summary

The consequences of the pharmacological manipulation of metabotropic and AMPA glutamate receptor-mediated events in the rat brain were investigated in this thesis. $[^{14}C]2$-deoxyglucose autoradiography was used to explore modifications in physiological brain function following the systemic administration of two novel selective agonists with actions on group II metabotropic glutamate receptors (mGluRs) and following the intracerebral manipulation of the hippocampus using a selective AMPA antagonist. The putative role of group II mGluRs in neuroprotection was also examined. An *in vivo* model of cerebral ischaemia together with two *in vitro* models of neurotoxicity with group II mGluR agonist intervention were used to study the potential of group II mGluR agonists in protecting cellular elements from neurotoxic insults.

Mapping brain function with group II selective mGluR agonists

Local rates of cerebral glucose use were measured using the $[^{14}C]2$-deoxyglucose autoradiographic technique to examine the functional consequences of the systemic administration of the novel mGluR agonist LY354740, and a related analogue LY379268, in the conscious rat.

Both LY354740 (0.3, 3.0, 30 mg/kg) and LY379268 (0.1, 1.0, 10 mg/kg) produced dose-dependent changes in glucose utilisation. LY354740 produced anatomically widespread reductions in glucose use, while LY379268 affected a smaller number of brain regions which displayed increases in glucose metabolism. After LY354740 (3.0mg/kg) administration, 4 out of 42 brain regions demonstrated statistically significant changes from vehicle treated controls: red nuclei (-16%), mammillary body (-25%), anteroventral thalamic nucleus (-29%) and the superficial layer of the superior colliculus (+50%). An additional 15 regions displayed significant reductions in function-related glucose use (P<0.05) in animals

treated with LY354740 (30mg/kg). In contrast, LY379268 (0.1, 1.0, 10mg/kg) produced changes in glucose metabolism in only 20% of the brain regions analysed. Significant increases in glucose use (P<0.05) were evident in the superficial layer of the superior colliculus (+81%), locus coeruleus (+57%), genu of the corpus callosum (+31%), cochlear nucleus (+26%), inferior colliculus (+20%) and the molecular layer of the hippocampus (+14%). Three regions displayed significant decreases: mammillary body (-34%), anteroventral thalamic nucleus (-28%) and the lateral habenular nucleus (-24%). Both compounds displayed a similar anatomical pattern of altered glucose metabolism in the limbic system. Reductions were noted in the anteroventral thalamic nucleus, lateral habenular nucleus, molecular layer of the hippocampus and the mammillary body (P < 0.05) following both agonists. Glucose utilisation in components of different sensory systems were altered following the activation of mGluR2/3. In animals treated with LY354740, reductions in function-related glucose use were observed in areas associated with vision, while those treated with LY379268 demonstrated elevated glucose utilisation in primary auditory areas.

This study has demonstrated that the [^{14}C]2-deoxyglucose autoradiographic technique provides a reliable means of mapping functional events in the brain. It has highlighted fundamental differences in the regional effects of the two agonists and has served to demonstrate the important functional involvement of the limbic system together with the participation of components of different sensory systems in response to the activation of mGluR2 and mGluR3 with LY354740 and LY379268.

Regional mapping of cerebral function following hippocampal manipulation

The [^{14}C]2-deoxyglucose autoradiographic technique was used to investigate changes in brain function during, and following, the localised 7 day infusion of the selective AMPA/kainate receptor antagonist LY326325 in the conscious rat.

During the period of drug infusion, anatomically circumscribed changes in glucose use were measured in animals treated with LY326325 compared with aCSF (artificial cerebrospinal fluid) treated control animals. Reductions in glucose utilisation were demonstrated in the molecular layer of the dorsal hippocampus (-23%, $P<0.002$) but not in the molecular layer of the ventral hippocampus. The maximal reduction in glucose use measured in the molecular layer of the hippocampus was observed adjacent to the implant site, along a dorsal axis relative to the implant site. Other than a marked elevation in function-related glucose use in the superficial layers of the entorhinal cortex, rates of glucose utilisation in the remaining regions of the CNS were minimally affected during the period of drug infusion.

Following the period of LY326325 infusion, glucose use in the molecular layer of the dorsal hippocampus in animals treated with LY326325 returned to levels comparable with aCSF treated animals. The elevation in glucose use observed in the entorhinal cortex during the period of drug infusion was also not evident. However, a 17% reduction in glucose use was observed in the red nucleus of LY326325 animals. Function-related glucose use in aCSF treated animals both during the period of drug infusion and after drug infusion did not differ significantly.

This study reveals that intrahippocampal infusions of LY326325 can reduce synaptic activity as measured by glucose use selectively in the hippocampus in a reversible manner. Infusions of this kind may provide invaluable insight into memory processes that are thought to involve the hippocampus.

Neuroprotection *in vivo* and *in vitro* using group II mGluR agonists

The effects of LY354740 and LY379268 were assessed in the middle cerebral artery occlusion model of focal ischaemia in rats. LY354740 (0.3, 3.0 or 30.0 mg/kg) or LY379268 (10.0mg/kg) were administered subcutaneously 30 minutes prior to and 3 hours

after the induction of ischaemia. Twenty four hours after the ischaemic insult, the brains were processed for the evaluation of infarct volumes. No significant reduction in infarct volumes was observed in animals treated with LY354740 (30mg/kg) (199 ± 22 mm^3) compared with vehicle treated controls (191 ± 18 mm^3). Similarly, no reduction in infarct volumes was seen following LY379268 (10mg/kg) (97 ± 11 mm^3) compared with vehicle treated controls (101 ± 8 mm^3). These data provide no support for the view that group II metabotropic glutamate receptors have a major influence on reducing the volume of ischaemic damage in this model.

LY379268 treated brain tissue in animals in which the middle cerebral artery (MCA) had been occluded was assessed together with vehicle treated MCA-occluded animals at a cellular level using immunohistochemistry to determine whether any cellular or mechanistic changes were distinguishable from the vehicle-treated group. Immunohistochemical analysis carried out at one coronal level (anterior co-ordinate 7.19 mm), using markers for amyloid precursor protein (APP), transforming growth factor-β1 (TGF-β1), TGF-β2, fragment end labelling of DNA and for mGluR2/3, demonstrated no changes in APP accumulation score or in the number of mGluR2/3 immunoreactive cells. However, labelling for TGF-β1 demonstrated a significant reduction in the number of immunoreactive cells at the core of the ischaemic lesion following LY379268 compared with vehicle treated controls. In contrast, TGF-β2 immunoreactivity was increased by 25% at the boundary of the ischaemic lesion compared to vehicle treated controls. In addition, animals treated with LY379268 displayed significant reductions in the number of terminal deoxynucleotidyl transferase (TdT) labelled cells both at the boundary and at the core of the lesion, compared with vehicle treated controls. This data provides evidence that activation of mGluR2/3 by LY379268 reduces apoptotic-like cell death and results in the increased production of TGF-β2. To establish whether astrocytes were involved in the production of TGF-β2, primary

cultures were incubated with the agonists LY354740 and LY379268. The results showed that astrocytes were capable of producing and secreting TGF-β2 following treatment with LY354740 and LY379268. This response was abolished in cultures simultaneously incubated with the mGluR2/3 selective antagonist LY341495 indicating that the response is specifically mediated through mGluR2/3.

In a separate series of experiments *in vitro*, the neuroprotective effects of LY354740 and LY379268 were explored using staurosporine-induced toxicity in neuronal cell cultures. Both LY354740 and LY379268 (1μm) significantly reduced lactate dehydrogenase (LDH) efflux, a marker of cell damage and death, caused by staurosporine.

Collectively, these data provide evidence that group II mGluRs may not have a neuroprotective role in focal models of cerebral ischaemia, where damage to cells occurs quickly, but that their activation may reduce cell death in instances where the slowly evolving cellular damage is protracted to allow defensive intracellular events to take place. In addition, such defensive intracellular events are likely to involve glial-neuronal signalling.

CHAPTER 1

INTRODUCTION

1.1 Glutamate in the CNS

Glutamate, together with aspartate, are excitatory amino acids found in great abundance in the brain. They have well established roles in protein synthesis, as key intermediates in ammonia metabolism, and as precursors for other neurotransmitters such as γ-aminobutyric acid (GABA). A transmitter role for glutamate and aspartate was first proposed in the 1950s after observations that sodium glutamate could activate central nervous system (CNS) neurones (Hayashi, 1954). Since then, the role of glutamate as a neurotransmitter in the CNS, and the elucidation of excitatory amino acid receptors have been extensively studied. The availability of potent and selective excitatory amino acid agonists and antagonists together with the advent of molecular biological techniques has resulted in the discovery of distinct receptor types.

At least 4 classes of receptors exist. Three are ion-channel linked receptors, or ionotropic receptors (iGluR) and are named after their preferred agonists:- N-methyl-D-aspartate (NMDA), kainate-preferring (KA), and α-amino-3-hydroxy-5-methyl-4-isoxazolepropionic acid (AMPA). The remaining class of receptor are the metabotropic receptors (mGluR), which are coupled to second messenger systems. While the properties of all the receptor types will be outlined, attention will be focused on the metabotropic glutamate receptors.

1.2 Ionotropic glutamate receptor classification

The ionotropic glutamate receptor subtypes are traditionally defined by the actions of specific agonists and are divided into NMDA and non-NMDA receptors (AMPA and kainate receptors). Through DNA cloning, the clear separation between the NMDA receptors and non-NMDA receptors that was demonstrated pharmacologically was given a

molecular basis (Hollman *et al.*, 1989). The protein sequences between the subunits of the NMDA receptors and the non-NMDA receptors differed substantially (Hollman *et al.*, 1989; Moriyoshi *et al.*, 1991; Monyer *et al.*, 1994). Moreover, studies demonstrated that there is no significant sequence homology or receptor structure similarity between glutamate receptors and other ligand-gated ion channels including the GABA$_A$, nicotinic acetylcholine, glycine or serotonin receptors. Unlike other ionotropic receptors which have 4 transmembrane domains (TMD) and an extracellular C-terminus, the ionotropic glutamate receptors appear to have an intracellular C-terminus and only three 'real' TMD. (Hollman *et al.*, 1994; Kuryatov *et al.*, 1994; Wo & Oswald, 1994). In this model, rather than crossing the membrane fully, the second TMD is considered to lie in close proximity to the intracellular surface of the plasma membrane or make a hairpin turn in the membrane.

The following sections outline the functional characteristics, pharmacology and molecular biology of these receptors.

1.2.1   The NMDA receptor

The availability of specific agonists and antagonists and the use of radioligand binding studies has led to extensive studies over the last 40 years that have provided detailed characteristics of NMDA receptors. At resting membrane potentials the channel is voltage-dependently blocked (at potentials more negative than -20 or -30 mV) by Mg^{2+} ions. Activation of the receptor by glutamate, aspartate or related amino acids leads to a voltage-dependent conductance in neurones resulting from the removal of the Mg^{2+} blockade and the opening of the cation-permeable ion channel (Na$^+$, K$^+$ and Ca^{2+}). Thus NMDA receptor-induced synaptic currents are characteristically slow in onset and have a long duration, decaying over several hundred milliseconds. This type of activation results in

a large influx of Ca^{2+} into the cell which can elicit long-term metabolic or structural changes.

Compounds that act on NMDA receptors are classified according to their site of action. The competitive NMDA antagonists, such as 3-(2-carboxypiperazin-4-yl)propenyl-1-phosphonoate (CPP-ene), act on the glutamate/NMDA recognition site. In conjunction with the glutamate recognition site, drugs can act at:

a) a regulatory site which binds glycine (strychnine insensitive). NMDA receptor activity is not possible without glycine. D-serine and D-alanine are active at this binding site and act as co-agonists at the NMDA receptor. Modulation of the glycine site has been used to experimentally manipulate NMDA receptor activity (e.g. 3-amino-1-hydroxy-2-pyrolidone, HA-966).

b) a site within the channel that binds phencyclidine and related compounds. Agents which act on this site are classed as non-competitive NMDA antagonists (e.g. MK-801) as the responses mediated are voltage- and use-dependent. Other ligands include dissociative anaesthetics such as phencyclidine and ketamine. They have a low therapeutic ratio as the side effects associated with these compounds are psychotomimetic and cardiovascular in nature (Muir & Lees, 1995).

c) the polyamine modulatory binding site where the polyamines spermine and spermidine act as agonists and putrescine and arcaine act as antagonists.

d) an inhibitory divalent cation site that binds Zn^{2+}. In contrast to Mg^{2+}, the inhibition by Zn^{2+} is not voltage-dependent and interacts at a different site. One function of this site could be to modulate NMDA function because of the high concentrations of Zn^{2+} present in nerve terminals.

Activation of the NMDA receptor is also subject to modification by H^{+} concentration and redox state. Acidic pH inhibits NMDA receptor activation while reducing

agents enhance NMDA receptor activation and Ca^{2+} influx (Levy *et al.*, 1990; Sucher *et al.*, 1990). Compounds that act on NMDA receptors selectively are outlined in table 1.1.

Molecular biology of the NMDA receptors

NMDA receptors exist in multiple forms and most probably as pentameric assemblies. Expression studies have revealed that NMDA-receptors are composed heteromerically of two subunits, the NR1 subunit (103 kDa) and the NR2 subunit (133 kDA) (Moriyoshi *et al.*, 1991). The NR1 subunit is a fundamental component of all native NMDA receptors and can be assembled into homomeric NR1 receptor channels (albeit with a small current response). The NR1 subunit has 8 possible splice variants, NR1A-NR1H (Zukin & Bennett, 1995), that arise from the permutations of a short insertion near the N-terminus (4 variants) or a deletion in the C-terminus (3 variants) together with the main isoform (Westbrook, 1994). Four NR2 subunit types exist, NR2A-NR2D, which form the native NMDA when co-expressed with the NR1 receptors (Gasic & Hollman, 1992). The NR2 subunits are modulatory subunits that have no NMDA activity but potentiate and differentiate the NMDA receptor activity depending on which of the NR2 subunits are incorporated. For example, NR1-NR2A and NR1-NR2B channels are more sensitive to the Mg^{2+} blockade and display the highest affinity sites for glycine binding compared with other heteromeric channels (Monyer *et al.*, 1992). Both the Ca^{2+} permeability and Mg^{2+} block in the NMDA receptor channel are determined by a site corresponding to the TMD2 RNA editing site in the AMPA receptor. Pharmacological diversity of the NMDA receptors is affected by subunit composition. For example, eliprodil and ifenprodil are NR2B specific antagonists.

The binding sites for glutamate and glycine on recombinant NR1-NR2B receptors have been identified using site-directed mutagenesis studies (Kuryatov *et al.*, 1994). In both

subunits, the binding sites have significant and structural homology with the bacterial amino-acid proteins that bind protein or ions first recognised in AMPA receptors. The subunits possess two domains similar to that of bacterial periplasmic binding proteins. One domain is homologous with the leucine, isoleucine, valine binding protein (LIVBP) and the other is homologous with the lysine, arginine, ornithine binding protein (LAOBP). A schematic representation is illustrated in figure 1.2. The similarities to bacterial binding proteins are discussed in section 1.3.

1.2.2 The non-NMDA receptors

Until very recently, the lack of pharmacological tools to discriminate between AMPA and KA receptors caused much confusion regarding the functionally distinct actions mediated by each receptor. Consequently, the kainate receptor is the least characterised of the glutamate receptors.

The AMPA receptor has at least three separate binding sites at which agonists or antagonists can act;

a) the glutamate binding site, e.g. 2,3-Dihydro-6-nitro-7-sulfamoyl-benzo(F)quinoxaline (NBQX).

b) the desensitisation site; AMPA receptors show rapid desensitisation.

c) the intra-ion channel binding sites where certain substances such as the Joro spider toxin acts to block the ion channel (Ozawa *et al.*, 1998).

Agonists acting on the AMPA receptor lead to the activation of conductance channels that exhibit little voltage-dependence, are permeable to Na^+ and K^+, and which may be permeable or impermeable to Ca^{2+} depending on the receptor structure. Receptor activation by KA results in the opening of a cation channel permeable to Na^+, and sometimes to Ca^{2+}.

A distinctive characteristic of non-NMDA receptors are their rapid desensitisation to glutamate. This is thought to play a role in the shaping of synaptic currents and in synaptic depression at some synapses (Trussell & Fishbach, 1989; Trussell et al., 1993). At AMPA receptors, AMPA and glutamate but not KA induce a rapid and strong desensitising response in the receptors, while desensitisation is marked at KA receptors following KA activated currents. A number of agents have been shown to reduce this rapid desensitisation. Concanavalin A (ConA) blocks rapid glutamate desensitisation at native and recombinant KA receptors (Huettner, 1990; Partin et al., 1993). ConA is less potent at AMPA receptors but the diuretic agent cyclothiazide (CTZ) and also aniracetam blocks desensitisation at native and recombinant AMPA receptors with no effect at KA receptors (Wong & Mayer, 1993; Yamada & Tang, 1993). A recent compound 4-[2-(phenyl-sulfonylamino)ethylthio]-2,6-difluoro-phenoxyacetamide (PEPA) which is structurally distinct from the pyrrolidinones such as aniracetam, and the benzothiazide compounds such as CTZ, has been found to potentiate AMPA receptor responses (Sekiguchi et al., 1997).

Characterisation of the AMPA receptor has been advanced greatly with the aid of the competitive antagonist 2,3-Dihydro-6-nitro-7-sulfamoyl-benzo(F)quinoxaline (NBQX) the most potent centrally active AMPA antagonist. This was the first AMPA/KA receptor antagonist with selectivity and systemic activity. Receptor binding studies and electrophysiological studies demonstrated that it has a 30-fold higher affinity for AMPA receptors over KA receptors in the CNS, and no affinity for NMDA receptor binding sites (Sheardown et al., 1990). Subsequently, a second class of AMPA antagonists has emerged, that are non-competitive and do not exhibit voltage- or use-dependency, e.g. GYKI 52466 and GYKI 53655. They act to increase the rate of desensitisation of AMPA receptors by binding to the CTZ binding or a neighbouring site (Palmer & Lodge, 1993). GYKI 53655 has made possible the functional isolation of KA receptors. The antagonist 5-nitro-6,7,8,9-
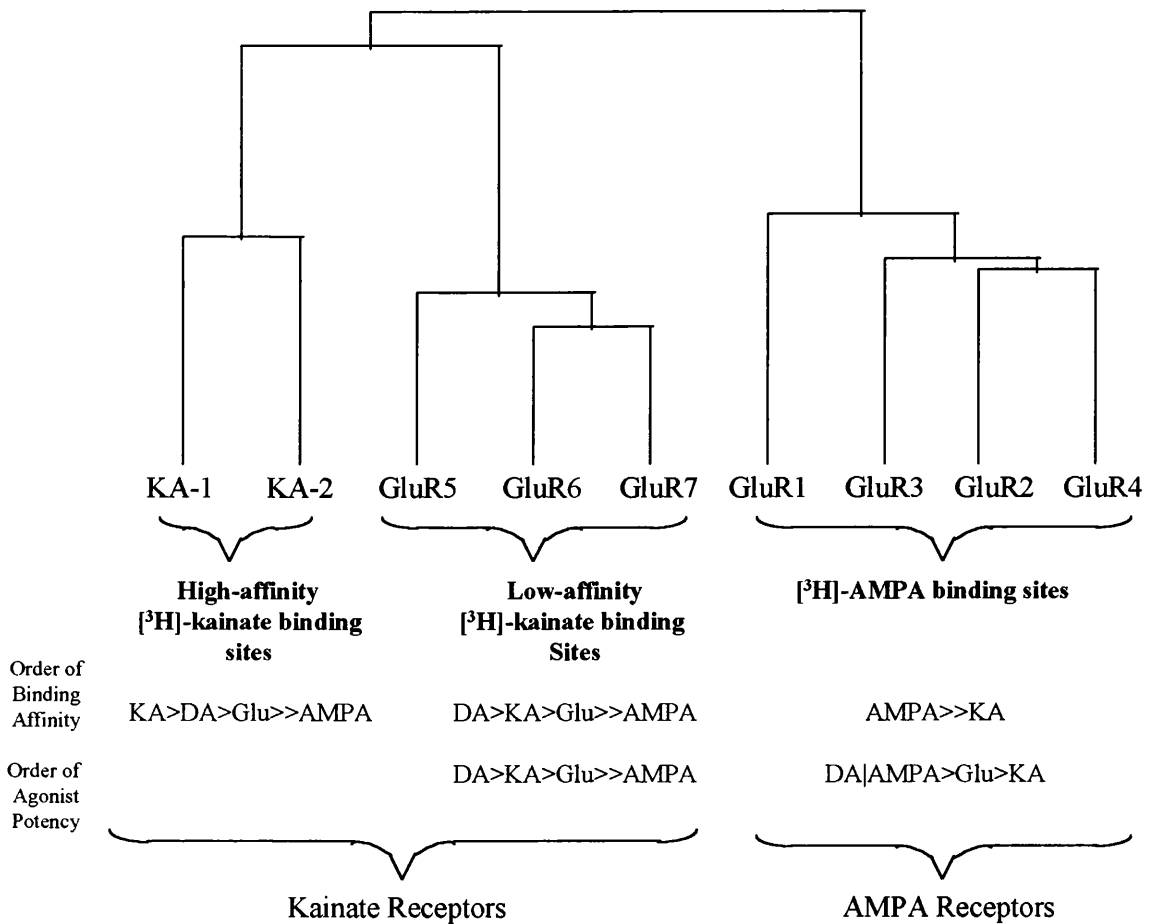
Figure 1.1.   Structural relationship among cloned AMPA and kainate receptor subunits.

The line length separating the subunits represents their evolutionary distance.
Order of low affinity binding, K_D = 50-100 nM, high affinity binding, K_D = 5 nM.
KA=kainate; DA=domoate; Glu=L-glutamate.

(From Bettler & Mulle, 1995)

tetrahydrobenzo[g]indole-2,3-dione-3-oxime (NS102) is routinely used at kainate receptors, but has poor selectivity. A newly developed glutamate analogue, 2S,4R-4-methylglutamate (SYM 2081), is a promising ligand that has demonstrated the ability to desensitise KA receptor mediated currents selectively and potently (Wilding & Huettner, 1997). The agents that selectively act on AMPA and KA receptors are summarised in table 1.1 (for a comprehensive review of AMPA receptor pharmacology, see Gill & Lodge, 1997). In hindsight, comparing the properties of the recombinant KA receptors with the native receptors, most of the electrophysiological actions of KA described in the brain have been attributed to AMPA receptors rather than KA receptors. Only in rare instances has it been possible to find pure populations of kainate receptors *in vivo* and even now the physiological role of kainate receptors remain obscure. The characterisation of KA receptors has not been easy because of their desensitising properties and the masking of their currents by the larger AMPA receptor-mediated currents (Lerma *et al.*, 1993). Investigation of the physiological roles of KA-preferring receptors is just starting in earnest (Castillo *et al.*, 1997; Clarke *et al.*, 1997; Rodríguez-Moreno *et al.*, 1997; Lerma, 1997).

Molecular biology of AMPA and KA receptors

The first glutamate receptor was cloned in 1989 and was named GluR1 (Hollman *et al.*, 1989). It is generally believed that 4 genes encode AMPA receptor subunits (GluR1-4) and 5 encode KA receptor subunits. The kainate receptors comprise of GluR5-7, known as the "low affinity" subunits and the "high affinity" KA1-2 (Bettler *et al.*, 1992; Lomeli *et al.*, 1992). All non-NMDA glutamate receptor subunits are approximately 900 amino acid residues in length of about 100 kDa and the sequence relationship of these genes reflect the traditional pharmacological classification (figure 1.1). AMPA receptors exist either as homomeric or heteromeric oligomers of the different subunits. The different assemblies of

the subunits results in major changes in the functional properties of the native AMPA receptors.

Molecular analysis has provided evidence for much structural and functional diversity. Many splice variants have been described in the N- and C-terminals of AMPA and KA receptor subunits (Bettler & Mulle, 1995). For instance, each KA subunit is subject to splicing and the GluR1/-2/-3/-4 subunits exist in alternatively spliced 'flip' and 'flop' variants which are spatially and temporally regulated (Monyer *et al.*, 1991). The isoforms differ in their expression in cells and have different kinetic properties (Sommer *et al.*, 1990). They have been shown to differ in their time course of desensitisation. Channels assembled with flop variants generally show a faster desensitisation than those with flip forms (Mosbacher *et al.*, 1994). Also their response to drugs modifying desensitisation differ (Partin *et al.*, 1993).

The functional properties of AMPA and KA receptors can also be altered by RNA editing (Sommer *et al.*, 1991; Köhler *et al.*, 1993). This manifests as variations in the conductance levels of a receptor subtype according to the subunits present (Swanson *et al.*, 1997). For example, recombinant expression studies show that the subunit GluR2 gives rise to heteromeric receptors low in Ca^{2+} permeability, characteristic of most native AMPA receptors (Hollman *et al.*, 1991). This contrasts with homomeric and heteromeric receptors assembled from the GluR1/-3/-4 subunits that are relatively permeable to Ca^{2+}. This property has been mapped to a single residue. The change in a single amino acid at the 'Q/R' site in the TMD2 segment of subunits determines the Ca^{2+} permeability. Mutagenesis studies have shown that this site also determines the sensitivity of the ion channels to spider and wasp toxins such as argiotoxin and Joro spider toxin, which have less effect on GluR2 containing receptors and serve as probes to detect the presence or absence of GluR2 subunits (Blaschke *et al.*, 1993). The change in this amino acid is the product of an RNA

editing mechanism that converts the glutamine codon (CAG) present into an arginine codon (CGG). The positive charge of arginine prevents the permeation of divalent cations in AMPA receptors. GluR1/-3/-4 subunits have the glutamine residue (Q), whereas the GluR2 subunit has the arginine residue (R). GluR5 and GluR6 subunits can also be edited to have the arginine residue. RNA editing of the Q/R site in the second domain has also been observed for the KA receptor subunit GluR6 and produces a similar effect on rectification as the AMPA subunits (discussed below), but an opposite effect on calcium permeability. Those that have the arginine residue have a higher calcium permeability than GluR6 with glutamine. However, this depends on additional RNA editing of 2 codons in TMD1 (Köhler et al., 1993). The corresponding site in NMDA receptors is also responsible for Ca^{2+} and Mg^{2+} permeability. Recently, editing at another site was identified in the extracellular TMD3-TMD4 loop of GluR subunits which determines a switch from the encoded arginine (R) to glycine (G) (Lomeli et al., 1994). Editing at this site is specific for GluR2, 3 and 4, and is about 80-90% complete in adult rat brain. Immediately adjacent to this editing site is the flip/flop splicing site. Similar to the flip/flop site, this RNA editing site is involved in controlling desensitisation and recovery rates of AMPA receptor responses, and edited forms show a slower desensitisation rate(Seeburg, 1996).

Using heterologous expression systems it was demonstrated that AMPA subunits can assemble into both homomeric and heteromeric receptor configurations with distinct functional properties (Boulter et al., 1990; Keinänen et al., 1990). Homomeric receptors of GluR1, GluR3 and GluR4 are Ca^{2+} permeable and show inwardly rectifying I/V relations whereas GluR2 form Ca^{2+} impermeable channels with linear I/V relations (Hume et al., 1991). When GluR2 is co-expressed with any of the other AMPA receptor subunits, channels with properties similar to GluR2 are formed (Hollman et al., 1991). It also seems that only a very few cells lack the GluR2 subunit. Examples are the Bergmann glia cells
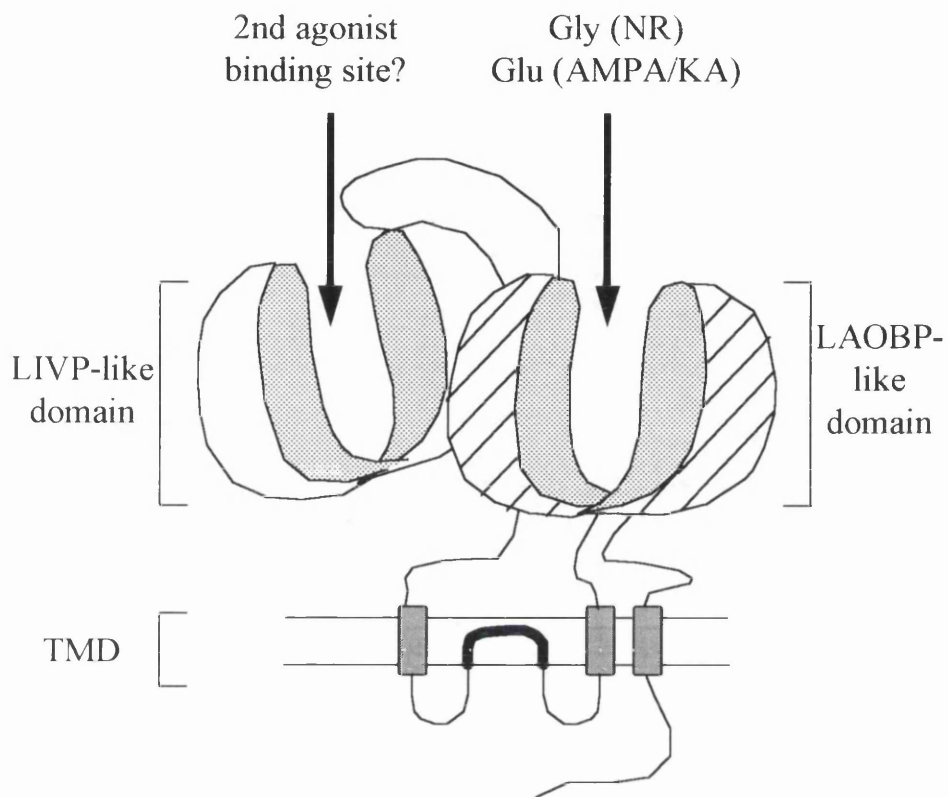
Figure 1.2   Schematic representation of the topology of an iGluR.

The channel pore domain is highlighted in black
LIVP = Leucine, isoleucine, valine binding protein; LAOBP = Lysine, arginine, ornithine binding protein; TMD = transmembrane domain

(Adapted from Pin & Bockaert, 1995)

Table 1.1   Ionotropic glutamate receptor pharmacology.

RECEPTOR CLASSES	Agonists	Antagonists	Comments / References
NMDA transmitter site	NMDA L-Glutamate Methanoglutamate L-Aspartate Ibotenate Quinolinate homocysteate	CPP CPP-ene D-AP5 D-AP7 CGS-19755	Curtis & Watkins, 1963
Channel		PCP MK-801 TCP Ketamine SKF 10047 CNS 1102 dextromethorphan memantine	Clineschmidt *et al.*, 1982; Kemp *et al.*, 1987.
Glycine site	Glycine D-Serine D-Alanine D-Cycloserine (P)	HA-966 (P) Kynurenate 7-Cl-Kynurenate ACEA 1011, 1021	Davies & Watkins, 1973; Kulagowski *et al.*, 1994
Polyamine site	Spermine Spermidine Histamine	Ifenprodil Arcaine Eliprodil	Spermine and Spermidine enhance the affinity for MK-801 Eliprodil/ifenprodil NR2B selective
AMPA	AMPA L-Glutamate Quisqualate Kainate Willardiines	NBQX CNQX DNQX LY293558 GYKI 52466 GDEE Argiotoxin Joro spider toxin	GYKI 52466 is non-competitive and inhibits GluR6 Argiotoxin is use-dependent channel blocker - no block in receptors with edited GluR2 subunit Haldemann & McLennan, 1972; Krogsgaard-Larsen *et al.*, 1980; Ornstein *et al.*, 1993; Sheardown *et al.*, 1990
Kainate	AMPA Kainate L-Glutamate Domoate Quisqualate Willardiines	CNQX DNQX NS-102 Methahexitone	AMPA agonist at GluR5, GluR6/KA-2 and dorsal root ganglion neurones Methahexitone active on AMPA and GABA receptors CNQX less potent at GluR6 than at other receptors

Agents are not necessarily ranked in order of potency. (P) = partial agonist.
AMPA: α-amino-3-hydroxy-5-methylisoxazole proprionate; **CGS-19755**: (+)cis-4-phosphonomethyl-2-piperidinecarboxylate; **CNQX**: 6-cyano-7-nitro-quinoxaline-2,3-dione; **CPP**: 3-3(2-carboxypiperazin-4-yl)propyl-1-phosphate; **CPP-ene**: 3-(2-carboxypiperazin-4-yl)propenyl-1-phosphonoate; **D-AP5**: (D-)2-amino-5-phosphopentanoate; **DNQX**: 6,7-nitro-qunoxaline-2,3-dione; **GDEE**: glutamic acid diethyl ester; **GYKI 52466**: 1-(4-aminophenyl)-4-methyl-7,8-methylenedioxy-5H-2,3-benzodiazepine; **HA-966**: 3-amino-1-hydroxy-2-pyrolidone; **LY293558**; **MK-801**: dibenzocycloheptene-imine; **PCP**: phecyclidine, **TCP**: 1-(1-thienyl- cyclohexyl)-piperidine

(Burnashev *et al.*, 1992) and a subset of hippocampal neurones (type II cells) (Bochet *et al.*, 1994).

Only KA receptor subunits GluR5 and GluR6 form functional homomeric receptors (Bettler *et al.*, 1992; Sommer *et al.*, 1992; Köhler *et al.*, 1993) and can also assemble as heteromeric receptors in pairwise combination with the KA-1 or KA-2 subunits (Herb *et al.*, 1992; Sakimura *et al.*, 1992). GluR5 and GluR6 exhibit fast desensitisation kinetics to KA/glutamate while the inclusion of KA subunits into GluR6 and GluR7 receptors make them sensitive to AMPA (Herb *et al.*, 1992). Additionally, heteromeric GluR5/KA-2 receptors present faster inactivation kinetics than homomeric GluR5 receptors.

Despite extensive research, all attempts to incorporate GluR7 subunit into a functional recombinant receptor has been unsuccessful until recently. Schiffer *et al.* (1997) have cloned and characterised a novel carboxy-terminal splice variant of GluR7, named GluR7b. They have demonstrated that these two subunits can generate functional homomeric kainate receptors with distinct pharmacological properties. GluR7 showed approximately a 10 fold higher EC_{50} for glutamate compared to other cloned AMPA or kainate receptors. In addition, GluR7 could be co-expressed with KA-1 and KA-2 subunits to form functional heteromeric receptors. Interestingly, these receptors were insensitive to domoate, unlike all other non-NMDA receptor subunits. The authors concluded that this receptor may play a unique role under conditions of strengthened neurotransmission in the CNS. Although reports suggest that KA receptor subunits do not form mixed channel complexes with AMPA receptor subunits, both types of receptors can be expressed in the same neurone or glial cell and may localise in different subcellular sites (Vickers *et al.*, 1993; Patneau *et al.*, 1994; Wenthold *et al.*, 1994). The model of glutamate binding is thought to be the same as for NMDA receptors (figure 1.2) and the TMD2 domain of each

subunit is thought to contribute directly to the lining of the cation channel (Sucher *et al.*, 1996).

1.2.3   Current concepts of ionotropic glutamate receptor subunit identification

In order to understand all the roles of these receptors, there is undoubtedly a need to identify all the subunits that make up the subtypes, so that the individual characteristics of each subunit may be differentiated and the nature of the subunit co-assemblies understood. Although this identification process has progressed rapidly, there is recent evidence that suggests many more discoveries are to be made. For example, the expression of recombinant NMDA receptors can exhibit different properties from the native NMDA receptors on neurones, such as pharmacology or antibody reactivity. This may well be due to unidentified native partner subunits (Sucher *et al.*, 1996; Barnard, 1997). Additional evidence also suggests that types of ionotropic glutamate receptors exist in the mammalian CNS that have not yet been identified. The cloned δ1 and δ2 subunits (Lomeli *et al.*, 1993) which have a 15-25% sequence homology to NMDA and non-NMDA receptor subunits have failed to express functionally alone or with any other known subunit.

Further subunits have been described recently. The non-NMDA receptors have an extracellular N-terminal. Distinct from the established non-NMDA receptors, structurally related subunits of ~50 kDa have been reported that have most of the extracellular N-terminal domain missing (Wo & Oswald, 1994). These are kainate binding proteins found in abundance in non-mammalian vertebrates. These proteins bind selectively to KA and not AMPA and occur on neurones in frogs (Wada *et al.*, 1989). From the *Xenopus laevis* toad, a short GluR-like protein was purified which binds to AMPA and KA with high affinity, and upon reconstitution in a lipid bilayer, could participate in a glutamate-activated channel (Henley *et al.*, 1992). This subunit has been termed XenU1 and is unlike the kainate-binding

proteins and all previously known non-NMDA subunits. In addition, XenU1 does not replace the conventional receptors because *Xenopus* also contains the known receptor subunits for AMPA and KA which have been demonstrated to be >95% identical to their rat equivalents (Ishimaru *et al.*, 1996). Expression data suggests however that a partner subunit is required for XenU1 and a novel subunit has been cloned from *Xenopus* - XenNR1G cDNA (Soloviev *et al.*, 1996). This encodes a 99.6 kDa subunit closely related to the NR1 subunit seen in mammalian NMDA receptors. When expressed alone, no functional response was evident, but after co-expression of XenNR1G and XenU1, consistent and strong current responses to NMDA and non-NMDA receptor agonists were obtained. Electrophysiological studies have provided evidence that these receptors exist as a new type of ionotropic glutamate receptor (Soloviev *et al.*, 1996). It has been termed a 'unitary receptor' for glutamate, i.e. one that combines the agonist sites of NMDA and non-NMDA receptors on different subunits, but in one heteromeric receptor molecule. These receptors exhibit the fundamental attributes of the NMDA receptor-channel complex; a voltage-dependent Mg^{2+} block and glycine dependence, but are stimulated by non-NMDA agonists, and may exist in mammals. These receptors, together with the δ-subunits identified, illustrate that the full repertoire of ionotropic glutamate receptors is still unknown.

1.3   Metabotropic glutamate receptor classification

The existence of metabotropic glutamate receptors mGluRs was only discovered in 1985 when it was reported that glutamate stimulated phospholipase C in cultured striatal neurones via a receptor that did not belong to the NMDA, AMPA or KA families (Sladeczek *et al.*, 1985). Independently, L-AP4 had previously been recognised as a specific ligand for a new glutamate receptor subtype (Foster & Fagg, 1984). Subsequent research revealed L-AP4 to act as an agonist on presynaptic glutamate receptors, depressing

glutamate release at excitatory synapses and shown to be coupled to G-proteins (Koerner & Johnson, 1992; Nawy & Jahr, 1990). It is now recognised that the then named L-AP4 receptor is a member of the mGluR family. Unlike the ionotropic glutamate receptors, early characterisation and classification of the mGluRs resulted from molecular biological techniques. Pharmacologically, mGluRs were distinguished from the ionotropic glutamate receptors by the use of the non selective (mGluR subtype) agonist *trans*-1-aminocyclopentane-1,3-dicarboxylic acid (*trans*-ACPD), or its 1S, 3R-isomer, which modifies inositol phosphate (IP) metabolism (Palmer *et al.*, 1989; Schoepp *et al.*, 1991).

Molecular biology of the metabotropic glutamate receptors

The first mGluR cDNA was cloned independently by two groups and is now generally named mGluR1a (Masu *et al.*, 1991; Houamed *et al.*, 1991). Its deduced amino acid sequence revealed that this receptor shared no sequence homology with any other G-protein coupled receptor. The ensuing search for mGluR-related cDNA has led to the isolation of 7 other genes and several splice variants that encode mGluRs and are named mGluR1-mGluR8.

Splice variants have been demonstrated for mGluR1, mGluR4 and mGluR5 (Tanabe *et al.*, 1992; Pin *et al.*, 1992; Minakami *et al.*, 1994). To date, the human homologues of mGluR1a, b and d, mGluR2, mGluR3, mGluR4, mGluR5a, b, mGluR7 and mGluR8 have been cloned (Minakami *et al.*, 1994; Laurie *et al.*, 1996; Desai *et al.*, 1995; Flor *et al.*, 1995a, 1995b; Emile *et al.*, 1996; Daggett *et al.*, 1995; Wu *et al.*, 1998). The primary sequence of the human receptors show 93-99% homology with the rat homologues, while a mGluR cloned from *Drosophila melanogaster* called DmGluRA shows 45% sequence homology with the mammalian mGluR3 (figure 1.3). The mGluRs also show significant homology with the recently cloned GABA$_B$ receptor (Kaupmann *et al.*, 1997).

The 8 mGluRs can be subdivided into three groups principally on the basis of their amino acid sequence, but also in terms of their pharmacological properties and transduction mechanisms (figure 1.3). mGluRs of the same group show about 70% sequence identity, whereas between groups this decreases to around 45%. The receptors are much larger than all previously identified G-protein coupled receptors and do not share any sequence homology, thus defining a new family of receptors. This new family of receptors may not be restricted to glutamate receptors and may include additional members. Evidence for this comes from the isolation of a Ca^{2+}-sensing receptor cDNA from a bovine parathyroid cDNA library. It has a 30% sequence identity with the mGluRs but is not sensitive to mGluR agonists but to cations such as Mg^{2+}, Gd^{3+} and neomycin (Brown *et al.*, 1993).

All the mGluRs possess a large N-terminal extracellular domain, seven putative TMDs separated by short intra- and extra-cellular loops and a cytoplasmic C-terminal domain variable in length (figure 1.4). The role of the C-terminal domain is not known, but may be the target of various kinases due to the numerous phosphorylation sites and serine/threonine residues present that could regulate receptor activity. The model of the glutamate binding site emerged from the molecular modelling of the N-terminal domain of mGluR1 (O'Hara *et al.*, 1993). Nakanishi *et al.* (1990) first noticed that there were similarities in sequence between the N-terminal domain of AMPA receptors and bacterial periplasmic glutamine-binding proteins, especially with the leucine, isoleucine, valine binding protein (LIVBP). The mGluR1 N-terminal domain also exhibited homology with the bacterial binding protein. This similarity is not evident at the primary sequence level, but is prominent when the sequences are aligned with respect to their three-dimensional compatibility. The resulting model of the N-terminal domain displays 2 globular lobes connected by hinge regions that close like a clamshell on binding of the ligand. By constructing chimeric receptors, it was demonstrated that the second intracellular loop of

17
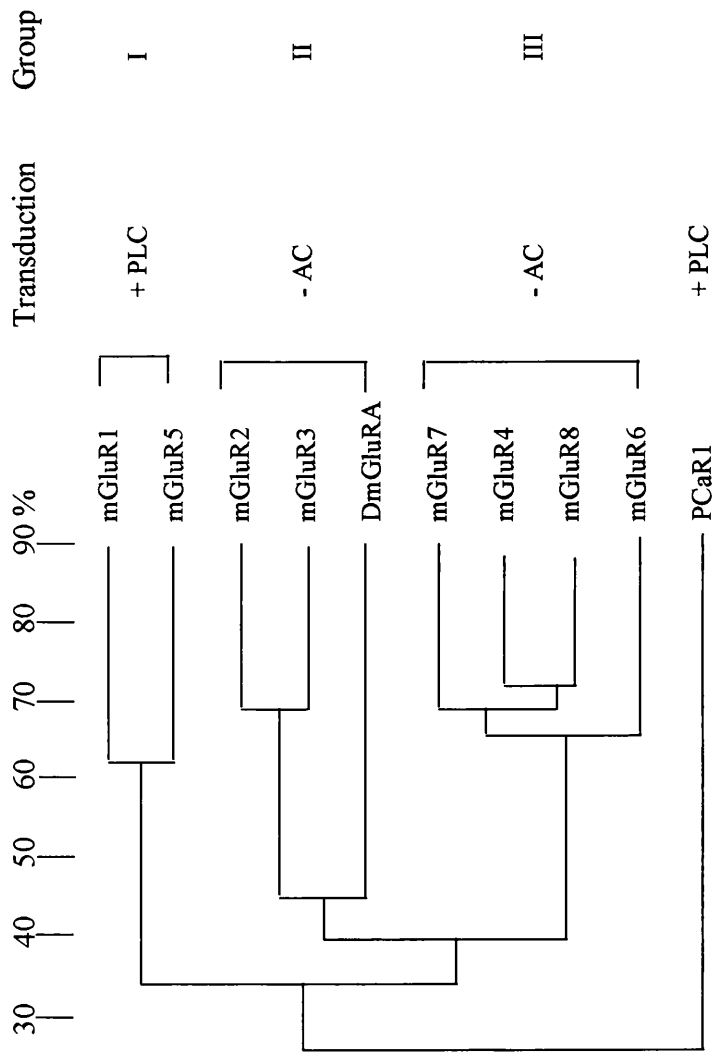
Figure 1.3   Classification of the mGluR family.

Dendrogram of the members of the mGluR family including the *Drosophilia* mGluR (DmGluRA) and the bovine parathyroid Ca2+-sensing receptor (PCaR). PLC = Phospholipase C; AC = Adenylate cyclase

(From Conn & Pin, 1997)

mGluRs is critical in G-protein coupling specificity (Pin *et al.*, 1994; Gomeza *et al.*, 1996).

The mechanism by which a ligand induces the conformational changes required for G-protein activation remain to be discovered. For a comprehensive review of the structure of the mGluRs, see Conn & Pin, (1997).

Like the iGluRs, evidence suggests that novel mGluRs may also exist that have not been discovered as yet. For example, in cortical slices, there appears to be an mGluR that couples to phosphoinositide hydrolysis that does not correspond to any of the previously cloned mGluR subtypes (Chung *et al.*, 1998). Furthermore, a novel mGluR is thought to exist that couples to the activation of phospholipase D (Holler *et al.*, 1993; Boss *et al.*, 1994).

1.3.1 Group I receptors

Cloned group I mGluRs, including the splice variants (mGluR1a-c,e and mGluR5a and b), stimulate phospholipase C (PLC), demonstrated by the hydrolysis of phosphatidylinositol (PI) (Masu *et al.*, 1991; Houamed *et al.*, 1991). Hydrolysis of the membrane phosphatidylinositol-4,5-bisphosphate by PLC produces two second messengers; diacylglycerol (DAG) which activates protein kinase C (PKC) and inositol 1,4,5-trisphosphate (IP_3) which leads to the release of calcium from intracellular stores. Stimulation of cAMP formation has also been reported for mGluR1a and it has been attributed to a direct coupling to adenylate cyclase (AC) through G_s-protein (Aramori & Nakanishi, 1992), though this is not certain. In addition, it is not known whether this heterologous coupling is a result of the expression of the receptors at high levels in non-neuronal cells or is due to low G-protein selectivity in neurones. It has also been reported recently that mGluR activation (suggested to be mGluR1) increases cGMP levels in cerebellar slices and that the response can be blocked by nitric oxide synthase inhibitors

(Okada, 1992). While no functional differences have been detected between the expressed splice variants mGluR5a and mGluR5b, the mGluR1a variant has been shown to generate faster responses and activate AC when compared with the truncated isoforms mGluR1b and mGluR1c (Pin *et al.*, 1992; Pickering *et al.*, 1993) It is thought that the functional difference is caused by a difference in the coupling efficiency of the receptors to the G-proteins (Prézeau *et al.*, 1996). A pre-synaptically located mGluR shown to couple to PI hydrolysis is thought to exist that enhances the release of glutamate, but only in the presence of arachidonic acid (Herrero *et al.*, 1992).

For both clonal cell lines and native receptor-mediated responses, group I receptors are selectively activated by the compound 3-5-hydroxyphenylglycine (DHPG). Other selective agonists are summarised in table 1.2. Although qualitatively similar, the potencies of the majority of these agonists are significantly greater upon mGluR5 receptors. Selective antagonists for this group of receptors are emerging. Recently, the synthesis of substituted derivatives of a prototypic mGluR antagonist, 4-carboxyphenylglycine (4-CPG) has produced compounds LY367385 and 2-methyl-4C3HPG that possess improved selectivity for mGluR1a over mGluR5a (table 1.2). However, these agents have been demonstrated to activate group II receptors at higher concentration.

1.3.2 Group II receptors

Expression of cloned group II mGluRs (mGluR2 and 3) is coupled to the inhibition of adenylate cyclase (Tanabe *et al.*, 1992). This response is inhibited by pertussis toxin which suggests the involvement of a G_i-type of G-protein. They have also been shown to inhibit N-type Ca^{2+} channels through a pertussis toxin sensitive pathway (Ikeda *et al.*, 1995). Consistent with studies in expression systems, activation of group II mGluRs inhibits forskolin-induced increases in cAMP accumulation in brain slices and cultures (Schoepp *et*
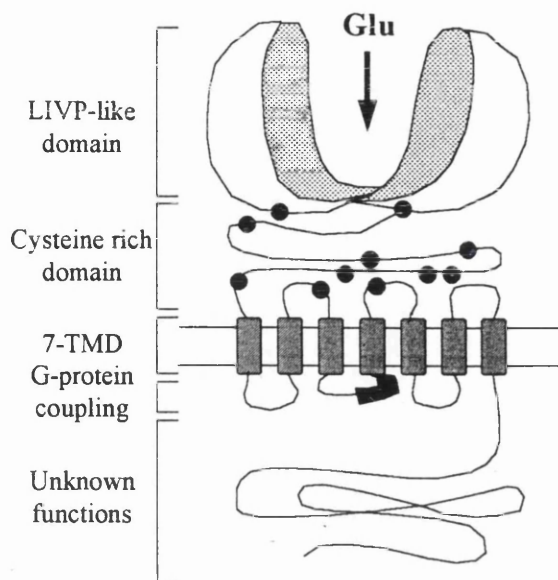
Figure 1.4   Schematic representation of the topology of an mGluR.

The region rich in cysteine residues is indicated with black circles. The segment in the second intracellular loop is important for G-protein coupling specificity is indicated in black. LIVP = Leucine, isoleucine, valine binding protein
TMD = transmembrane domain

(From Conn & Pin, 1997)

al., 1995a; Wright & Schoepp, 1996). However, as the measurement of inhibition of cAMP has been through the AC activator forskolin, rather than responses of receptors that activate AC to agonists, it is not clear whether group II mGluRs actually couple to inhibition of neurotransmitter-induced increases in cAMP accumulation in native systems. Indeed, there is evidence to suggest that that the activation of group II potentiates rather than inhibits cAMP accumulation resulting from G_s-coupled receptor agonists (e.g. vasoactive intestinal polypeptide, the β-adrenergic receptor agonist isoproterenol) in the hippocampus (Winder & Conn, 1996).

Group II mGluRs are selectively activated by (2R, 4R)-4-aminopyrrolidinedicarboxylic acid, (2R, 4R)-APDC (Schoepp *et al.*, 1995a). Other agonists which result in the activation of mGluR2 and mGluR3 are presented in table 1.2. (2S,2'R,3'R)-2-(2'3'-dicarboxycyclopropyl) glycine (DCG-IV) is the most widely used group II agonist, but is not wholly selective for these receptors. The novel group II agonists LY354740 (Bond *et al.*, 1997) and LY379268 (Monn *et al.*, in press) used in this thesis are, at present, the most potent compounds for this class. They are the first mGluR agonists to be bioavailable following systemic administration, and are potent at nanomolar concentrations. The structure of the ligands are given in figure 1.5. The pharmacology of these agonists are discussed extensively in chapter 8, section 8.1. Selective antagonists for group II receptors are also available. For the majority of the antagonists, their activities have been reported only for mGluR2 and not mGluR3 receptors, but differences may emerge in native receptors where both the receptors may contribute to the pharmacological responses.

1.3.3 Group III receptors

Group III mGluRs (mGluR4, 6, 7 and 8) are also negatively coupled to adenylate cyclase via a pertussis toxin sensitive G-protein when expressed in certain cells and in native systems (Nakajima *et al.*, 1993; Okamoto *et al.*, 1994). The inhibition observed in expression systems is often smaller than that seen with the group II mGluRs and it has been suggested that this is because this transduction pathway is not the preferred pathway. For example, mGluR6 and possibly mGluR8 are likely to negatively couple to a cGMP phophodiesterase in its native environment of the retina (Shiells & Falk, 1992). Unlike the group II mGluRs, the group III mGluRs have been shown to couple to the inhibition of G_s-activated adenylate cyclase in the hippocampus (Wright & Schoepp, 1996).

COO⁻

Glutamate

⁺H₃N COO⁻

H

HO₂C

LY354740

H

H CO₂H

NH₂

H

O

HO₂C

LY379268

H

H CO₂H

NH₂
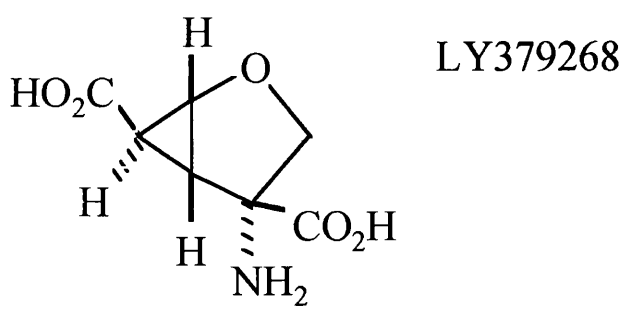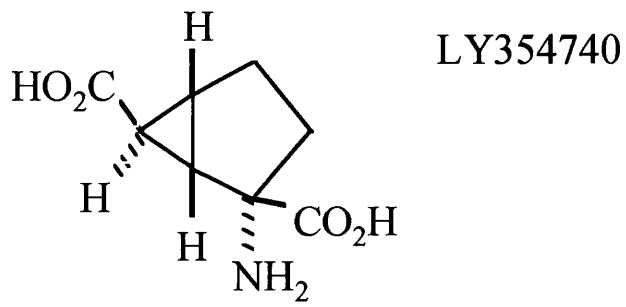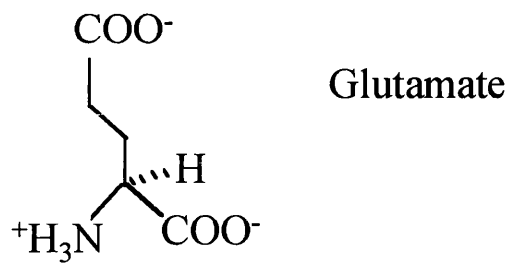
Figure 1.5 Structure of glutamate, LY354740 and LY379268.

Table 1.2   Metabotropic glutamate receptors: characteristics and pharmacology.

	Members	Effector	G-protein	Selective agonists	Selective antagonists	Comments	References
Group I	mGluR1 mGluR5	↑ PLC	$G_{q/11}$	(S)-3,5-DHPG (RS)-3H-PG t-ADA CHPG Quisqualate DHPMP	AIDA (S)-CBPG CPCCOEt LY367385 LY357366 2-methyl-4C3HPG	CHPG active at mGluR5a only; LY367385 and 2-methyl-4C3HPG more selective on mGluR1a than mGluR5a	Ito et al., 1992; Birse et al., 1993; Manahan-Vaughan et al., 1996; Doherty et al., 1997; Pellicciari et al., 1995; Clarke et al., 1997; Bruno et al., 1999
Group II	mGluR2 mGluR3	↓ AC	$G_{i/o}$	(2R,4R)-APDC LY354740 LY379268 DCG-IV	MCCG PCCG-IV LY341495 EGLU	PCCG-IV active at mGluR4; DCG-IV also active at NMDA receptors	Schoepp et al., 1995b; Bond et al., 1997; Knöpfel et al., 1995; Thomsen et al., 1996; Jane et al., 1996; Monn et al., in press
Group III	mGluR4 mGluR6 mGluR7 mGluR8	↓ AC	$G_{i/o}$	L-AP4 L-SOP	MAP4 CPPG MSOP		Toms et al., 1996; Jane et al., 1994; Thomsen & Suzdak, 1993

t-ADA: trans-azetidine-2,4-dicarboxylate

AIDA: (RS)-1-aminoindan-1,5-dicarboxylic acid

L-AP4: L-2-amino-4-phosphonobutyrate

(2R, 4R)-APDC: (2R,4R)-aminopyrrolidine-2,4-dicarboxylate

(S)-CBPG: (S)-(+)-2-(3')-carboxybicyclo[1.1.1]pentylglycine

CHPG: (RS)-2-chloro-5-hydroxyphenylglycine

2-methyl-4C3HPG: 2-methyl-4-carboxy-3-hydroxyphenylglycine

CPCCOEt: cyclopropan[b]chromen-1a-carboxylate

CPPG: (RS)-α-cyclopropyl-4-phosphon-phenylglycine

DCG-IV: (2S,2'R,3'R)-2-(2'3'-dicarboxycyclopropyl)glycine

(S)-3,5-DHPG: (S)-3,5-dihydroxyphenylglycine

DHPMP: (RS)-amino-(3,5-dihydroxyphenyl)methyl phosphinic acid

EGLU: (2S)-α-ethylglutamate

(RS)-3H-PG: (RS)-3-hydroxylphenylglycine

LY341495: (2S-2-amino-2-(1S,2S-2-carboxycyclopropan-1-yl)-3-(xanth-9-yl)propanoic acid

LY354740: (+)-2-aminobicyclo[3.1.0]hexane-2,6-dicarboxylate

LY367885: (-)-2-methyl 4-carboxyphenylglycine

LY379268: (1R,4R,5S,6R)-2-oxa-4-aminobicyclo[3.1.0]hexane-4,6-dicarboxylate

MAP4: α-methyl-L-AP4

MCCG: methyl carboxycyclopropyl glycine

MSOP: (RS)-α-methylserine-O-phosphate

PCCG-IV: 2-(2'-catrboxy-3'-phenylcyclopropyl)glycine

L-SOP: L-serine-O-phosphate

While this group contains the largest number of receptors, they are the least well characterised pharmacologically. The pharmacology of group III receptors differs tremendously from groups I and II and they are selectively activated by L-amino-4-phosphonobutyrate, L-AP4 (Nakanishi, 1992). The actions of L-AP4 are mimicked by the structurally related (and endogenous to the CNS) L-serine-O-phosphate (L-SOP) (Thomsen & Suzdak, 1993). Interestingly, mGluR4 receptors are largely unaffected by any of the broad spectrum phenylglycine derivatives, the structure upon which most of the mGluR ligands are based. Table 1.2 summarises the selective agonists and antagonists of group III mGluRs.

1.4   Distribution and physiological roles of glutamate receptors

1.4.1   Ionotropic glutamate receptors

Distribution of the ionotropic glutamate receptors

The distribution of the different receptors has been extensively studied. The general distribution of the NMDA receptors in the rat CNS has been mapped using radiolabelled NMDA antagonists (Maragos *et al.*, 1986; Monaghan & Cotman, 1985). This method permits the identification of the location of binding sites but does not allow a measure of functional receptor activity. NMDA receptors are found predominantly in the forebrain with the highest levels of NMDA binding sites to be found in the hippocampal CA1 region. Moderate levels of NMDA binding sites are present in the dentate gyrus and the CA3. NMDA receptors are widespread in the cortex, but particularly in the frontal, anterior cingulate and pyriform cortices. However, a laminar pattern of receptor density exists in the cortex; two bands of receptors are seen in cortical layers I-III and V. High levels of NMDA receptors are present in sub-cortical regions such as the dorsal-lateral septum, amygdala, striatum and nucleus accumbens. Brain regions associated with sensory functions also

contain a moderate level of NMDA receptors, including visual structures such as the superior colliculus superficial layer and lateral geniculate body and auditory structures such as the medial geniculate body and cochlear nucleus. Low levels of NMDA receptors are found in motor regions, for example the red nucleus and the pontine nucleus. The distribution of the different NR subunits have been determined by *in situ* hybridisation (Monyer *et al.*, 1992; Moriyoshi *et al.*, 1991). While NR1 is widely distributed, NR2 subunits are differentially distributed in the CNS. For example NR2C expression levels are present in the cerebellum only, while NR2A and NR2B are found predominantly in the hippocampus, cortex and thalamus and NR2D is found mainly in the olfactory bulb (Monyer *et al.*, 1992; Buller *et al.*, 1994; Salt & Eaton, 1996). Expression patterns of NR2 subunits are also regulated developmentally in rodents suggesting that different spatial and temporal patterns of expression of NR2 allow for the fine tuning of NMDA receptor functions.

AMPA receptors are distributed abundantly and widely throughout the CNS. Using radioligand binding studies, the highest levels were seen in the hippocampal CA1 and CA3 regions. High levels of binding were also seen in the molecular layer of the dentate gyrus and superficial layers of the cerebral cortex. Other brain regions found to be rich in [^{3}H]AMPA binding included the striatum, nucleus accumbens, septum and amygdala (Monaghan *et al.*, 1984; Rainbow *et al.*, 1984). AMPA receptors are also present in several types of glial cells (Bowman & Kimelberg, 1984; Burnashev *et al.*, 1992; Müller *et al.*, 1992). Following the molecular identification of the receptor subunits, AMPA receptor distributions have been localised at the mRNA level and at the protein level (Rogers *et al.*, 1991; Petralia and Wenthold, 1992; Martin *et al.*, 1993). As a result of these studies, GluR1-4 were shown to have regional expression patterns. In the cortex, GluR2 mRNA is expressed uniformly in all layers while GluR1, 3 and 4 mRNAs differ among layers. In the hippocampus, GluR1, 2 and 3 mRNAs are abundantly expressed in the pyramidal cell layer

and dentate gyrus. Studies indicate that AMPA receptor subunits are expressed predominantly in the flop forms in the adult brain (Sommer *et al.*, 1990) and that only a few neuronal types lack the GluR2 subunit. Indeed, a recent study has provided evidence that calcium permeable AMPA receptors in the hippocampus (i.e. GluR2 lacking) are found exclusively at mossy fibre synapses (Tóth & McBain, 1998). In addition, it is believed that in the hippocampus distinct AMPA receptors are expressed on single neurones that are associated with specific afferent pathways. This suggests that information is likely to be transmitted onto the postsynaptic cell in a synapse specific manner (Tóth & McBain, 1998).

Radioligand binding studies using [^{3}H]kainate have revealed that binding sites are abundant throughout the entire CNS. Brain areas such as the hippocampal CA3 region and cerebellar granular layer show intense labelling. KA receptor densities are high in cortical layers V and VI, the reticular nucleus of the thalamus, striatum and hypothalamus (Monaghan & Cotman, 1982). The anatomical distribution of KA receptor subunits has also been determined more recently using *in situ* hybridisation (Bahn *et al.*, 1994; Bischoff *et al.*, 1997). All 5 subunits are expressed by the majority of brain cells. KA2 mRNA appears to be almost universally expressed while KA1 transcripts are seen mainly in the CA3 and dentate gyrus of the hippocampus. GluR5 mRNA expression is seen in the cingulate and piriform cortex while GluR6 is most abundantly expressed in cerebellar granule cells. Evidence suggests KA receptors can coexist with AMPA receptor subunits on the same cells but do not co-assemble with one another (Mackler & Eberwine, 1993).

Ionotropic glutamate receptor mediated responses

AMPA receptor subunits are found clustered at postsynaptic sites and a major role of the ionotropic glutamate receptors is the transmission of normal synaptic activity along excitatory pathways. Glutamate mediated excitatory post-synaptic potentials (EPSPs) are

made up of 2 components. Stimulation of the AMPA receptors are responsible for the stimulatory fast EPSP (Davies *et al.*, 1989), while the NMDA receptor is activated only after depolarisation and because of its slower conductance appears to be involved in the amplification of excitatory responses. Together, they underlie excitatory synaptic currents. Several lines of evidence suggest that AMPA and NMDA receptors are co-localised and are commonly activated by a near instantaneous rise and rapid decay of glutamate (Jones & Baughman, 1991) Therefore, it seems likely that the AMPA receptor has a relatively low affinity and becomes unbound very quickly after the clearance of glutamate whereas NMDA receptors have a higher affinity which results in a prolonged binding (Lester *et al.*, 1990). Because of the multitude of combinations of receptor subunits, large differences in the kinetics of non-NMDA synaptic currents that have been observed between different neuronal populations may result from differential clearance of glutamate from the synaptic cleft (Livsey & Vicini; 1992; Barbour *et al.*, 1994) but may also reflect the differences in the functional properties of the receptors such as desensitisation characteristics (Viklicky *et al.*, 1991). As already mentioned, the role of KA receptors is less clear because the synaptic responses have been difficult to demonstrate (Castillo *et al.*, 1997; Vignes & Collingridge, 1997). This is largely due to the finding that KA produces large non-desensitising current responses at AMPA receptors. However, the presence of functional KA receptors in the hippocampus suggests the involvement of KA receptors in fast glutamatergic transmission. Electrophysiological data supports the idea that NMDA and AMPA or KA receptors work together to mediate post-synaptic excitation.

Physiological roles of the ionotropic glutamate receptors

Given their widespread distribution, they are involved in virtually all central nervous system functions. The ionotropic glutamate receptors not only mediate fast excitatory

transmission but also participate in brain plasticity. NMDA receptors are proposed to be involved in the mechanisms of synaptic plasticity in the developing and mature brain. For example, NMDA receptors are involved in the developing visual and olfactory systems (Cline et al., 1987; Lincoln et al., 1988) and have been linked to neuronal survival and differentiation (Headley & Grillner, 1990). A multitude of evidence indicates that the NMDA and AMPA glutamate receptors are important in the hypothetical cellular mechanisms of memory formation - long-term potentiation (LTP) and long-term depression (Collingridge & Bliss, 1987; Thompson, 1986). LTP is a long lasting increase in synaptic transmission evoked by either a high frequency stimulation of synaptic pathways, or by pairing presynaptic activity with postsynaptic depolarisation (Bliss & Lømo, 1973). The former is most commonly used and LTP is induced by delivering a high frequency tetanus (such as 10 bursts of 200 Hz for 75 ms, with an interburst interval of 10 s is frequently used for *in vivo* experiments).The potentiation of synaptic efficacy is dependent on an increase in intracellular Ca^{2+}. Because of the voltage-dependent feature of NMDA receptors, they are thought to be essential to the induction and maintenance of LTP (Bliss & Collingridge 1993).

The hippocampus has been implicated in memory formation and all excitatory projection pathways to, within, and from the hippocampus, use glutamate as a transmitter. The involvement of NMDA receptors in the hippocampus in learning and memory in rats has been previously demonstrated. Studies have shown the importance of NMDA receptors in the induction of LTP in the Schaffer collateral-CA1 field of the hippocampus and is commonly known as NMDA-dependent LTP (Bliss & Collingridge, 1993). The high frequency stimulation of the Schaffer collaterals leads to an association between NMDA receptor activation and postsynaptic depolarisation. This allows the removal of the Mg^{2+} block of the NMDA receptor associated channel. The Ca^{2+} influx resulting from the opening

of the NMDA receptor activates postsynaptic Ca^{2+} sensitive enzymes which leads to the potentiation of the synaptic efficacy by either pre- or post-synaptic modifications. Similarly Ca^{2+} permeable AMPA receptors are expected to provide a synaptically activated route for Ca^{2+} entry for the modulation of LTP, and GluR1 subunits are thought to be particularly important for LTP (Vanderklish *et al.*, 1992). Traditionally, LTP is thought to result from an increase in transmitter release and an enhanced postsynaptic AMPA/KA response (Bliss & Collingridge, 1993). Recent studies using GluR2 KO mice have suggested that LTP in the CA1 occurs post-synaptically and results from a recruitment of new AMPA receptors or an increase in the conductance of receptors (Mainen *et al.*, 1998). NMDA receptor involvement in learning and memory has also been demonstrated behaviourally using spatial memory tasks (Morris *et al.*, 1986). More recently, using cre-lox transgenic technology, Tsien *et al.* (1996a) were able to produce mice where the NR1 gene was disrupted in CA1 pyramidal cells but was normally expressed in other parts of the brain. Together with finding that NMDA receptor-mediated currents and LTP were abolished in the CA1 synapses, the mice exhibited impaired spatial memory (Tsien *et al.*, 1996b; McHugh *et al.*, 1996). Not all memory processes are dependent on LTP, and NMDA receptors have been shown to be involved in these LTP-independent processes. For example, NMDA receptor antagonists interfere with working memory (Adler *et al.*, 1998), which is a short-lasting form of memory that is maintained by neuronal activity rather than synaptic modification (Funahashi *et al.*, 1989). Recently, Lisman *et al.* (1998) showed that the voltage-dependent excitatory postsynaptic potentials produced by NMDA receptors can lead to selective excitation of neurones in the prefrontal cortex that is needed to maintain novel items in working memory.

KA receptors are believed to have presynaptic roles. Studies have implicated KA receptors in generating epileptiform activity at CA3 mossy fibre terminals and the

suppression of synaptic release of glutamate at CA1 synapses. Although other groups have reported that KA enhances transmitter release (Ozawa *et al.*, 1998), reports have suggested that KA receptor activation, specifically GluR5 subunits, downregulates GABAergic inhibition in hippocampal CA1 pyramidal neurones (Clarke *et al.*, 1997; Rodriguez-Moreno *et al.*, 1997).

Finally, glutamatergic pathways from the cerebral cortex to the striatum appear to be involved in the regulation of voluntary motor behaviour. Indeed, there is evidence of the involvement of cortico-striatal, cortico-subthalamic and subthalamic-pallidal/nigral glutamatergic projections in Parkinson's disease (Greenamyre & O'Brien, 1991)

1.4.2 Metabotropic glutamate receptors

Distribution of the metabotropic glutamate receptors

In situ hybridisation and immunohistochemical studies of the rat brain have demonstrated that the mGluRs are expressed in neuronal and glial populations throughout the brain. The receptor subtypes show distinct patterns of distribution with differential expression both regionally and between cell types within a region. The distribution of each group of mGluRs is discussed in turn below.

mGluR1 expression has been demonstrated in many of the target areas of putative glutamatergic projection fibres such as the hippocampus - especially CA2-CA4, striatum, olfactory tubercle, thalamus (except reticular nucleus), substantia nigra, red nucleus, superior colliculus, cochlear nucleus and Purkinje cells of the cerebellum (Shigemoto *et al.*, 1992). mGluR5 are distributed differently from mGluR1 mRNA. They are specifically localised to pyramidal cells throughout the CA1-CA4 and granule cells of the dentate gyrus and Golgi cells in the cerebellum (Abe *et al.*, 1992). Both mGluR1a and mGluR5 are localised at the periphery of postsynaptic densities and therefore respond to concentrations

of glutamate that are sufficiently high to spread away from the central region of the synapse (Baude *et al.*, 1993; Shigemoto *et al.*, 1996).

Studies have revealed that mGluR2 are essentially localised to the main and accessory olfactory bulb, cerebral cortices (particularly in the entorhinal cortex), striatum, molecular layers of the hippocampus and dentate gyrus, mammillary body, medial habenular nucleus, thalamic (reticular, anterior and midline) nuclei and cerebellar Golgi neurones (Ohishi *et al.*, 1993a & b, 1994; Hayashi *et al.*, 1993; Neki *et al.*, 1996a & b; Petralia *et al.*, 1996). Through these studies, there is evidence to suggest that mGluR2 are located presynaptically at perforant and mossy fibres of the hippocampus, as well as postsynaptically. Additionally they appear to be discretely localised to presynaptic terminals of GABAergic granule cells. The localisation of mGluR3 reveal that they are distributed more widely in forebrain neurones and glia. They are prominently expressed in neurones in the cerebral cortex, reticular thalamic nucleus, striatum, caudate putamen, dentate gyrus and in glial cells throughout the brain (Tanabe *et al.*, 1993; Petralia *et al.*, 1996). Moderate expression of mGluR3 are also seen in the superficial layer of the superior colliculus, lateral amygdaloid nucleus and Golgi cells of the cerebellum (Ohishi *et al.*, 1993b). mGluR3 are also distributed in white matter where they are expressed in oligodendrocytes. In contrast to mGluR2, they are only weakly expressed in the olfactory bulb. A recent *in vitro* binding study was able to characterise rat mGluR2 and mGluR3 more selectively with the group II specific agonist LY354740 (Schaffhauser *et al.*, 1998). They found that the distribution of binding sites for [^{3}H]LY354740 in sections of rat brain correlated well with mGluR2 over mGluR3 when compared to previous immunohistochemical or *in situ* hybridisation studies. In particular, the highest density of binding was seen in the anteroventral thalamic nuclei, cerebellar granule layer, retrosplenial cortex and in the molecular layer of the hippocampus.

Of the group III receptors, *in situ* hybridisation studies have shown that mGluR8 mRNA expression is seen in the main olfactory bulb of the mouse and that they are located presynaptically (Kinoshita *et al.*, 1996a). Of the remaining receptors, mGluR4 is most intensely expressed in the cerebellar granule cells (especially mGluR4a) and are thought to act as autoreceptors on axon terminals of parallel fibres (Kinoshita *et al.*, 1996b). They are also found in the superficial layers of the entorhinal cortex, mammillary body and thalamic nuclei. The distribution of mGluR7 mRNA in the rat brain has been shown to be more widely distributed than mGluR4 mRNA (Ohishi *et al.*, 1995). They are present on axon terminals of the mitral/tufted cell in the main olfactory bulb, cortical regions, CA1 and 3 of the hippocampus, granule cells of the dentate gyrus and locus coeruleus. They are also expressed in the regions displaying mGluR4 mRNA mentioned above. The mGluR6 is unique among glutamate receptors and displays the most restricted expression of all the mGluRs. This receptor appears to be exclusively expressed at an appreciable level in the inner layer of the retina, at ON-bipolar cells (Nakajima *et al.*, 1993). Moreover, it appears that this receptor is the only example of a G-protein coupled receptor responsible for fast synaptic transmission in the CNS (Nakanishi, 1994).

Within any brain region, differential expression of receptor subtypes is also seen. For example, *in situ* hybridisation has revealed that the most dominant subtypes in the CA1 of the hippocampus are mGluR5 and mGluR7 on neurones and apical dendrites, while mGluR1 are found in abundance on the stratum oriens. In the CA2 region, mGluR4 and mGluR7 are widely expressed and the CA3 expresses mGluR1, mGluR5 and mGluR7 on neurones with a lower amount of mGluR2. mGluR4 are seen to be located presynaptically on mossy fibre terminals. Also in the cerebellum there is prominent expression of three subtypes; mGluR1 are found predominantly in Purkinje cells, mGluR2 in Golgi cells, while mGluR4 are seen in the granule cells. In addition, within the cerebellum, two separate populations of Golgi cells

have been demonstrated. The majority of cells contain mGluR2 and are segregated from Golgi cells possessing mGluR5. No cells were demonstrated to show mGluR2 and mGluR5 simultaneously (Ohishi *et al.*, 1993a, 1994, 1995; Neki *et al.*, 1996b). This precise segregation of the mGluRs seems to suggest that the individual subtypes have specialised functions.

mGluR mediated responses

As the mGluRs couple to second messenger systems, they could conceivably affect many aspects of cell function. They have been shown to modulate voltage-dependent and voltage-independent ion channel function, increasing or decreasing excitability along with potentiating or inhibiting synaptic transmission.

Potassium channels are common targets for modulation by mGluRs which can result in a dramatic increase in cell excitability, attributed to mGluR1 and mGluR5 (Davies *et al.*, 1995; Gereau & Conn, 1995b), or an inhibitory effect, due possibly to group I or II receptors (Rainnie *et al.*, 1994). The receptors are capable of exerting direct excitatory effects on neurones by activating non-selective cation channels including the Na^+/Ca^{2+} exchanger, and the activation of a Ca^{2+}- activated non-specific cation current (Crépel *et al.*, 1994; McBain *et al.*, 1994). There is also some evidence to suggest that mGluRs may couple to cation channels by a G-protein independent mechanism (Zheng *et al.*, 1995). The activation of mGluR are thought to reduce currents through the various voltage-dependent calcium channels. Inhibition of N-type currents in cortical neurones are likely to be mediated by both group I and II mGluRs (Choi & Lovinger, 1996), while group II mGluRs mediate the inhibition of Ca^{2+} channels in cultured granule cells (Chavis *et al.*, 1995).

Glutamatergic circuits can be modulated through the activation of mGluRs. The mGluRs provide a mechanism by which glutamate can modulate or fine-tune activity at the

same synapses at which it elicits fast synaptic responses. One of the most prominent physiologic effects of mGluR agonists throughout the CNS is the reduction of transmission at glutamatergic synapses. This is typically mediated by the presynaptic mGluRs that serve as autoreceptors to reduce glutamate release. mGluRs of all three groups can act as autoreceptors in different brain regions. In the adult hippocampal CA1, the autoreceptors were revealed to be group I and III mGluRs, most likely the mGluR5 and mGluR7 subtypes (Gereau & Conn 1995a & b; Manzoni & Bockaert, 1995). Other examples of autoreceptors can be found at the mossy fibre synapses (group II and III involvement) and cortico-striatal synapses (group II) (Manzoni *et al.*, 1995; Lovinger & McCool, 1995).

The mechanisms by which autoreceptors regulate glutamate release from presynaptic terminals is not clear. One mechanism could result from the reduction of voltage-sensitive calcium currents (VSCCs). Alternative mechanisms could be due to the direct modulation of presynaptic Ca^{2+} currents that trigger exocytosis, or modulation of the exocytotic machinery itself, or the activation of presynaptic potassium currents. Evidence exists for these mechanisms. For example, 1S, 3R-ACPD was found to reduce transmission at excitatory synapses in the visual cortex, and this effect was blocked by the K^+ channel blocker 4-aminopyridine (Sladeczek *et al.*, 1993). However, more recent work has revealed that transmitter release is through direct modulation of the Ca^{2+} current (Takahashi *et al.*, 1996).

A novel mechanism by which mGluR activation can reduce transmission at glutamatergic synapses in the hippocampus has been discovered in recent years. Winder & Conn (1996) concluded that co-activation of mGluRs and β-adrenergic receptors leads to an increase in cAMP which results in the activation of presynaptic adenosine receptors at the Schaffer collateral terminals. However, this response was found to be initiated in glia (accumulation of cAMP) rather than in neurones. Thus, the group II mGluRs (most

probably mGluR3) located on glia are involved in a novel form of glial-neuronal communication and could be pivotal in regulating synaptic transmission in the hippocampus when noradrenergic inputs are active. In contrast, presynaptic mGluR activation can increase glutamate release under certain conditions. This has been seen when mGluRs are activated in the presence of arachidonic acid (Herrero *et al.*, 1992; Collins & Davies, 1993). Increased glutamate release has been demonstrated at the Schaffer collateral-CA1 synapse where autoreceptors are also present. Thus it seems the potentiation of glutamate release, which occurs when mGluRs are activated in the presence of arachidonic acid, is sufficient to overcome the autoreceptor mediated depression of transmission at this synapse.

As well as serving as autoreceptors, mGluRs can serve as presynaptic heteroceptors at GABAergic synapses, reducing GABA release and inhibitory synaptic transmission. Again, it seems that members of all three groups are capable of this function. Of the brain regions studied, group II mGluRs can reduce transmission at inhibitory synapses in the accessory olfactory bulb and thalamus (Salt & Eaton, 1995; Hayashi *et al.*, 1993). This property has also been seen for group I and group III mGluRs in the CA1 area of the hippocampus and thalamus respectively (Gereau & Conn, 1995a; Salt & Eaton, 1995). Another role of the mGluRs is their ability to regulate excitatory and inhibitory transmission by modulating the currents through the glutamate and GABA receptor channels. They have been demonstrated to potentiate and reduce currents through both NMDA and non-NMDA receptors. This action is highly variable in different cell populations and suggests unique roles for mGluRs in regulating synaptic transmission in different brain regions (Bleakman *et al.*, 1992; Cerne & Randic, 1992; Colwell & Levine, 1994).

There is now increasing evidence for the specific subcellular localisation of mGluRs on neurones and synaptic terminals (Pin & Duvoisin, 1995). Group I receptors are generally located at postsynaptic sites, whereas group II and III receptors can occur at both

presynaptic and postsynaptic sites. More specifically, it appears that functional receptors can be found located at the periphery of synapses. The mGluR1a receptors are thought to be localised at the periphery of the post-synaptic membrane (Baude *et al.*, 1993), unlike the iGluRs which occupy the 'core' of the synapse. Also, mGluR2 has been shown to be located pre-terminally on axonal processes and in the rat hippocampus, and presynaptic mGluR7 is located within the synaptic grid where vesicle docking and exocytosis takes place (Shigemoto *et al.*, 1996). Thus, they are only expected to be activated by excessive amounts of glutamate such as that released during synaptic hyperactivity and not during normal synaptic transmission. Indeed, recent work by Scanziani *et al.* (1997) has provided evidence for this at hippocampal mossy fibre synapses in the guinea pig. Using mGluR antagonists MCPG (α-methyl-4-carboxy-phenylglycine) and MCCG (2S, 3S, 4S)-methyl-2-(carboxycyclopropyl)-glycine) to block the receptors, synaptic responses were measured at two different frequencies. It was shown that the antagonist increased the amplitude of synaptic responses during a 1 Hz train, but not during the control 0.05 Hz stimulation. This indicated that the modulation was mediated by mGluR2 and that they were activated only during the higher frequency stimulation. Thus, as mGluR agonists are known to depress transmission at mossy fibre synapses, the removal of the block resulted in a rapid inhibition of transmitter release. This use-dependent activation of presynaptic mGluRs represents a negative feedback mechanism for controlling the strength of synaptic transmission.

The group I receptors mGluR1 and mGluR5 have been shown to exhibit distinct intracellular calcium responses in transfected cells. Electrophysiological studies have demonstrated that glutamate evokes a single-peaked, non-oscillatory $[Ca^{2+}]_i$ in mGluR1 expressing cells and oscillatory $[Ca^{2+}]_i$ response in mGluR5 expressing cells (Kawabata *et al.*, 1996). This is thought to result from a single amino acid substitution at the G protein interacting carboxy-terminal domain and that the oscillatory response is determined by a
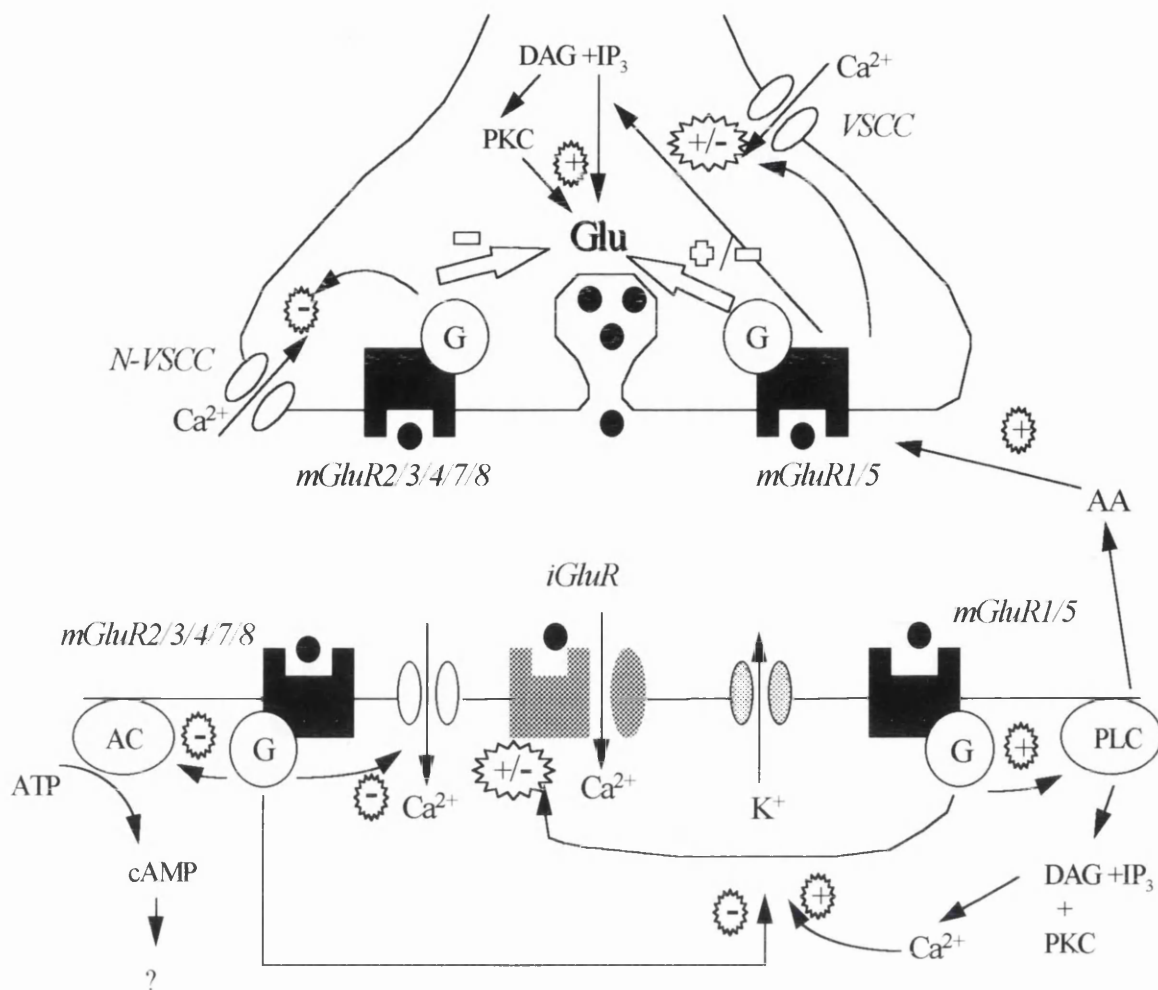
Figure 1.6   Schematic view of the putative roles of mGluRs at glutamatergic synapses.

Presynaptically, mGluRs may potentiate the release of glutamate by activating protein kinase C (PKC) or by potentiating the activity of the calcium channels. They may also inhibit the release of glutamate by inhibiting N-type voltage sensitive calcium channels (VSCCs). Arachidonic acid (AA) can act as a retrograde messenger after being released by diacylglycerol (DAG) and act on group I mGluRs to enhance glutamate release. Postsynaptically, mGluRs can modulate the activity of NMDA and AMPA receptors, different potassium channels (calcium activated, inward rectifier channel), and VSCCs. G = G protein; IP_3 = inositol 1,4,5-trisphosphate; PLC = phospholipase C.

specific PKC phosphorylation at the threonine residue of mGluR5 (Kawabata et al., 1996). Thus, the two closely related mGluR subtypes mediate diverging intracellular signalling in glutamate transmission (Nakanishi et al., 1998). This again hints at specialised functions for the different receptors.

Physiological roles of the metabotropic glutamate receptors

As a consequence of the discovery of better agonists and antagonists, and the development of gene-knockout techniques, the mGluRs have been shown to be involved in many brain functions.

A substantial body of evidence indicates that mGluRs also have important roles in development and plasticity. For example, in development, the peak of excitatory amino acid stimulated PI hydrolysis is seen between 6 and 12 days of age in neonatal rats and this correlates well with periods of intense synaptogenesis (Palmer *et al.*, 1990). Their involvement in memory and learning is provided by studies of synaptic plasticity.

Receptors such as mGluRs that are capable of enhancing NMDA receptor activity and increase the intracellular Ca^{2+} concentration are expected to facilitate the induction of LTP, or even to induce LTP, as experiments have shown that hippocampal long-term potentiation requires the influx of Ca^{2+} through receptors and additional activation of PLC and AC dependent signal cascades (Blitzer *et al.*, 1995; Collingridge & Bliss, 1995). Moreover, an increase in the levels of IP_3 is also thought to be important in LTP since it can release Ca^{2+} from internal stores. Indeed, studies suggested that NMDA receptor activation appeared not to be sufficient to induce LTP. Several reports have demonstrated that NMDA-dependent LTP in the hippocampus requires the activation of mGluRs *in vivo* (Bashir *et al.*, 1993; Manahan-Vaughan & Reymann, 1996; Manahan-Vaughan *et al.*, 1996). Of the 8 cloned mGluRs, receptors of group I have been implicated most strongly in

LTP (Pin & Duvoisin, 1995). Early reports yielded conflicting results. The potentiation of NMDA/AMPA mediated currents have been described in which a broad-spectrum mGluR ligand was used to induce LTP in CA1 and CA3 of the hippocampus, but these results were not reproduced by others (Chinestra *et al.*, 1993; Manzoni *et al.*, 1994). Experiments in 'knock-out' mice have provided evidence for the involvement of mGluRs in LTP. Independent groups have found that in these animals LTP is reduced, but with ambiguous results (Conquet *et al.*, 1994; Aiba *et al.*, 1994).

Evidence for the role of the group I subtypes in LTP and memory is beginning to be elucidated from studies using gene-targeting techniques. Recent work with mutant mice that express no mGluR5 but normal levels of the other glutamate receptors suggest mGluR5 plays a regulatory role in NMDA receptor dependent LTP, such as that seen in the CA1 region and dentate gyrus of the hippocampus (Lu *et al.*, 1997). Consistent with this, they found that LTP remained intact in the mossy fibre synapses on the CA3 region which is an NMDA receptor independent pathway. Behaviourally, the mutant mice were also impaired in two different spatial learning tasks which are known to depend on an intact hippocampus - the water maze and contextual fear conditioning (Morris, 1981; Philips & LeDoux, 1992). In contrast, previous studies using a mutated mGluR1 gene revealed that LTP was impaired in the NMDA-independent pathways in the hippocampus (mossy fibre synapses of the CA3) (Aiba *et al.*, 1994).

Behaviourally, the impairment of spatial memory has been observed after MCPG (non selective mGluR antagonist) injection in the hippocampus, i.c.v injection of 1S, 3R-ACPD, and in mGluR1 knock-out mice (Riedel *et al.*, 1994; Conquet *et al.*, 1994; Aiba *et al.*, 1994; Pettit *et al.*, 1994). Spatial memory acquisition, which is believed to be hippocampus dependent, requires the modulation of mGluRs as the blockade of these receptors during learning causes amnesia (Riedel & Reymann, 1996). Also, it was observed

that the effect of blockade of mGluRs is limited to a time window during and shortly after the acquisition learning as blocking the receptors hours after the learning event does not interfere with memory formation nor memory recall (Riedel & Reymann, 1996).

In the cerebellum, long-term depression (LTD) of parallel fibre Purkinje cell synapses is a well defined phenomenon. A role for PLC-coupled mGluRs, especially mGluR1 which is highly expressed in Purkinje cells, has been suggested here (Linden, 1994). It is thought to arise from the co-activation of AMPA and mGluR receptors together with an increase in the concentration of intracellular Ca^{2+} induced by Purkinje depolarisation.

The activation of mGluRs also appears to be important for NMDA-independent LTP, such as VSCC-dependent LTP (Little et al., 1995). Recent work has demonstrated that the group I antagonists MCPG and 4-CPG were effective at blocking both NMDA and VSCC-dependent LTP (Manahan-Vaughan et al., 1998). As both forms of LTP activate multiple second messenger pathways, it is thought that these two forms of LTP share some common induction pathways which involve mGluRs.

The involvement of group II receptors in LTP has also been studied. Behnisch et al. (1998) provided evidence that while mGluR2 and mGluR3 are not essential for the induction of long term potentiation in the CA1 region of the hippocampus, they may be involved in feedback mechanisms in long-term potentiation. Group II receptors are thought important in other forms of learning. For example, mGluR2 are predominantly expressed presynaptically on granule cells of the accessory olfactory bulb. Activation of these receptors leads to the suppression of GABAergic inhibition and the enhancement of olfactory memory (Kaba et al., 1994).

LTD (long term depression), like LTP is also thought to be a fundamental process involved in learning and memory (Bliss & Collingridge, 1993). In the hippocampus,

repetitive low frequency stimulation can reverse LTP by a process known as depotentiation (Barrionuevo *et al.*, 1980). A similar type of homosynaptic depression can also be induced without first inducing LTP known as homosynaptic LTD (Dudek & Bear, 1992). Given the widespread expression of mGluR2 presynaptically on mossy fibres the role of these receptors was explored in synaptic plasticity in CA3 by targeted disruption of the mGluR2 gene (Yokoi *et al.*, 1996). It was demonstrated that LTP induced by tetanus was not impaired, but homosynaptic LTD induced by low frequency stimulation was almost totally abolished. However, the mutants performed normally in water maze learning tasks.

It is speculated that the role mGluRs play in the participation of memory formation is to modulate the signal-to-noise ratio of the CNS; that is, they set a ratio in order to filter out unimportant information and amplify important information. Under normal conditions, spontaneous neuronal activity is supposed to constitute a 'noise'. During a particular learning event, activation of mGluRs might produce a signal, and this increase in the signal-to-noise ratio is transformed into memory. Blockade of group I mGluRs by MCPG for example, prevents the changes in the signal-to-noise ratio and thus leads to amnesia. Other mGluRs might reduce the noise and generate signals. Stimulation of group II or III mGluRs may depress excitation due to the inhibition of voltage-activated Ca^{2+} channels or the presynaptic reduction of transmitter release (Glaum & Miller, 1993).

The mechanisms involved in the induction and early expression of LTP are currently extensively studied. Less is known about the maintenance of LTP which appears to be critically dependent on protein synthesis and mRNA synthesis. Study into LTP maintenance has led to the hypothesis that the induction of LTP is associated with the setting of a 'synaptic tag' at activated synapses whose role is to sequester plasticity-related proteins that go on to serve to stabilise temporary synaptic changes and extend their persistence (Frey &

Morris, 1998). It has been speculated that the presently unknown identity of the tag may interact with mGluRs and aid in the sequestration of proteins.

With the exclusive localisation of mGluR6 in the retina, the mGluRs have an important role in visual transmission (Nomura *et al.*, 1994). Electrophysiological evidence indicates that mGluR6 mediates postsynaptic responses on ON-bipolar cells (i.e. excitation of ON pathway following light exposure) by enhancing cGMP hydrolysis, analogous to that of signal transduction in photoreceptors (Nawy & Jahr, 1990).The mGluRs have also been demonstrated to be involved in the central control of cardiac activity (Pawloski-Dahm & Gordon, 1992). The microinjection of 1SR,3RS-ACPD into the nucleus tractus solatarius was demonstrated to induce cardiovascular responses that mimic the baroreflex response (e.g. hypotension and bradycardia). It is believed that mGluRs could provide novel centrally acting agents for the treatment of high blood pressure (Pawloski-Dahm & Gordon, 1992).

1.5   Glutamate and neurodegeneration

In addition to being crucially involved in physiological circumstances, glutamate also appears to be involved in acute and chronic neurological disorders. Knowledge that glutamate was toxic to neurones dates back to 1957 (Lucas & Newhouse). It was not until 14 years later that the investigation of the action of glutamate and glutamate analogues led to the hypothesis of excitotoxicity (Olney *et al,.* 1971) and the concept that the excessive activation of glutamate receptors can mediate neuronal degeneration and cell death (Olney, 1969). Support for the excitotoxicity hypothesis grew when the neuronal pathology induced by glutamate and glutamate analogues were revealed to be similar to that associated with a wide range of neurological insults such as ischaemia and epilepsy (Rothman, 1984; Auer *et al.*, 1984; Olney *et al.*, 1986). In accordance with this, a massive release of glutamate as

well as other neurotransmitters (e.g. aspartate, GABA, glycine) was demonstrated during and following experimental ischaemia models (Benveniste *et al.*, 1984; Globus *et al.*, 1988; Andine *et al.*, 1991; Mitani & Kataoka, 1991). Although glutamate is also believed to be involved in several forms of chronic neuronal degeneration, such as Alzheimer's disease or Huntingdon's disease (Meldrum & Garthwaite, 1990; Beal, 1992). The literature concerning chronic degeneration is not reviewed because the focus of the thesis was on acute excitotoxicity associated with ischaemia.

The question of the mechanisms of glutamate neurotoxicity has since been addressed both *in vitro* and *in vivo* by the development of models of cerebral ischaemia (Choi, 1988; Macrae, 1992; McAuley, 1995). There are several main types of *in vivo* ischaemia models, grouped into global and focal models (transient and permanent and partial and complete). Global models have often been stated to be models of cardiac arrest producing selective cell death, while focal models are said to be of greater relevance to acute ischaemic stroke producing brain infarction (Macrae, 1992). Focal ischaemia differs in a variety of ways from global ischaemia. A major difference is that focal ischaemia has a dense core of ischaemic tissue that is destined to die, together with a therapeutically susceptible zone at the periphery of the lesion called the penumbra, where the potential for collaterization exists (Ginsberg & Pulsinelli, 1994). Models in which the middle cerebral artery (MCA) of the rat is occluded are extensively used to study focal cerebral ischaemia because of their relevance to the human clinical setting as this vessel is most often occluded in man (Mohr *et al.*, 1986). In addition, the rat is the species of choice not only because of economical considerations but also because the cranial circulation in the rat is proposed to be similar to that in humans (Yamori *et al.*, 1976), especially when compared with other species such as the cat, dog and gerbil.

Of the numerous models of focal ischaemia (for review of models see Macrae, 1992; McAuley, 1995), the subtemporal approach with diathermy originally described by Tamura and co-workers (1981) has emerged as the standard method of MCA occlusion. The MCA is electrocoagulated proximal to the origin of the lateral lenticulostriate artery and results in the severe reduction in cerebral blood flow (<25ml/100g/minutes) within the territory of the MCA known as the ischaemic core (cortex, caudate putamen, globus pallidus, regions of the internal capsule and adjacent white matter) with blood flow reduced to a lesser degree (20-25% normal flow) at the penumbra (Hossman, 1994). The ischaemic penumbra disappears as the duration of the ischaemia increases and after a certain time will no longer be receptive to therapeutic intervention. Certain factors can complicate the outcome of the ischaemic insult and have to be taken into consideration. These include the animal species, strain, sex, age, nature of the ischaemia (global/focal, temporary/permanent), physiological variables such as temperature and blood pressure. Consequently, some neuroprotection studies have reported conflicting results.

In vitro models of ischaemia and neurotoxicity have been developed and used successfully to provide valuable information about the cellular mechanisms of injury not possible *in vivo*. For example, *in vitro* ischaemia is generated by severe energy depletion, either by the direct removal of vital substrates, or by a pharmacological intervention such as Iodoacetate, an inhibitor of glycolysis (Goldberg *et al.*, 1997). The direct removal of the energy substrates oxygen and glucose is usually preferred, as it avoids problems associated with metabolic inhibitors such as the difficult removal of the agents from cells. It has been demonstrated that when neuronal cultures are deprived of both oxygen and glucose, they are killed approximately 10-fold more rapidly than in the absence of either oxygen or glucose alone (Goldberg *et al.*, 1997). The cell death seen following an acute insult such as hypoxia and hypoglycaemia is characterised by cell body swelling, early membrane lysis and

random DNA breakage and is generally categorised as necrosis. Recently, increased attention has been focused on neuronal apoptosis (marked by cell body shrinkage, membrane blebbing, chromatin condensation and internucleosomal fragmentation of cellular DNA) because of suggestions that it may contribute to neuronal loss in certain disease states, including hypoxia/hypoglycaemia and neurodegenerative diseases (Linnik *et al.*, 1993). Staurosporine-induced cell death is considered to be mediated primarily through the activation of apoptotic pathways (Koh *et al.*, 1995). Staurosporine acts as a broad spectrum inhibitor of cAMP-dependent protein kinase, Ca^{2+}-calmodulin kinase type II, tyrosine kinases and protein kinase C. Previous studies have demonstrated the ability of staurosporine to induce apoptosis in non-neuronal cell types and in cells of the CNS (Koh *et al.*, 1994).

1.5.1 Ionotropic glutamate receptors and mechanisms of excitotoxicity

The exact mechanisms that lead to cell death are still unclear but it is well recognised that Ca^{2+} plays a critical role. In 1977, Nicholson *et al.* demonstrated that anoxia triggered the rapid translocation of Ca^{2+} from extracellular to intracellular spaces of cerebellar tissues. This and subsequent work led to the hypothesis of calcium-mediated cell death in ischaemia, hypoxia, hypoglycaemia and status epilepticus (Siesjö, 1981). It was originally assumed that only certain populations of neurones with high densities of calcium channels were vulnerable to these insults. However, an important step forward was made when the subsequent work of Choi (1987) demonstrated that cultured neurones exposed to glutamate showed a delayed cell death that was calcium mediated, and that removal of extracellular calcium protected the neurones. The conclusion drawn was that the excitotoxic hypothesis and the calcium hypothesis of cell death were intimately linked.

Much of the interest in mechanisms of neurotoxicity has been focused on the NMDA receptor, reflecting its high Ca^{2+} permeability and it's ability to mediate abnormal rises in intracellular Ca^{2+}. Much evidence also exists for the involvement of non-NMDA receptors in pathological processes because of their appreciable Ca^{2+} permeability. AMPA receptors lacking the GluR2 subunit may play a role in the vulnerability of hippocampal neurones to ischaemic injury. Thus Pellegrini-Giampietro *et al.* (1992) reported that transient global forebrain ischaemia induced a selective decrease in GluR2 mRNA levels in the hippocampus and this preceded any histological signs of cell damage. This would lead to the increased formation of Ca^{2+}-permeable AMPA receptors. The hypothesis predicts that Ca^{2+} entry through GluR2-lacking AMPA receptors in neurones that normally express Ca^{2+}-impermeable channels contributes to the delayed cell death seen in global ischaemia because such channels do not intrinsically have any compensatory mechanisms for Ca^{2+} buffering (Pellegrini-Giampietro *et al.*, 1997).

Under normal physiological conditions, calcium fluxes are tightly regulated by means of the $3Na^{+}$-Ca^{2+} exchange and by an ATP regulated Ca^{2+}-$2H^{+}$ exchanger (Blaustein, 1988; Carafoli, 1987). In order to maintain calcium homeostasis, mechanisms must also exist for terminating both glutamate and calcium transients. These include the re-uptake of glutamate through an electrogenic Na^{+}/glutamate symporter, ATP-dependent Ca^{2+} pumps in the endoplasmic reticulum (ER), reuptake by glia, Ca^{2+}- or ATP-dependent K^{+} channels and GABA-activated Cl^{-} channels (Attwell & Mobbs, 1994; Pellerin & Magistretti, 1994; Kennedy, 1989; Erecinska & Silver, 1994). Thus with the concentration of intracellular calcium maintained, $[Ca^{2+}]_i$ is only seen to rise transiently during cell activation. For example, glutamate (AMPA) receptor activation results in the passage of Na^{+} into the cell, which in turn leads to the depolarisation of the postsynaptic membrane. The depolarisation has two possible effects; 1) it relieves the Mg^{2+} block of the calcium permeable channel

gated by the NMDA receptor and 2) it opens voltage-sensitive calcium channels (VSCCs). In addition, there may be mobilisation of intracellular calcium stores following mGluR mediated activation of IP_3 and Ca^{2+}-permeable AMPA receptors. Therefore, elevations in $[Ca^{2+}]_i$ can be induced by a number of pathways.

The prolonged elevations of $[Ca^{2+}]_i$ that follow pathological insults such as ischaemia can damage neurones in many ways. In ischaemia, the reduction in blood flow causes a decline in ATP levels and leads to the failure of the Na^+/K^+ pump, which in turn results in depolarisation and the activation of glutamate receptors. The depolarisation leads to the opening of VSCC and calcium influx into the cell. The increase in intracellular calcium also causes a release of glutamate that results in the prolonged exposure of post-synaptic receptors to glutamate and to further influx of Na^+ and Ca^{2+} ions. Re-uptake of glutamate becomes impaired through the suppression of ATP levels and this can lead to non-vesicular release of glutamate. This results in the accumulation of intracellular calcium in neurones followed by the destabilisation of the ATP-driven Ca^{2+}-2H exchanger. It can also result in the reversal of the Na^+/Ca^{2+} exchanger due to the Na^+ influx through voltage-gated channels and also as a result of activating AMPA receptors. While levels of free calcium within a cell are very low (0.1μmol/L), the total cell calcium content is about 10 000 times higher and calcium is found bound to proteins or phospholipids, or sequestered into the ER, calciosomes and mitochondria. It is clear that the cell contains enough calcium to substantially increase $[Ca^{2+}]_i$ if it becomes released into the cytosol or displaced from its binding sites. Calcium can also be released by PLC-coupled events, mediated by receptors. Furthermore, the re-sequestration of calcium back into the ER requires ATP (Kristián & Siesjö, 1998). Increasing levels of calcium eventually activate immediate early genes and proteases such as calpains, which lead to the destruction of cytoskeletal components (Siman & Noszek, 1988) and also activation of phospholipases and endonucleases leading to the

membrane damage and DNA fragmentation. Calcium also affects the activity of protein kinases (e.g. PKC, PKA), phosphatases, and activates enzymes that give rise to the production of reactive oxygen species such as hydrogen peroxide (H_2O_2), the superoxide anion (O_2^-), and nitric oxide (NO) (Tymianski & Tator, 1996; Choi, 1988) which in turn can modulate $[Ca^{2+}]_i$ directly (Siesjö et al., 1994).

The mechanism described above is a well recognised scheme implicated in excitotoxicity. However, in recent years, research interests have focused on calcium metabolism of the mitochondria. It is well known that calcium accumulation leads to mitochondrial damage (Nicholls, 1985). It is assumed that following an insult of limited duration, a sustained perturbation of cell calcium metabolism leads to a slow gradual rise in $[Ca^{2+}]_i$ (Deshpande et al., 1987). The rise in calcium eventually exceeds a 'set point' for calcium sequestration in the mitochondria, and they start to accumulate calcium until they are overloaded and become dysfunctional (Martins et al., 1988). The damage triggered was originally thought to indicate the activation of mitochondrial phospholipase A_2 (PLA$_2$) which broke down the lipid backbone of the inner mitochondrial membrane to produce a non-specific increase in mitochondrial membrane permeability (Gunter & Pfeiffer, 1990). Recent evidence suggests that the increase in permeability involves the assembly of a proteinaceous pore - the MPT (mitochondrial permeability transition) pore which allows the passage of ions and molecules (Gunter & Pfeiffer, 1990; Zoratti & Szabó, 1995; Duchen et al., 1993; Bernardi & Petronilli, 1996).

The neuropathological state that has been described following the exposure of neurones to glutamate, or a glutamate analogue, is one of cellular swelling - in particular swelling of the mitochondria. This has been causally linked with chloride influx (Rothman, 1985), but the swelling process is now thought to reflect the assembly of an MPT pore in the inner mitochondrial membrane which allows the release of Ca^{2+} and Mg^{2+} along with

other compounds. A consequence of this is the abrupt production of reactive oxygen species. MPT pore formation is triggered by a number of factors, but is thought to occur principally as a result of oxidative stress and calcium accumulation (Duchen *et al.*, 1993; Crompton *et al.*, 1988; Richter *et al.*, 1995). Studies *in vitro* have demonstrated that cyclosporin A inhibits the MPT pore (Zoratti & Szabó, 1995). While *in vivo*, it was discovered that cyclosporin A, provided it could pass the blood-brain barrier, dramatically reduces CA1 damage following a brief forebrain ischaemia (Uchino *et al.*, 1995). However, these results have to be interpreted with caution as cyclosporin can produce other effects (e.g. immunosuppression, modulation of NO production). Of the reactive oxygen species produced following an increase in $[Ca^{2+}]_i$, NO and peroxynitrite predispose to an MPT pore and could potentially act as triggers of a pore opening in partially calcium loaded mitochondria (Schweizer & Richter, 1994; Packer & Murphy, 1995).

A second hypothesis involves the synthesis of the respiratory complexes in the mitochondria (Abe *et al.*, 1995). Briefly, the enzymes (i.e. the respiratory complexes) required to allow the passage of electrons along the respiratory chain and extrude H^+ are encoded for by mitochondrial and nuclear DNA. For this process, the mitochondria must therefore be transported to the nucleus along the cytoskeletal elements, such as dynorphin and kinesin. The suggestion put forward is that this process grinds to a halt when the cytoskeleton is broken down by calcium activated proteases and calcium-dependent disassembly of the microtubules (Siman *et al.*, 1996). This would result in reduced activities of the mitochondrial enzymes and a subsequent depletion in the generation of ATP.

Free radicals play an important role in excitotoxic and ischaemic processes (Watson & Ginsberg, 1989). Free radicals are produced predominantly in the mitochondria and also in the arachidonic acid cascade of phospholipid metabolism. The production of free radicals leads to lipid peroxidation and degradation of proteins which may subsequently compromise

intracellular calcium regulation (Floyd & Carney, 1992). Thus, free radicals promote the elevation of $[Ca^{2+}]_i$, which in turn increases free radical production by mechanisms involving the production of arachidonic acid (Sanfeliu et al., 1990; Verity, 1993). The production of the free radical NO is increased in response to increased $[Ca^{2+}]_i$. It has been shown the NOS containing neurones (1-2% of all neurones in the cortex) are resistant to NMDA toxicity (Koh & Choi, 1988; Uemura et al., 1990). Calcium stimulates constitutive nitric oxide synthase (cNOS) through Ca^{2+}-calmodulin which results in the formation of NO. Therefore, the activation of NMDA glutamate receptors can trigger NO synthesis via the associated influx of calcium. NO may be cytotoxic directly by inhibiting enzymes in the mitochondria, resulting in perturbations in energy metabolism and in enzymes involved in DNA synthesis, such as ribonucleotide reductase activity (Dawson et al., 1992; Kwon et al., 1991). A major pathway through which NO mediates cell death is thought to be its interaction with O_2^- anion and the subsequent formation of peroxynitrite ($ONOO^-$) (Beckman et al., 1991; Koppenol et al., 1992). Peroxynitrite also decomposes to other reactive oxygen species thus activating lipid peroxidation. Other studies using knockout mice have identified the specific NOS isoforms important to ischaemic injury. Animals deficient in neuronal NOS (nNOS) appear to be more resistant to ischaemic tissue damage than wild types (Huang et al., 1994). However, the involvement of NO in the pathophysiology of brain injury remains controversial. Studies have also provided evidence that NO is not involved (Demerle-Pallardy et al., 1991). Studies by Lipton et al. (1993) suggest that the dual roles of NO in excitotoxicty may depend upon its redox state. The reduced ion, nitrogen monoxide (NO^-) is thought to be responsible for the neurotoxic action of NO via a reaction with superoxide leading to the formation of peroxynitrite. Conversely, the oxidised nitrosonium ion (NO^+) is believed to react with the redox modulatory site of the NMDA receptor and block neurotransmission.
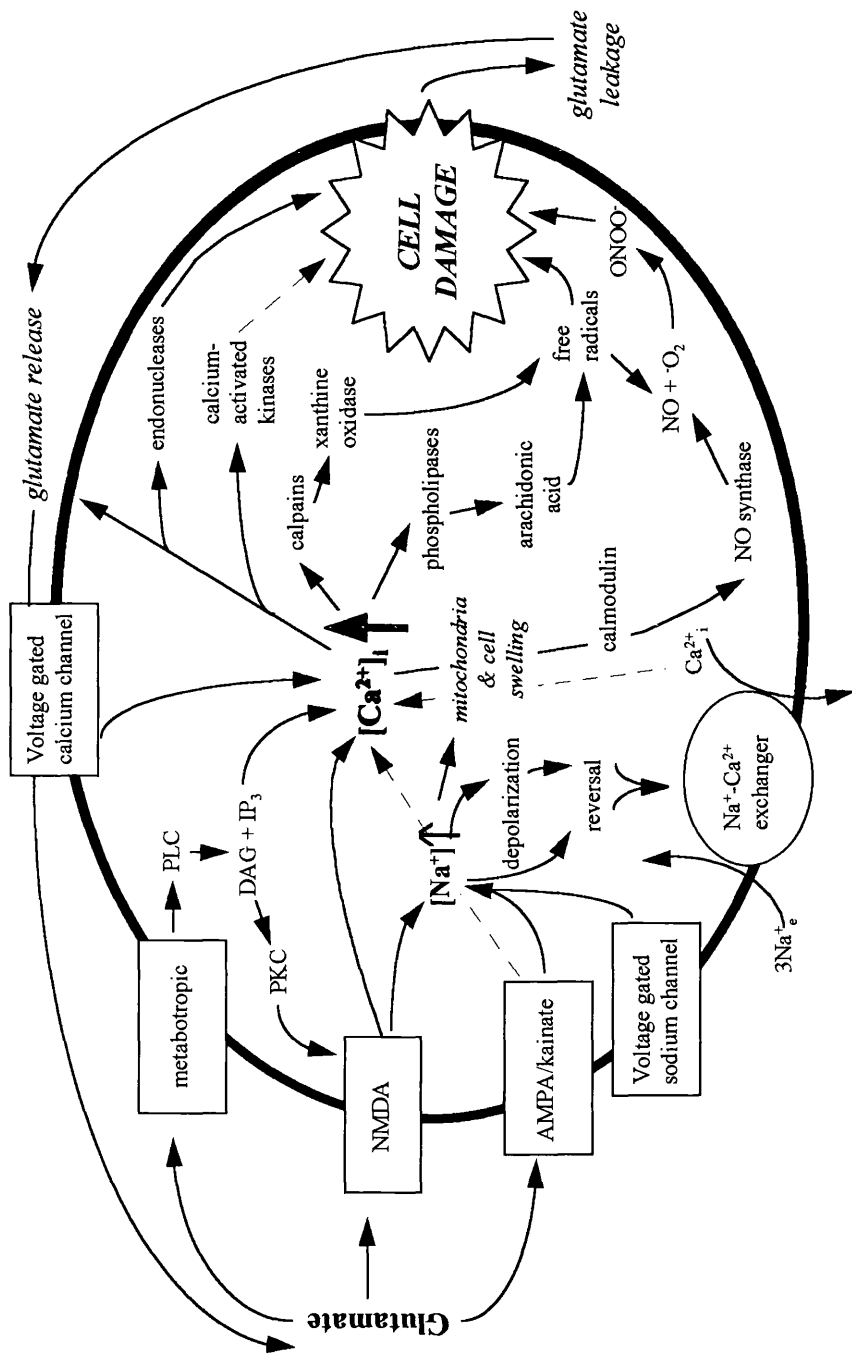
Figure 1.7   Proposed mechanisms by which intracellular calcium may be increased in neurones in glutamate excitotoxicity.

(Adapted from Gill & Lodge 1997)

1.5.2 Existing neuroprotective strategies for glutamate-induced toxicity

In order to effectively treat neurotoxic insults, in this case ischaemia, an appreciation of the mechanisms involved in causing cell damage and death is required. Thus, a number of pharmacological strategies have been proposed as possible mechanisms for attenuating the neurotoxic actions of glutamate and have been studied in models of excitotoxic and ischaemic cell death *in vitro* and in animal models of acute ischaemic stroke.

The post-synaptic manipulation of glutamate receptors has been the most obvious line of consideration. Initial efforts concentrated on NMDA receptor subtypes because of their Ca^{2+} permeability. Functional inhibition of NMDA receptors can be achieved through actions at different sites such as the primary transmitter site, the glycine binding site, polyamine site and PCP site. Glutamate receptor antagonists have been demonstrated to effectively reduce neuronal damage in experimental models of ischaemia and hypoxia. In global ischaemia, NMDA receptor antagonists provide little protection. However, the competitive antagonists CGS19755 and CPP have been shown to provide neuroprotection when given before the ischaemic insult (Boast *et al.*, 1988). NMDA receptor antagonists of all types, for example the non-competitive antagonists MK-801, dextromethorphan, CNS1102 and eliprodil, appear to be effective in providing neuroprotection in models of focal ischaemia (Gotti *et al.*, 1988; Park *et al.*, 1988, 1992; Toulmond *et al.*, 1993). However, inhibition of these different sites can lead to serious side effects and behavioural profiles such as loss of memory, limiting their clinical utility.

AMPA receptors can also be inhibited by both allosteric and competitive antagonists. The potent AMPA antagonist NBQX was a candidate used to examine the role of non-NMDA receptors in ischaemia (Gill & Lodge, 1991), but due to its pharmacokinetics, chemical properties and side effects (such as renal precipitation), it was not developed further. The administration of AMPA receptor antagonists alone or in

combination with NMDA are neuroprotective in models of global ischaemia (Sheardown *et al.*, 1990; Kaku *et al.*, 1991; Mosinger *et al.*, 1991). AMPA antagonists have been shown to provide partial protection against damage induced by global ischaemia when given post-ischaemically (Buchan *et al.*, 1991a; Li & Buchan, 1993). However, in focal ischaemia, AMPA antagonists of both types, e.g. LY293558 and GYKI 52466, also diminish the volume of infarction (Buchan *et al.*, 1991b; Bullock *et al.*, 1994; Gill *et al.*, 1992; Smith & Meldrum, 1992; Degraba *et al.*, 1994). By blocking AMPA receptors, membrane depolarisation is prevented, which in turn will attenuate NMDA receptor activation and voltage-sensitive Ca^{2+} channels, thereby reducing Ca^{2+} entry. AMPA antagonists appear to be more potent neuroprotectants against the delayed neuronal death seen after severe forebrain ischaemia (4 vessel occlusion). A rationale for the neuroprotective effects of AMPA antagonists against delayed neuronal degeneration is the possible alteration in the expression of the receptors after ischaemia. It has been shown that there is a decrease in the expression of GluR2 following severe forebrain ischaemia. As the GluR2 subunit determines the calcium permeability of the AMPA receptors, this would result in increased calcium permeability, and cell damage. The use of AMPA antagonists may inhibit this response. Alternatively, AMPA receptors may become more responsive after ischaemia and are upregulated, as seen during the maintenance phase of LTP (Davies *et al.*, 1989).

In view of the importance of calcium in mediating neuronal damage and death, calcium channel antagonists (compounds that block calcium fluxes through voltage-operated calcium channels) have been investigated for their usefulness in neuroprotection. Initial studies used compounds that had been optimised for their anti-hypertensive properties such as nimodipine (Alps *et al.*, 1988). The results from these calcium antagonists are conflicting. For example, nimodipine has been reported to be neuroprotective in some but not all focal ischaemia studies in the rat, and global ischaemia

models (Bielenberg *et al.*, 1990; Alps *et al.*, 1988). It is thought that the conflicting data may be due to in part the confounding effects of systemic hypotension. The neuronal VSCC antagonist SB201823A which has reduced cardiovascular effects, has been shown to be neuroprotective in both global and focal cerebral ischaemic models (Barone *et al.*, 1995; Ginsberg, 1995). Following on from this, studies have demonstrated that calpain inhibitors (enzyme activated by high levels of intracellular calcium) reduce ischaemic damage and infarct volume in focal ischaemia (Rami & Krieglstein, 1993).

Oxygen free radicals are important in the cascade of cellular events leading to cell death following cerebral ischaemia. By conjugating the enzyme responsible for removing superoxide, superoxide dismutase (SOD), to polyethylene glycol the circulation half-life of SOD can be increased by many hours. Liu *et al.* (1989) demonstrated that this reduced infarct volume in permanent MCA occlusion by around 25%. In addition, compounds that inhibit lipid peroxidation (e.g. tirilizad) also provide neuroprotection in various experimental models (Hall *et al.*, 1994). Nitrone-based free radical traps are also possible strategies for neuroprotection. Using these compounds, free radicals are intercepted and incorporated into the nitrone agents to form a spin adduct that can no longer undergo other reactions. The potential of these agents in cerebral ischaemia arose serendipitously following studies with phenyl-tert-butylnitrone (PBN) with little or no side effects (Carney & Floyd, 1991). Evidence suggests that the action of PBN is not wholly attributable to trapping free radicals. Zhao *et al.* (1994) demonstrated that brain infarct volume was reduced following MCA occlusion, even when administered 3 hours post-ischaemia. Thus it seems that PBN may block neurodegenerative processes initiated by, that are temporally separate from, the post-ischaemic burst of oxyradicals which is most likely thought to be genomic regulation (Hensley *et al.*, 1997).

Another possible approach to the protection of neurones in ischaemia is to modulate Na^+ channels (down-modulate) and K^+ channels (opening of channels). The down regulation of Na^+ channels during periods of limited oxygen supply appears an effective way of reducing energy expenditure because a large proportion of energy consumed by excitable cells is used to maintain the Na^+ and K^+ gradients across the membrane. Cell membranes are selectively permeable to K^+ under physiological conditions and for this reason the activation of K^+ channels opposes depolarisation and thus will reduce membrane excitability and neuronal activity (Suzuki et al., 1995). The down regulation of Na^+ channels remains beneficial even after the ischaemia. Lamotrigine and its derivatives act on Na^+ channels and have been demonstrated to protect against ischaemic damage (Wiard et al., 1995; Smith & Meldrum, 1995). Other agents such as riluzole, lubeluzole (Pratt et al., 1992; De Ryck et al., 1994) are also capable of protecting against ischaemic damage. The transport of L-glutamate may also represent a site at which excitatory transmission may be controlled. More specifically, in the presence of high levels of glutamate, the increased transport of glutamate away from the synaptic cleft could serve as a protective mechanism to prevent excitotoxic damage.

On the basis of the exciting experimental data showing neuroprotection in the various animal models of cerebral ischaemia, a multitude of clinical trials have been carried out in ischaemic stroke patients. However, out of all the studies completed, only the USA trial for the thrombolytic agent recombinant tissue plasminogen activator (rt-PA) has proved successful (Adams et al., 1996).

Presently, there is much interest in secondary neuronal death, such as that seen with CNS inflammatory processes which occur days after an ischaemic insult. An emerging strategy for the treatment of stroke is directed at inflammatory cytokines (Feuerstein et al., 1996). Various experimental studies have implicated roles for several inflammatory

molecules in the pathophysiology of stroke. The dramatic expression of cytokines has been detected after an ischaemic insult. These include tumour necrosis factor-α, TNF-α (Wang *et al.*, 1994), interleukin-1β, IL-1β (Liu *et al.*, 1993), transforming growth factor-β, TGF-β (Wießner *et al.*, 1993) and interleukin-6, IL-6 (Wang *et al.*, 1995), as well as various chemokines. While some cytokine-suppressive drugs have been suggested as a possible therapeutic targets in stroke (Elford *et al.*, 1995; Loddick & Rothwell 1996), recent studies have shown that the production of certain cytokines may be beneficial in limiting neuronal cell death associated with excitotoxicity, such as the TGF-βs (McNeill *et al.*, 1994). The TGF-βs are expressed abundantly in the nervous system and are multifunctional, pleiotropic molecules with major roles in the control of cell differentiation and proliferation, extracellular matrix metabolism, cellular migration and immunosuppression. In addition to the interest in the inflammatory response following ischaemia, it is increasingly recognised that white matter in the CNS is highly vulnerable to cerebral ischaemia (Pantoni *et al.*, 1996) and its protection should be considered alongside that of grey matter. Amyloid precursor protein (APP) is a transmembrane glycoprotein associated with the cytoskeleton. It is ubiquitously expressed in the nervous system and undergoes fast anterograde axonal transport in the peripheral nervous system. Disruption of APP transport is believed to reflect axonal injury; it has been demonstrated to be a sensitive marker of axonal damage in head injury (Blumbergs *et al.*, 1994; Gentleman *et al.*, 1995) and accumulation of APP has been shown as a result of ischaemic insults (Kalaria *et al.*, 1993; Stephenson *et al.*, 1992).

1.6   Emerging roles of metabotropic glutamate receptors in brain pathology

Due to the ubiquitous distribution of mGluRs, they have the potential to participate in a wide variety of functions in the CNS. Because of this, they may also be involved in a

wide range of neurologic and psychiatric disorders. The involvement of mGluRs in pathology was initially suggested when enhancements of excitatory amino acid stimulated PI hydrolysis were demonstrated in brain slice preparations subjected to various stimuli (Iadorola et al., 1986; Nicoletti et al., 1987; Seren et al., 1989).

mGluRs may have a role in chronic neurodegenerative disorders. Recent evidence indicates that mGluRs may be potential drug targets for the therapy of Parkinson's disease (Greenamyre et al., 1994). The activation of mGluRs is also thought to interfere with the pathophysiological events underlying Alzheimer's disease. Activation of recombinant mGluR1a has been shown to increase the release of soluble forms of amyloid precursor protein APP (Lee et al., 1995). This might be accompanied by a reduction in β-amyloid production (Gabuzda et al., 1993). In contrast, apoptosis induced by β-amyloid is substantially reduced by agonists of group II and group III mGluRs (Copani et al., 1995).

Hypothetically, one of the most potential and beneficial effects of mGluR agonists and antagonists is their use in reducing of excitotoxic neuronal damage that occurs after stroke or traumatic brain injury. From the putative mechanisms described above, selective antagonists of mGluRs involved in potentiating responses to the activation of iGluRs could be effective in reducing excitotoxicity, as could agonists at mGluR autoreceptors.

As previously described, the role of ionotropic glutamate receptors in excitotoxic insults such as ischaemia prompted the search for neuroprotective agents. Protecting against excitotoxicity using iGluR antagonist therapy has revealed serious shortcomings, such as compromised fast excitatory synaptic transmission (Ginsberg, 1995). Metabotropic glutamate receptors are possible targets for neurodegenerative disorders as they have the potential to overcome the limitations associated with agents active at ionotropic glutamate receptors. Evidence shows that they are expected to mediate excitatory synaptic transmission only under certain circumstances, such as synaptic hyperactivity (Conn et al.,

1995). Thus, mGluRs could influence both the induction and the progression of neuronal degeneration without hampering the efficiency of fast excitatory synaptic transmission.

When this thesis was first undertaken, interest in the involvement of mGluRs in acute excitotoxicity was still in its infancy due to the absence of good pharmacological tools. Preliminary studies had revealed that NMDA-induced neurotoxicity in cortical cultured cells was attenuated with *trans*-ACPD (active isomer is 1S,3R-ACPD), and that this observation was extended to a mouse model of permanent focal ischaemia (Koh *et al.*, 1991; Chiamulera *et al.*, 1992). However, the local or intracerebroventricular infusion of *trans*-ACPD resulted in the degeneration of striatal and hippocampal neurones (McDonald & Schoepp, 1992), while intrahippocampal injections resulted in limbic seizures and hippocampal cell loss (Sacaan & Schoepp, 1992). The dichotomy in results can be attributed to the fact that *trans*-ACPD has a broad spectrum of activity and is able to activate various mGluR subtypes. This has led to the hypothesis that individual mGluR subtypes can differentially affect the processes associated with neurodegeneration and has resulted in a succession of predominantly *in vitro* studies exploring the roles of mGluRs in excitotoxicity. Studies with the mGluR2/3 selective agonists 2R,4R-APDC and DCG-IV, and group III selective agonists L-AP4 and L-SOP, also demonstrated protective effects against hypoxic- and NMDA-induced excitotoxic neuronal cell death (Bruno *et al.*, 1994; Buisson & Choi, 1995; Buisson *et al.*, 1996). Similarly, *in vivo* studies demonstrated that intraventricular injections of DCG-IV produced anticonvulsive and neuroprotective effects against kainic acid induced excitotoxicity (Miyamoto *et al.*, 1997). Thus it is generally assumed that the activation of group II or III receptors will facilitate neuroprotection by reducing synaptic excitation (Nicoletti *et al.*, 1996).

The situation with group I receptors however is still not entirely clear. It is thought that the activation of mGluR1 or mGluR5 will increase neuronal excitation and excitability,

and therefore exacerbate neuronal damage. Activation of an mGluR coupled to PI hydrolysis could increase calcium levels either by IP_3-mediated release of calcium from intracellular stores, such as the ER, or by DAG activation of PKC leading to the facilitation of calcium currents through NMDA receptors. This is believed to be a consequence of excessive mGluR-mediated potentiation of NMDA currents through the ability of PKC to remove the Mg^{2+} block. Consistent with this idea, Bruno et al., (1995b) demonstrated that agonists selective for group I mGluRs led to the amplification of NMDA-induced neuronal degeneration in cultured cortical cells, and also that the activation of mGluR1 exacerbated post-traumatic neuronal injury (Mukhin et al., 1996). Similarly MCPG, a broad spectrum mGluR antagonist, was shown to protect hippocampal CA1 neurones from hypoxia and hypoglycaemia in vitro (Opitz et al., 1994). In contrast, Ferraguti et al. (1997) provided evidence to suggest that the inactivation of mGluR1 does not prevent excitotoxic neuronal damage following MCA occlusion in the mouse. Again, the apparent contradictory results can now be explained by the involvement of these agents with more than one mGluR subtype. This however does not explain the absence of neuroprotection demonstrated following the targeted gene disruption of mGluR1 (Ferraguti et al., 1997).

Recent studies using the new and selective group I mGluR antagonists, AIDA and LY367385, appear to substantiate the hypothesis that activation of mGluR1 and mGluR5 are detrimental to the CNS (Strasser et al., 1998; Bruno et al., 1999). Neuroprotection may also be subject to the timing of group I mGluR manipulation (Schröder et al., 1999). Although there has been limited in vivo data because of the lack of systemically active, centrally bioavailable, mGluR selective ligands with which to explore the involvement of these receptors in excitotoxicity, the absence of mGluRs in target organs of the autonomic nervous system suggests they should be devoid of major peripheral side effects and mGluRs may be promising drug targets. Recent evidence for the role of group II mGluRs in

excitotoxicity is further discussed in context within the results section of this thesis in chapter 8, section 8.4.

1.7 Imaging cerebral function with [^{14}C]2-deoxyglucose autoradiography

[^{14}C]2-deoxyglucose autoradiography ([^{14}C]2-DG) allows functional activity within the brain to be assessed quantitatively. Through the measurement of local rates of glucose utilisation, this technique permits the visualisation and the quantitation of glucose metabolism in discrete anatomical regions throughout the CNS. Inferences about cerebral function can be drawn using the [^{14}C]2-DG autoradiographic technique for two reasons. Firstly, under normal physiological conditions, the energy requirements of cerebral tissue are derived almost exclusively from the aerobic metabolism of glucose. Secondly, functional activity and energy metabolism in the CNS are directly and intimately associated (Sokoloff, 1977).

The technique takes advantage of the biochemical characteristics which result from the modification of the glucose molecule to 2-deoxyglucose, which differs only in the substitution of the hydroxyl group on the second carbon atom to a hydrogen atom. The entry of 2-deoxyglucose from the blood into the brain is mediated by the same saturable carrier that transports glucose across the blood-brain barrier. In the CNS, both sugars compete for hexokinase which result in their phosphorylation, and it is at this point in the biochemical pathway that the metabolism of the two diverge. Glucose-6-phosphate is metabolised further via the glycolytic and tricarboxylic acid cycle pathways eventually to produce CO_2 and water. The product 2-deoxyglucose-6-phosphate however, is not a substrate for glucose-6-phosphate dehydrogenase or glucose-6-phosphate isomerase and its catabolism ceases at this point. Therefore, once 2-deoxyglucose-6-phosphate is formed, it is

essentially trapped and accumulates as it is formed in the cerebral tissues (the hydrolysis of 2-deoxyglucose-6-phosphate back to 2-deoxyglucose does not present a problem as levels of glucose-6-phosphatase are present only in very low levels), thus allowing the application of the quantitative autoradiographic technique.

Sokoloff *et al.* (1977) developed a theoretical model based on the biochemical properties of 2-deoxyglucose (figure 1.8) in which the relationships can be mathematically defined and an operational equation derived if the following assumptions are made:

1)   Plasma glucose concentration and the rate of glucose consumption are constant throughout the period of the procedure.

2)   Each tissue compartment is homogeneous, and that the concentrations of [^{14}C]2-DG and glucose within each compartment are uniform and exchange directly with the plasma.

3)   [^{14}C]2-DG is present only in tracer concentrations (molecular concentrations of free [^{14}C]2-DG essentially equal to zero).

The operational equation which defines R_i, the rate of glucose consumption per unit mass of tissue 'i' in terms of the measurable variables 1) arterial plasma [^{14}C]2-DG concentration (C_p^*) and arterial plasma glucose levels (C_p) at specified times (t) throughout the experiment to the time of killing (T), and 2) the total concentration of [^{14}C] in the tissue (C_i) at the time of killing (T), is illustrated in figure 1.9. The rate constants K_1^*, K_2^* and K_3^*, which define the distribution of tracer between plasma and brain tissue compartments, and the lumped constant (λ, Φ and kinetic constants for hexokinase) which maintains the steady state rates of [^{14}C]2-DG and glucose phosphorylation in the brain, are not measured in each experiment. The values for these constants were previously determined in animals by Sokoloff *et al.* (1977) in the original description of the method.

PLASMA   **BRAIN TISSUE**

Precursor pool   *Metabolic products*

$[^{14}C]$-Deoxyglucose $\quad$ K_1^* $\quad$ $[^{14}C]$-Deoxyglucose $\quad$ K_3^* $\quad$ $[^{14}C]$-Deoxyglucose-6-Phosphate
(C_P^*) $\qquad$ K_2^* $\qquad$ (C_E^*) $\qquad\qquad$ (C_M^*)

Glucose $\qquad$ K_1 $\qquad$ Glucose $\qquad$ K_3 $\qquad$ Glucose-6-Phosphate
(C_P) $\qquad$ K_2 $\qquad$ (C_E) $\qquad\qquad$ (C_M)

hydrolysis by
glucose-6-phosphatase

$CO_2 + H_2O$
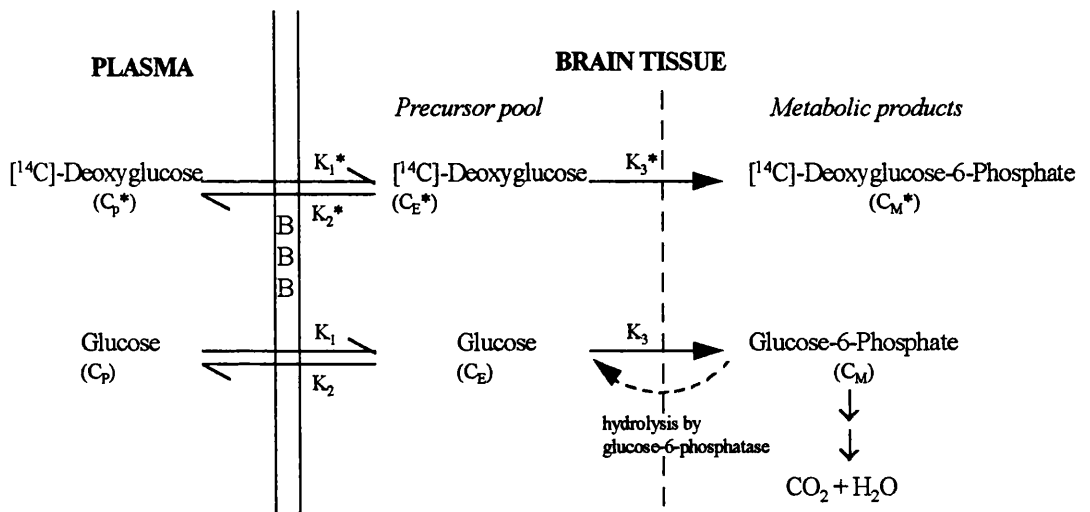
Total tissue ^{14}C concentration $C_i^* = C_E^* + C_M^*$

Figure 1.8 **Schematic representation of the biochemical behaviour of $[^{14}C]2$-deoxyglucose in the brain.**

C_P^* and C_P represent the concentrations of $[^{14}C]2$-deoxyglucose and glucose in arterial plasma respectively.

C_E^* and C_E represent their respective concentrations in tissue precursor pools that serve as substrates for hexokinase.

C_M^* and C_M represent the concentrations of $[^{14}C]2$-deoxyglucose-6-phosphate and glucose-6-phosphate in tissue respectively.

$K_1^{(*)}$, $K_2^{(*)}$, $K_3^{(*)}$ represent the rate constants for carrier mediated transport of $[^4C]2$-deoxyglucose from plasma to tissue, from tissue back to plasma, and phosphorylation by hexokinase respectively.

(From Sokoloff *et al.*, 1977)

Different energy-dependent processes contribute to the rate of glucose utilisation within neurones, including processes involved with neurotransmitter synthesis and release and the maintenance of ionic gradients by ionic pumps. The different cellular elements within cerebral tissue will also have varying requirements for energy consumption. It has been estimated that neurones account for approximately 75% of the total oxygen consumption in the CNS (Siesjö, 1978). The dynamic alterations in glucose utilisation reflect predominantly nerve terminal electrical activity (Schwartz *et al.*, 1979). The

$$R_i = \frac{C_i^*(T) \; - \; K_1^* e^{-(K_2^*+K_3^*)T}\displaystyle\int_0^T C_P^* e^{(K_2^*+K_3^*)t}\, dt}{\left[\dfrac{\lambda \cdot V_m^* \cdot K_m}{\phi \cdot V_m \cdot K_m^*}\right]\left[\displaystyle\int_0^T \left(\dfrac{C_P^*}{C_P}\right) dt \; - \; e^{-(K_2^*+K_3^*)T}\displaystyle\int_0^T \left(\dfrac{C_P^*}{C_P}\right) e^{(K_2^*+K_3^*)t}\, dt\right]}$$

Figure 1.9   The operational equation of the [^{14}C]2-deoxyglucose method.

The rate of glucose utilisation R_i in any region of cerebral tissue is calculated from the operational equation. All symbols are the same as those defined in figure 2.1
λ represents the ratio of tissue distribution volumes for deoxyglucose and glucose, Φ equals the fraction of glucose which, once phosphorylated, will continue to be metabolised via the glycolytic pathway, $K_m^{(*)}$ and $Vm^{(*)}$ represent the Michaelis-Menten constants of hexokinase for deoxyglucose$^{(*)}$ and glucose.

(From Sokoloff et al., 1977)

remainder of energy consumption in the brain relates to ionic fluxes and ionic transport which can be manipulated only after the inhibition of electrical activity (i.e. flat EEG) (Crane et al., 1978; Astrup et al., 1981).

As alterations in glucose use correspond to the activity in axonal pathways, changes in glucose use will not be restricted to receptor localisation, but also the neuronal pathways connected to those regions. For this reason, the technique has been successfully applied to many diverse situations. For an extensive review of the applications of the [^{14}C]2-DG technique, interested readers should refer to the review by McCulloch (1982). A major application of the [^{14}C]2-DG technique has been to characterise the functional consequences associated with a particular neurotransmitter system, either by the administration (systemically/locally) of putative receptor agonists or antagonists, or by using stereotaxically placed lesions. Over the past 20 years, the [^{14}C]2-DG technique has provided much insight into the circuitry associated with the majority of the known neurotransmitter

systems in the CNS. A small number of studies are briefly outlined here to present a few of the applications of the $[^{14}C]$2-DG technique. The most extensively studied system has been that of dopamine. Dopaminergic systems have been manipulated sytemically, through the use of agonists and antagonists, and also locally by stereotaxic lesions of dopaminergic pathways. Such studies have demonstrated that changes in glucose metabolism are restricted in their anatomical distribution. The systemic administration of dopaminergic agonists led to elevations in glucose use in regions containing dopamine receptors, such as the substantia nigra and striatum. However, alterations in glucose utilisation were also demonstrated in brain regions lacking dopamine receptors but which are influenced by dopaminergic activity, such as the inferior olivary nucleus and thalamic nuclei. Intracerebral approaches such as the lesioning of dopaminergic pathways or injecting dopaminergic agents directly into brain regions, have also been used to manipulate neuronal activity. For example, a combination of systemically administered apomorphine and lesions of retinal input to primary visual structures helped in determining the involvement of retinal dopaminergic receptor activation in visual processes (McCulloch et al., 1980).

Extensive studies have been carried out to investigate the consequences of GABA receptor manipulation. Using the systemic administration of the $GABA_A$ agonists muscimol and 4,5,6,7-tetrahydroisoxazole[5,4-c]pyridin-3-ol (THIP), these ligands were demonstrated to depress glucose utilisation throughout the CNS (Kelly & McCulloch, 1982, 1984; Kelly et al., 1986). An interesting application of the autoradiographic technique has been the use of a ranking function (f function) to allow the systematic and objective interpretation of data obtained (Ford et al., 1985). This approach was applied to studies investigating GABAergic manipulations. Through the use of the f function, regional heterogeneity in the metabolic responses of brain structures to GABA ligands were

revealed. Differences in the cerebral functional effects of the benzodiazepine, diazepam, was separated from the effects of the GABA$_A$ agonists muscimol and THIP.

Since glutamate is widely used in the CNS as a neurotransmitter, and is associated with the pathogenesis of a variety of neurodegenerative disorders, the functional consequences of glutamate receptor manipulations have also been studied extensively. Selective NMDA receptor antagonists together with selective AMPA receptor antagonists have been used to examine cerebral function in both physiologic and pathologic conditions.

Systemic pharmacologic manipulations using NMDA receptor antagonists have been carried out extensively. Using a variety of competitive antagonists (e.g. CPP, CGS 19755 and CGS 37849) and non-competitive antagonists (e.g. MK-801, ketamine and PCP), studies have revealed that the functional consequences after receptor blockade both at the glutamate recognition site and in the receptor ion channel are essentially the same. The non-competitive NMDA antagonists result in selective and substantial increases in function-related glucose use in cortical and subcortical limbic structures and basal ganglia, while the competitive NMDA antagonists result in more modest reductions in glucose use in these areas (Meibach *et al.*, 1979; Nelson *et al.*, 1980; Hargreaves *et al.*, 1993; Sharkey *et al.*, 1994).The differences in the magnitude of the responses displayed by the different NMDA receptor antagonists has been attributed to the use-dependent nature of the glutamate receptor blockade of MK-801 or PCP, which is intensified by increasing glutamatergic transmission.

The systemic antagonism of AMPA receptors by agents such as NBQX and LY293558 result in alterations in glucose use that differ from the effects produced by the competitive and non-competitive antagonists of the NMDA receptors. AMPA antagonists produce marked, anatomically widespread and dose-dependent reductions in glucose use throughout the brain, unlike the selective changes seen following NMDA receptor

manipulation (Suzdak & Sheardown, 1993; Browne & McCulloch, 1994). The consequences of the pharmacologic manipulations of NMDA and AMPA receptors are discussed in relation to findings obtained in this thesis in chapter 8.

1.8 Aims of thesis

The extensive study of ionotropic glutamate receptors has revealed a multitude of functions in the brain and led to speculation about their involvement in the pathology of neurodegenerative diseases such as ischaemia. While it has been demonstrated that NMDA and AMPA receptor antagonists such as MK-801 and NBQX are potent neuroprotectants, the use of such agents in the clinical setting has not proved possible. Similarly, the roles of mGluRs in the CNS are thought to be as diverse, and thus could have the potential to influence the therapy of a variety of CNS disorders. However, progress has been hindered due to a lack of subtype-specific and systemically active ligands.

The aims of this thesis are to investigate the consequences of metabotropic and AMPA glutamate receptor activation in the rat brain using selective ligands with an emphasis on group II mGluR activation. The consequences of antagonism were also examined for AMPA. The studies examine the impact of glutamate receptor activation following pharmacological manipulations under physiological and pathological conditions using a variety of *in vitro* and *in vivo* techniques.

Aim 1:   To investigate the effects on cerebral function following glutamate receptor manipulation using two novel, systemically active metabotropic receptor agonists that have been demonstrated to be highly potent and selective for group II mGluRs *in vitro*, LY354740 and LY379268. Using [^{14}C]2-deoxyglucose autoradiography, the effects of these agents on glucose utilisation in the rat brain will be examined and compared. In

addition, the study will investigate if the effects following the systemic administration of LY354740 and LY379268 are similar to those displayed following systemic NMDA and AMPA receptor antagonists.

Aim 2:   To investigate the consequences of cerebral function following the selective modification of neuronal activity by direct intracerebral injection of the selective AMPA antagonist LY326325. [^{14}C]2-deoxyglucose autoradiography will also be used in this study to determine whether AMPA receptor blockade in the hippocampus is similar to that seen following intracerebral blockade of NMDA receptors.

Aim 3:   To explore the neuroprotective role of group II mGluRs in cerebral ischaemia. A model of permanent cerebral ischaemia together with LY354740 and LY379268 drug intervention will be used to test the hypothesis that activation of group II mGluRs are neuroprotective. Together with the traditional histological analysis to measure infarct volume, immunohistochemical analysis of ischaemic brain tissue treated with LY379268 will also be carried out to determine cellular changes in the brain following permanent cerebral ischaemia.

Aim 4:   To explore the possible mechanisms of actions of group II mGluRs in acute excitotoxicity using cell culture models of neurotoxicity. This study will use two mechanistically disparate challenges of hypoxia/hypoglycaemia and staurosporine-induced neurotoxicity to investigate the events involved in mediating neuroprotection by LY354740 and LY379268. In addition, astrocytes will also be used to determine their possible role in the protection mechanism.

CHAPTER 2

METHODS

2.1 *In vivo* [^{14}C]2-deoxyglucose autoradiography

2.1.1 Preparation of animals for [^{14}C]2-deoxyglucose measurement

Male adult rats were placed in a perspex chamber and anaesthetised initially with 5% halothane in a nitrous oxide and oxygen gas mixture (70:30). Maintenance of anaesthesia was achieved using 0.8-1.0% halothane, administered via a face mask. The right femoral blood vessels were exposed by blunt dissection and polyethylene cannulae containing heparinised saline (5 IU/ml) were inserted 0.5cm into the right femoral artery and vein to allow the sampling of blood and the injection of [^{14}C]2-deoxyglucose, respectively. The cannulae were secured in place using 4/0 silk thread and a small quantity of adhesive (superglue) was applied as a precautionary measure. By making a small cut through the skin at the nape of the neck, the cannulae were passed subcutaneously and externalised using a sterilised stainless steel guide cannula (International Market Supply, UK). Xylocaine® anaesthetic gel was applied liberally to the femoral incision site and the incision site sutured. The externalised cannulae were secured in place by sutures, and again a small quantity of adhesive was applied. The cannulae were trimmed to a shorter length, out of the reach of the animal, and plugged. The halothane anaesthesia was discontinued and the rats allowed to recover from the effects of the anaesthetic for a minimum of two hours before any further manipulation. Arterial blood pressure and rectal temperature were monitored continuously throughout the surgical procedure and heating lamps were used to maintain normal body temperature.

2.1.2 Cannulae preparation

Cannulae (Portex Ltd., UK) were prepared manually at least 24 hours before they were required for use in [^{14}C]2-DG autoradiography experiments. A length (approximately 2cm) of cannula with an external diameter 0.96mm, internal diameter 0.58mm, was inserted

(1mm) into a cannula (cut to approximately 20cm) with an external diameter 1.4mm, internal diameter 0.63mm. The join was then sealed with standard Araldite epoxy adhesive and allowed to air-dry.

2.1.3   The [^{14}C]2-deoxyglucose procedure

Local cerebral glucose utilisation was measured in fully conscious, freely moving rats by means of the [^{14}C]2-DG technique originally described by Sokoloff *et al.* (1977). The period of measurement of cerebral glucose utilisation was initiated by the administration of an intravenous pulse of 50µCi [^{14}C]2-DG (specific activity 55.0 mCi/mol; Amersham Life Science) in 0.7ml saline, injected over 30 seconds. Timed arterial blood samples (approximately 100µl) were drawn at fixed time points over the next 45 minutes. The blood samples were immediately centrifuged (Microfuge E; Beckman) and the arterial plasma aliquots assayed to determine the concentrations of ^{14}C and glucose by means of liquid scintillation counting and semi-automated glucose oxidase enzyme assay (Glucose Analyser 2, Beckman), respectively. Forty-five minutes after the isotope administration, the rats were sacrificed with halothane and their brains were removed quickly and carefully. The brains were then frozen in isopentane at -42°C for 10 minutes, mounted onto swivel headed microtome chucks and embedded in Lipshaw matrix ready for processing for quantitative autoradiography.

2.1.4   Liquid scintillation analysis

In order to calculate the plasma integral required in the operational equation for the determination of rates of local cerebral glucose utilisation, the plasma history of [^{14}C]2-DG over the experimental period of 45 minutes had to be measured. A plasma sample of 20µl from each of the blood samples obtained at each time point was pipetted into a scintillation

vial containing 1ml distilled water. To each vial, 10ml scintillation fluid was added (Ecoscint, National Diagnostics) and shaken thoroughly. A vial containing 20μl of ^{14}C-standard of known specific activity was also counted to act as an internal control. Radioactivity was counted in a refrigerated scintillation counter (Packard Tri-Carb, 1900CA) and the mean disintegrations per minute (dpm) were calculated from triplicate counts of 4 minutes each.

2.1.5 Preparation of autoradiograms

Previously mounted brains were stored at -20°C for as short a period as possible (less than 2 days). The brains were cut serially into 20μm thick coronal cryostat sections at -22°C. Triplicate sections were collected according to the cutting schedule utilised (cutting schedules varied between studies depending on the regions of specific interest), mounted onto 20mm x 40mm glass coverslips and dried rapidly on a hotplate at 60°C. The coverslips were then glued onto thin card in sequence. Autoradiograms were generated by exposing the brain sections with medical X-ray film (Biomax™ MR film, Eastman Kodak Company) in light-tight cassettes for 3 days, together with a series of precalibrated [^{14}C]-methyl methacrylate standards (range 44-1475nCi/g tissue equivalents). After 3 days, the films were developed (developer 5 minutes, stop bath 1 minute, fixer 10 minutes, followed by half an hour in running water).

2.1.6 Quantitative densitometric image analysis

Local rates of glucose utilisation were determined from the [^{14}C]2-DG autoradiograms with quantitative densitometric analysis using a computer based densitometer (Micro Computer Imaging Device; MCID, Imaging Research Inc., Ontario, Canada). Densitometric measurements represent the amount of digital signal collected from

the sample, in this case X-ray film, and are expressed initially as grey levels from 0 (represents black) to 255 (represents white). The image analyser then converts the measured grey levels into optical density values ranging from 0 (white) to 2.4 (black). After raw data input and calibration to the ^{14}C film standards (figure 2.1), which relates optical density to the known concentrations of radioactivity (nCi/g), the quantification of isotope concentrations and consequently local cerebral glucose use (μmol/100g/minutes) were measured in discrete brain regions in each animal. Measurements were made by placing the autoradiographic sections under the camera (at the same magnification and light intensity as that used for the calibrations) and positioning a frame over each anatomical region of interest. The size of the measuring frame varied (1mm^2- 9mm^2), depending on the anatomical region (e.g. 1mm^2 for small nuclei such as the locus coeruleus; 9mm^2 for large anatomical regions such as the caudate nucleus). For each anatomical region of interest, the mean optical density was calculated from readings made in 3-6 sections per animal (maximum n=12). Anatomical structures in the rat brain were defined with reference to a stereotaxic atlas (Paxinos & Watson, 1986).

2.2   Hippocampal stereotaxic surgery

The study utilising stereotaxic surgery in this thesis was carried out in collaboration with the University of Edinburgh and Université de Bordeaux I. I would like to thank Professor Richard Morris, Dr. Gernot Riedel and Dr. Jacques Micheau for performing the stereotaxic surgery described in this thesis.

2.2.1   Intrahippocampal stereotaxic placement of cannulae

The chronic implantation of cannulae and minipumps into the hippocampus was performed under general anaesthetic using standard stereotaxic techniques.
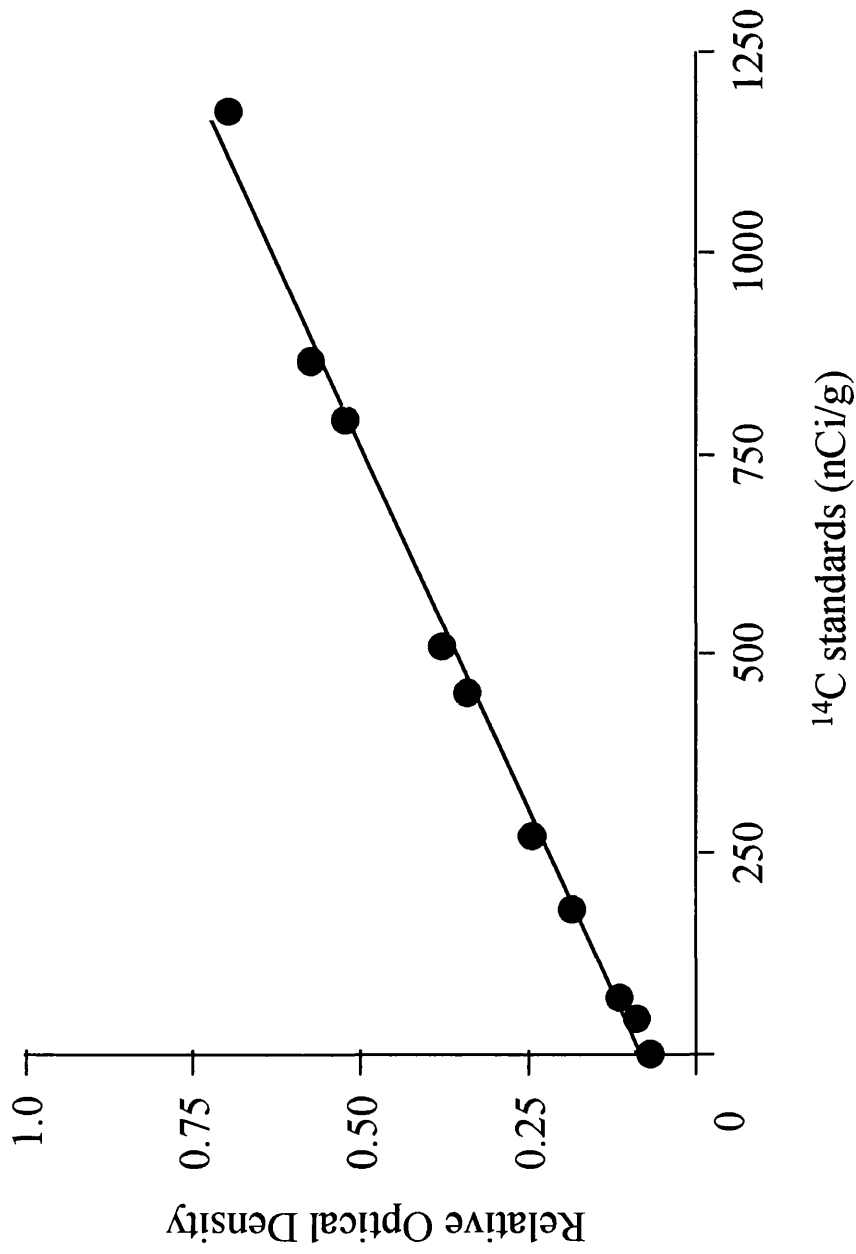
Figure 2.1   Representative example of ^{14}C standard curve for [^{14}C]2-DG autoradiography.

Calibration of the film standards relates the optical density to the known concentrations of radioactivity (nCi/g). This allows the subsequent calculation of local cerebral glucose use in separate brain areas to be measured.

Male adult rats (Harlan Olac, Bicester, UK) were placed in a perspex chamber and anaesthetised with 5% halothane in a nitrous oxide and oxygen gas mixture (70:30). Anaesthetic was maintained by intraperitoneal (i.p.) injections of Avertin (tribromoethanol, 10 ml/kg). The fur on the skull cap was shaved and the animal placed on a stereotaxic frame (Electromedical) with the head placed horizontally (tooth bar at -3.5mm). The skull and bregma were exposed by making a longitudinal midline incision in the scalp and the skin was moved out of the way with tweezers. Any connective tissue on the skull surface was removed with a scalpel. The co-ordinates of the cannulae placement were identified and marked in pencil on the skull surface, with respect to the bregma position. Two small burr holes were made through the skull with a drill at the respective locations. After perforating the dura with a syringe needle, previously prepared L-shaped 27 gauge-tipped stainless steel infusion cannulae connected to 7 day minipumps (ALZA 1007D, pumping rate of 0.5µl/hr for 7 days) by flexible polyethylene tubing, were implanted bilaterally in the dorsal hippocampus at bregma co-ordinates of AP -4.5mm, L/R ±3.0mm, to a depth of -3.0mm below the dura. In order to keep the cannulae fixed in place, three additional burr holes were drilled above frontal and occipital regions into which small stainless steel screws were anchored. Dental cement was then applied to the skull, cannulae, and screws, to secure the whole apparatus. The minipumps were placed in a cavity below the skin of the neck. Finally, the skin flaps were folded back and sutured. To avoid infections, the wound was cleaned and a topical antibiotic (Aureomycin) was applied liberally over the wound. Animals were allowed to recover from the anaesthetic under heating lamps until consciousness was regained. Animals were then placed individually into cages lined with post-operative pads together with a small quantity of rat chow softened with water. The animals were returned to their normal housing conditions and examined regularly for the next 24 hours to check on

their recovery. On subsequent days, animals were given replacement softened diet, and checked daily to monitor their recovery.

All surgical tools were cold sterilised in Novasapa while cannulae and screws were sterilised in ethanol (96%).

2.2.2 Avertin preparation

A concentrate of tribromoethanol was first prepared. In complete darkness, 62ml of tertiary-amyl-alcohol was added to 100g of tribromoethanol crystals. This was mixed thoroughly and stored in a brown-tinted bottle in the dark as the concentrate is very sensitive to light. For a working preparation of the anaesthetic, 5ml of absolute alcohol was added to 62.5ml of 0.9% saline and mixed thoroughly. To this mixture, 1.25ml of the previously prepared concentrate was added and stirred overnight. The final anaesthetic solution should be clear in appearance and the concentrate should be thoroughly dissolved.

2.3   Focal cerebral ischaemia in the rat

The surgical procedure of MCA occlusion in the rat described in this thesis was performed by Dr. Marc Soriano.

2.3.1 Preparation of animals

All the experiments were carried out in adult male Fischer 344 rats (250-350g body weight) obtained from Harlan Olac, Bicester, UK. Animals were kept under 12-hour light-dark cycle and allowed free access to food and water.

Male adult rats were placed in a perspex chamber and anaesthetised initially with 5% halothane in a nitrous oxide and oxygen gas mixture (70:30). When the animal was deeply anaesthetised, i.e. loss of righting reflex, non-surgical tracheal intubation was performed.

75

For this, a cork board was sandwiched upright between two lead bricks. A length of silk thread was knotted to form a loop and secured at the top of the cork board and suspended over the side of the board. The rat was then suspended onto the loop of silk thread by its top teeth to open the mouth and trachea. The tongue was gently held out of the way using forceps and the rat was intubated by introducing a 16G intubation tube into the trachea (Quik-Cath II; 51 mm L, Baxter; the stainless needle is blunted down to sit within the tube). Once in place, the needle was removed and rats were attached to a ventilator (Linton Instruments) and anaesthetic was maintained with 1.5% halothane. The femoral artery was cannulated with a polythene catheter for monitoring physiological variables. Blood pressure (Gould Instruments), blood gases (pCO_2 and pO_2)and pH were monitored throughout the surgical procedure (288 Blood Gas System, Ciba-Corning), while glucose samples were taken immediately after cannulation, pre-occlusion and 10 minutes post-occlusion (Glucose Analyser-2, Beckman).

2.3.2 Middle cerebral artery occlusion

Left MCA occlusion was carried out according to the method of Tamura *et al*. (1981) with minor modifications. The animal was placed on its side and the left eye was closed with a suture. Following a vertical scalp incision between the eye and the ear (using the whisker closest to the ear as an anatomical landmark), the temporalis muscle was divided along the plane of its fibre bundles and retracted in order to expose the zygomatic arch, which was kept intact (figure 2.2). With the aid of an operating microscope, a subtemporal craniectomy was carried out using a dental drill. To ensure that overheating of the skull and brain did not occur, the craniectomy was kept cool with sterile saline solution. After exposure of the left MCA, the dura was cut and removed with micro-scissors. The MCA was electrocoagulated using diathermy immediately over the olfactory tract and the
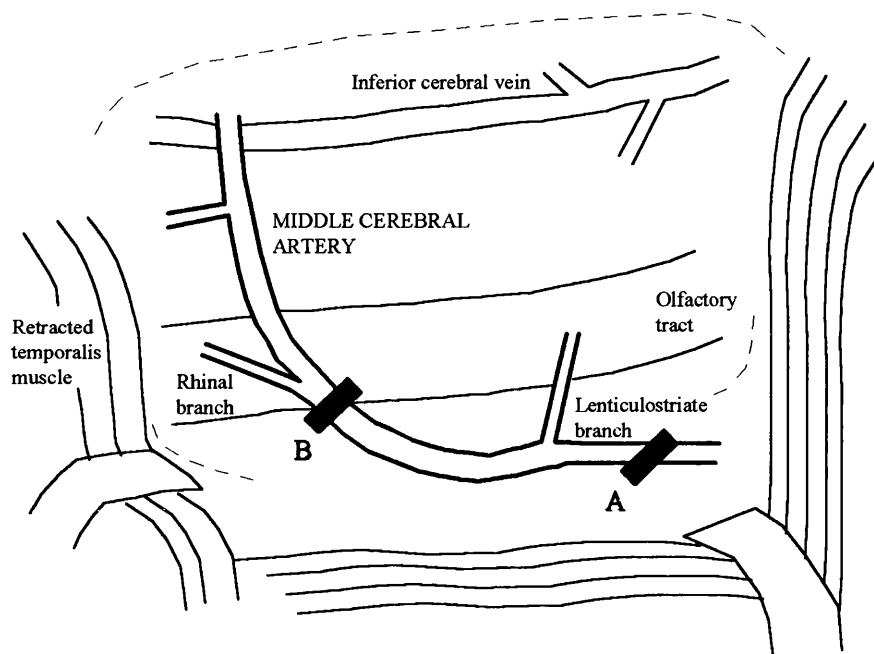
Figure 2.2   Middle cerebral artery exposure.

Sites of proximal (A) and distal (B) middle cerebral artery occlusion.

(From McAuley, 1995)

coagulation was extended proximally to the origin of the lenticulostriate arteries. The MCA was bisected with micro scissors to ensure the complete cessation of blood flow, and wounds were sutured with 4/0 silk thread. A subcutaneous (s.c.) injection of sterile saline (2ml) was given to prevent dehydration. Halothane anaesthesia was discontinued and the animal was then ventilated on pure oxygen until signs of consciousness were evident, and extubated. Throughout the surgical procedure, body temperature was monitored with a rectal probe and maintained at 37.5 °C with a heating blanket. Animals were placed in an incubator during initial recovery period and then returned to their normal housing conditions. Any animals which displayed adverse signs of suffering were withdrawn from the study and humanely killed.

2.3.3   Tissue processing

Twenty four hours following the MCA occlusion, the animals were sacrificed with 5% halothane and the brains were carefully removed and frozen in isopentane at -42°C for 10 minutes. The brains were cut into 20 µm thick serial coronal cryostat sections at -22°C at the 8 pre-selected coronal levels per animal, from anterior 10.5 mm to posterior 1.02 mm (Osborne *et al.*, 1987). Triplicate sections were mounted onto microscope slides and stained with haematoxylin and eosin (H & E) (appendix 3) for histological lesion assessment. Figure 2.3 presents the 8 stereotaxic levels at which histopathological assessment is carried out.

2.3.4   Measurement of the volume of infarction

Ischaemic damage is most widely identified by quantitative histopathology. This method allows the distribution and area (and consequently the volume) of ischaemic damage to be assessed at 8 coronal levels throughout the MCA territory (Osborne *et al.*, 1987).
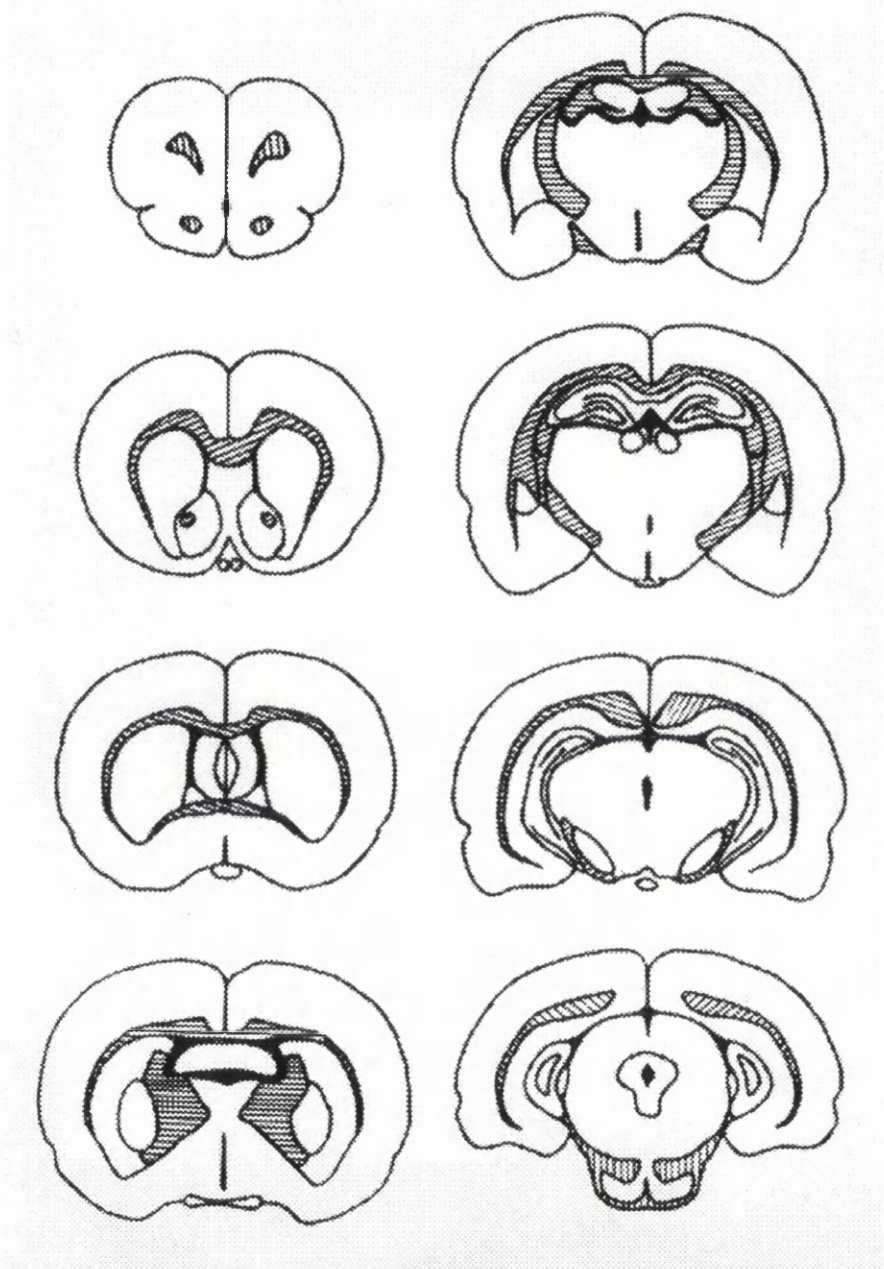
Figure 2.3   Stereotaxic levels for the histopathological assessment of ischaemic damage in the rat.

The minimum number of stereotaxic levels which must be assessed to yield accurate volumetric measurements of infarction is 8 (Osborne *et al.*, 1987). The levels are represented here along with their respective anatomical landmarks.

Areas of ischaemic damage and brain swelling were assessed using a computer based image analysis system (MCID, Imaging Research Inc.). As this system involves the counting of discrete pixels which make up the projected image in question, area measurements are obtained by counting the pixels enclosed within a target outline. Therefore, in order for data to be expressed in real spatial units, the pixels were referenced to a spatial reference scale. Calibrations were made using a cross-hair calibration graticule of 40mm. Both vertical and horizontal axes were calibrated, with distance displayed as a function of pixels/mm. Area measurements were made by placing the H & E stained coronal sections under the camera (at the same magnification as that used for the calibrations) and drawing round the boundary of the ischaemic area projected onto the monitor. The mean area was calculated from the triplicate sections at each coronal level. The approximate volumes of ischaemic damage for each animal were then attained by integrating each of the 8 areas of damage measured (mm^2) with the known distance between the stereotaxic co-ordinates of these levels.

All analyses were carried out in a blinded fashion.

2.4   *In vitro* models of neurotoxicity

2.4.1   Primary cortical astrocyte culture

Dissection

The method for obtaining cultures of mixed glia from neonatal rat cerebral cortices is based on that of McCarthy & de Vellis (1980). Neonatal rat pups (day 0-3) were killed by decapitation, and the heads were kept moist with 70% ethanol. These were secured in place with straight watchmaker's forceps, and the brains removed by cutting a 'V' into the skull, from a point at its base to the eyes, on both sides. The skull was removed to expose the dorsal surface of the brain. With a pair of curved watchmaker's forceps, the brains were

gently lifted out and placed into small petri dishes (Falcon) containing Ca^{2+}-and Mg^{2+}-free Hank's Balanced Salt Solution (HBSS-CFMF). The cerebellum was held in place with forceps and the cerebral cortices were detached from the body of the brain and transferred to fresh HBSS-CFMF. With the aid of a dissecting microscope, the hippocampus was removed by dissecting along the extension of the lateral ventricles. The caudate and septal nuclei were also removed to leave a cortical cup. The meninges were removed from the surface of the cortices. The cortices were placed into a sterile petri dish containing a fresh volume of HBSS-CMF.

Dissociation, plating and maintenance of cells

The cortices were cut into small cubes ($0.5mm^3$) with a scalpel and the fragments were placed into a 50ml centrifuge tube (Falcon). The tissue fragments were incubated with collagenase (2000 U/ml solution, diluted 1:3) and 0.25% trypsin (1:3 dilution) for 20 minutes at 37°C. Following enzymatic digestion, soya bean trypsin inhibitor and DNase (SBTI-DNase; see appendix 2), were added to inactivate the trypsin and digest any free DNA. The fragments were first triturated gently through a 10ml serological pipette (10x). Trituration was repeated carefully to avoid frothing using a 21G needle and a 23G needle (4x). The cell suspension was centrifuged for 10 minutes at 1000 rpm (Universal 16/16R; Hettich). The supernatant was discarded, and the cells re-suspended in a known volume of culture medium (20% foetal calf serum in Dulbecco's Modified Eagles Medium (20% FCS-DMEM), containing 2mM glutamine, 25µg/ml gentamicin) and counted using a haemocytometer. The cell solution was diluted 1:10 for counting, together with the addition of trypan blue (20%) to exclude the inclusion of non-viable cells. The cells were diluted to a final concentration of 1.5×10^6 cells/ml and plated into $75cm^2$ Primaria culture flasks (Falcon), 10ml per flask. Cultures were kept at 37°C in a humidified 5% CO_2/95% air

incubator. After 3 days in culture, the medium was replaced with 10% FCS-DMEM. Cells were then subsequently fed twice a week with 5% FCS-DMEM. Once the cells reached confluence, they were purified using the shaking method of McCarthy & de Vellis (1980).

Purification of specific cell types from mixed astroglial cultures

After approximately 12 days in culture, the confluent mixed cultures were used to prepare purified cultures of type 1 astrocytes via the shaking method (McCarthy & de Vellis, 1980). Mixed glial cultures consist of process-bearing cells (O-2A progenitors, oligodendroglia and type 2 astrocytes) growing on top of a confluent layer of type 1 astroglia. The shaking process detaches the process-bearing cells from the bed layer to leave an enriched population of type 1 astrocytes. The procedure for generating primary cultures of O2-A progenitors, microglia, oligodendroglia, type 2 or type 1 astrocytes is provided in figure 2.4.

Prior to shaking, the caps of the culture flasks were tightened to retain the 5% CO_2/95% air atmosphere and shaken on a bench top orbital shaker (Forma Scientific, Life Sciences International) at 260 rpm for $1^1/_2$ hours at 37°C. The medium was discarded and 10ml fresh 5% FCS-DMEM was added to each flask. The flasks were then returned to the incubator for 1 hour to equilibrate CO_2 with the fresh medium. The flasks were returned to the bench top orbital shaker following the incubation period, where they were shaken at 260 rpm for 18 hours at 37°C. The medium from each flask was removed, the adherent cells were rinsed with unsupplemented DMEM, and the cells subcultured to a plating density of 3 x 10^6 cells/ 75cm^2 flask. The enriched type 1 astrocyte cultures were then returned to the incubator, and maintained by feeding with 5% FCS-DMEM twice a week. Cells were used in experiments at least 3 weeks after the initial plating.

Day 0-12   Mixed brain cell culture from rat cerebral cortex

Day 12   Preshake (260 rpm, 1.5 hr), collect nonadherent cells

Shake (260 rpm, 18 hr)   Incubate 37 C, 1 h

Collect adherent cells

Microglia-enriched culture

Day 13   Adherent, flat cells   Nonadherent, process-bearing cells
                                    Contains 0-2A progenitor cells

5% FCS-DMEM   *5% FCS-DMEM*   *Chemically defined*
                       + ACM   *medium*

Type 1 astroglia-enriched   Type 2 astroglia-enriched   Oligodendroglia-enriched
culture   culture   culture

Figure 2.4   Schematic representation of the protocol used to prepare type 1 and type 2 astroglia, oligodendroglia and microglia.

(Modified from Levison & McCarthy, 1991)

2.4.2 Primary cortical neuronal cultures

Dissection

Neuronal cortical cultures were obtained from the method of Rose *et al.* (1993). Time-mated female rats (Bantin & Kingman, Hull, UK) were euthanased by CO_2 followed by cervical dislocation. Embryos at day 16-18 of gestation (E16-18) were released from their placentas into a large square petri dish (Sterilin) containing ice-cold HBSS-CFMF. The embryos were decapitated and the heads placed into fresh HBSS-CFMF medium on ice. For each head, a sterile 30mm upturned petri dish lid was used as a stand. Each head was placed gently onto the lid and placed under a dissecting microscope. The heads were anchored in place and the skin and developing bone were cut from the base of the head up, towards the dome and nose, in a straight line. Using straight and curved watchmaker's forceps, the membranes were teased aside to expose the brain and the cortices were removed from the skull to leave the cerebellum behind. An arc of cortex was then removed from both hemispheres (parallel to midline) with a scalpel. As much of the meninges were removed as possible and the cortical tissue fragments were transferred to a universal containing ice cold dissecting medium (DMEM - 4500g/l glucose; 1% v/v nystatin).

Dissociation, plating and maintenance of cells

Dissecting medium was added to the tissue fragments to give a volume of 9ml. To this, 1ml 2.5% trypsin was added and the mixture was incubated for 30 minutes at 37°C. The enzymatic digestion was stopped by replacing the medium with 9ml serum-containing medium together with 1ml DNase I (0.5mg/ml). The fragments were triturated gently with flamed glass Pasteur pipettes and the cell suspension was centrifuged at 1000 rpm for 8 minutes at 15°C. The supernatant was discarded and the cells were re-suspended in 20ml culture medium (10% v/v non dialysed heat inactivated FCS, 1mM glutamine, 1% v/v

gentamicin and 1% v/v nystatin in Neurobasal medium) and counted using a haemocytometer. Cells were cultured at a final plating density of 6×10^5 cells/ml onto 24 well plates (0.5ml/well) previously treated with poly-D-lysine (5μg/ml prepared in sterile distilled water). 1ml was added to each well for at least 1 hour. The poly-D-lysine was aspirated and the plates used directly. Cultures were kept at 37°C in a humidified 5% CO_2/95% air atmosphere. After two days in culture, non-neuronal division was halted by exposure to 5μM cytosine arabinoside in serum-free medium containing B27 supplement. Subsequent to this, half the culture medium was replaced at 3-5 day intervals and the cultures were maintained for 10-14 days prior to use in experiments.

2.4.3 Induction of hypoxia and glucose deprivation

After the appropriate time in culture in 24 well plates, cells were deprived of glucose and oxygen to produce an *in vitro* model of hypoxia and glucose utilisation. Glucose free PBS Dulbecco's Balanced Salt solution (PBS-DBSS) containing 1% v/v HEPES was sonicated for approximately 10 minutes to remove the majority of dissolved oxygen in the medium. This was followed by gassing the balanced salt solution with N_2 gas for at least an hour. The existing cell culture medium was aspirated and the medium was replaced with 495μl of the N_2-gassed PBS Dulbecco's balanced salt solution. The plates were replaced into a 5% O_2/5% CO_2/90% N_2 hypoxic incubator for the required length of time. Following the oxygen and glucose deprivation, the media were replaced with 495μl serum free Neurobasal medium (no extra glucose added) and the plates incubated in a 5% CO_2/90% air atmosphere. The media were removed for assay of LDH levels 24 hours after the initial insult.

For neuroprotection studies, 5µl of 100X concentration of ligand was added to the appropriate cultures for the duration of the oxygen and glucose deprivation and again for the following incubation in glucose-supplemented and normoxic conditions.

2.4.4 Induction of staurosporine induced neurotoxicity

After the appropriate time in culture in 24 well plates, the existing culture medium was aspirated and replaced with 490ul Neurobasal medium (serum and glucose free with 1% HEPES, 1% glutamine and 10uM glycine). 5µl of 1µM staurosporine (in DMSO) was added to the appropriate wells. The plates were replaced into the incubator for 48 hours and the supernatants were removed for the assessment of neuronal injury. For neuroprotection studies, 5µl of the 100X concentration of agonist was added to the wells 15 minutes prior to the addition of staurosporine.

2.5   Immunohistochemistry

In this section, the immunohistochemical techniques used in this thesis will be described. Due to the different requirements of the studies undertaken, the staining techniques employed for *in vivo* and *in vitro* material are dealt separately.

2.5.1 *In vivo* material

Immunostaining was carried out using the standard method used in our laboratory, the avidin-biotin method (figure 2.5). Avidin has a high affinity for biotin, and this technique exploits this highly efficacious and specific reaction. Biotin molecules are conjugated to antibodies, which are then bound to a complex comprising of avidin and a biotinylated enzyme to produce an amplified signal at the antigen binding site. Immunostaining for the

detection of DNA fragmentation was carried out using a commercially available kit with separate instructions for use. This procedure is also described.

All immunohistochemistry was carried out in 4% paraformaldehyde fixed, paraffin-embedded tissue. Sections were first de-waxed thoroughly in histoclear for 10 minutes. The process of rehydration of the sections of tissue was initiated by immersion into absolute alcohol for 10 minutes. This was repeated with fresh absolute alcohol for another 5 minutes. Endogenous peroxidase within the tissue was removed by incubating the tissue in 3% hydrogen peroxide in methanol for 30 minutes. The slides were then washed in water for 10 minutes, followed by a rinse in 50mM phosphate buffered saline (PBS). If necessary, the slides were treated with a proteolytic enzyme (0.4% pepsin in 0.01M HCl), or detergent (0.2% Triton-X in PBS) depending on the antigen to be demonstrated. Any excess PBS was blotted carefully from around the sections and the slides were placed individually into a humidity chamber. Using a hydrophobic marker pen, an outline was drawn around each section on the slide to limit the volume of solutions to be applied. Each section of tissue was incubated with 300μl blocker containing normal serum from the animal species used to prepare the secondary antibody (5% bovine serum albumin (BSA), 10% normal serum in PBS) for 1 hour at room temperature. The excess blocker was removed and the sections were covered with optimally diluted primary antibody. Antibodies were diluted in 0.1% BSA and 1.5% normal serum in PBS. The sections were incubated with the primary antibody overnight at 4°C. Following overnight incubation, the antibody solution was removed and the sections washed thoroughly in PBS for 2 x 5 minutes. Each section was incubated with 300μl of the appropriate secondary antibody (directed against the immunoglobulin from the species used to prepare the primary antibody), diluted 1:100 in PBS for 1 hour at room temperature. During this incubation, the avidin-biotin horseradish
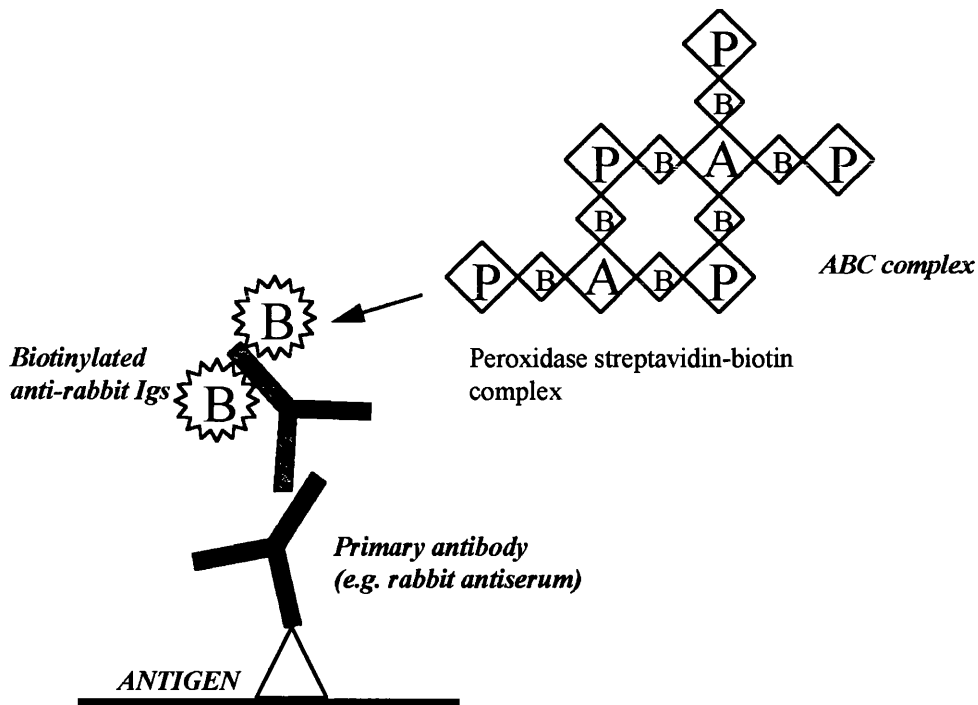
Figure 2.5   The avidin-biotin complex immunolabelling method.

(Adapted from Jackson & Blythe, 1993)

peroxidase complex (ABC complex) was prepared (1 drop solution A and B in 4.9ml PBS; Vector), mixed and allowed to stand for 1 hour. The sections were washed in PBS for 2 x 5 minutes and then incubated with the ABC complex for 1 hour. The sections were then washed with PBS for 2 x 5 minutes and the peroxidase reaction was developed using the chromogen diaminobenzidene (DAB) to produce a brown coloured end product (2 drops buffer, 2 drops H_2O_2 and 4 drops DAB; Vector). The reaction was stopped after a maximum incubation time of 5 minutes (inter-study development times variable) with PBS. The sections were washed with PBS (2 x 5 minutes) followed by water (2 x 5 minutes). The sections were then counterstained with H & E (see appendix 3 for protocol), dehydrated

through alcohol (70%, 90% and 100%), cleared with histoclear and mounted in synthetic mounting medium, DPX.

Negative controls were generated following the described method, but omitting the primary antibody incubation (figure 2.6).

Fragment end labelling of DNA using terminal deoxynucleotidyl transferase (TdT)

Staining for DNA fragmentation was carried out using the commercially available kit obtainable from Oncogene Research Products, Calbiochem (TdT-FragEL™). In principle, TdT binds to exposed 3'-OH ends of DNA fragments and catalyses the addition of biotin-labelled and unlabelled deoxynucleotides. Biotinylated nucleotides are detected using a streptavidin-horseradish peroxidase conjugate. The chromogen DAB reacts with the labelled sample to generate an insoluble brown substrate at the site of DNA fragmentation. The sections are subsequently counterstained with methyl green.

Sections were first de-waxed in a similar fashion to the method described for the *in vivo* material. Slides were immersed in histoclear for 5 minutes followed by immersion into absolute alcohol for 5 minutes. This was repeated using fresh absolute alcohol for another 5 minutes. Sections were then rehydrated by immersing consecutively into 90%, 80% and 70% ethanol for 3 minutes each. The slides were then rinsed briefly with 1X TBS (20mM Tris pH 7.6, 140mM NaCl). To limit the volumes applied to the slides, each section was encircled using a hydrophobic slide marker and placed in a humidity chamber. Sections were permeabilised by incubation with 20 µg/ml proteinase K, 100 µl/section for 20 minutes (1 µl of 2 mg/ml Proteinase K in 10mM Tris pH 8, added to 99 µl 10mM Tris per section). It is important at this step not to overincubate. Slides were rinsed with 1X TBS and any excess buffer was blotted and the slides carefully dried around each section. Endogenous peroxidase was inactivated by incubating the tissue in 3% hydrogen peroxide in methanol
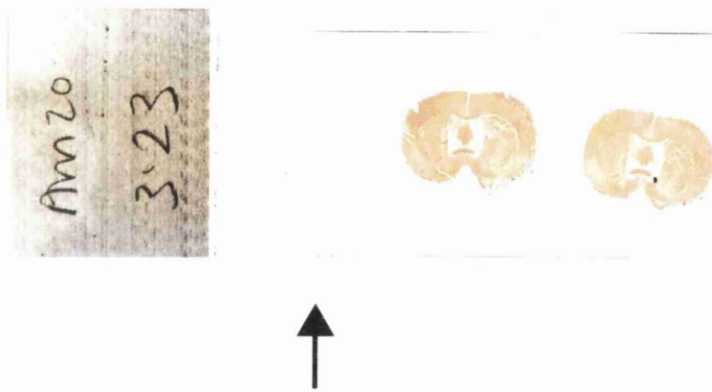
Figure 2.6   Immunohistochemistry; generation of negative controls.

Representative example of methodological negative control (arrow). This demonstrates the methodological non-specificity of the immunolabelling technique employed. Negative controls were generated using the method describes in section 2.5.1, but omitting the primary antibody incubation step.

for 5 minutes. The slides were rinsed again in TBS and dried carefully.

Equilibration and labelling of TdT was carried out by incubating each section with 100 µl of 1X TdT equilibration buffer for 30 minutes (dilution of 5X TdT equilibration buffer - 1M sodium cacodylate, 0.15 M Tris, 1.5 mg/ml BSA, 3.75mM $CoCl_2$, pH 6.6 - with distilled water). During this incubation, the TdT labelling reaction mixture was prepared on ice by mixing 57 µl of TdT labelling reaction mixture (mixture of labelled and unlabelled deoxynucleotides at an optimal ratio) with 3 µl of TdT enzyme for each section. The equilibration buffer was blotted carefully and the labelling reaction mixture was applied immediately to each section and incubated at 37°C for 1.5 hours. Following the incubation, the slides were rinsed with TBS. The labelling reaction was terminated by incubating the slides with 0.5 M EDTA, pH 8 for 5 minutes. The slides were rinsed with TBS and excess buffer blotted carefully. Sections were blocked by incubating with 4% BSA in PBS for 10 minutes. This was carefully blotted and 1X streptavidin peroxidase conjugate (prepared in 4% BSA/PBS) was immediately applied to each section. The sections were incubated at room temperature for 30 minutes. DAB solution was freshly prepared 5 minutes before the end of the incubation (1 DAB tablet, 1 H_2O_2/urea tablet in 1 ml of tap water). Following incubation with the conjugate, slides were rinsed with TBS and each section was incubated with the DAB for 10-15 minutes. The slides were rinsed with distilled water and counterstained with 0.3% methyl green for 3 minutes. The counterstain was removed and the slides were dipped 2-4 times into absolute ethanol. Slides were blotted briefly and the slides were dipped again into fresh absolute alcohol. The slides were blotted again and then dipped 2-4 times into histoclear. Excess histoclear was wiped away and the slides were mounted in DPX and left to dry for 24 hours.

2.5.2 *In vitro* material

For the visualisation of cultured cells, immunofluorescent techniques were employed, where the labelled antibody is visualised directly from its emitted fluorescence. The method described was used for the simultaneous identification of two antigens. The cells were grown on poly-l-lysine coated glass coverslips (5μg/ml prepared in sterile distilled water, 1 hour incubation) in 4 well plates (Nunc, GibcoBRL) for at least three weeks as detailed in section 2.4.1. The cells were rinsed with PBS and fixed with 4% paraformaldehyde containing 4% sucrose for 20 minutes followed by a 10 minutes incubation with -20°C methanol (see appendix 2). Following fixation, the cells were rinsed with PBS, 2 x 1 minutes. Coverslips were then returned to PBS. Each coverslip was incubated with 300μl blocker containing normal serum from the animal species used to prepare the secondary antibodies (2% BSA, 10% normal goat serum and 5% normal horse serum in PBS) for 1 hour at room temperature. The blocker was removed with a disposable pasteur pipette and the sections were covered with the two optimally diluted primary antibodies (the concentrations used are outlined in individual studies). Antibodies were diluted in 1% BSA and 1.5% normal serum in PBS. The coverslips were incubated with the two primary antibodies overnight at 4°C. Following the overnight incubation, the coverslips were rinsed thoroughly in PBS for 3 x 5 minutes. The cultures were incubated with fluorochrome-conjugated antibodies directed against the immunoglobulins from the species used to prepare the primary antibodies for 1 hour in the dark at room temperature. Fluorochromes used in this thesis were fluorescein and texas red (Vector; 1:100), which can be visualised by their green and red fluorescence, respectively. The coverslips were rinsed again in PBS for 3 x 5 minutes and mounted onto slides using a polyvinyl alcohol-based mountant containing an anti-bleaching agent (protocol in appendix 2). All slides were stored

in the dark at 4°C and viewed under the microscope within a week of staining to avoid loss of fluorescence.

2.6   Assessment of neuronal damage

2.6.1   Lactate dehydrogenase efflux assay for cell damage and death

Two separate protocols for the assessment of lactate dehydrogenase (LDH) efflux were used in this thesis as a proportion of the LDH assays were carried out at Lilly Research Centre, Eli Lilly and Company. Both methods are described.

Cytotoxicity detection kit

The Cytotoxicity Detection Kit (Boehringer Mannheim) is a sensitive colourimetric assay for the quantification of cell death based on the measurement of LDH activity released from the cytosol of damaged cells into the supernatant. LDH activity is determined by an enzymatic test: In the first step NAD^+ is reduced to NADH and H^+ by the LDH catalysed conversion of lactate to pyruvate. In the second step, the catalyst (diaphorase) transfers H/H^+ from NADH and H^+ to the tetrazolium salt INT (2-[4-iodophenyl]-3-[4-nitrophenyl]-5-phenyltetrazolium chloride) which is reduced to formazan (figure 2.7). This colour reaction is then measured spectrophotometrically. An increase in the amount of dead or damaged cells results in an increase of LDH activity in the culture supernatant. This increase in the amount of enzyme activity directly correlates to the amount of formazan formed. Thus, the amount of colour formed in the assay is proportional to the number of lysed cells.

Following the harvesting of supernatants for the assessment of LDH efflux, 100µl of supernatant was transferred, in duplicate, into clear 96 well flat bottomed microtitre plates (Falcon). The reaction mixture was prepared immediately prior to use; 11.25ml of the dye
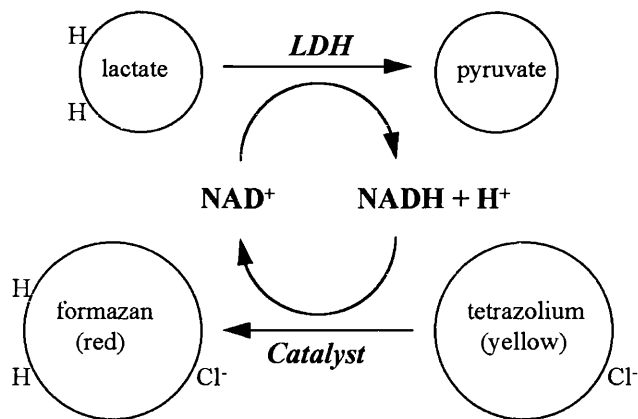
Figure 2.7   Diagrammatic representation of the enzymatic reaction used in the Cytotoxicity Detection Kit.

solution was added to 250µl of the catalyst solution mixed. 100µl of the reaction mixture was then added to each of the wells and the plates were incubated in the dark for 15 minutes. Absorbance of the samples were measured at 490 nm using an ELISA plate reader, with a reference wavelength of 650 nm.

Lactate dehydrogenase kit

This procedure for determining LDH efflux (Sigma Diagnostics) is based on the spectrophotometric method of Wroblewski and LaDue (1955). The activity of LDH is measured by monitoring the rate at which the substrate pyruvate is reduced to lactate. The reduction is coupled with the oxidation of NADH which is followed spectrophotometrically in terms of the rate of decrease in absorbance at 340 nm (figure 2.8).

Following the harvesting of supernatants from astrocytes cultured in 75cm^2 flasks, the volume of supernatant was concentrated from 10ml to approximately 0.5-1ml using Centriplus™ concentrators (Centriplus-3, Amicon). Supernatants were centrifuged at 3000g

for $6\frac{1}{4}$ hours at 4°C, and the retentate supernatant was recovered by an inverted spin at 2000g for 4 minutes at 4°C. The concentrated volumes of supernatant were used for the assessment of LDH efflux. Firstly, the temperature controlled cuvet compartment of the spectrophotometer was set at a known temperature between 20° and 39°C. In triplicate, 2.85ml phosphate buffer and 50μl of the supernatant sample were added to a NADH vial and mixed. This was left to incubate in a water bath at 25°C for 20 minutes. The solution was brought to the temperature of the cuvet compartment and 0.1ml sodium pyruvate solution was added to the vial and mixed. The contents of the vial were then transferred to a cuvet of 1cm lightpath. The absorbance at 340nm was read and recorded at 30 second intervals for 3 minutes, versus water as reference. The period when the decrease in absorbance produced was linear with time was selected, and the ΔA per minute for this period was determined. LDH activity was then calculated from:

$$\text{LDH (units/ml)} = \frac{\Delta A \text{ per minutes x TCF}}{0.001 \text{ x } 0.05 \text{ x lightpath (cm)}}$$

where 0.001 = ΔA equivalent to 1 unit of LDH activity in a 3ml volume with 1cm lightpath

at 25°C

0.05 = sample volume in cuvet (ml)

TCF = temperature correction factor (Table 2.1; 1.0 at 25°C)

Therefore, if a lightpath of 1cm is used, the following equation is derived:

LDH (units/ml) =   ΔA per minutes x 20,000 x TCF

One unit of LDH activity is defined as the decrease in A_{340} by 0.001 per minute at 25°C in a 3ml reaction mixture in a cuvet of 1cm lightpath.

$$\text{Pyruvate} + \text{NADH} \xleftrightarrow{\hspace{2cm}} \text{Lactate} + \text{NAD}$$
$$(\text{high } A_{340}) \qquad\qquad\qquad (\text{low } A_{340})$$

Figure 2.8   **LDH assay of Wroblewski and LaDue (1955): Enzymatic reaction.**

Table 2.1   **Temperature Correction Factors for calculating LDH activity.**

Cuvet temperature (°C)	TCF	Cuvet temperature (°C)	TCF
20	1.45	30	0.73
21	1.37	31	0.69
22	1.25	32	0.65
23	1.16	33	0.62
24	1.06	34	0.58
25	1.00	35	0.55
26	0.93	36	0.53
27	0.88	37	0.51
28	0.82	38	0.48
29	0.78	39	0.46

2.6.2 Measurement of DNA fragmentation

DNA fragmentation was quantified using a nucleosome ELISA immunoassay kit for measurement of mono- and oligo-nucleosome formation in cell extracts (Calbiochem). Free mono- and oligo-nucleosomes are captured on pre-coated DNA binding proteins. They are then detected following the binding of a biotin-labelled antibody (Anti-histone 3) to the histone component of the nucleosomes and streptavidin-linked horseradish peroxidase conjugate. The resultant colour reaction produced in the assay is proportional to the number of nucleosomes in the sample. The Nucleosome ELISA kit includes all the necessary reagents required for carrying out the procedure.

Following induction of *in vitro* neurotoxicity, samples were prepared for the Nucleosome assay. The culture media from the cells cultured in 24 well plates were carefully removed and each well replaced with 1ml of lysis buffer containing 0.2mM phenylmethylsulphonyl fluoride (PMSF). The cells were vortexed and incubated for 30 minutes on ice. The plates were then centrifuged at 3000 rpm for 30 minutes at 4°C and frozen for at least 18 hours at -20°C before proceeding any further in the assay. Samples were thawed and components of the Nucleosome ELISA were brought to room temperature. In order to measure the free nucleosomes in unknown sample supernatants, a standard curve of known nucleosome concentration was prepared. The Nucleosome Standard was prepared to a concentration of 30 nucleosome units per ml (30 U/ml) with distilled water and lysis buffer. The standard was further diluted with lysis buffer to concentrations of 10, 3.3, 1.1 and 0.366 U/ml by making three-fold serial dilutions. Lysis buffer was used as a background control (0 U/ml).

All samples were diluted in lysis buffer containing PMSF (1:10). Samples and standards were then added to the microtitre plate, 100μl into each well in duplicate. The plate was covered with a plate sealer and incubated at room temperature for 3 hours.

Following this incubation time, the wells were washed thoroughly 3 times with 1X wash buffer (25ml of 20X wash buffer to 475ml distilled water). Any residual buffer was removed by tapping onto a paper towel after each wash. 100μl of the detector antibody, biotinylated polyclonal anti-histone 3 antibody, was added into each well. Again the plate was covered with a plate sealer, and the plate was incubated at room temperature for 1 hour. The wells were washed three times with 1X wash buffer as before. Each well was incubated with 100μl of 1X streptavidin conjugate (400X streptavidin horseradish peroxidase conjugate diluted 1:400, mixed and filtered with a 0.2μm syringe), the plate covered with a plate sealer, followed by incubation at room temperature for 30 minutes. The wells were washed twice with 1X wash buffer as before, then the whole plate was flooded with distilled water, the contents removed, and any residual water tapped off the plate onto paper towel. The chromogenic substrate solution was added, 100μl to each well in the plate and incubated in the dark for 30 minutes at room temperature. Following substrate incubation, 100μl of stop solution (2.5M sulphuric acid) was added to each well, in the same order as the previously added substrate solution. Finally, the plate was read on a spectrophotometric plate reader at dual wavelengths of 450/595 nm. The average absorbance value was obtained from the duplicate standard and sample readings. A standard curve was constructed (figure 2.9) by plotting absorbance for each standard versus concentration of each standard (U/ml), and the nucleosome concentration of each sample was determined by interpolation from the standard curve.

2.7   Western blot analysis

Western blot analysis was carried out in astrocytes cultured in 75cm^2 flasks. Cells were treated according to the study being carried out, and the supernatants collected into Centriplus™ concentrators (Centriplus-3) for concentration into a smaller volume without
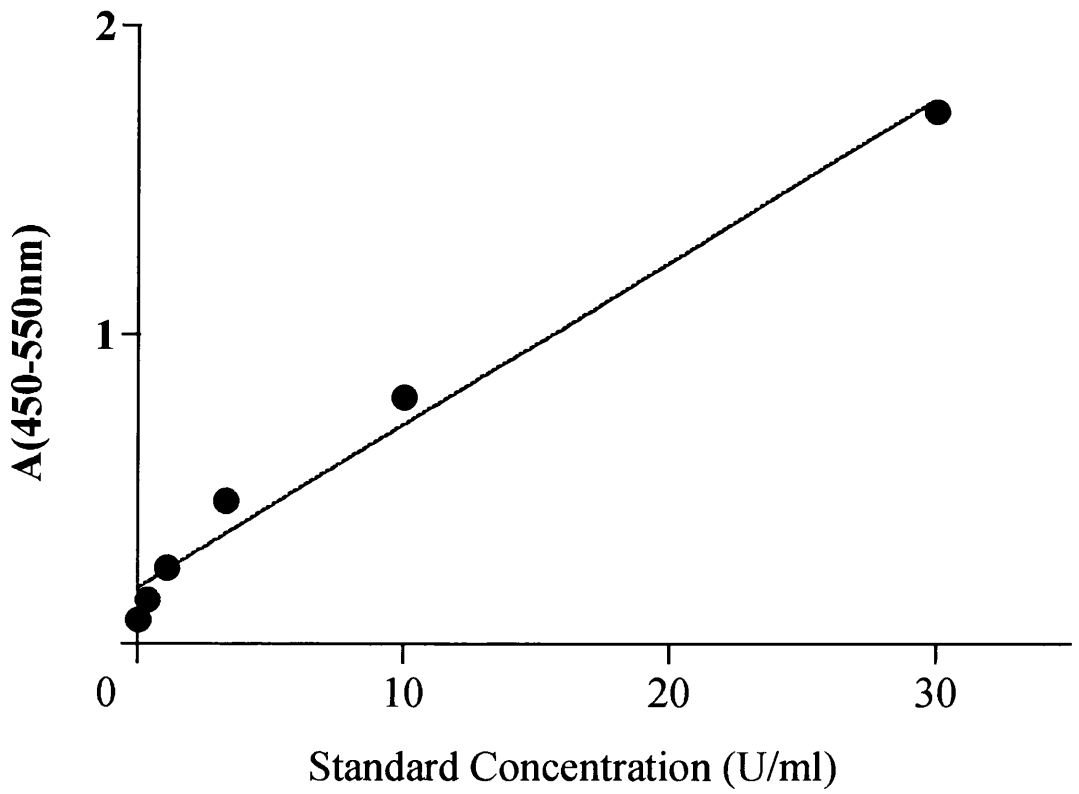
Figure 2.9 **Representative standard curve for the measurement of nucleosomes in unknown samples.**

losing any protein. To the supernatants, 1% FCS was added to keep any proteins stable. The supernatants were centrifuged at 3000g for $6^1/_4$ hours at 4°C and the retentates recovered by an inverted spin of 2000g for 4 minutes at 4°C. The flasks containing the cells were rinsed in sterile PBS and treated with 1ml lysis buffer/flask (see appendix 2) containing 0.2mM PMSF (prepared in ethanol). Flasks and concentrated-supernatants were then frozen at -70°C until required for protein determination. Before the determination of protein, the samples were removed and thawed at room temperature. The astrocytes were removed from the flasks into eppendorf tubes using a cell scraper, while the supernatants were similarly transferred to eppendorfs. The cell samples and supernatants were then homogenised using a hand-held homogeniser (Anachem) and placed on ice.

2.7.1 Protein determination of unknown samples

In order to measure the protein concentration from unknown samples, a standard curve using Bovine Serum Albumin (BSA) of known concentration was prepared. The Bio-Rad protein assay was used to determine protein concentration.

BSA was prepared at 1mg/ml in lysis buffer and a standard curve was prepared in duplicate (table 2.2). A representative standard curve is shown in figure 2.10.

Table 2.2   Standard curve for protein determination

PROTEIN CONCENTRATION (μg/ml)	BSA VOLUME (μl)	WATER VOLUME (μl)
0	0	800
1	1	799
2	2	798
5	5	795
10	10	790
15	15	785
20	20	780
25	25	775
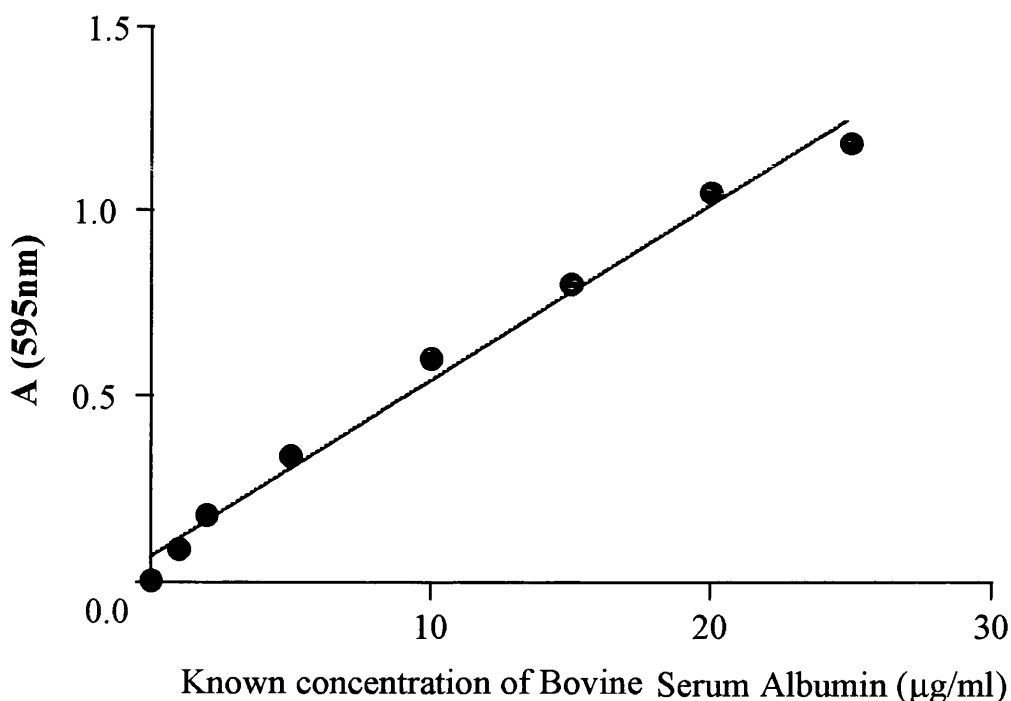
Figure 2.10   Representative standard curve for the measurement of protein in unknown samples

The unknown samples were diluted 1:10, and 10μl of each of the diluted samples was added to 790μl of water in duplicate. 200μl of the Bio-Rad protein assay solution was then added to all the tubes and mixed. Spectrophotometric absorbance readings were made at 595nm and a standard curve of absorbance versus protein concentration (μg/ml) was produced. From the mean absorbance of the unknown samples, the protein concentrations were determined from the standard curve.

2.7.2   SDS-PAGE electrophoresis

Gel plates and spacers were cleaned in water followed by ethanol and assembled in the gel setter, ensuring that there were no leaks. An 8% resolving gel was prepared using

Prosieve-50 (appendix 2) to allow the detection of high and low molecular weight proteins. Polymerisation was initiated with 10% ammonium persulphate (APS) and 10% TEMED. The gel was poured between the gel plates quickly and carefully, and a layer of distilled water was added to the surface of the gel to prevent it from drying out. The gel was allowed to polymerise for at least 1 hour at room temperature. Once set, the water was removed, and any excess was blotted. A 5% stacking gel (appendix 2) was prepared and poured onto the resolving gel, the comb inserted and left to polymerise for a further hour, after which the comb was removed and the wells rinsed with running buffer (72g glycine, 15g Tris, 50ml 10% SDS prepared to a volume of 5l with distilled water). The gels were loaded into a vertical electrophoresis unit and the reservoirs filled $^3/_4$ full with running buffer. Prior to loading, the protein samples were denatured by boiling with 2X sample buffer (appendix 2), 1:1, for 5 minutes. Each sample was then loaded into the gel at a protein concentration of 25µg/ml together with Bio-Rad prestained broad-range protein standards, 20µl/lane, using a Hamilton syringe. A note was made of the sample loading to aid gel identification later. The gel was then run overnight in cooled running buffer at a constant current of 11mA.

2.7.3 Western blotting

Following the gel run, the protein was transferred from the gel to polyvinyl difluoride (PVDF) membrane using the method of wet transfer. The top gel plate was removed, the stacker gel cut away with a scalpel, and the resolving gel was soaked in transfer buffer (72g glycine, 15g Tris, 1l methanol prepared to a final volume of 5l) for 15-20 minutes. A corner of the gel was cut away to aid orientation. Blotting paper, two sheets per membrane, were cut to the same size as the sponges used in the transfer tank. PVDF membranes were cut to the same size as the gel (12 x 13 cm). While the gels were soaking

in transfer buffer, the blotting paper and sponges were thoroughly soaked in transfer buffer, while the PVDF membranes soaked in methanol for a few seconds. The membranes were then transferred to distilled water to remove the methanol for 1-2 minutes, followed by soaking in transfer buffer. For wet transfer of the proteins, a sponge was placed on top of the outer mesh. A sheet of blotting paper was laid on top followed by the gel. The PVDF membrane was carefully placed on top followed by the second sheet of blotting paper. At this stage, any air bubbles that may have formed between the gel and the membrane were rolled out carefully. Another sponge was placed on top of the blotting paper and the whole apparatus was held in place by attaching the second mesh. The transfer set-up was placed into the transfer tank so that the membrane faced the anode, and the proteins were transferred for 3 hours at 80V. Following successful transfer of proteins onto the membrane, the PVDF membrane was rinsed thoroughly in 0.2% Tween 20-Tris buffered saline (T-TBS), pH 7.5 (appendix 2). To block non-specific sites, membranes were incubated with 5% Marvel in T-TBS for 1 hour at room temperature. Membranes were washed thoroughly in T-TBS, 3 x 10 minutes. Optimised concentrations of primary antibodies were prepared in T-TBS and incubated with the membranes overnight at 4°C. The primary antibodies were poured off and the membranes were washed in T-TBS for 3 x 10 minutes. Horseradish peroxidase conjugated secondary antibodies directed against the immunoglobulins from the species used to prepare the primary antibodies were prepared in 3% Marvel/TBS-T, at the required concentration, and incubated with membranes for 1 hour at room temperature. The blots were washed with T-TBS thoroughly for 3 x 10 minutes. Visualisation of the protein bands was carried out using the enhanced chemiluminescence (ECL) method. While the membranes were washing, the ECL reagent was prepared in a 1:1 solution to obtain a final volume of $0.125ml/cm^2$ membrane. The membranes were blotted of any excess T-TBS and placed onto SaranWrap, proteins facing upwards. Membranes

were incubated with the ECL reagent for 1 minute precisely. Working quickly, membranes were carefully blotted vertically onto a sheet of blotting paper to remove any excess ECL reagent. The membranes were then placed protein side down onto SaranWrap (pre-cut). The SaranWrap was closed, avoiding any pressure on the membrane, to form an envelope. The membranes were placed into film cassettes protein side up, and in the dark, a sheet of autoradiography film (Fujifilm) was placed on top of each membrane. The cassette was closed and the membrane exposed to the film for 15 seconds initially. The films were immediately developed to assess the optimal exposure time required.

Following ECL detection, the same membranes were reprobed with a variety of antibodies. The membranes were first stripped of the bound antibodies by submerging the membrane in stripping buffer (100mM 2-mercaptoethanol, 2% sodium dodecyl sulphate, 62.5mM Tris-HCl, pH 6.7) and incubated at 50°C for 30 minutes with occasional agitation. The membranes were washed in TBS-T, 2 x 10 minutes and then blocked in 5% Marvel in TBS-T for 1 hour at room temperature. Immunodetection could then be carried out again as described above.

CHAPTER 3

MAPPING BRAIN FUNCTION WITH GROUP II SELECTIVE

METABOTROPIC GLUTAMATE RECEPTOR AGONISTS

3.1 Introduction

Existing ligands for mGluR2 and mGluR3 have been useful for investigating the properties of these receptors *in vitro*, but their utility as pharmacological tools *in vivo* has been limited for a number of reasons. Previous studies have shown that some so-called 'selective' mGluR ligands can also activate other classes of glutamate receptors. For example, the most widely used mGluR 2/3 agonist to date (2S, 1'R, 2'R, 3'R)-2-(2', 3'-dicarboxycyclopropyl) glycine, DCG-IV, is also a relatively potent NMDA receptor agonist (Wilsch *et al.*, 1994). In addition, none of the existing compounds for mGluR2 or mGluR3 have demonstrated potent central effects after systemic administration.

The two recently developed mGluR agonists, (1SR,2SR,5RS,6SR)-2-aminobicyclo[3.1.0]hexane-2,6-dicarboxylate, LY354740 (Monn *et al.*, 1997) and a heterobicyclic amino acid related to this molecule, (1R,4R,5S,6R)-2-oxa-4-aminobicyclo[3.1.0]hexane-4,6-dicarboxylate, LY379268 (Monn *et al.*, in press) are novel, potent agonists selective for Group II mGluRs. They are the first mGluR2/3 selective agonists to be effective when administered systemically (Monn *et al.*, 1996; in press; Bond *et al.*, 1997; Schoepp *et al.*, 1997) and their pharmacology are discussed in chapter 8, section 8.1. However, the precise action of these ligands centrally is poorly defined. Insight into the functional events within individual brain regions is possible by measuring the rates of local cerebral glucose utilisation using the [^{14}C]2-deoxyglucose autoradiographic technique (Sokoloff *et al.*, 1977). For the purpose of the present study, the [^{14}C]2-DG autoradiographic technique was employed to determine the functional events in the brain following the systemic administration of LY354740 or LY379268.

3.2   Methods

3.2.1   Animal preparation and [^{14}C]2-deoxyglucose measurement

Forty-three male Sprague-Dawley rats weighing between 300-400g (Harlan Olac, Bicester, UK) were used for this study. All animals were allowed to acclimatise to their surroundings for at least 5 days before surgery. Rats were housed under natural daylight conditions, and food and water were provided *ad libitum*. On the day of the experiment, the animals were anaesthetised and cannulated (section 2.1.1). Following recovery from the anaesthetic, rats were placed into individual boxes and body temperature was kept normothermic with heating lamps. The [^{14}C]2-DG procedure was then carried out as detailed in section 2.1.4.

3.2.2   Drug administration and physiological monitoring

The compounds LY354740 (0.3, 3.0, 30.0mg/kg) and LY379268 (0.1, 1.0, 10.0mg/kg) were dissolved in 0.7ml saline (0.9%). An intravenous bolus injection of either agent was administered via the femoral vein catheter, 10 minutes prior to the injection of [^{14}C]2-DG. Control animals (n = 11) received vehicle (0.9% saline).

Any physiological effects of the agonists were also measured. Mean arterial blood pressure was monitored (Gould Instruments) for at least 20 minutes before the pulse of [^{14}C]2-DG was administered and then subsequently discontinued. Rectal temperature was monitored throughout the experiment. Arterial blood samples were also taken 10 minutes before, and 5 and 45 minutes after, drug administration for analysis of pCO_2, pO_2 and pH levels (n = 40).

3.2.3 Data analysis

Local rates of glucose utilisation were determined in 43 separate brain regions using quantitative densitometric analysis. As the consequences of the systemic administration of mGluR agonists on brain function were unknown, brain regions were chosen from the rostral to the caudal extent of the brain for analysis. All the data were analysed initially by ANOVA to identify brain regions associated with significant alterations in glucose use, followed by two-tailed Student's unpaired t-test. A Bonferroni correction factor of 3 was applied to the probability values to take into account the comparisons between each control and drug treatment groups. Each drug was compared with contemporaneous, randomised vehicle treated control animals.

The extent of responsiveness of each of the 43 regions measured to LY354740 (0.3, 3.0, 30mg/kg) and LY379268 (0.1, 1.0, 10mg/kg) was assessed by applying an arithmetic function (f). This arithmetic function incorporates all the dose response data available for each of the brain regions and enables a 'rank order of responsiveness' for each region to be obtained. The f value is derived from:-

$$f = \Sigma(x_c - x_{Ti})^2$$

where x_c is the mean of $\log_e$(glucose use) for the control group members, and x_{Ti} is the mean of $\log_e$(glucose use) for the ith dose of the treatment group, T. The reliability of this method of data handling has previously been described (Ford $et\ al.$, 1985). A frequency distribution of responsiveness was generated for LY354740 and LY379268.

3.3   Results

3.3.1   Physiological parameters

The intravenous administration of LY354740 (0.3, 3.0, 30mg/kg) and LY379268 (0.1, 1.0, 10mg/kg) produced no detectable changes in mean arterial blood pressure or

blood gas levels. However, both compounds induced a small increase in rectal temperature 45 minutes after the administration of the agonists (tables 3.1-3.2).

Prior to drug administration, all the rats exhibited signs of inquisitive behaviour, with intermittent periods of movement and grooming. They all responded to auditory, visual, and tactile stimulation. Following the administration of LY354740 and LY379268, marked changes in the gross behaviour between the two different treatment groups of the rats were noted. No major overt changes in behaviour of LY354740 treated animals were observed, although they appeared less active than the vehicle treated controls. In contrast, animals treated with LY379268 (10mg/kg) appeared especially hypersensitive to auditory stimuli. Following the administration of the drug, the rats would appear less active with little body movement. However, noises would trigger a noticeable startle response which remained for the duration of the experiment. Plasma glucose levels were significantly increased 45 minutes after LY379268 (10 mg/kg) compared with control levels. Similar changes in glucose levels were not detected following LY354740 administration.

3.3.2 LY354740 and local cerebral glucose utilisation

The function-related glucose utilisation values associated with LY354740 are presented in tables 3.3-3.7. LY354740 (0.3, 3.0, 30mg/kg) produced anatomically widespread changes in glucose utilisation in a dose-dependent manner throughout the CNS. Only one region, the superficial layer of the superior colliculus, displayed significant increases in glucose use with LY354740, while 18 regions displayed significant decreases in glucose use. No significant changes in glucose use were detected in any regions in animals treated with LY354740 (0.3 mg/kg). However, at LY354740 (3.0 mg/kg), 4 out of the 42 brain areas measured demonstrated statistically significant changes from the vehicle treated controls: red nuclei (-16 %), mammillary body (-25 %), anterior thalamus (-29 %) and the

superficial layer of the superior colliculus (+50 %). An additional 15 brain regions displayed statistically significant reductions in function related glucose use (P<0.05) in animals treated with LY354740 (30 mg/kg). Function-related glucose use was significantly reduced in over 50% of the cortical regions measured in animals treated with LY354740 (30 mg/kg). In order to determine whether this depression in glucose use affected all layers of the cortex, local rates of glucose utilisation were measured in layers II/III, IV and V/VI in the parietal cortex. Table 3.4 demonstrates that the magnitude of the reductions in glucose use after LY354740 was similar in all cortical layers examined and did not exhibit any selectivity.

The magnitude of the f values provides an indication of how pronounced the alterations in glucose use were within a particular region across the entire dose-response relationship (a high value signifies the most pronounced alterations). Thus the application of the f rank allows the regional responses of LY354740 to be rank ordered (table 3.8) and the frequency distribution of responsiveness to be generated. The most pronounced changes after LY354740 (i.e. largest f values) were seen in the anteroventral thalamic nucleus, mammillary body, superficial layer of the superior colliculus, anterior cingulate cortex and lateral habenular nuclei ($f > 0.15$). For other regions, the f values were normally distributed around a mean of 0.05 (figure 3.7). This distribution of f values reflects the relative homogeneous effects of LY354740 on function related glucose utilisation globally in the CNS.

3.3.3 LY379268 and local cerebral glucose utilisation

LY379268 (0.1, 1.0 and 10 mg/kg) produced anatomically circumscribed and dose-dependent changes in glucose utilisation (tables 3.3-3.7). Six regions displayed significant increases in glucose use after LY379268 (the superficial layer of the superior colliculus, locus coeruleus, genu of the corpus callosum, cochlear nucleus, inferior colliculus and the

molecular layer of the hippocampus) and 3 regions displayed significant decreases (mammillary body, anteroventral thalamic nucleus, and the lateral habenular nucleus). Following LY379268 (0.1 mg/kg), only the locus coeruleus demonstrated a statistically significant increase in glucose use from the vehicle treated controls. After LY379268 (1 mg/kg) significant alterations in glucose use were observed in the superior colliculus (+63%), locus coeruleus (+57%), molecular layer of the hippocampus (+14%) and the genu of the corpus callosum (+31%). In no region were significant reductions in glucose use observed after LY379268 (1 mg/kg). After LY379268 (10 mg/kg) significant alterations in glucose use were observed in the superficial layer of the superior colliculus (+81%), locus coeruleus (+52%), mammillary body (-34%), anteroventral thalamic nucleus (-28%), lateral habenular nucleus (-24%), cochlear nucleus (+26%) and inferior colliculus (+20%). As a result of the changes in glucose use demonstrated in cortical regions of animals treated with LY354740, local rates of glucose utilisation were measured in layers II/III, IV and V/VI of the sensory motor cortex (table 3.4). This region was chosen because of the sensory changes in behaviour noted in animals treated with LY379268 (10 mg/kg). Glucose use in the sensory motor cortex was not significantly altered statistically (the issue of statistical analysis is discussed further in appendix 4). However, a demonstrable trend of increasing glucose use with increasing LY379268 dose can be seen in the sensory motor cortex (all layers), which then returned to levels comparable with vehicle treated controls at the highest dose of 10 mg/kg.

The frequency distribution and rank order of responsiveness are presented in figure 3.7 and table 3.8, respectively. The anatomically circumscribed effects of LY379268 demonstrated by the numerical data were also apparent from the skewed distribution of f values obtained from the dose response data with LY379268. Brain areas in which the most pronounced changes were identified; i.e. where $f > 0.15$ were the superficial layer of the

Table 3.1   LY354740: Physiological variables.

Time (relative to drug administration) /minutes	Vehicle	LY354740 (mg/kg)		
		0.3	3.0	30
Rectal temperature (°C)				
-10	37.6 ± 0.2	37.7 ± 0.2	37.6 ± 0.1	37.7 ± 0.1
0	37.5 ± 0.3	37.7 ± 0.2	37.7 ± 0.1	38.0 ± 0.2
5	37.5 ± 0.3	37.7 ± 0.2	37.8 ± 0.1	37.7 ± 0.2
45	37.4 ± 0.3	37.8 ± 0.2	38.2 ± 0.1*	38.2 ± 0.2*
Mean arterial blood pressure (mmHg)				
-10	115 ± 5	121 ± 3	113 ± 3	117 ± 2
0	113 ± 6	120 ± 5	116 ± 4	118 ± 2
5	113 ± 5	119 ± 5	123 ± 5	121 ± 4
Arterial plasma glucose (mM)				
-10	5.9 ± 0.5	6.3 ± 0.2	6.0 ± 0.5	6.2 ± 0.5
45	7.8 ± 0.2	7.0 ± 0.3	7.4 ± 0.3	8.0 ± 0.6
pCO_2 (mmHg)				
-10	31 ± 4	31 ± 4	32 ± 2	30 ± 4
5	29 ± 1	32 ± 1	29 ± 2	29 ± 3
45	35 ± 2	37 ± 3	28 ± 1	37 ± 3
pO_2 (mmHg)				
-10	110 ± 13	96 ± 7	102 ± 13	92 ± 3
5	88 ± 3	94 ± 5	117 ± 16	90 ± 1
45	97 ± 3	95 ± 4	119 ± 15	90 ± 3
pH				
-10	7.5 ± 0.01	7.4 ± 0.02	7.4 ± 0.01	7.4 ± 0.01
5	7.4 ± 0.01	7.4 ± 0.01	7.4 ± 0.01	7.4 ± 0.01
45	7.4 ± 0.01	7.4 ± 0.00	7.4 ± 0.03	7.4 ± 0.01
number of animals	5	5	5	5

Data are presented as mean $\pm$ SEM. *$P < 0.05$ for statistical comparison between vehicle and drug treated groups at each time point (ANOVA, Student's unpaired t-test with Bonferroni correction)

Table 3.2   LY379268: Physiological variables.

| Time (relative to drug administration) /minutes | Vehicle | LY379268 (mg/kg) | | |
		0.1	1.0	10
Rectal temperature (°C)				
-10	37.8 ± 0.2	37.7 ± 0.2	38.1 ± 0.1	38.1 ± 0.3
0	37.8 ± 0.2	37.6 ± 0.2	38.0 ± 0.1	38.0 ± 0.2
5	37.9 ± 0.2	37.7 ± 0.2	38.0 ± 0.1	37.9 ± 0.2
45	37.7 ± 0.3	37.7 ± 0.2	38.8 ± 0.2 *	37.9 ± 0.3
Mean arterial blood pressure (mmHg)				
-10	124 ± 3	120 ± 3	123 ± 3	121 ± 3
0	123 ± 3	121 ± 5	125 ± 4	125 ± 3
5	126 ± 4	125 ± 5	127 ± 4	131 ± 3
Arterial plasma glucose (mM)				
-10	5.8 ± 0.4	5.0 ± 0.5	5.4 ± 0.6	6.2 ± 0.3
45	8.0 ± 0.3	8.0 ± 0.1	7.8 ± 0.3	10.2 ± 0.2***
pCO$_2$ (mmHg)				
-10	41 ± 5	36 ± 5	40 ± 4	41 ± 1
5	36 ± 4	39 ± 2	42 ± 1	37 ± 1
45	37 ± 3	39 ± 5	39 ± 4	41 ± 3
pO$_2$ (mmHg)				
-10	98 ± 8	112 ± 7	96 ± 2	93 ± 8
5	98 ± 5	94 ± 2	107 ± 10	100 ± 2
45	101 ± 2	107 ± 6	98 ± 5	102 ± 4
pH				
-10	7.4 ± 0.02	7.4 ± 0.01	7.4 ± 0.02	7.5 ± 0.01
5	7.4 ± 0.03	7.4 ± 0.02	7.4 ± 0.02	7.5 ± 0.01
45	7.4 ± 0.02	7.4 ± 0.01	7.4 ± 0.02	7.4 ± 0.02
number of animals	5	5	5	5

Data are presented as mean $\pm$ SEM. *P<0.05, ***P<0.001 for statistical comparison between vehicle and drug treated groups at each time point (ANOVA, Student's unpaired t-test with Bonferroni correction)

Table 3.3   Glucose utilisation following administration of LY354740 and LY379268: Primary visual and auditory system.

STRUCTURE	LY354740				LY379268				fVALUE	
	Vehicle	0.3	3.0	30	Vehicle	0.1	1.0	10	LY354740	LY379268
Primary visual system										
Visual cortex (layer IV)	103 ± 7	87 ± 2	87 ± 9	75 ± 4*	90 ± 3	95 ± 3	90 ± 5	88 ± 5	0.149	0.004
Lateral geniculate body	83 ± 4	70 ± 3	80 ± 7	81 ± 3	69 ± 6	73 ± 3	86 ± 6	85 ± 6	0.028	0.106
Superior colliculus:										
superficial layer	87 ± 5	78 ± 4	130 ± 11***	128 ± 5***	73 ± 4	77 ± 3	119 ± 7***	132 ± 7***	0.328	0.599
deep layer	92 ± 5	81 ± 2	80 ± 4	70 ± 2***	77 ± 4	80 ± 2	79 ± 2	68 ± 2	0.112	0.018
Vestibular nucleus	126 ± 5	112 ± 4	123 ± 3	103 ± 4**	109 ± 4	109 ± 3	114 ± 5	104 ± 5	0.056	0.004
Primary auditory system										
Auditory cortex (layer IV)	132 ± 6	136 ± 2	134 ± 10	110 ± 6	126 ± 5	139 ± 9	145 ± 7	127 ± 5	0.035	0.030
Medial geniculate body	121 ± 6	114 ± 5	113 ± 8	100 ± 4	101 ± 5	105 ± 5	110 ± 4	102 ± 5	0.048	0.008
Inferior colliculus	180 ± 8	173 ± 6	168 ± 8	164 ± 6	162 ± 7	164 ± 6	180 ± 8	194 ± 11*	0.016	0.044
Superior olivary nucleus	136 ± 9	131 ± 4	119 ± 6	112 ± 7	119 ± 6	123 ± 4	128 ± 4	118 ± 8	0.056	0.006
Cochlear nucleus	152 ± 5	146 ± 5	142 ± 10	146 ± 8	140 ± 7	146 ± 7	161 ± 7	176 ± 8**	0.008	0.076
Number of animals	6	5	5	7	5	5	5	5		

Data are presented as mean ± SEM (μmol/100g/minutes)

*P<0.05, **P<0.01, ***P<0.001 for statistical comparison between vehicle and drug treated groups (ANOVA, Student's unpaired t-test with Bonferroni correction)

f values produce a measure of regional responsiveness and the values were derived from the above data using the arithmetic function described in section 3.2.3

Table 3.4   Glucose utilisation following administration of LY354740 and LY379268: Cortical regions.

STRUCTURE	LY354740 (mg/kg)				LY379268 (mg/kg)				fVALUE	
	Vehicle	0.3	3.0	30	Vehicle	0.1	1.0	10	LY354740	LY379268
Parietal cortex:										
layer II/III	99 ± 5	92 ± 3	93 ± 9	78 ± 3 *					0.0675	
layer IV	123 ± 7	115 ± 4	110 ± 10	93 ± 3 **	98 ± 2	104 ± 3	103 ± 3	94 ± 4	0.0933	0.008
layer V/VI	99 ± 4	93 ± 3	90 ± 8	80 ± 2 *					0.0538	
Sensory motor cortex:										
layer II/III					86 ± 3	95 ± 4	105 ± 5	90 ± 7		0.056
layer IV	133 ± 7	123 ± 6	119 ± 10	109 ± 5	108 ± 3	123 ± 4	133 ± 8	114 ± 11	0.0581	0.064
layer VI					83 ± 3	90 ± 3	105 ± 8	84 ± 7		0.058
Anterior cingulate cortex	117 ± 11	100 ± 3	101 ± 14	78 ± 4 **	101 ± 4	104 ± 4	104 ± 5	85 ± 7	0.2126	0.031
Frontal cortex	115 ± 8	106 ± 3	106 ± 10	88 ± 4*	105 ± 3	111 ± 3	114 ± 7	102 ± 6	0.0843	0.013
Prefrontal	125 ± 8	124 ± 5	121 ± 12	106 ± 3	101 ± 8	114 ± 3	117 ± 5	99 ± 5	0.0296	0.038
Number of animals	6	5	5	7	5	5	5	5		

Data are presented as mean ± SEM (μmol/100g/minutes)

*P<0.05, **P<0.01, ***P<0.001 for statistical comparison between vehicle and drug treated groups (ANOVA, Student's unpaired t-test with Bonferroni correction)

f values produce a measure of regional responsiveness and the values were derived from the above data using the arithmetic function described in section 3.2.3

Table 3.5   Glucose utilisation following administration of LY354740 and LY379268: Extrapyramidal and sensory motor regions.

STRUCTURE	LY354740 (mg/kg)				LY379268 (mg/kg)				fVALUE	
	Vehicle	0.3	3.0	30	Vehicle	0.1	1.0	10	LY354740	LY379268
Caudate-putamen	116 ± 8	109 ± 4	112 ± 8	96 ± 4	88 ± 5	96 ± 3	99 ± 5	100 ± 7	0.0425	0.034
Globus pallidus	64 ± 3	57 ± 2	56 ± 5	54 ± 2	53 ± 2	55 ± 1	59 ± 4	53 ± 3	0.0661	0.013
Substantia nigra:										
pars compacta	82 ± 3	73 ± 2	75 ± 5	67 ± 3**	70 ± 3	77 ± 2	77 ± 3	74 ± 2	0.0649	0.022
pars reticulata	50 ± 2	47 ± 1	49 ± 4	50 ± 1	48 ± 3	53 ± 2	52 ± 1	48 ± 1	0.0048	0.022
Thalamus:										
mediodorsal	108 ± 7	93 ± 4	92 ± 9	81 ± 2**	95 ± 6	104 ± 5	102 ± 4	86 ± 5	0.1322	0.023
ventrolateral	88 ± 4	78 ± 4	80 ± 6	77 ± 3	71 ± 5	77 ± 2	79 ± 4	72 ± 6	0.0433	0.021
Subthalamic nucleus	92 ± 4	82 ± 3	80 ± 7	80 ± 2	83 ± 3	84 ± 3	87 ± 4	80 ± 3	0.0540	0.004
Inferior olivary nucleus	71 ± 5	75 ± 2	82 ± 6	73 ± 3					0.0261	
Red nucleus	87 ± 4	76 ± 2	73 ± 5*	65 ± 2***	70 ± 2	75 ± 1	72 ± 4	65 ± 2	0.1309	0.011
Cerebellum:										
cortex	62 ± 3	58 ± 1	59 ± 3	55 ± 2	59 ± 3	67 ± 3	63 ± 3	56 ± 3	0.0178	0.025
white matter	36 ± 2	37 ± 1	35 ± 3	35 ± 1	37 ± 3	38 ± 1	39 ± 3	29 ± 1	0.0020	0.057
Number of animals	6	5	5	7	5	5	5	5		

Data are presented as mean ± SEM (μmol/100g/minutes)

*P<0.05, **P<0.01, ***P<0.001 for statistical comparison between vehicle and drug treated groups (ANOVA, Student's unpaired -test with Bonferroni correction)

f values produce a measure of regional responsiveness and the values were derived from the above data using the arithmetic function described in section 3.2.3

Table 3.6   Glucose utilisation following administration of LY354740 and LY379268: Limbic system and other brain regions.

STRUCTURE	LY354740 (mg/kg)				LY379268 (mg/kg)				fVALUE	
	Vehicle	0.3	3.0	30	Vehicle	0.1	1.0	10	LY354740	LY379268
Hippocampus (molecular layer)	83 ± 3	82 ± 1	81 ± 2	67 ± 3***	69 ± 3	74 ± 4	79 ± 1*	69 ± 2	0.0476	0.023
Dentate gyrus	68 ± 3	71 ± 1	69 ± 2	58 ± 3*	59 ± 2	63 ± 3	63 ± 1	58 ± 2	0.0290	0.008
Lateral habenular nucleus	102 ± 8	101 ± 7	100 ± 9	69 ± 4**	88 ± 4	94 ± 3	92 ± 6	67 ± 7*	0.1522	0.079
Median raphe nucleus	91 ± 5	88 ± 2	83 ± 6	70 ± 3**	77 ± 4	84 ± 4	74 ± 4	66 ± 1	0.0799	0.033
Mammillary body	115 ± 6	103 ± 3	87 ± 8**	66 ± 2***	94 ± 6	99 ± 5	89 ± 4	62 ± 2***	0.3989	0.172
Amygdala	48 ± 3	45 ± 2	53 ± 4	45 ± 2	43 ± 1	44 ± 1	51 ± 3	47 ± 4	0.0201	0.041
Septal nucleus	51 ± 3	44 ± 2	49 ± 5	42 ± 2	43 ± 3	44 ± 1	48 ± 3	40 ± 3	0.0663	0.020
Nucleus accumbens	90 ± 6	83 ± 2	81 ± 5	74 ± 2	73 ± 5	82 ± 2	89 ± 6	81 ± 5	0.0538	0.055
Pons	67 ± 3	57 ± 3	60 ± 5	53 ± 3*	54 ± 3	56 ± 2	55 ± 2	50 ± 1	0.0982	0.009
Locus coeruleus	±	±	±	±	44 ± 4	62 ± 2***	69 ± 2***	67 ± 2***		0.490
Hypothalamus	50 ± 4	41 ± 3	47 ± 6	47 ± 2	42 ± 2	41 ± 1	47 ± 3	48 ± 2	0.0508	0.030
Anteroventral thalamic nucleus	129 ± 8	123 ± 4	92 ± 10**	70 ± 2***	109 ± 4	119 ± 5	101 ± 6	78 ± 5**	0.5006	0.123
Number of animals	6	5	5	7	5	5	5	5		

Data are presented as mean ± SEM (μmol/100g/minutes)

*P<0.05, **P<0.01, ***P<0.001 for statistical comparison between vehicle and drug treated groups (ANOVA, Student's unpaired t-test with Bonferroni correction)

f values produce a measure of regional responsiveness and the values were derived from the above data using the arithmetic function described in section 3.2.3

Table 3.7   Glucose utilisation following administration of **LY354740** and **LY379268: White matter.**

STRUCTURE	LY354740 (mg/kg)				LY379268 (mg/kg)				ƒVALUE	
	Vehicle	0.3	3.0	30	Vehicle	0.1	1.0	10	LY354740	LY379268
Internal capsule	40 ± 4	34 ± 2	36 ± 4	35 ± 1	31 ± 1	31 ± 1	36 ± 3	33 ± 3	0.0539	0.029
Corpus callosum	44 ± 2	38 ± 1	38 ± 3	38 ± 2	34 ± 3	36 ± 2	39 ± 2	34 ± 2	0.0620	0.020
Genu of the corpus callosum	33 ± 3	26 ± 1	31 ± 3	28 ± 1	26 ± 1	27 ± 1	34 ± 3*	31 ± 3	0.0696	0.110
Number of animals	6	5	5	7	5	5	5	5		

Data are presented as mean ± SEM (μmol/100g/minutes)

*P<0.05, **P<0.01, ***P<0.001 for statistical comparison between vehicle and drug treated groups (ANOVA, Student's unpaired t-test with Bonferroni correction)

ƒ values produce a measure of regional responsiveness and the values were derived from the above data using the arithmetic function described in section 3.2.3

superior colliculus, locus coeruleus, mammillary body and the anteroventral thalamic nucleus.

3.3.4   Comparison of LY354740 and LY379268

Both LY354740 and LY379268 produced dose-dependent changes in glucose utilisation. The numerical alteration in glucose use, the computed f values and visual inspection of the autoradiograms, indicate that there were some similarities in the regional response to both metabotropic glutamate agonists, i.e. the increased glucose use in the superficial layer of the superior colliculus and the marked reductions in glucose use in 3 limbic areas (mammillary body, anteroventral thalamic nucleus, lateral habenular nucleus) after both agonists (figure 3.1-3.4). Despite these similar effects, the overall patterns of glucose use response to the two metabotropic agents were quite dissimilar (figure 3.5). LY354740 produced anatomically widespread reductions in glucose use while LY379268 affected a smaller number of brain regions which displayed increases in glucose metabolism. More specifically, following LY354740 administration, there were widespread reductions in glucose use not just in limbic areas, but also in the cerebral cortex and motor areas (substantia nigra, red nucleus). In autoradiograms from animals treated with LY354740, there was a loss of anatomical detail and sharpness of image reflecting the widespread metabolic depression. Following LY379268, there was no widespread reduction in glucose use, with the mean rate of glucose use tending to be greater than in vehicle-treated animals. In a number of regions, for example, some auditory relay nuclei and the hippocampus, the increased glucose use achieved statistical significance. In contrast to the LY354740 autoradiograms, the autoradiograms from animals treated with LY379268 showed excellent anatomical detail and sharpness of image.

118

Further comparisons of the functional consequences of LY354740 and LY379268 in the brain can be achieved by examination of the f ranking function. An f value is generated for each brain region independently for the effects of LY354740 or LY379268. By inspecting the f ranking hierarchies of the two agonists (table 3.8), it can be seen that some regions of the brain were extremely sensitive (largest f values) to both LY354740 and LY379268. These brain regions were the superficial layer of the superior colliculus, mammillary body and the anteroventral thalamic nucleus. At the other end of the spectrum, brain regions moderately and minimally responsive to LY354740 and LY379268 were different. Considering the overall pattern of the f ranking hierarchies, the profiles of the agonists in the brain appear to differ. The heterogeneity of the regional responses of the two agonists is demonstrated by their different f value frequency distributions, and in addition, is highlighted by the absence of association between the calculated f values (figure 3.7-8). Using Spearman's rank-order correlations, the overall correlation coefficient for all regions generated $r = -0.075$ ($P = 0.65$), indicating that the two compounds have selectively different sites of action in the brain. However, from both the numerical data and f values, both compounds displayed some similar changes in glucose use in the limbic system. The correlation coefficient for limbic areas produced $r = 0.44$ ($P = 0.47$), which suggests that the effects of the two agonists in the limbic system are slightly more similar.
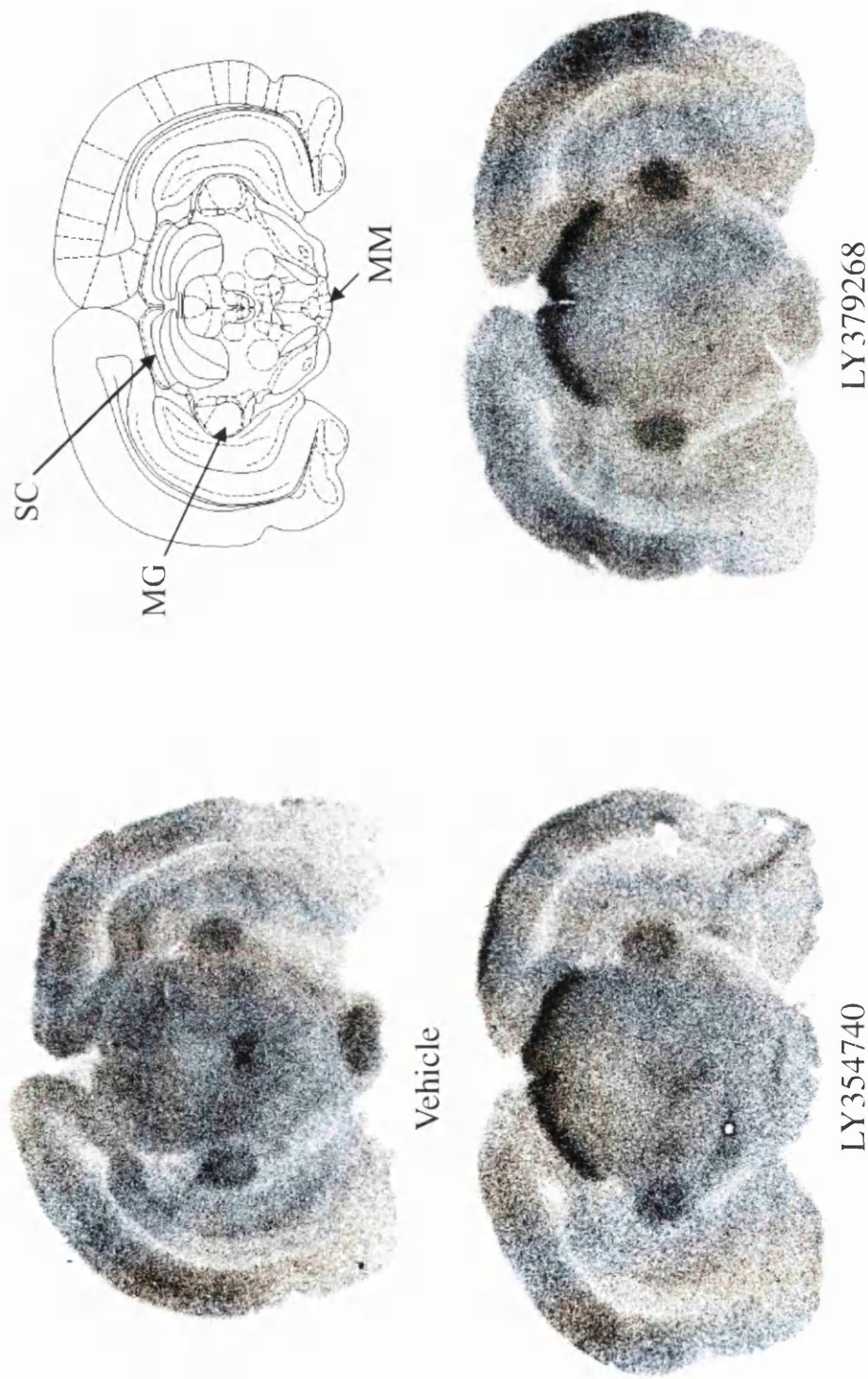
Figure 3.1   Glucose use in the superficial layer of the superior colliculus is sensitive to LY354740 and LY379268.

Representative autoradiograms illustrating the similar changes in glucose utilisation in the superficial layer of the superior colliculus (SC) following vehicle, LY354740 (30mg/kg) and LY379268 (10mg/kg). Note also the reduction in glucose use in mammillary body following both agonists.

MG = medical geniculate body. MM = mammillary body.
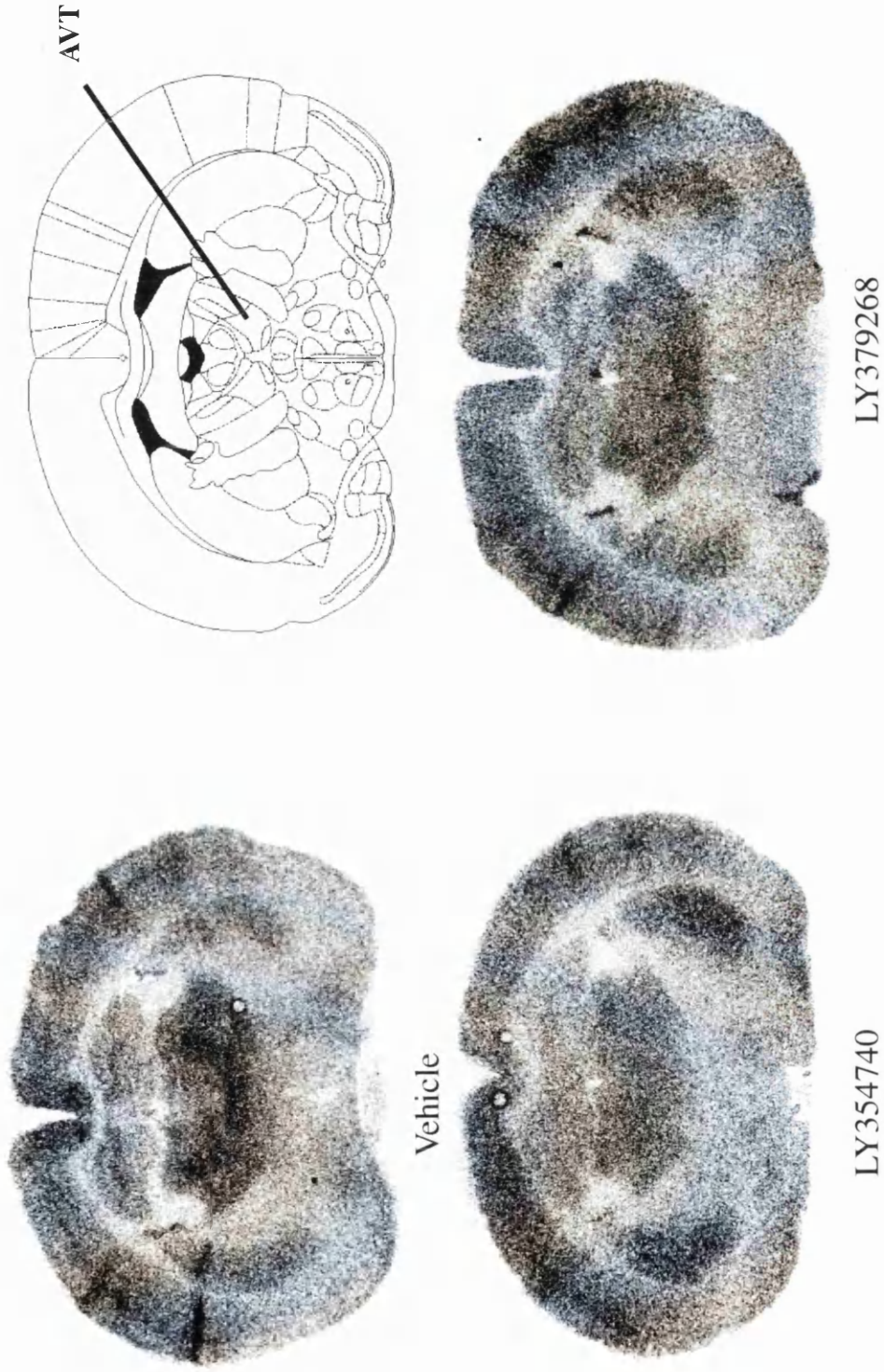
Figure 3.2   Glucose use in the anteroventral thalamic nucleus is sensitive to LY354740 and LY379268.

Representative autoradiograms illustrating the similar changes in glucose utilisation in the anteroventral thalamic nucleus (AVT) following: vehicle, LY354740 (30mg/kg) and LY379268 (10mg/kg).

MAMMILLARY BODY
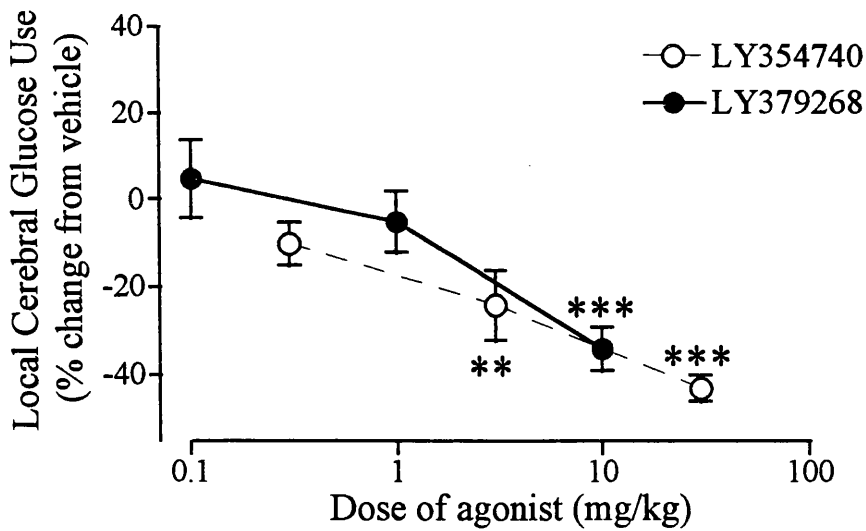
ANTEROVENTRAL THALAMIC NUCLEUS
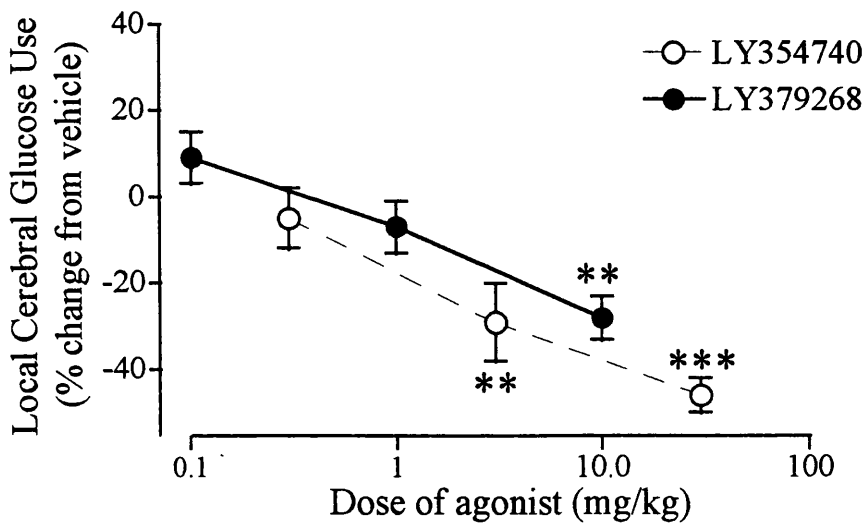
Figure 3.3   mGluR agonists and local cerebral glucose use: homogeneous responses to LY354740 and LY379268.

The data are presented as % change in glucose utilisation relative to glucose use in vehicle treated control animals (mean ± SEM). In both the mammillary body and anteroventral thalamic nucleus, LY354740 produces a greater magnitude of glucose use reduction.
*$P<0.05$, **$P<0.01$, ***$P<0.001$ (ANOVA followed by Student's t-test with Bonferroni correction).

LATERAL HABENULAR NUCLEUS
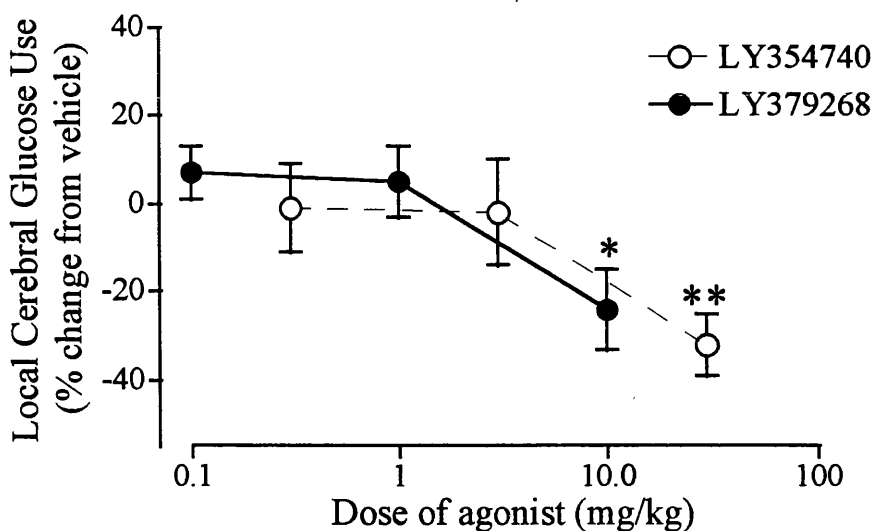
SUPERIOR COLLICULUS
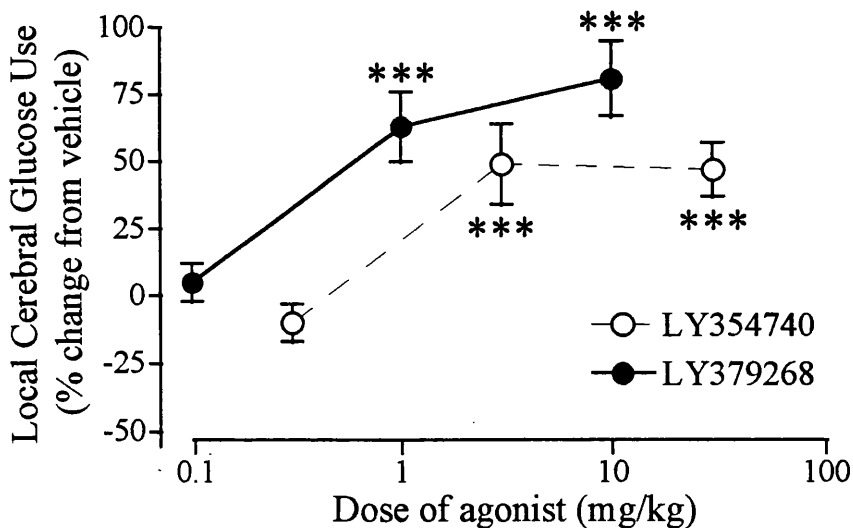
Figure 3.4 **mGluR agonists and local cerebral glucose use: homogeneous responses to LY354740 and LY379268.**

The data are presented as % change in glucose utilisation relative to glucose use in vehicle treated control animals (mean ± SEM). While the magnitude of glucose use reductions is similar in the lateral habenular nucleus following both LY354740 and LY379268, note the greater potency of LY379268 over LY354740 in the superficial layer of the superior colliculus.

*P<0.05, **P<0.01, ***P<0.001 (ANOVA followed by Student's *t*-test with Bonferroni correction).

VISUAL CORTEX
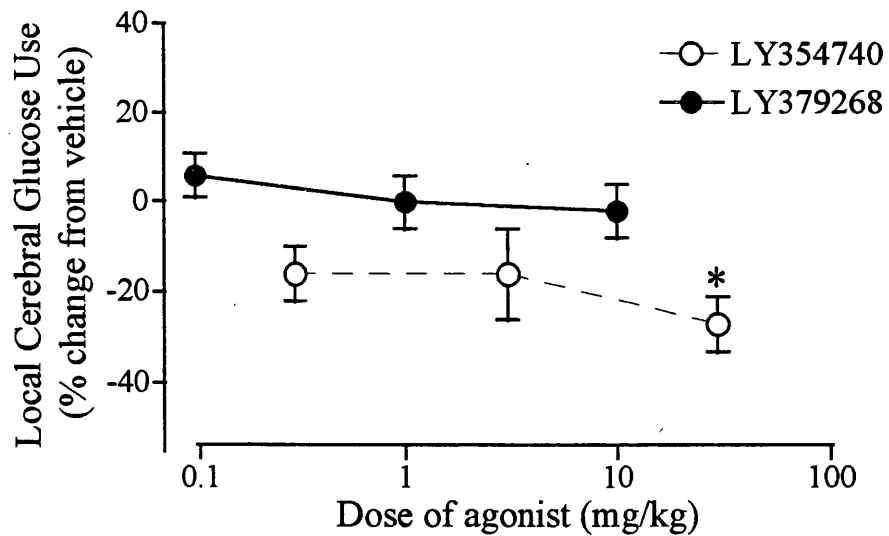
COCHLEAR NUCLEUS
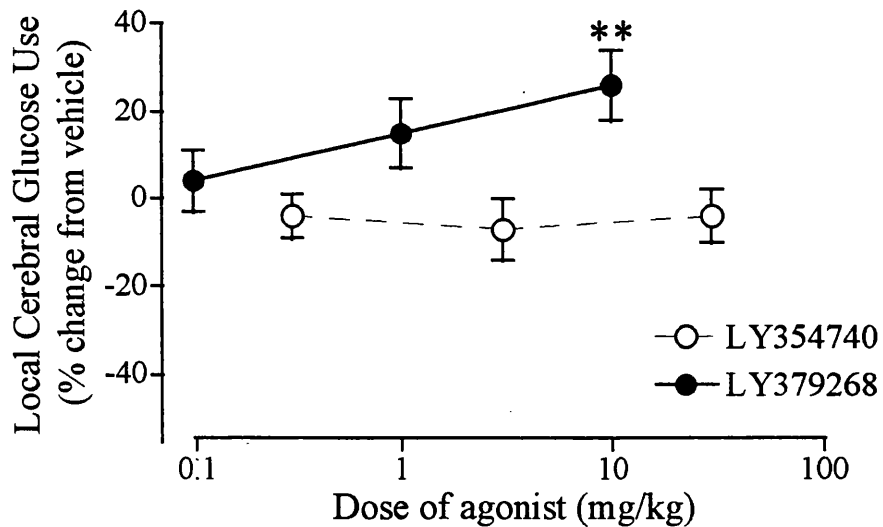
Figure 3.5   **mGluR agonists and local cerebral glucose use: heterogeneous responses to LY354740 and LY379268.**

The data are presented as % change in glucose utilisation relative to glucose use in vehicle treated control animals (mean ± SEM). While LY354740 produces a significant reduction in glucose use in part of the visual system, LY379268 produces a significant elevation in glucose use in a region of the auditory system.

*$P<0.05$, **$P<0.01$ (ANOVA followed by Student's t-test with Bonferroni correction).

124

CEREBELLAR CORTEX
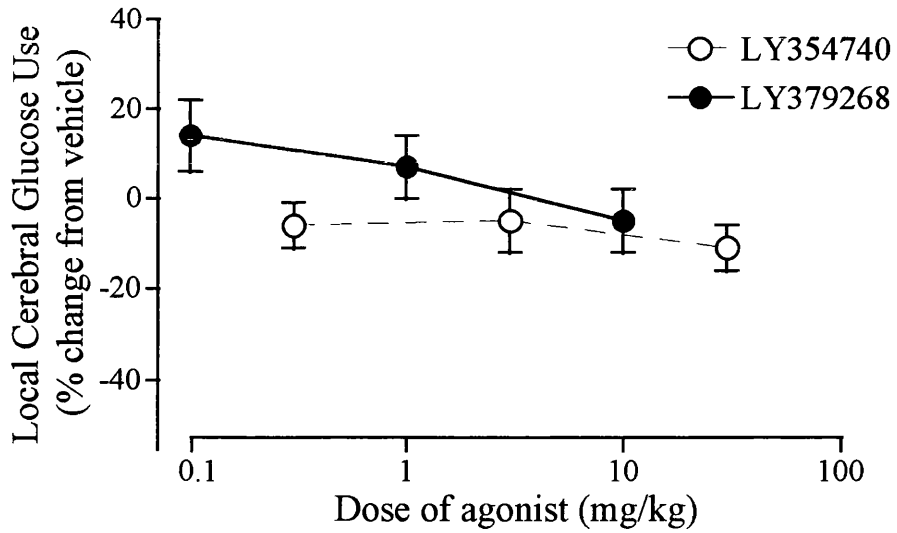
SUBSTANTIA NIGRA PARS RETICULATA
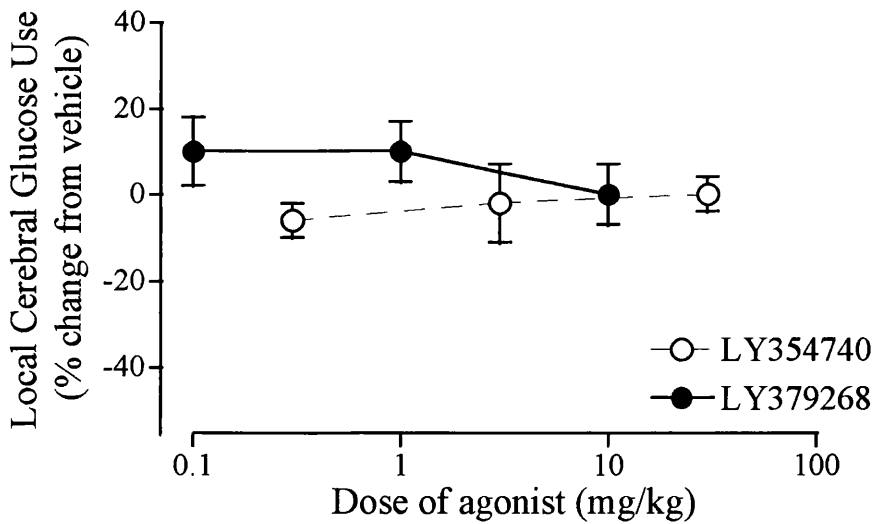
Figure 3.6   mGluR agonists and local cerebral glucose use: minimal responses to LY354740 and LY379268.

The data are presented as % change in glucose utilisation relative to glucose use in vehicle treated control animals (mean ± SEM). Both the cerebellar cortex and substantia nigra pars reticulata were insensitive to alterations in glucose use by LY354740 and LY379268.

Table 3.8   LY354740 and LY379268: Hierarchy of regional responsiveness.

BRAIN REGIONS	
LY354740	**LY379268**
Anteroventral thalamic nucleus	**Superficial layer of superior colliculus**
Mammillary body	**Locus coeruleus**
Superficial layer of superior colliculus	**Mammillary body**
Anterior cingulate cortex	Anteroventral thalamic nucleus
Lateral habenular nucleus	Genu of the corpus callosum
Visual cortex	Lateral geniculate body
Mediodorsal thalamus	Lateral habenular nucleus
Red nuclei	Cochlear nucleus
Deep layer of superior colliculus	Sensory motor cortex (layer IV)
Pons	Sensory motor cortex (layer V/VI)
Parietal cortex (layer IV)	Cerebellar white matter
Frontal cortex	Sensory motor cortex (layer II/III)
Median raphe nucleus	Nucleus accumbens
Genu of the corpus callosum	Inferior colliculus
Parietal cortex (layer II/III)	Amygdala
Septal nucleus	Prefrontal cortex
Globus pallidus	Caudate
Substantia nigra pars compacta	Median raphe nucleus
Corpus callosum	Anterior cingulate cortex
Sensory motor cortex (layer IV)	Hypothalamus
Vestibular nucleus	Auditory cortex
Superior olivary nucleus	Internal capsule
Subthalamic nucleus	Cerebellar hemisphere
Internal capsule	Hippocampus - molecular layer
Nucleus accumbens	Mediodorsal thalamus
Parietal cortex (layer V/VI)	Substantia nigra pars compacta
Hypothalamus	Substantia nigra pars reticulata
Medial geniculate nucleus	Ventrolateral thalamus
Hippocampus - molecular layer	Septal nucleus
Ventrolateral thalamus	Corpus callosum
Caudate-putamen	Deep layer of superior colliculus
Auditory cortex	Frontal cortex (layer IV)
Prefrontal cortex	Globus pallidus
Dentate Gyrus	Red nucleus
Lateral geniculate body	Pons
Inferior olivary body	Medial geniculate body
Amygdala	Dentate gyrus
Cerebellar cortex	Parietal cortex (layer IV)
Inferior colliculus	Superior olivary body
Cochlear nucleus	Vestibular nucleus
Substantia nigra pars reticulata	Visual cortex (layer IV)
Cerebellar white matter	Subthalamic nucleus

The sensitivity of each of the 43 brain regions investigated following LY354740 and LY379268 administration are ranked in order of decreasing magnitude of effect by their respective f values. Regions highlighted in bold font have been arbitrarily classified into a group considered the 'most responsive', where f values > 0.15.
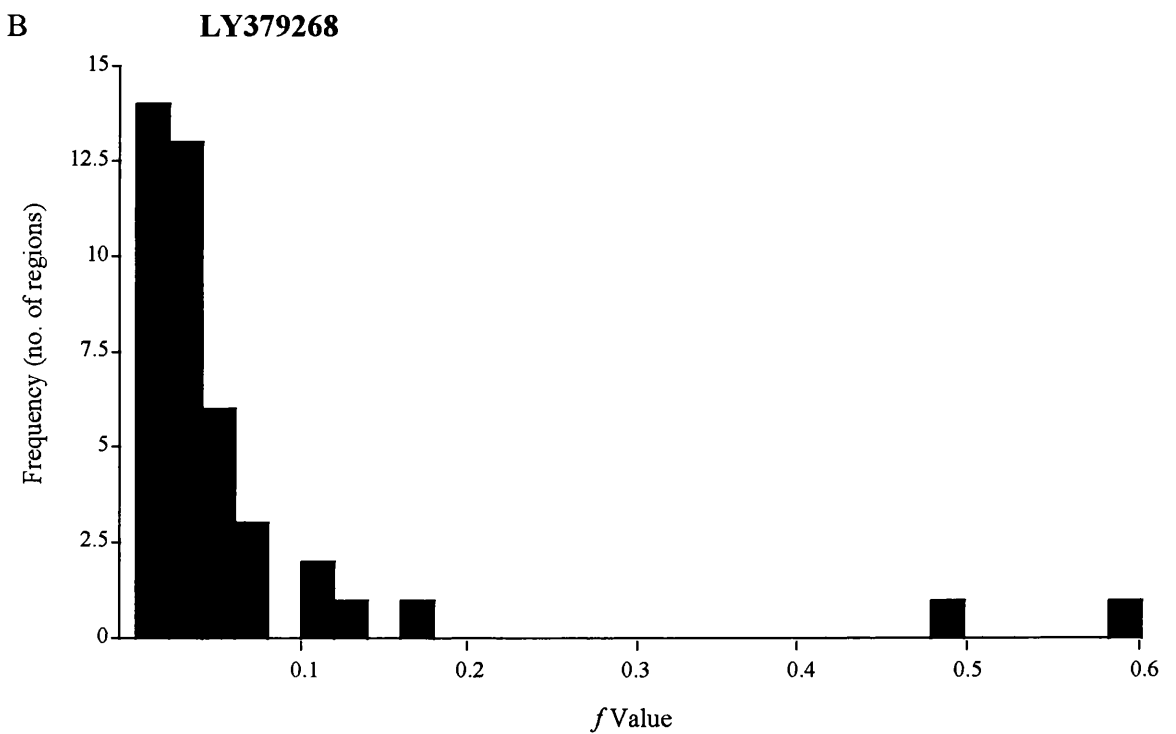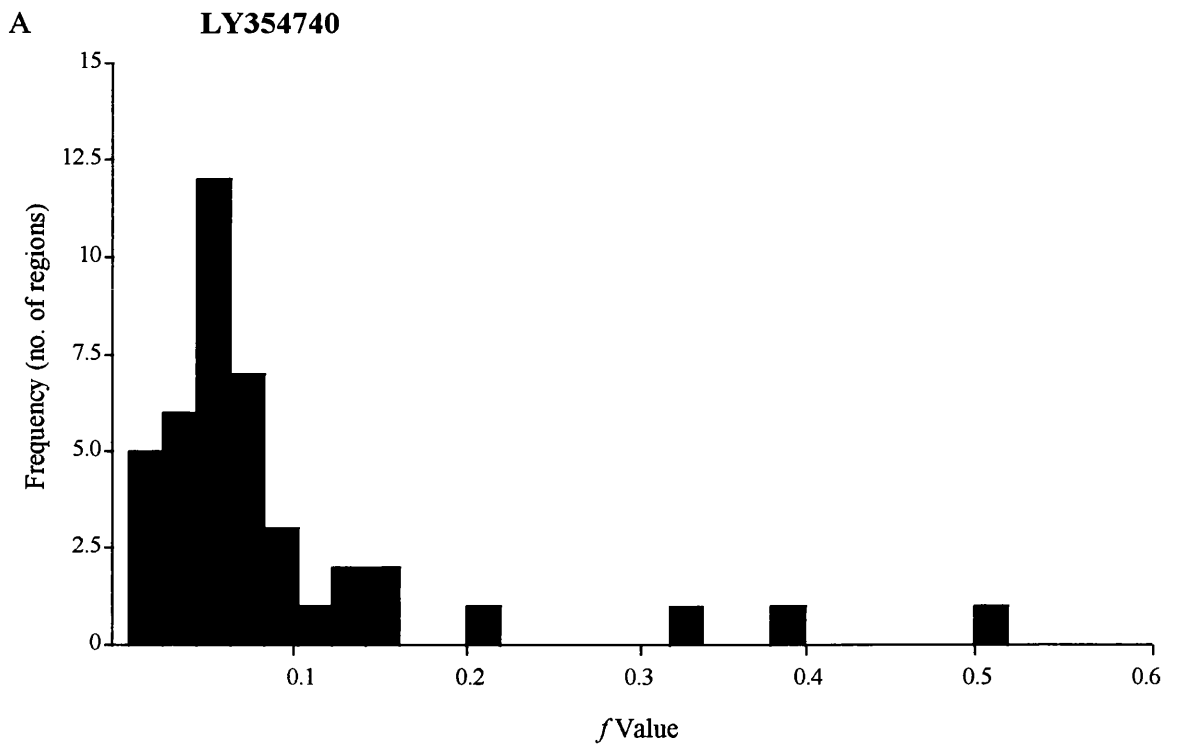
Figure 3.7   Frequency distributions of f values for LY354740 and LY379268.

The f values obtained from the arithmetic function indicate the responsiveness of individual brain regions to the drug treatment. (A) Following LY354740, the distribution of f values was relatively homogeneous with values being normally distributed around 0.05. (B) Following LY379268, the response of brain regions was more heterogeneous and the f values showed a much more skewed distribution.

127
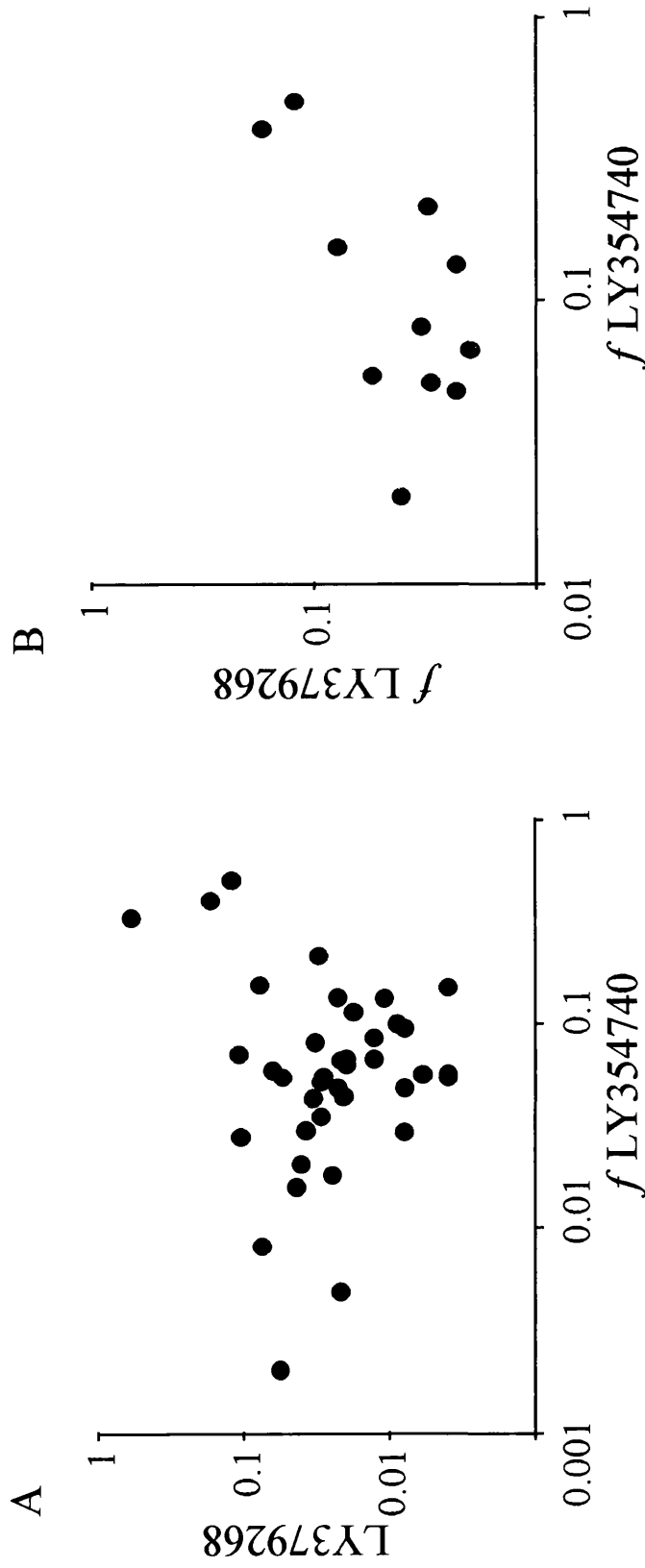
Figure 3.8 **LY354740 and LY379268: Relationship between *f* values for glucose use.**

The relationship between the extent of responsiveness of glucose use in the 43 brain regions to LY354740 and LY379268 Each point represents the *f* value obtained from all the dose response data in an individual brain region in response to each agonist. A) The overall correlation coefficient for all regions, r = -0.075 (P = 0.65) indicating the two compounds have selectively different sites of action. B) The correlation coefficient for limbic areas, r = 0.44 (P = 0.47) which suggests the effects of the two agonists are more similar here. Each point represents one of the following regions of the limbic system: mammillary body; anteroventral thalamic nucleus; lateral habenular nucleus; nucleus accumbens; amygdala; median raphe nucleus; anterior cingulate cortex; hypothalamus; mediodorsal thalamic nucleus and septal nucleus.

128

3.4   Summary and technical considerations

In this study, the effects of two new mGluR agonists, LY354740 and LY379268, on local cerebral glucose use were examined. Although mGluRs are currently extensively studied and characterised, this was the first time the functional consequences resulting from the systemic activation of mGluR2/3 by selective agonists were described.

The results of the study show that the systemic administration of LY354740 produced major changes in the rates of local cerebral glucose utilisation in 19 of the 42 regions measured, while with LY379268, only 9 out of 42 regions were substantially affected. The additional use of the ranking function f provides a system which allows the interpretation of data from the entire dose-response relationship. The utility of the f ranking function has been previously demonstrated by Kelly *et al.* (1986). In this present study, by using all of the available data, distinct patterns of altered local cerebral glucose utilisation were established for both metabotropic agonists and used to supplement percentage changes in function-related glucose use, or significance levels in specific regions. Irrespective of how the data were analysed, a number of similarities and more obviously, dissimilarities were identified in the regional responses of local glucose use to the two metabotropic glutamate agonists. Glucose use in a number of anatomically interconnected regions of the limbic systems (anteroventral thalamic nucleus, mammillary body, lateral habenular nucleus) were sensitive to reduction by both LY354740 and LY379268. Glucose use in the superior colliculus (superficial layer) was increased by both metabotropic agonists. In contrast, LY354740 provoked anatomically widespread reductions in glucose use, notably in the cerebral cortex and visual system, whereas LY379268 elicited circumscribed increases in glucose use in the auditory relay nuclei and locus coeruleus.

One of the central assumptions made in the original derivation of the operational equation of the [^{14}C]2-deoxyglucose method requires that plasma glucose concentration

remains constant throughout the experimental procedure. However, plasma glucose levels were significantly increased 45 minutes after LY379268 (10 mg/kg) compared with control levels (table 3.2), with plasma glucose levels peaking at their highest levels 10-25 minutes into the experimental procedure. This clearly does not satisfy the constraints and thus invalidates the operational equation and lumped constant of the [^{14}C]2-deoxyglucose method (Schuier et al., 1981). Savaki et al., (1980) developed a method for the measurement of the turnover rate constant (or the half-life) of the free glucose content of brain. As a result of these studies, the method could be applied to the [^{14}C]2-deoxyglucose technique for the measurement of local cerebral glucose utilisation in conditions with changing arterial plasma glucose concentrations (for example, in conditions such as stress where plasma glucose may fluctuate continuously during the procedure). For this, a new operational equation was derived to take into account changing plasma glucose levels, based on the original operational equation by Sokoloff et al. (1977). Using this method for the animals treated with LY379268 (10 mg/kg), the final plasma integral in both white and grey matter differed by less than 3% compared with the final plasma integral values obtained using the original method. Therefore, this difference would have negligible effects on the final outcome of local rates of glucose utilisation.

The results of this study are discussed in chapter 8, section 8.2.

CHAPTER 4

FUNCTIONAL MAPPING FOLLOWING

LIMBIC SYSTEM MANIPULATION

4.1   Introduction

The [^{14}C]2-DG technique has been applied extensively to characterise the functional consequences associated with the pharmacological manipulations of specific receptor populations, such as glutamate receptors. Past studies have successfully contributed to our understanding of the anatomical circuits influenced by ionotropic glutamate receptor activity (Nehls et al., 1988; McCulloch & Iversen, 1991; Browne & McCulloch, 1994). Similarly, the study carried out in chapter 3 has revealed selective circuits influenced by group II mGluR activity and augmented our current understanding of the functional consequences of systemic glutamatergic manipulations.

In contrast to the widespread changes in glucose utilisation following the systemic administration of agents, the [^{14}C]2-DG technique has also been successfully used to explore the functional consequences following more selective and localised manipulations of the CNS. While investigations of NMDA receptor activity have been carried out using direct intracerebral injections of selective antagonists, no such studies have been performed for AMPA receptors and mGluRs. Therefore the aim of this study was to explore the consequences of cerebral function following selective AMPA and mGluR manipulation of the hippocampus.

Local rates of function-related glucose use were assessed in animals during and following the intrahippocampal infusion of the selective AMPA/KA receptor antagonist LY326325. Unfortunately, this study was limited to the investigation of AMPA receptor manipulation. At the time this study was carried out, LY354740 was under clinical development and LY379268 was being considered for clinical use. Company policy restricted their use in research, and for this reason, LY354740 and LY379268 could not be used in this study. LY326325 is a different salt of the better known decahydroisoquinoline compound LY293558 (Ornstein et al., 1993; Schoepp et al., 1995b). LY326325 was

chosen to inactivate the hippocampus because it has previously been demonstrated to be systemically active and to reduce glucose utilisation homogeneously throughout the brain (Browne & McCulloch, 1994). In addition, LY326325 is water soluble, which avoids the use of solvents such as dimethyl sulphoxide (DMSO) and the possible brain damage associated with its use. An advantage of this type of study is the unique opportunity it provides to simultaneously complement and combine other studies, such as the effects of intrahippocampal LY326325 infusion in behavioural and electrophysiological studies .

4.2 Methods

4.2.1 Stereotaxic surgery

Adult male hooded-Lister rats (Harlan Olac, Bicester, UK) weighing between 200-250g (n=19) were used for this study. All animals were allowed to acclimatise to their surroundings for at least 5 days before any surgery under normal housing conditions. Animals were first anaesthetised with 5% halothane and anaesthetic was maintained by i.p. injection of Avertin (tribromoethanol, 10ml/kg). Stereotaxic surgery was carried out as described in section 2.2. Animals were implanted bilaterally with 7 day minipumps containing either LY326325 or aCSF (artificial cerebrospinal fluid). Following surgery, animals were returned to their normal housing conditions and checked regularly until they were used for the autoradiographic procedure.

4.2.2 [^{14}C]2-deoxyglucose measurements

Local cerebral glucose utilisation measurements were carried out in conscious, freely moving animals using [^{14}C]2-DG autoradiography as described in section 2.1. Adjacent coronal brain sections to those obtained for autoradiography were taken for H & E staining to aid the identification of the cannulae injection site, and any resulting areas of

brain damage. For this study, as the pharmacological manipulation was localised to intracerebral hippocampal injections, the brain regions chosen for analysis reflected primarily the hippocampus and it's anatomical connections. Local rates of glucose use were determined in 34 separate brain regions with quantitative densitometric analysis in a blinded fashion. All the data were analysed by two-tailed Student's unpaired t-test.

The [^{14}C]2-DG autoradiographic procedure was carried out 4 days after minipump implantation to examine the functional consequences of hippocampal inactivation (minipump ran for 7 days), or following 11 days to determine brain function after the exhaustion of the drug/vehicle in the minipump.

4.2.3 Drug administration

Artificial cerebrospinal fluid (aCSF)

To make 1l of aCSF, stock solutions A and B were firstly prepared. For solution A, 8.66g of NaCl; 0.225g KCl; 0.205g CaCl$_2$2H$_2$O and 0.165g MgCl$_2$6H$_2$O were added to 500ml pyrogen-free sterile water. For solution B, 0.115g Na$_2$HPO$_4$ and 0.025g NaH$_2$PO$_4$H$_2$O were added to 500ml pyrogen-free sterile water. Solutions A and B were then added in equal volumes.

LY326325

LY326325 was dissolved in aCSF to give a 1.5mM stock solution (pH adjusted to 7.2). LY326325 was administered at a concentration of 0.375mM via the minipumps and the cannulae at a rate of 0.5µl/hour (Drs. J Micheau & G Riedel, personal communication). Control animals received bilateral minipump infusions of aCSF.

4.3 Results

4.3.1 General Observations

Following stereotaxic surgery, recovery from the effects of anaesthesia was slower than with halothane as a direct result of the administration route of the anaesthetic (i.p. injection rather than a gas mix). Once the animals had regained consciousness, changes in behaviour were noticed. All animals were less active than before the surgical procedure. This loss of activity remained for the next couple of days together with a loss in weight (table 4.1). By 4 days after surgery, weight loss was still evident in animals but they all exhibited signs of normal inquisitive behaviour. No changes in behaviour were observed between animals at 4 days after surgery and animals at 11 days after surgery.

Gross examination of the autoradiograms revealed that damage had occurred in some animals at the cortical level of the brain. This damage was observed usually at the level of the frontal/prefrontal cortex and was attributed to either the heat generated from the drill-bit used for the stereotaxic surgery, or actual physical damage produced by the screws used to keep the stereotaxic assembly in place. Damage caused by the needle tract was clearly evident in all brains at the site of the injection. Consequently, brain regions selected for densitometric analysis were chosen only if they were free from artefactual damage.

4.3.2 Function-related glucose use 4 days following stereotaxic surgery

The function-related glucose utilisation values associated with LY326325 infusion are presented in tables 4.2-4.5. Anatomically circumscribed changes in glucose use were measured in animals treated with LY326325 compared with aCSF treated control animals. During the period of drug infusion (4 days), a reduction in glucose utilisation of 23% in the dorsal hippocampus, stratum lacunosum moleculare, (P<0.002) was evident (bregma -3.30 mm), while the ventral hippocampus, stratum lacunosum moleculare (bregma = -5.80 mm),

Table 4.1 Intrahippocampal manipulation of AMPA receptors using LY326325 infusion: weight of animals.

Day following surgery	Weight			
	4 days		11 days	
	aCSF	LY326325	aCSF	LY326325
0	336 ± 9	394 ± 19	340 ± 4	343 ± 9
1	330 ± 9	387 ± 16	324 ± 6	335 ± 10
2	315 ± 14	375 ± 15	312 ± 6	321 ± 11
3	318 ± 14	371 ± 17	312 ± 10	321 ± 9
4	317 ± 14	365 ± 18	313 ± 6	317 ± 10
5			318 ± 7	326 ± 7
6			319 ± 7	329 ± 8
7			319 ± 9	332 ± 8
8			326 ± 10	336 ± 11
9			325 ± 10	336 ± 11
10			328 ± 9	333 ± 13
11			336 ± 10	346 ± 12
Number of animals	5	5	4	5

Data are presented as mean ± SEM (g).

135

was minimally affected (figure 4.1). These results reveal a spatially selective response in the hippocampus during the period of LY326325 infusion. The intrahippocampal infusion of LY326325 after 4 days produced minimal alterations in glucose use in the remaining regions of the CNS other than a possible elevation in glucose utilisation in the superficial layers of the entorhinal cortex afferent to the hippocampus (table 4.3 and figure 4.1).

4.3.3 Function-related glucose use 11 days following stereotaxic surgery

The results at 11 days after LY326325 infusion, a time when the drug was exhausted, are presented in tables 4.2-4.5. At 11 days after LY326325 infusion, glucose utilisation in the dorsal hippocampus stratum lacunosum moleculare returned to levels comparable to that observed with aCSF treated animals. The alteration in glucose use in the entorhinal cortex measured after 4 days LY326325 infusion was also not evident after 11 days. Function-related glucose use in these regions of LY326325 treated animals were indistinguishable from the aCSF treated animals. However, a 17% reduction in glucose utilisation was observed in the red nucleus of LY326325 treated animals at 11 days after drug infusion (table 4.4). A comparison of the data generated from both the time points of 4 days and 11 days after drug infusion reveal a generalised reduction in glucose utilisation in all brain regions in the 4 day treatment group.

4.3.4 Glucose utilisation in the hippocampus

Tables 4.2-4.5 illustrate the subtle changes in glucose use in the brains of animals treated with an infusion of LY326325. The most significant reduction in function-related glucose use was demonstrated in the stratum lacunosum moleculare of the hippocampus in a selective manner, affecting the dorsal but not the ventral hippocampus. This selective

Table 4.2 Glucose utilisation at 4 days (minipump active) and 11 days (minipump exhausted) after intrahippocampal LY326325 infusion: Primary visual system.

STRUCTURE	4 DAYS		11 DAYS	
	aCSF	LY326325	aCSF	LY326325
Visual cortex (layer IV)	82 ± 4	85 ± 8	88 ± 3	90 ± 5
Lateral geniculate body	64 ± 5	64 ± 4	80 ± 5	72 ± 4
Superior colliculus:				
superficial layer	76 ± 3	74 ± 4	89 ± 5	83 ± 3
deep layer	58 ± 1	56 ± 3	69 ± 3	61 ± 4
Number of animals	5	5	4	5

Data are presented as mean ± SEM (μmol/100g/min)
There were no significant differences between LY326325 treated animals and aCSF treated control animals at either time point (Student's unpaired t-test)

Table 4.3 Glucose utilisation at 4 days (minipump active) and 11 days (minipump exhausted) after intrahippocampal LY326325 infusion: Cortical regions.

STRUCTURE	4 DAYS		11 DAYS	
	aCSF	LY326325	aCSF	LY326325
Entorhinal cortex (superficial)	59 ± 2	67 ± 4	67 ± 2	65 ± 3
Posterior cingulate cortex	65 ± 4	54 ± 4	78 ± 4	83 ± 8
Sensorimotor cortex (layer IV)	85 ± 4	95 ± 5	97 ± 5	98 ± 7
Anterior cingulate cortex	70 ± 4	65 ± 3	81 ± 5	88 ± 7
Piriform cortex	85 ± 3	93 ± 4	93 ± 3	97 ± 5
Number of animals	5	5	4	5

Data are presented as mean $\pm$ SEM (μmol/100g/min)

There were no significant differences between LY326325 treated animals and aCSF treated control animals at either time point (Student's unpaired t-test)

Table 4.4   Glucose utilisation at 4 days (minipump active) and 11 days (minipump exhausted) after intrahippocampal LY326325 infusion: Extrapyramidal and sensory motor regions.

STRUCTURE	4 DAYS		11 DAYS	
	aCSF	LY326325	aCSF	LY326325
Caudate-putamen	72 ± 3	75 ± 2	87 ± 5	80 ± 5
Globus pallidus	41 ± 2	43 ± 1	47 ± 2	43 ± 3
Substantia nigra:				
pars compacta	59 ± 3	60 ± 4	72 ± 2	65 ± 3
pars reticulata	40 ± 3	42 ± 2	48 ± 3	41 ± 3
Thalamus:				
mediodorsal	73 ± 3	68 ± 3	87 ± 3	80 ± 6
ventrolateral	65 ± 4	66 ± 4	73 ± 4	64 ± 4
Red nucleus	61 ± 4	63 ± 3	72 ± 2	60 ± 3**
Cerebellar nucleus	72 ± 4	79 ± 3	84 ± 2	79 ± 6
Cerebellum:				
cortex	44 ± 1	49 ± 2	53 ± 1	51 ± 3
white matter	25 ± 3	29 ± 1	30 ± 1	30 ± 2
Number of animals	5	5	4	5

Data are presented as mean ± SEM (μmol/100g/min). **P<0.002 for statistical comparison between aCSF and LY326325 (11 day) group (Student's unpaired *t*-test)

139

Table 4.5 Glucose utilisation at 4 days (minipump active) and 11 days (minipump exhausted) after intrahippocampal LY326325 infusion: Limbic regions.

STRUCTURE	4 DAYS		11 DAYS	
	aCSF	LY326325	aCSF	LY326325
Hippocampus - ventral: molecular layer	65 ± 3	68 ± 3	73 ± 1	76 ± 4
Hippocampus - dorsal: molecular layer	57 ± 2	44 ± 1**	61 ± 4	62 ± 3
CA1	37 ± 2	32 ± 1	45 ± 4	41 ± 2
CA3	48 ± 3	43 ± 2	55 ± 4	49 ± 4
Dentate gyrus:				
ventral	47 ± 2	53 ± 3	55 ± 4	51 ± 2
dorsal	42 ± 2	38 ± 1	47 ± 2	43 ± 2
Lateral habenular nucleus	88 ± 4	89 ± 5	107 ± 5	98 ± 6
Median raphe nucleus	69 ± 3	67 ± 3	81 ± 3	79 ± 4
Mammillary body	82 ± 3	78 ± 4	93 ± 5	94 ± 5
Amygdala	35 ± 2	39 ± 1	42 ± 5	36 ± 2
Septal nucleus	48 ± 2	53 ± 2	53 ± 2	52 ± 3
Nucleus accumbens	63 ± 3	65 ± 2	72 ± 3	71 ± 4
Hypothalamus	33 ± 3	35 ± 2	38 ± 3	33 ± 2
Hypothalamus (at medial forebrain bundle)	49 ± 2	54 ± 3	54 ± 3	52 ± 4
Anteroventral thalamic nucleus	90 ± 4	91 ± 6	104 ± 6	109 ± 7
Number of animals	5	5	4	5

Data are presented as mean ± SEM (μmol/100g/min). ***P=0.002 for statistical comparison between aCSF and LY326325 (4 day) group (Student's unpaired t-test)

140
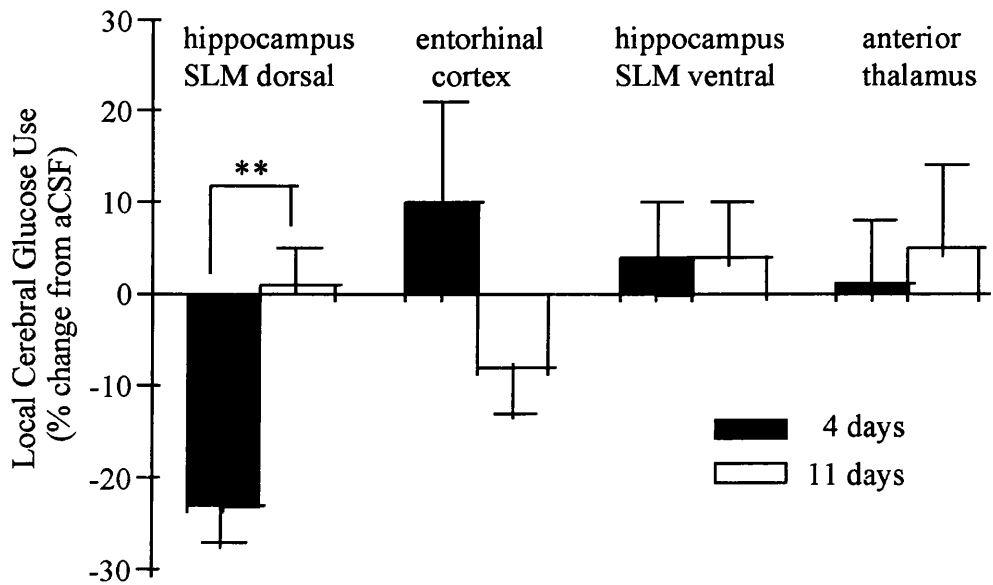
Figure 4.1   LY326325 and local cerebral glucose use.

The data are presented as % change in glucose utilisation relative to glucose use in aCSF treated control animals (mean ± SEM).
**P<0.002 (Student's unpaired *t*-test)

reduction initiated further analysis of the changes in glucose metabolism in the hippocampus in order to explore the extent of the reduction. To investigate the extent of hippocampal inactivation, as many densitometric readings were made in the hippocampus (stratum lacunosum moleculare) as were possible. However, to demonstrate these changes in the hippocampus quantitatively, several factors were taken into consideration. The injection site (placement of the stainless steel cannulae) was chosen as a reference point by which all the readings in each animal could be normalised. The injection site reference point was chosen on a separate occasion from the densitometric readings from the corresponding H & E sections in which the needle tract had reached the most ventral point in the hippocampus. Also, in order to overcome any issues of left-right asymmetry in the cut of the brain, the left and right hemispheres were initially considered separately. No demonstrable differences in glucose utilisation in the hippocampus between the left and right hemispheres were observed and so the data were pooled together (see appendix 5 for all left-right data). The results are presented in table 4.6 and illustrated in figure 4.2. Figure 4.2A illustrates that the maximal reduction in function-related glucose in the stratum lacunosum moleculare of the hippocampus was observed adjacent to the cannula implant site. In addition, the degree of hippocampal inactivation was greater along its dorsal axis relative to the implant site. Glucose utilisation in the hippocampus measured at 11 days after drug infusion (minipump exhausted) was indistinguishable from aCSF treated animals, although a disparity in glucose use was noted at the most dorsal portion of the hippocampus in aCSF treated animals compared with the LY326325 group (figure 4.2B). Figure 4.2C demonstrates that glucose use values were similar in the molecular layer of the hippocampus following aCSF treatment after 4 and 11 days. Figure 4.2D illustrates that a reduction in glucose use was observed in the hippocampus 4 days after LY326325 minipump implantation compared with hippocampal glucose use values after 11 days.

Table 4.6 Glucose utilisation at 4 days (minipump active) and 11 days (minipump exhausted) after LY326325 infusion: Stratum lacunosum moleculare of the hippocampus.

HIPPOCAMPUS (mm)	4 DAYS		11 DAYS	
	aCSF	LY326325	aCSF	LY326325
2.2 (≈ bregma -2.3 mm)	73 ± 5		64 ± 10	
2.0	69 ± 0.5		64 ± 8	
1.8	63 ± 4	67 ± 4	59 ± 2	72 ± 6
1.6	59 ± 2	56 ± 2	64 ± 4	75 ± 5
1.4	60 ± 1	53 ± 1	64 ± 4	72 ± 3
1.2	55 ± 1	50 ± 2	62 ± 3	71 ± 1
1.0	55 ± 1	45 ± 2	62 ± 5	67 ± 2
0.8	51 ± 2	41 ± 2	60 ± 5	64 ± 1
0.6	52 ± 2	40 ± 1	56 ± 3	62 ± 1
0.4	49 ± 2	40 ± 2	56 ± 3	57 ± 2
0.2	54 ± 1	39 ± 1	54 ± 2	57 ± 2
0 (= INJECTION SITE)	52 ± 2	41 ± 2	54 ± 1	56 ± 3
0.2	51 ± 2	43 ± 2	59 ± 3	57 ± 2
0.4	53 ± 4	45 ± 2	60 ± 2	63 ± 2
0.6	58 ± 2	49 ± 2	62 ± 3	62 ± 2
0.8	58 ± 3	55 ± 2	66 ± 3	67 ± 2
1.0	61 ± 2	56 ± 2	67 ± 3	67 ± 2
1.2	62 ± 3	62 ± 2	67 ± 2	70 ± 2
1.4	63 ± 2	64 ± 2	70 ± 1	71 ± 2
1.6	61 ± 2	65 ± 2	68 ± 1	72 ± 2
1.8	63 ± 1	67 ± 2	66 ± 1	72 ± 2
2.0	66 ± 2	66 ± 2	70 ± 2	73 ± 3
2.2	66 ± 2	69 ± 1	70 ± 2	74 ± 4
2.4		64 ± 2	72 ± 1	75 ± 4
2.6 (≈ bregma -7 mm)		74 ± 3	72 ± 1	72 ± 4
Number of animals	5	5	4	5

Data are presented as mean ± SEM (μmol/100g/min). The injection site '0' approximates to bregma = -4.52 mm (Paxinos & Watson, 1986).

A.   4 days: minipump active
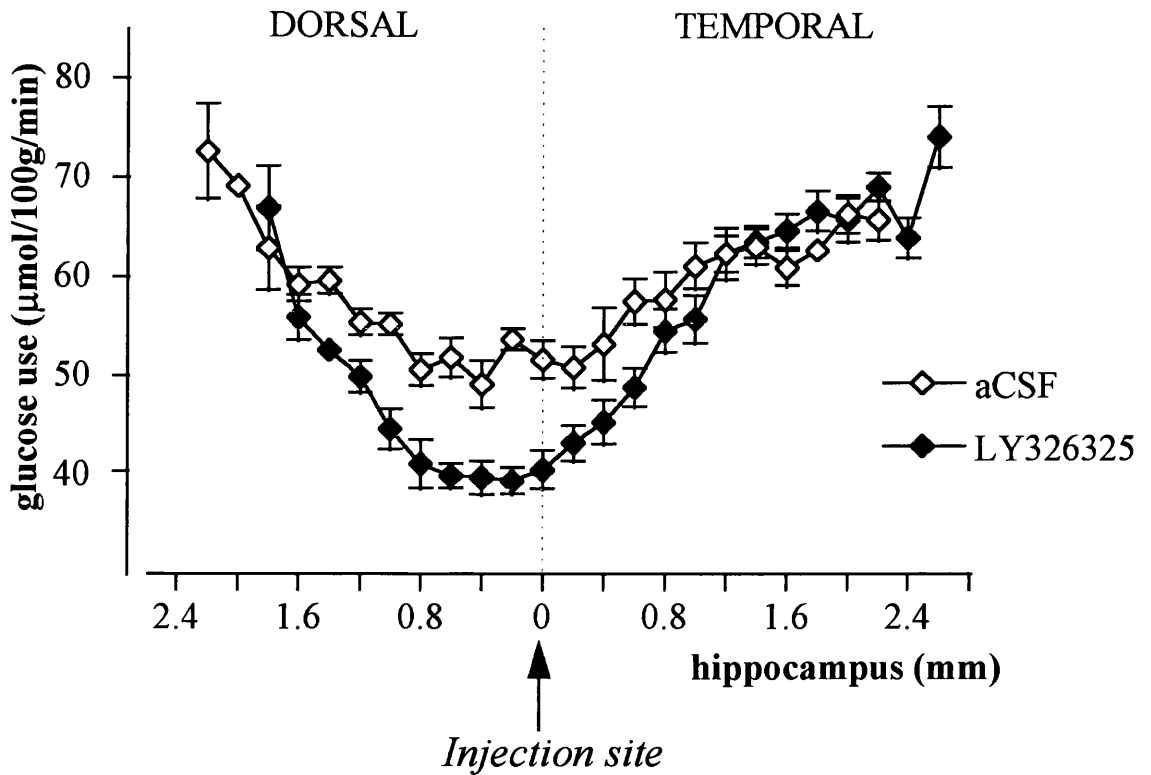
Figure 4.2A   Extent of the reduction of glucose use in the stratum lacunosum moleculare of the hippocampus: 4 days (minipump active).

The data are presented as mean ± SEM. The dotted line represents the site of injection (chosen from H & E stained sections). All data points to the left of the dotted line represent glucose use in the hippocampus at distances rostral to the injection site, while data points to the right of the dotted line represent glucose use in the hippocampus at distances caudal to the injection site.

B.   11 days: minipump exhausted
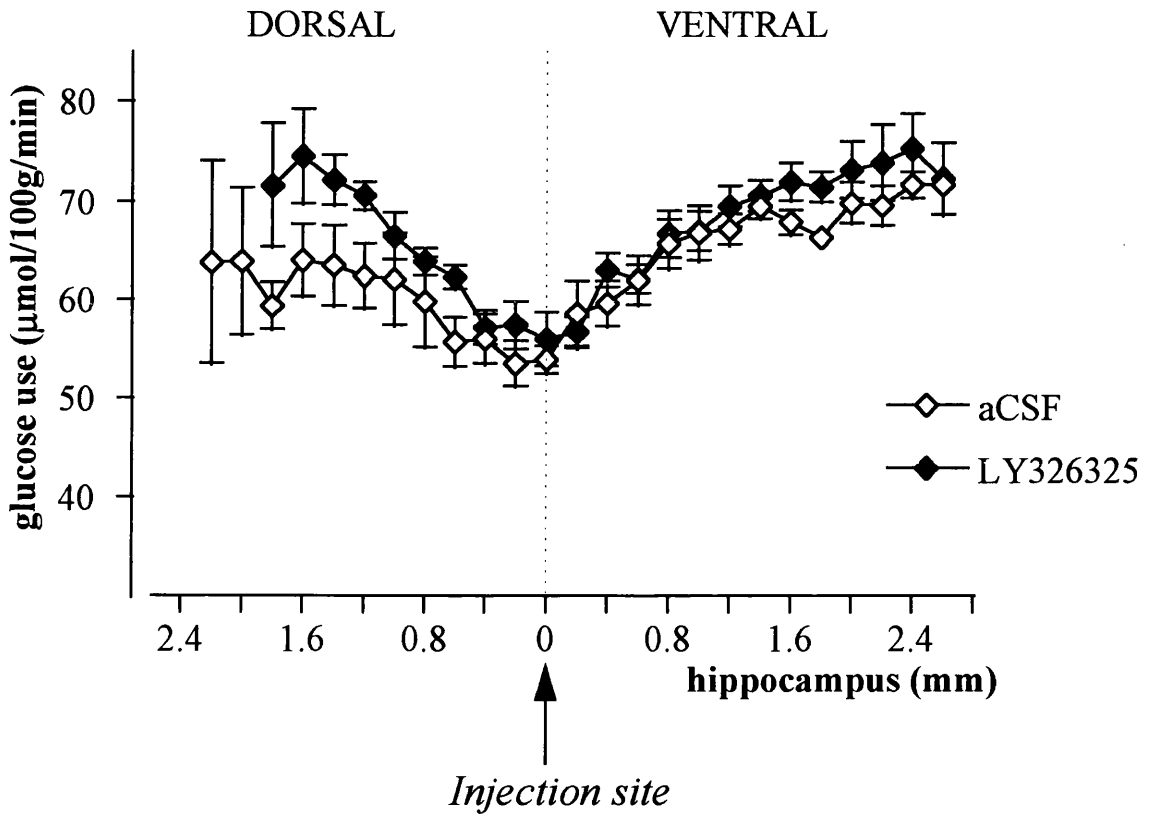
Figure 4.2B   Extent of the reduction of glucose use in the stratum lacunosum moleculare of the hippocampus: 11 days (minipump exhausted).

The data are presented as mean ± SEM. The dotted line represents the site of injection (chosen from H & E stained sections). All data points to the left of the dotted line represent glucose use in the hippocampus at distances rostral to the injection site, while data points to the right of the dotted line represent glucose use in the hippocampus at distances caudal to the injection site.

C.   bilateral aCSF treatment
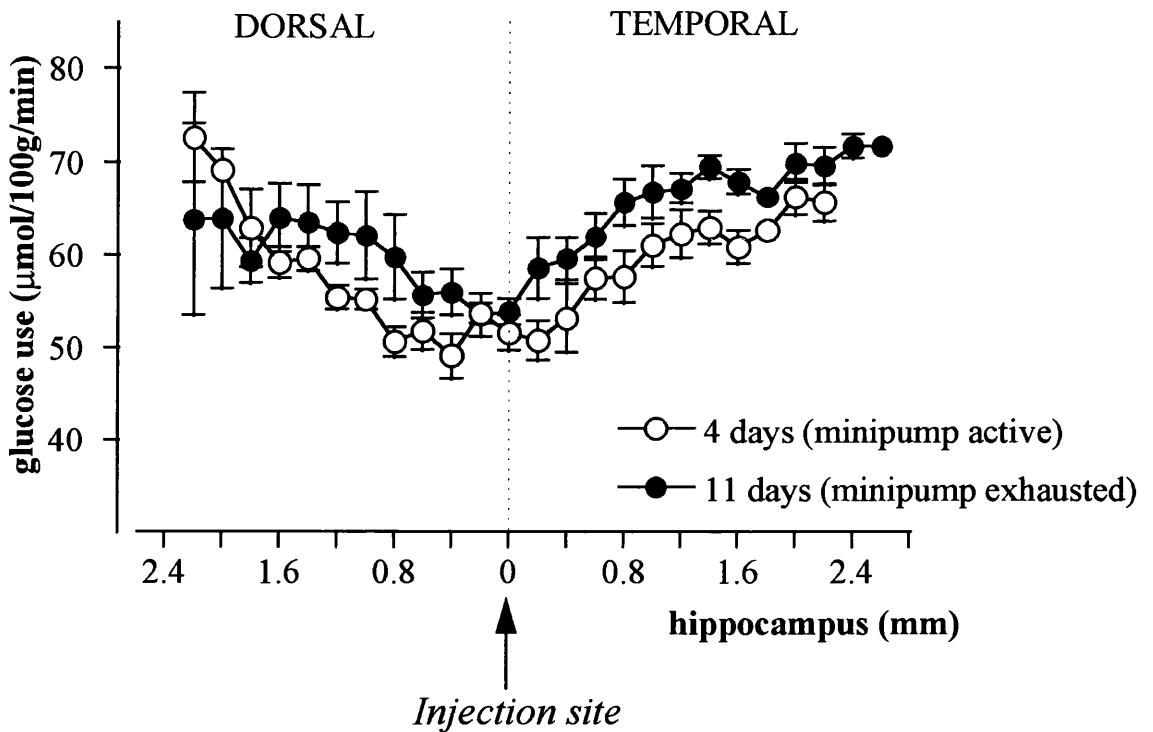
Figure 4.2C   Extent of the reduction of glucose use in the stratum lacunosum
moleculare of the hippocampus: comparison of aCSF treated groups at
4 days and 11 days.

The data are presented as mean ± SEM. The dotted line represents the site of injection
(chosen from H & E stained sections). All data points to the left of the dotted line represent
glucose use in the hippocampus at distances rostral to the injection site, while data points to
the right of the dotted line represent glucose use in the hippocampus at distances caudal to
the injection site.

D. bilateral LY326325 treatment
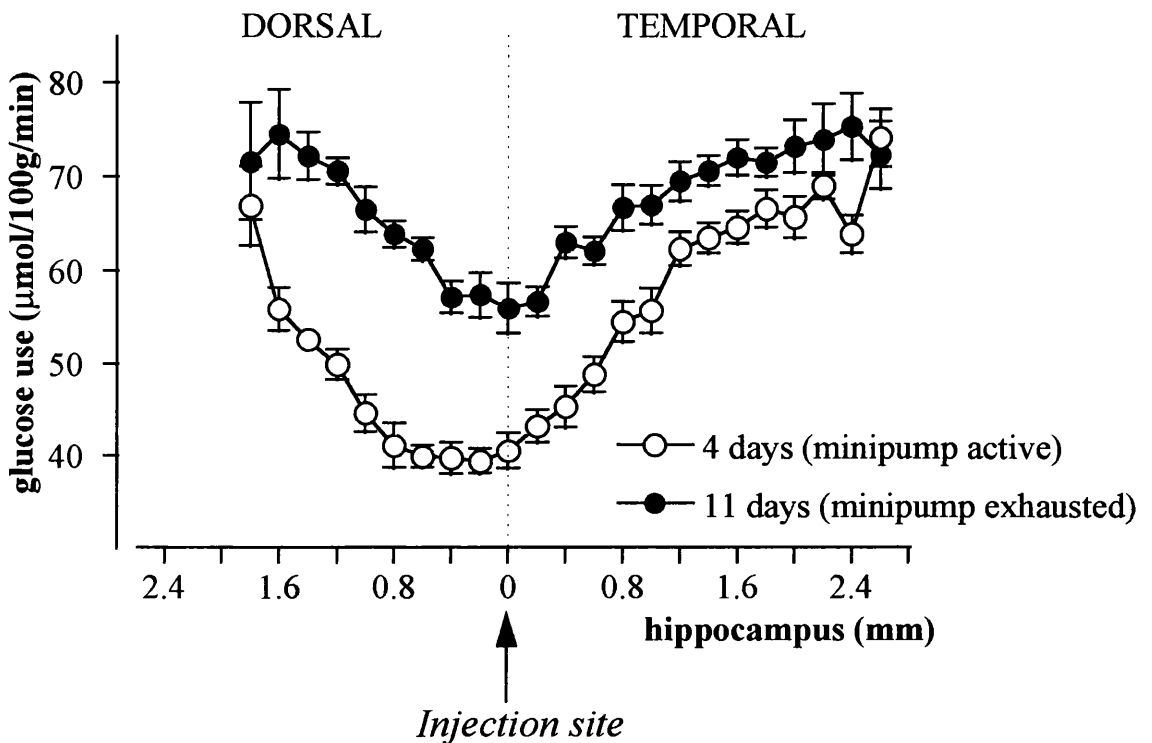
Figure 4.2D **Extent of the reduction of glucose use in the stratum lacunosum moleculare of the hippocampus: comparison of LY326325 treated groups at 4 days and 11 days.**

The data are presented as mean ± SEM. The dotted line represents the site of injection (chosen from H & E stained sections). All data points to the left of the dotted line represent glucose use in the hippocampus at distances rostral to the injection site, while data points to the right of the dotted line represent glucose use in the hippocampus at distances caudal to the injection site.

Figure 4.3   **Measurement of glucose use in the stratum lacunosum moleculare of the hippocampus: representative coronal line diagrams.**

DH = dorsal hippocampus; VPM = ventral posteromedial thalamic nucleus; TH = temporal hippocampus; MG = medial geniculate body.
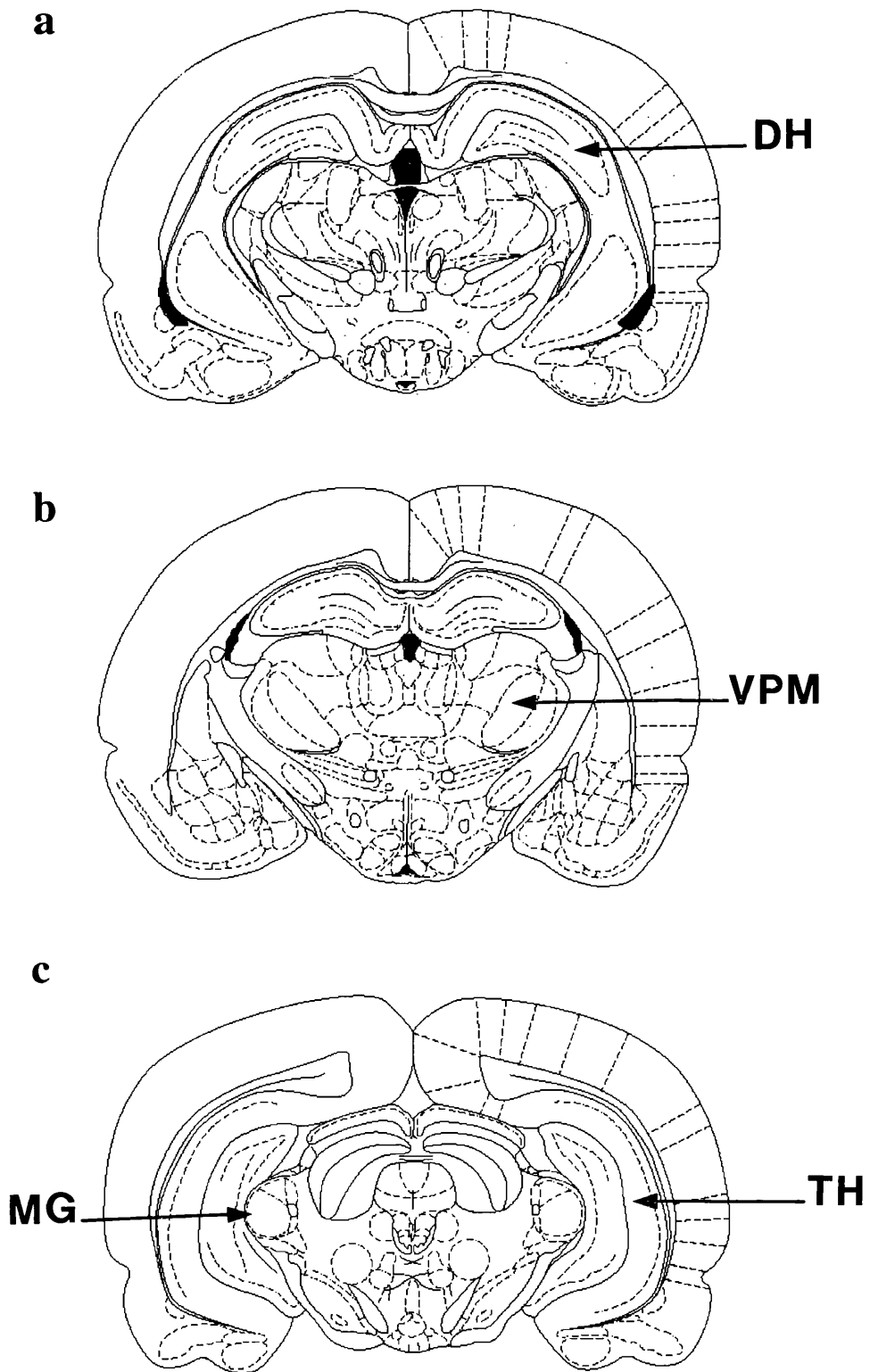
Figure 4.3 **Measurement of glucose use in the stratum lacunosum molecular of the hippocampus: representative coronal line diagrams.**

(As an aid to figure 4.2) The coronal line diagrams are presented to provide anatomical landmarks at various points of the hippocampus where glucose use was measured. a) the approximate site of injection (as recognised from the H & E stained brain sections), bregma = -4.52mm; b) the hippocampus at approx 1.6mm rostral to the injection site and c) the hippocampus at 1.6mm caudal to the injection site.

4.4 Summary and technical considerations

The results of this study demonstrate that the infusion of the AMPA receptor antagonist LY326325 produced selective and localised changes in the rates of local cerebral glucose utilisation in the brain. Specifically, the infusion of LY326325 reduced function related glucose utilisation in the stratum lacunosum moleculare of the hippocampus in a spatially selective manner; glucose utilisation was markedly affected in the dorsal aspect, with relatively little effect in the ventral portions of the hippocampus. In addition, the [^{14}C]2-DG data reveals that the functional response measured in the dorsal hippocampus during LY326325 infusion returns to levels comparable with aCSF treated animals after the infusion period. At 11 days after LY326325 infusion, the red nucleus showed a significant reduction in glucose utilisation compared to aCSF counterparts. Why this nucleus should be affected is not known. The data generated at both 4 days and 11 days after drug infusion revealed a generalised reduction in glucose utilisation in all brain regions in the 4 day treatment group. This non-specific alteration in glucose use reflects the response of the brain to the considerable trauma of the stereotaxic surgery itself (Kelly *et al.*, 1982; Kelly & McCulloch, 1984).

The energetic requirements of the brain are obtained almost exclusively from the aerobic oxidation of glucose. However, there are three other possible energy-generating substrates to glucose; the accumulation of lactate, the use of glycogen, and the use of ketone bodies, which are all important to the interpretation of [^{14}C]2-DG experiments. While lactate accumulation is well recognised in experimentally induced seizures, it is not normally associated with neuropharmacological manipulations (Siesjö, 1978). Levels of glycogen in the CNS are very low (less than 1% of the liver) and would only be able to support metabolic activity for a few minutes. In this instance, neither lactate accumulation nor glycogen utilisation would have affected the rate of glucose metabolism. The use of

ketone bodies as an alternative source of energy however, is capable of replacing glucose catabolism. Levels of ketone bodies in well-nourished animals are very low, and thus in normal situations, the contribution of ketone bodies to oxygen and energy metabolism is negligible. However, when animals are deprived of food, the levels of ketone bodies in the blood rise rapidly, such that their contribution to oxygen consumption has increased from less than 1% to greater than 20% (Ruderman *et al.*, 1974). Thus the disruption of the normal feeding behaviour of animals will lead to a greater contribution of ketone bodies to the energy generation in the CNS, and consequently the close coupling between the rate of glucose metabolism and functional activity will be compromised. Although the physiological data demonstrate that at 4 days after stereotaxic surgery the animals were continuing to lose weight, the animals were not deprived of food and thus it is predicted that ketone body metabolism would not have altered the outcome in glucose metabolism significantly in this study. For example, in the dorsal hippocampus, levels of glucose utilisation after 4 days aCSF treatment were seen to be indistinguishable from the 11 day aCSF treatment group. If ketone bodies were being used as an alternative source of energy, one would have expected much lower rates of glucose utilisation in the 4 day aCSF group.

In summary, this present study has revealed that a localised infusion of LY326325 directly into the hippocampus can reduce synaptic activity (i.e. function related glucose utilisation) in the dorsal stratum lacunosum moleculare of the hippocampus in a reversible manner. The significance of the results obtained from this study are discussed in section 8.3.

CHAPTER 5

THE EFFECTS OF THE SELECTIVE GROUP II

METABOTROPIC GLUTAMATE RECEPTOR AGONIST

LY354740 IN A RAT MODEL OF PERMANENT ISCHAEMIA

5.1   Introduction

The ionotropic glutamate receptors have been demonstrated to play a central role mechanistically in glutamate neurotoxicity. Therefore it is not surprising that metabotropic glutamate receptors are similarly thought to play an important role in the modulation of glutamate induced neurotoxicity (Nicoletti *et al.*, 1996). It has been generally assumed that the activation of group I mGluRs leads to increased neuronal excitation and excitability, and thus may have a contributing role in excitotoxic damage, while activation of group II or III mGluRs may be neuroprotective. It has been postulated that the neuroprotective effects of group II or III mGluR moderated ligands are mediated possibly through their ability to inhibit glutamate release presynaptically (Bruno *et al.*, 1995a). The aim of this study was to investigate whether the activation of group II mGluRs in the CNS by the bioavailable agonist LY354740 was neuroprotective following 24 hour permanent middle cerebral artery (MCA) occlusion in the rat.

5.2   Methods

5.2.1   Preparation of animals and MCA occlusion

Male Fischer 344 rats weighing between 250-300g were used in this study (Harlan Olac, Bicester, UK). Prior to experiments, animals were housed in cages of groups of 4 or 5 under natural daylight conditions, at a room temperature of approximately 21°C. Food and water were available *ad libitum*. Animals were anaesthetised initially with 5% halothane in a nitrous oxide: oxygen mix (70:30) until the righting reflex was lost. Animals were subsequently artificially ventilated following oral intubation, and anaesthetic was maintained with 1.5% halothane. Focal ischaemia was induced using an adapted method of Tamura *et al.* (1981) as described previously (section 2.3). The time of the diathermy was taken as the

exact time of the MCA occlusion. The anaesthetic was discontinued and the animals were allowed to recover for 24 hours. Once consciousness was regained, the animals were placed into individual cages lined with post-operative absorbent pads together with a small amount of rat chow softened with water. They were returned to their normal housing conditions and were examined regularly to check their status.

5.2.2   Drug administration

The animals received two subcutaneous doses of LY354740 (0.3, 3.0 or 30.0 mg/kg), or vehicle (0.9 % saline) in a volume of 0.5ml saline. The first injection was administered 30 minutes prior to the MCA occlusion under anaesthesia, while the second was administered three hours after the occlusion. All administrations of the drug/vehicle were performed in a blinded manner.

5.2.3   Histology and quantification of lesion size

Twenty four hours following the MCA occlusion, the animals were sacrificed with an overdose of halothane and decapitated. The brains were carefully removed and frozen in isopentane at -42°C. The brains were mounted and embedded in Lipshaw matrix and were cut into 20 μm thick serial coronal cryostat sections at -22°C. Sections were mounted onto microscope slides and stained with H & E (appendix 3). Areas of ischaemic damage and brain swelling were assessed by an observer blinded to the treatment groups at 8 pre-selected coronal levels per animal, from anterior 10.5 mm to posterior 1.02 mm (Osborne *et al.*, 1987) using the MCID computer based image analysis system. The approximate volumes of ischaemic damage for each animal were obtained by the method previously described (section 2.3.4). All the data were analysed for statistical significance using ANOVA.

5.3   Results

During the initial period of recovery, all animals appeared less active than before the surgical procedure with very little movement or signs of inquisitive behaviour. The behaviour of all animals was greatly improved by the next morning; all animals had taken soft diet, and they all exhibited signs of inquisitiveness. None of the animals exhibited any adverse signs of suffering, and the mortality rate was zero.

Following 24 hour permanent MCA occlusion, ischaemic damage was observed within the territory supplied by the occluded MCA. The histopathological appearance between ischaemic brain tissue in animals treated with LY354740 and vehicle were indistinguishable. A typical lesion produced by the permanent occlusion of the MCA is represented in figure 5.1. The area of ischaemic damage can be identified as the area of pallor in the H & E stained sections.

The effects on LY354740 on infarct volume are presented in table 5.1. At 24 hours after MCA occlusion, figure 5.2 illustrates that there were no significant decreases in infarct volume following treatment of LY354740 at any of the doses, F = 0.04 (df 3, 29). The distribution of the areas of ischaemic damage are also presented in figure 5.3. The difference between the volumes of the ipsilateral and contralateral hemispheres provided a measure of brain swelling. Figures 5.4-5.5 show that no significant differences in the volumes of brain swelling between animals treated with LY354740 and vehicle-treated control animals were identified, F = 0.3 (df 3, 29). In addition to generating absolute infarct volumes and volumes of brain swelling, the percentage infarct volumes for each animal were also obtained (figure 5.6). Figure 5.7 illustrates that brain swelling, as a result of ischaemia, is directly proportional to infarction volumes in all animals, irrespective of whether they received vehicle or drug (r = 0.75, P< 0.01).
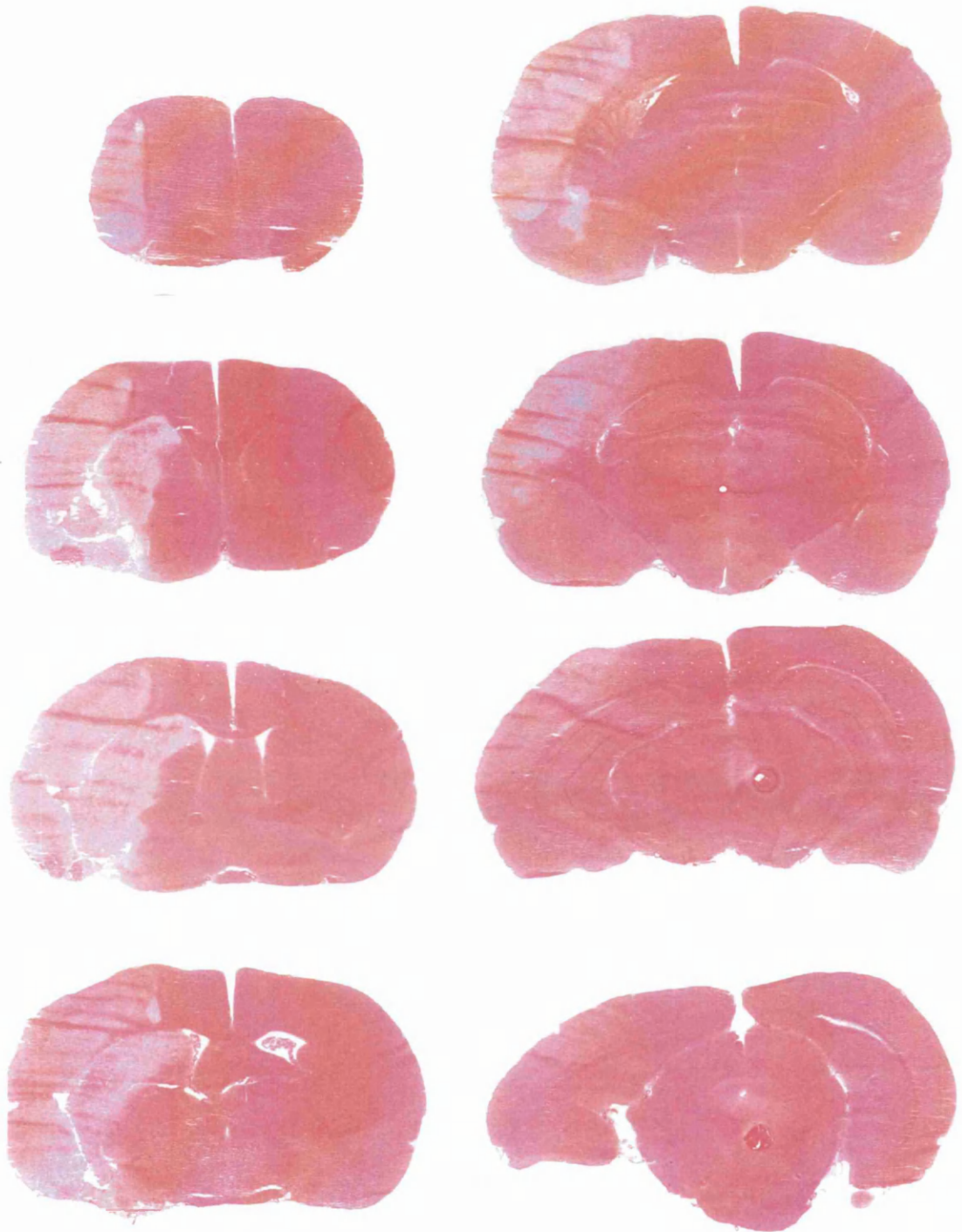
Figure 5.1   Focal ischaemic lesion.

A representative rat brain at the 8 pre-selected coronal levels stained with haematoxylin and eosin illustrating a typical lesion produced 24 hours after the permanent occlusion of the MCA. The region of ischaemic damage is identified as an area of pallor, affecting the ipsilateral striatum and cortex. Note also the swelling in the ipsilateral hemisphere compared with the contralateral hemisphere.

Table 5.1   LY354740 and the volume of ischaemic damage (mm^3) following permanent MCA occlusion.

VOLUME (mm^3)	VEHICLE	LY354740 (0.3 mg/kg)	LY354740 (3.0 mg/kg)	LY354740 (30 mg/kg)
Infarct	191 ± 18	193 ± 17	191 ± 14	199 ± 22
Hemisphere:				
Contralateral	532 ± 15	543 ± 14	513 ± 7	552 ± 16
Ipsilateral (non-infarcted)	433 ± 17	433 ± 17	418 ± 8	454 ± 11
Swelling	92 ± 7	84 ± 9	97 ± 12	102 ± 16
Number of animals	10	5	5	10

The data are presented as mean $\pm$ SEM (mm^3). LY354740 or vehicle (saline) were administered by 2 s.c. injections 30 minutes before and 3 hours after the MCA occlusion. There were no significant differences in volumes of infarct or swelling between vehicle or LY354740 treated animals (ANOVA)

INFARCTION
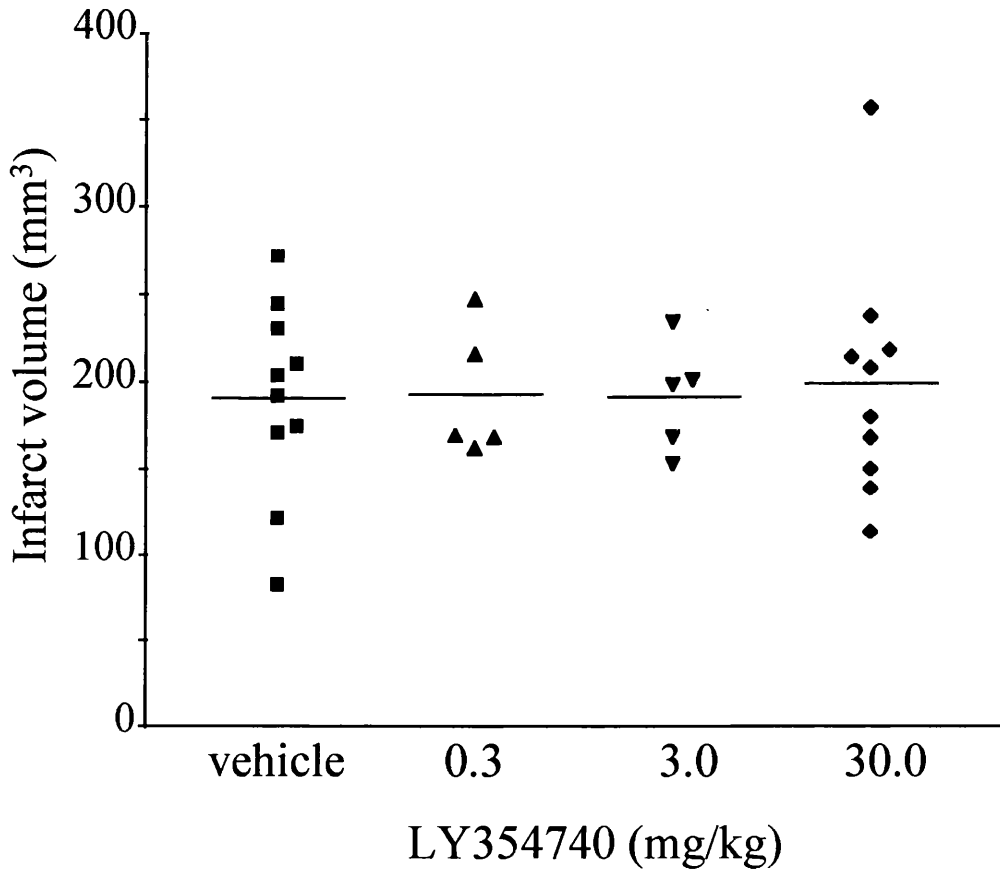
Figure 5.2   Volumes of infarction.

Areas of infarct were measured in H & E stained coronal sections from anterior 10.5 mm to posterior 1.02 mm. The volumes of ischaemic damage were obtained by integrating each of the areas measured with the known stereotaxic co-ordinates of the level. The data are presented as a scatter plot, each point representing an individual animal with the mean value presented as a horizontal bar. There were no differences in infarct volume between vehicle and any of the LY354740 drug treated groups (ANOVA).
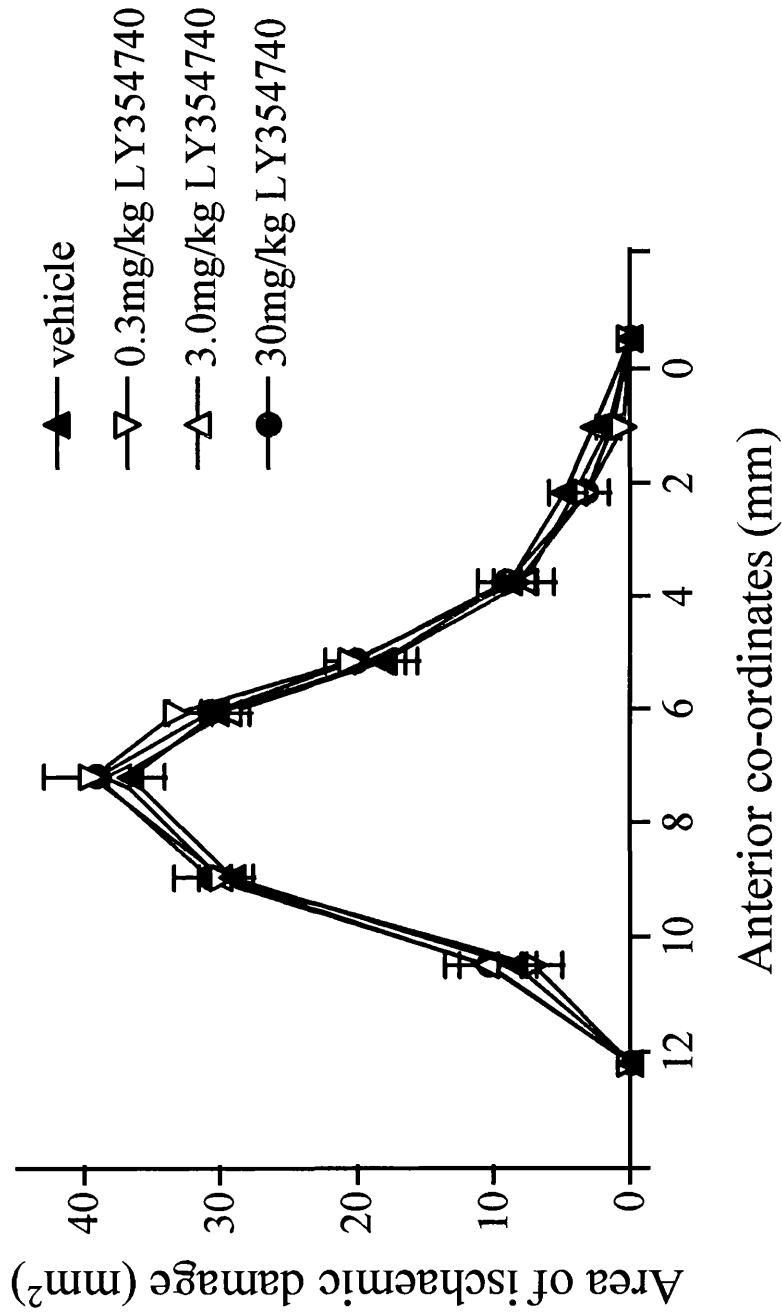
Figure 5.3   The distribution of the areas of ischaemic damage.

The areas of ischaemic damage in vehicle and LY354740 treated animals at each of the pre-selected stereotaxic levels (Osborne *et al.*, 1987).

BRAIN SWELLING
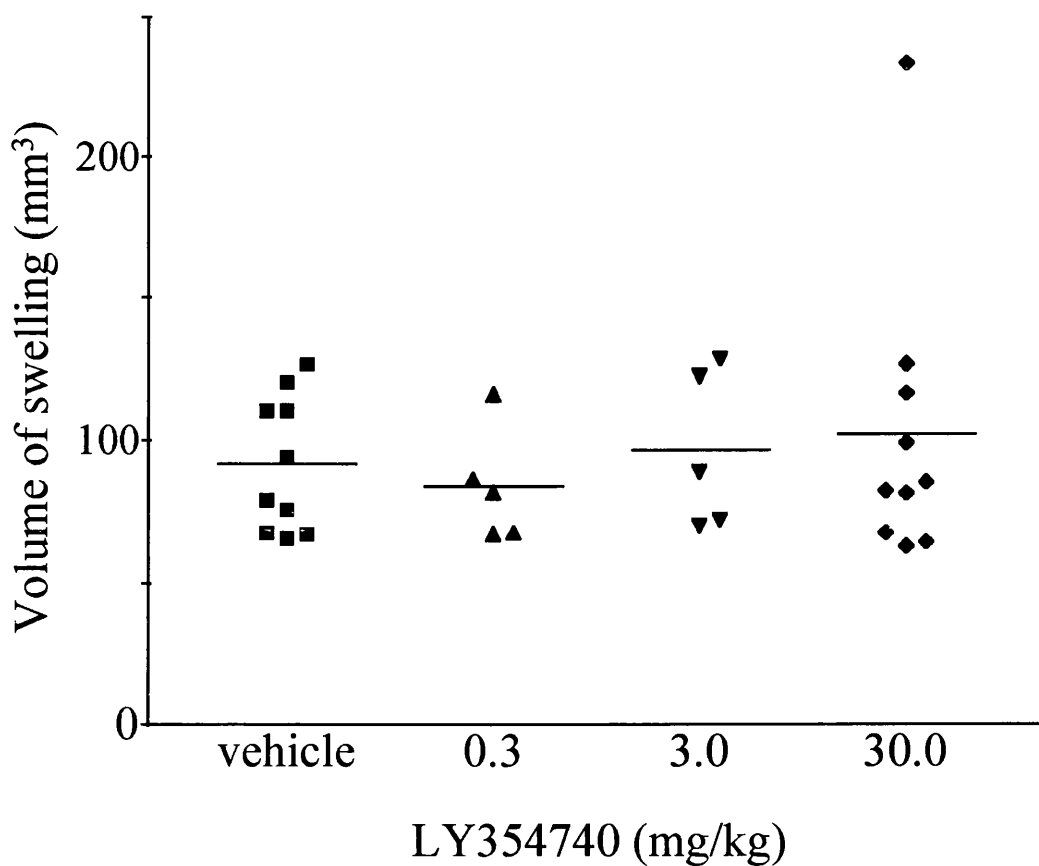
Figure 5.4   Volumes of brain swelling.

Ipsilateral and contralateral hemispheric areas were measured in H & E stained coronal sections from anterior 10.5 mm to posterior 1.02 mm. The respective volumes were obtained by integrating each of the areas measured with the known stereotaxic co-ordinates of the level and the difference between the volumes provided a measure of brain swelling. The data are presented as a scatter plot, each point representing an individual animal with the mean value presented as a horizontal bar. There were no differences in brain swelling between vehicle and any of the LY354740 drug treated groups (ANOVA).
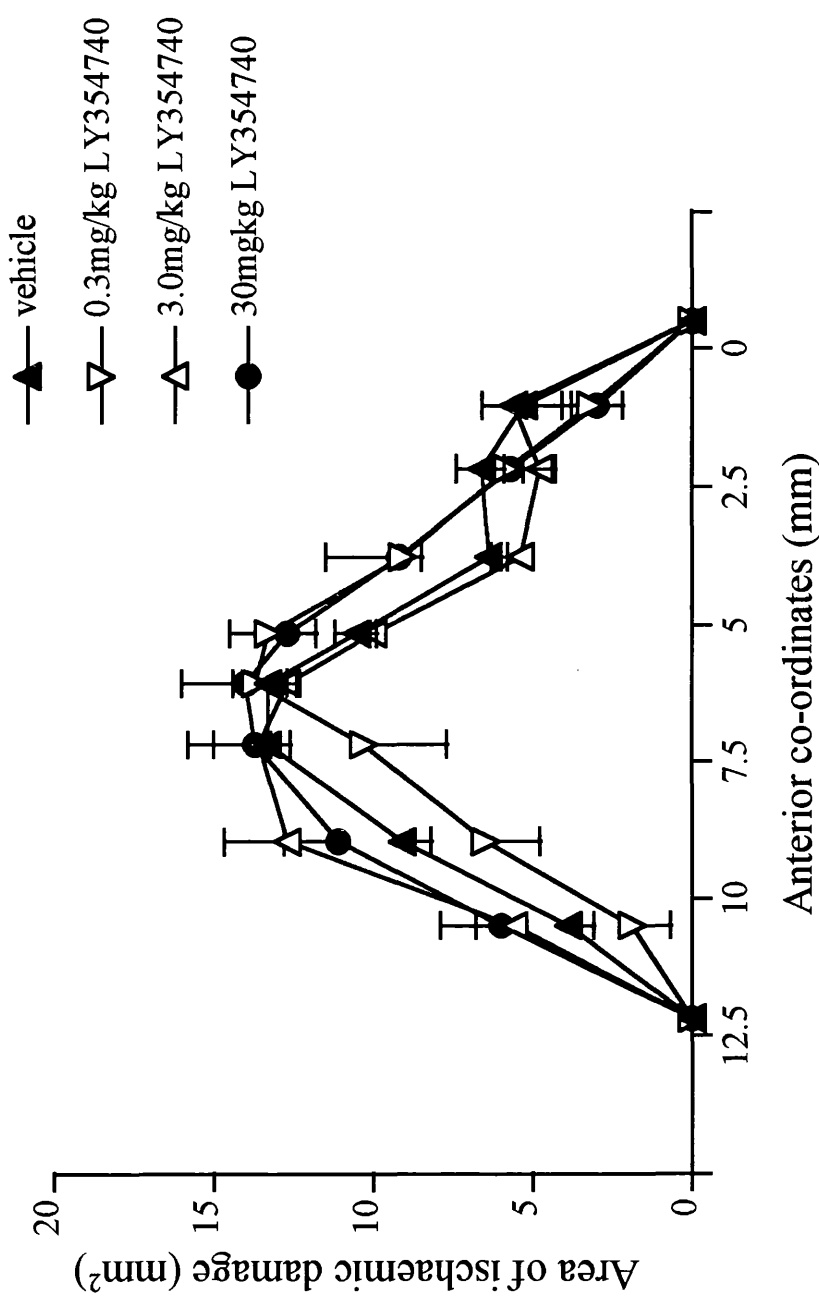
Figure 5.5   The distribution of the areas of brain swelling.

The areas of brain swelling in vehicle and LY354740 treated animals at each of the pre-selected stereotaxic levels (Osborne *et al.*, 1987).
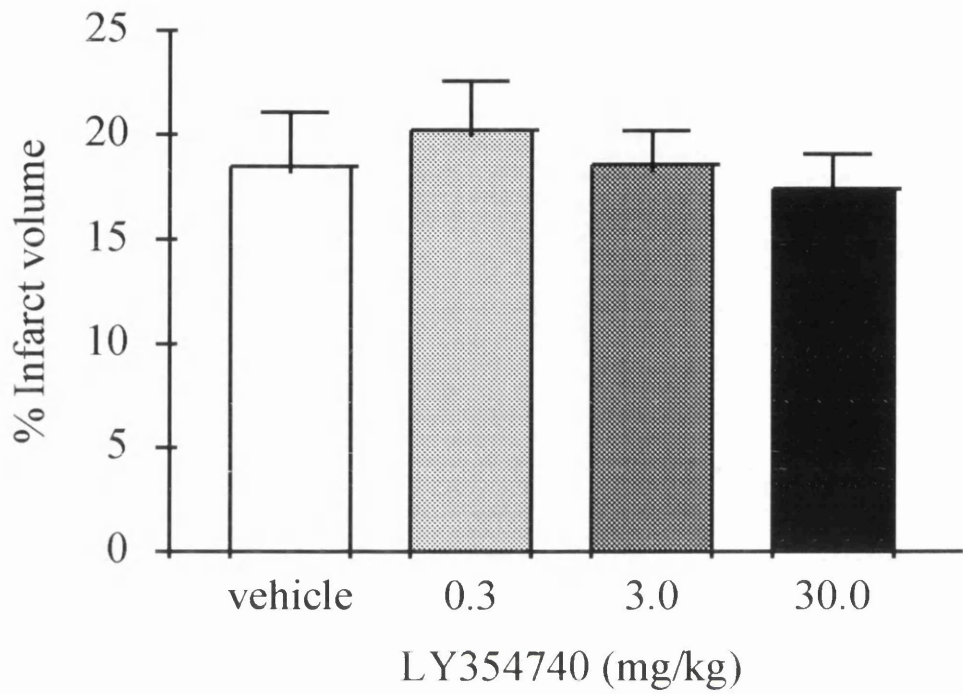
Figure 5.6   Percentage of ipsilateral hemisphere with ischaemic damage.

The percentage of ischaemic damage in each group was determined by measuring the area of the contralateral hemisphere and the area of non-infarcted tissue in the ipsilateral hemisphere (i.e. area of non-pallor) in H & E stained coronal sections from anterior 10.5 mm to posterior 1.02 mm. The respective volumes were obtained by integrating each of the areas measured with the known stereotaxic co-ordinates of the level and the percentage ischaemic damage was generated as described in the text. The data are presented as the mean ± SEM for vehicle controls (n=10); LY354740, 0.3mg/kg (n=5); LY354740, 3.0mg/kg (n=5) and LY354740, 30mg/kg (n=10). Analysis of the data by ANOVA revealed that there were no differences in the percentage infarct volume between vehicle and any of the LY354740 drug treated groups F=0.2 (df 3,29).
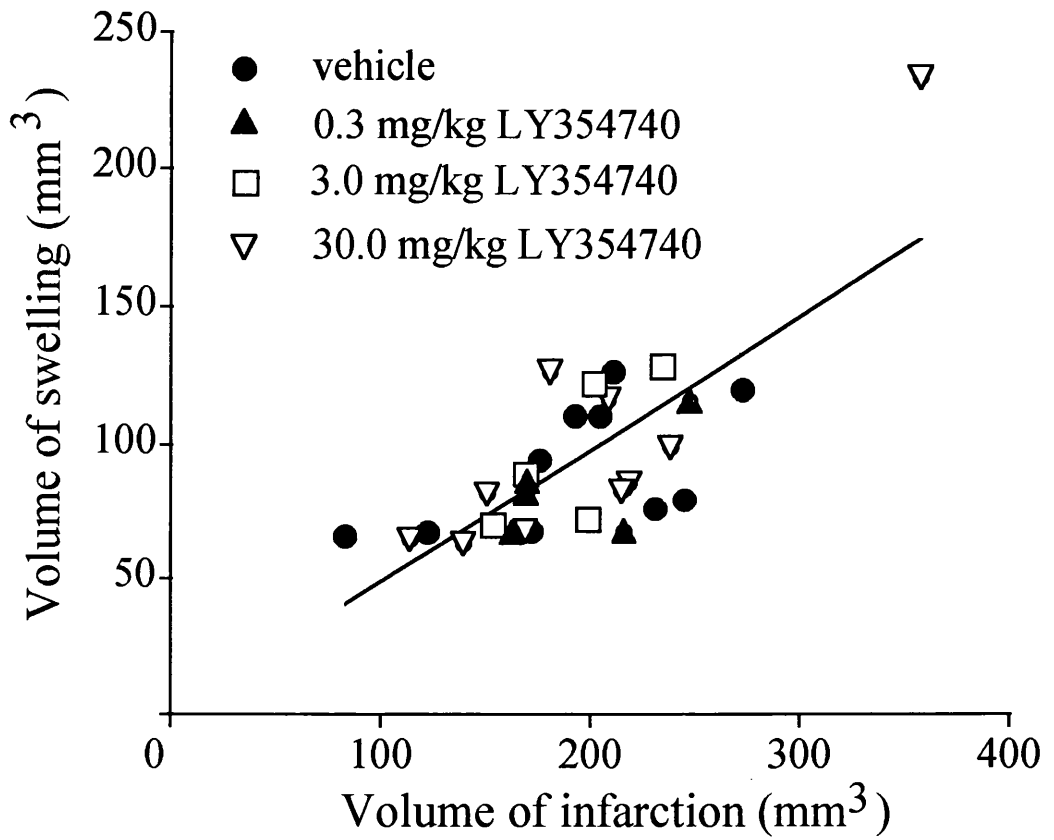
Figure 5.7 The relationship between the volume of infarction (mm^3) and the volume of ipsilateral hemispheric swelling (mm^3) in vehicle and LY354740 treated animals.

5.4   Summary and technical considerations

One of the fundamental problems involved with the determination of infarct volumes from experimental models of cerebral ischaemia is the enlargement of tissue by oedema which can vary from brain to brain. By using the method for measuring the percentage brain infarct volume described by Swanson and colleagues (1990), the potential error that is introduced by swelling is minimised. Irrespective of whether the data are analysed in absolute terms, or in percentage terms, the results from this study show that LY354740 failed to reduce ischaemic damage in the brain following a 24 hour permanent MCA occlusion model of cerebral ischaemia at any of the doses investigated.

In any neuroprotection study in which a drug has failed to alter the outcome, the adequacy of the dosing regimen must be taken into consideration. Levels of LY354740 in the brain were not determined in this study, but previous studies have demonstrated that the doses of LY354740 used in this study would be above levels needed to activate group II mGluRs *in vitro* (Battaglia *et al.*, 1997). Moreover, LY354740 administered at 10 mg/kg (i.v. and p.o), was shown to provide effective brain levels for more than 3 hours (Bond *et al.*, 1997). In addition, the [^{14}C]2-DG autoradiographic studies described in Chapter 3 demonstrated dose dependent changes in brain function (measured by glucose metabolism) following the systemic administration of LY354740 at the same doses used in this study. *Post hoc* power calculations indicated that the sample sizes and variance of the present study would have been capable of detecting changes of approximately 20 % ($\alpha = 5$ %, $\beta = 80$ %). Therefore, it is unlikely that the failure of LY354740 to reduce tissue damage can be attributed to the dosing regimen, or the inadequate power of the study.

Another factor which may influence the outcome in neuroprotection studies is the strain of animal used. It is well recognised that there are differences among rat strains in the hemispheric volumes of infarction. In 5 rat strains studied (Duverger & MacKenzie, 1988),

162

only the Fischer-344 strain demonstrated a consistent and sizeable infarcted volume following cerebral ischaemia. However, it could be possible that while the infarct size is consistent (compared with the variability seen in the Sprague-Dawley strain), the existence of penumbral tissue, and consequently the amount of salvageable tissue, may be compromised.

In summary, despite compelling evidence which suggest that group II metabotropic glutamate receptor agonists are neuroprotective (Buisson & Choi, 1995; Maiese *et al.*, 1995; Chiamulera *et al.*, 1992; Bruno *et al.*, 1996; Miyamoto *et al.*, 1997), LY354740 failed to demonstrate any neuroprotective effects after this model of permanent MCA occlusion in the rat. In direct contrast, a recent study demonstrated that LY354740 was able to substantially reduce damage in CA1 hippocampal neurones in a gerbil model of global ischaemia (Bond *et* al., 1998). The findings of this study and consequently the potential involvement of group II mGluR agonists in neurodegenerative conditions such as ischaemia are considered in section 8.4.

CHAPTER 6

INFLUENCE OF THE GROUP II METABOTROPIC

GLUTAMATE RECEPTOR AGONIST LY379268 IN CEREBRAL

ISCHAEMIA: A NEUROPATHOLOGIC ASSESSMENT

6.1 Introduction

The study carried out in chapter 5 with the mGluR2/3 selective agonist LY354740 revealed that this agent was unable to reduce the volume of ischaemic damage in the rat brain following a 24 hour permanent MCA occlusion model of focal cerebral ischaemia. The findings from the [^{14}C]2-DG study (chapter 3) revealed that although LY354740 and LY379268 are structurally similar, they appear to produce different functional responses in the brain. The aim of this study was to investigate whether LY379268, because of its different profile centrally, was neuroprotective following a 24 hour permanent MCA occlusion in the rat. A dose of 10mg/kg was chosen on the basis of its bioavailability in the brain as demonstrated in chapter 3. In addition to examining infarct size measurements, an attempt was also made to gain insight into the neuropathology of the ischaemic lesion in animals treated with LY379268. Thus, brain sections subjected to MCA occlusion were assessed for cellular changes using immunohistochemical endpoints. With the recent interest in the role of cytokines and white matter protection in cerebral ischaemia (chapter 1, section 1.5.2) immunohistochemical markers used in this instance included antibodies for TGFβ-1 and TGFβ-2 and APP. Given the recent evidence for the reduction of cell death following global ischaemia, the actions of group II mGluR agonists may be influenced by the mechanisms by which cells die. Therefore an antibody for the detection of DNA fragmentation was also used. Finally, an antibody for mGluR2/3 was used to investigate any possible changes in the receptors.

6.2 Methods

6.2.1 Preparation of animals and MCA occlusion

Male Fischer 344 rats weighing between 250-300g were used in this study (Harlan Olac, Bicester, UK). Prior to experiments, animals were housed under the normal conditions and food and water were available *ad libitum*. On the day of surgery, animals were anaesthetised initially with 5% halothane in a nitrous oxide: oxygen mix (70:30) until the righting reflex was lost. Animals were subsequently artificially ventilated following oral intubation, and anaesthetic was maintained with 1.5% halothane. Focal ischaemia was induced using an adapted method of Tamura *et al.* (1981) as described previously (section 2.3). The time of the diathermy was taken as the exact time of the MCA occlusion. The anaesthetic was discontinued and the animals were allowed to recover for the next 24 hours. Once consciousness was regained, the animals were placed into pre-prepared individual cages together with softened diet. They were returned to their normal housing conditions and were examined regularly to check their status.

6.2.2 Drug administration

All animals received two subcutaneous doses of LY379268 (10.0 mg/kg), or vehicle (0.9 % saline) in a volume of 0.5ml saline. The first injection was administered 30 minutes prior to the MCA occlusion under anaesthesia, while the second was administered three hours after the occlusion. All administrations of the drug/vehicle were performed in a blinded manner.

6.2.3 Tissue processing and quantification of lesion size

Twenty four hours following the MCA occlusion, the animals were re-anaesthetised with 5% halothane and perfused transcardially with 4% paraformaldehyde (appendix 3).

Following fixation, animals were decapitated and the heads post-fixed in fresh 4% paraformaldehyde overnight at 4°C. The brains were removed and processed for paraffin embedding. Brains were cut into 6 μm thick serial coronal sections on a microtome and mounted onto poly-l-lysine coated slides. The sections were then left at room temperature overnight to dry. The 8 pre-determined coronal levels (chapter 2, figure 2.3) necessary for the assessment of volumetric measurements of infarction were selected for each animal and stained with H & E. Areas of ischaemic damage were assessed by an observer blinded to the treatment groups using the MCID computer based image analysis system. The approximate volumes of ischaemic damage for each animal were obtained by the method previously described (section 2.3.4). The data were analysed for statistical significance using two-tailed unpaired Student's t-test.

6.2.4 Immunohistochemistry

Immunohistochemical analyses were carried out in adjacent sections to those used for the quantification of the ischaemic damage at the stereotaxic level of the septal nuclei/caudate (anterior co-ordinate = 7.19mm). All antibodies were individually titred to obtain the optimal working concentration. The subsequent antibodies were used at the following concentrations:

rabbit anti-mGluR2/3   1:75

rabbit anti-TGF-β1   1:100

rabbit anti-TGF-β2   1:400

mouse anti-APP   1:50

All staining was carried out as described in section 2.5.1. Staining for the amyloid precursor protein (APP) did not require enzymatic treatment. Antigen unmasking for mGluR2/3, TGF−β1 and TGF−β2 proteins required 0.4% pepsin treatment. Following

immunohistochemical labelling, all stained sections were cleared in histoclear and mounted using synthetic mounting medium, DPX. The slides were left to dry for 24 hours at room temperature before analysis under the microscope.

Subsequent quantification of the stained material was carried out using two different approaches. The APP stained coronal rat brain sections were analysed according to the semi-quantitative method of Yam *et al.*, (1998b). This method makes use of an arbitrary scoring system from 1-3. Thus, a score of one would indicate a low level of APP accumulation, a score of two intermediate/moderate level of APP accumulation, while a score of three reflects the greatest level of APP accumulation. The remaining material for the other protein markers were analysed by counting the number of cells stained selectively with the antibody within a 1 cm^2 counting grid. Figure 6.1 illustrates the method by which this was carried out. By reference back to the line diagrams generated for the quantification of the volume of ischaemia, the boundary of the lesion, i.e. border of dead or alive cells, could be ascertained. Once the boundary of the lesion was located, using the corpus callosum as an anatomical landmark, the grid counter was placed in such a manner so that it was aligned parallel with the border of the ischaemic damage. Four separate areas were counted; outwith the boundary of the ischaemic lesion, and then three consecutive adjacent areas progressing further into the ischaemic lesion. The cell counts were carried out three times and performed in a blinded fashion. The data were analysed at each level for statistical significance using two-tailed unpaired Student's *t*-test.
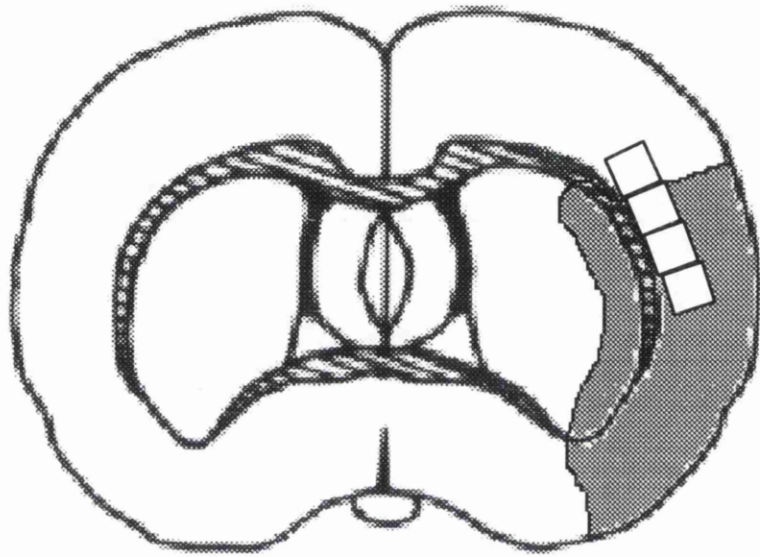
Figure 6.1   Analysis of immunohistochemical labelling of TGFβ-1, TGFβ-2 and mGluR2/3 for cell counting

Schematic representation of the brain areas analysed for staining with immunohistochemical markers. The 1 cm^2 grid used corresponds to an area of 0.5 mm^2 as a result of the magnification of the section.

6.3 Results

6.3.1 Effect of LY379268 on the size of the ischaemic lesion

All animals were again less active during the first few hours of recovery compared with their behaviour prior to the surgical procedure. Very little movement or signs of inquisitive behaviour were exhibited. However, by approximately 3-4 hours after MCA occlusion (coinciding with the second administration of the drug), marked changes in the general behaviour of LY379268 (10mg/kg) treated animals were noted. It was apparent that some of the animals (drug and vehicle treated) were experiencing a slight discomfort at having another s.c. injection, for example, moving around the cage and whimpering. LY379268 (10mg/kg) treated animals appeared to be especially hypersensitive to tactile and auditory stimuli and were very jumpy. By the next morning, the behaviour of all the animals were similar; they had taken soft diet, and they all exhibited signs of inquisitiveness. Important physiological parameters known to directly affect the variability in outcome were monitored. The values for these parameters are presented in table 6.1. No significant changes were identified in any of the parameters measured before or after the ischaemic insult (two-tailed paired Student's t-test). None of the animals exhibited any adverse signs of suffering, and the mortality rate was zero.

From the H & E stained sections of the rat brain, ischaemic damage was apparent within the territory supplied by the occluded MCA. The histopathological appearance between ischaemic brain tissue in animals treated with LY379268 and vehicle were indistinguishable, with a relatively even proportion of small and large areas of ischaemic damage. The effects on LY379268 on infarct volume are presented in table 6.2. A typical lesion produced by permanent occlusion of the MCA in this study is illustrated in figure 6.2 (for an actual H & E section, see appendix 6). At 24 hours after MCA occlusion, figure 6.3 illustrates that there were no significant decreases in infarct volume following treatment of

LY379268 (10 mg/kg). The distribution of the areas of ischaemic damage are also presented in figure 6.4.

6.3.2 Analysis of immunohistochemical labelling

APP

APP-specific staining was localised selectively at the borders of the ischaemic lesion in the subcortical white matter and in the myelinated fibre tracts within the caudate nucleus. Background non-specific staining was not evident in either the contralateral hemisphere or ipsilateral cortex. Varying levels of APP accumulation were seen in the animals and none of the animals displayed an absence of APP accumulation. The scores allocated to each of the animals (vehicle and LY379268 treatment) at the stereotaxic level of the septal/caudate nuclei are presented in table 6.3. It is clear that both treatment groups exhibit varying levels of APP accumulation and there is no separation between high and low scores of APP accumulation between the two groups. Examples of low (score of 1), moderate (score of 2) and high (score of 3) levels of APP accumulation are presented in figures 6.5-6.6. In addition, figure 6.7 illustrates that there is no correlation between APP accumulation and the volume of ischaemia.

Fragment end labelling of DNA

The immunohistochemical labelling of nucleosomal DNA fragments with terminal deoxynucleotidyl transferase (TdT) produced highly selective staining seen only in the region of the ischaemic lesion. Very little or no staining was evident in the contralateral hemisphere. Both the vehicle treated control group and the LY379268 treated group displayed a general increase in the number of labelled cells with increasing progression into

Table 6.1   Physiological variables monitored before and after MCA occlusion.

PARAMETER	VEHICLE		LY379268	
	before surgery	after surgery	before surgery	after surgery
Body temperature	37 ± 0.1	38 ± 0.2	37 ± 0.1	38 ± 0.1
Brain temperature	36 ± 0.1	37 ± 0.2	36 ± 0.3	36 ± 0.3
MABP	105 ± 2.7	94 ± 2.8	100 ± 3.4	97 ± 1.6
Plasma glucose	12 ± 0.9	10 ± 0.2	10 ± 0.4	9 ± 0.32
pCO2	37 ± 0.7	37 ± 0.7	36 ± 0.8	36 ± 1.0
pO2	155 ± 4.8	154 ± 5.3	161 ± 3.7	155 ± 4.0
pH	7.5 ± 0.01	7.5 ± 0.01	7.5 ± 0.00	7.5 ± 0.01
Number of animals	10		10	

Data are presented as mean values $\pm$ SEM.

There were no significant differences between parameters measured before or after the ischaemic insult in LY379268 treated animals or vehicle treated controls (Student's paired t-test).

Table 6.2   LY379268 and the volume of ischaemic damage (mm^3) following permanent MCA occlusion.

VOLUME (mm^3)	VEHICLE	LY379268 (10mg/kg)
Infarct:		
Hemispheric	101 ± 8	97 ± 11
Cortex	68 ± 8	63 ± 9
Caudate	26 ± 0.5	27 ± 1
Number of animals	9	9

The data are presented as mean $\pm$ SEM (mm^3). LY379268 (10mg/kg) or vehicle (saline) were administered by 2 s.c. injections 30 minutes before and 3 hours after the MCA occlusion. There were no significant differences in volume of infarct between vehicle or LY379268 treated animals (Student's unpaired t-test). Only 9 animals from each group were available for analysis due to cutting artefacts.
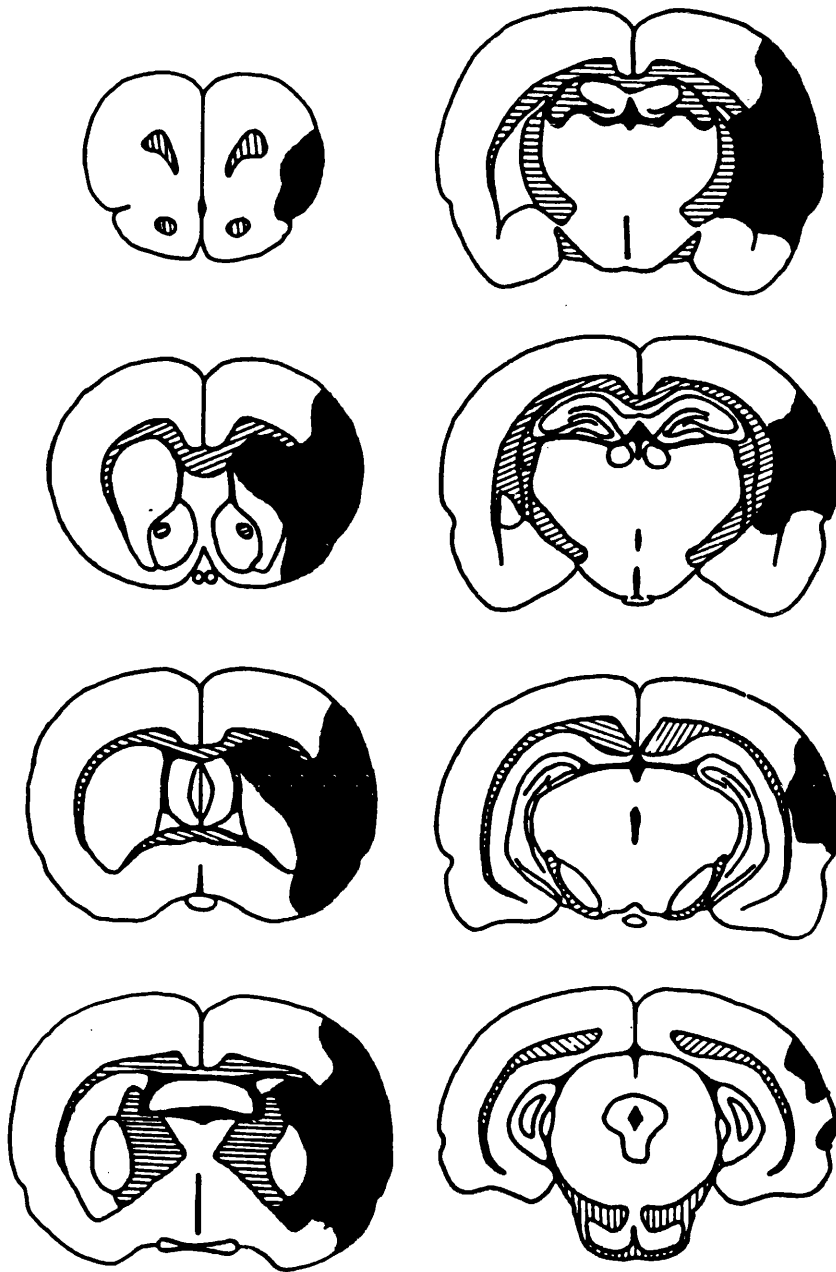
Figure 6.2   Focal ischaemic lesion.

A representative rat brain illustrating the distribution of the ischaemic damage produced 24 hours after the permanent occlusion of the MCA. The histopathological assessment of damage is mapped at the 8 stereotaxic levels, with the damaged areas highlighted in black.
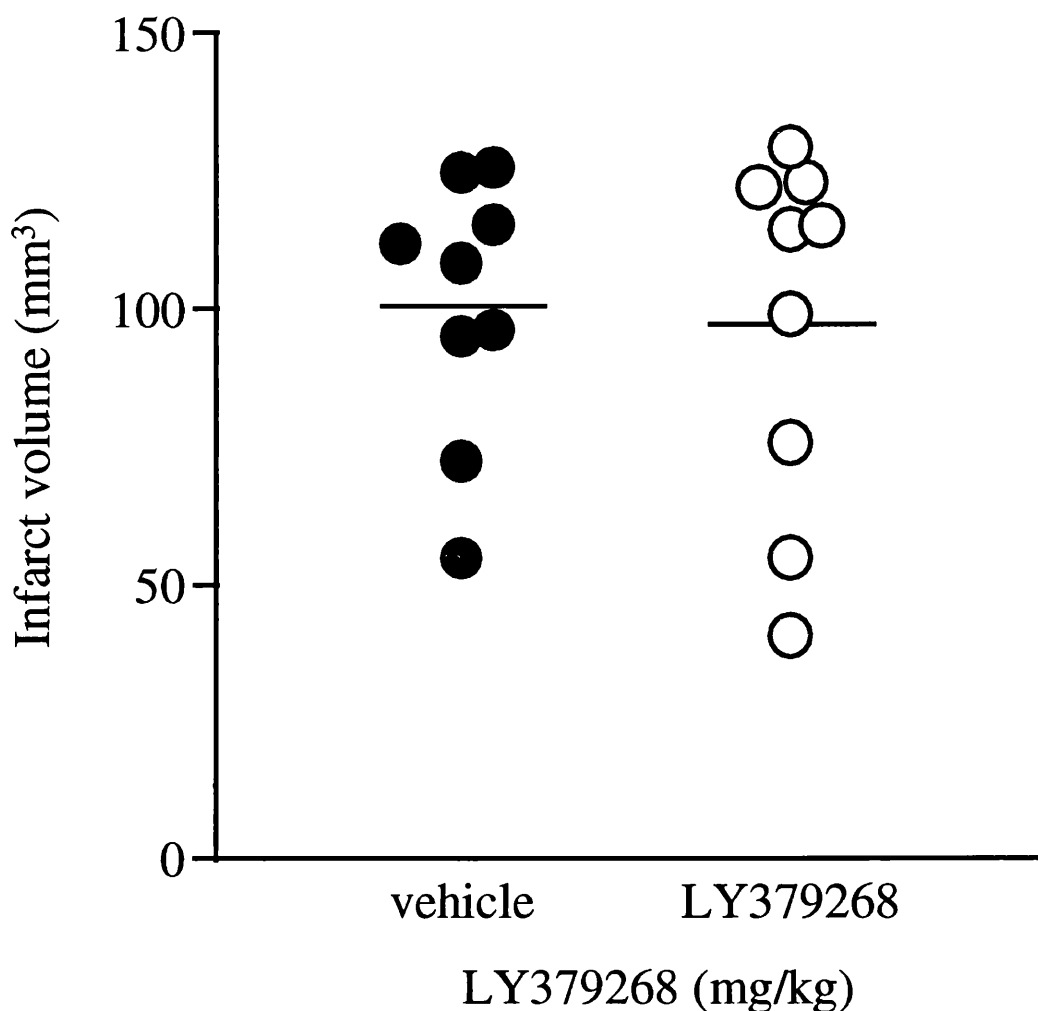
Figure 6.3   Volumes of infarction.

Areas of infarct were measured directly from the line diagrams of the stereotaxic levels from anterior 10.5 mm to posterior 1.02 mm. Areas were then calculated to take into account the magnification factor of the diagrams. Volumes of ischaemic damage were obtained by integrating each of the calculated areas with the known stereotaxic co-ordinates of the level. The data are presented as a scatter plot, each point representing an individual animal with the mean value presented as a horizontal bar. There were no differences in infarct volume between vehicle and the LY379268 treated group (Student's unpaired t-test)
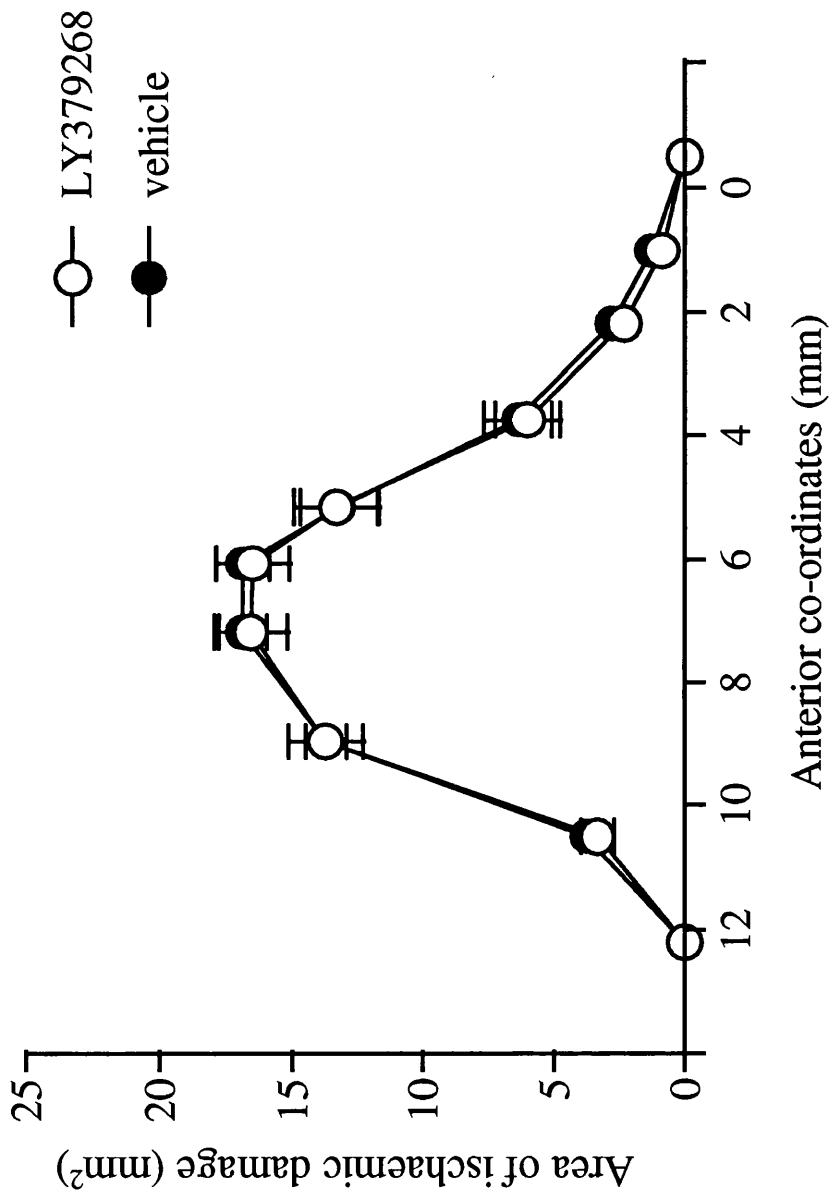
Figure 6.4 The distribution of the areas of ischaemic damage.

The areas of ischaemic damage in vehicle and LY379268 treated animals at each of the pre-selected stereotaxic levels (Osborne *et al.*, 1987).

Table 6.3 **APP accumulation and volumes of ischaemic damage.**

GROUP	APP SCORE	VOLUME OF ISCHAEMIC DAMAGE (mm^3)		
		hemisphere	cortex	caudate
Vehicle	2 ± 0.26	100.5 ± 8.0	67.9 ± 7.5	25.9 ± 0.5
LY379268	1.7 ± 0.26	97.3 ± 10.8	63.0 ± 9.4	27.0 ± 0.9
number of animals	10	9	9	9

Summary table of APP score at one stereotaxic level (anterior 7.19 mm) and volumes of ischaemic damage in vehicle and LY379268 treated groups.

Data are presented as mean values ± SEM.
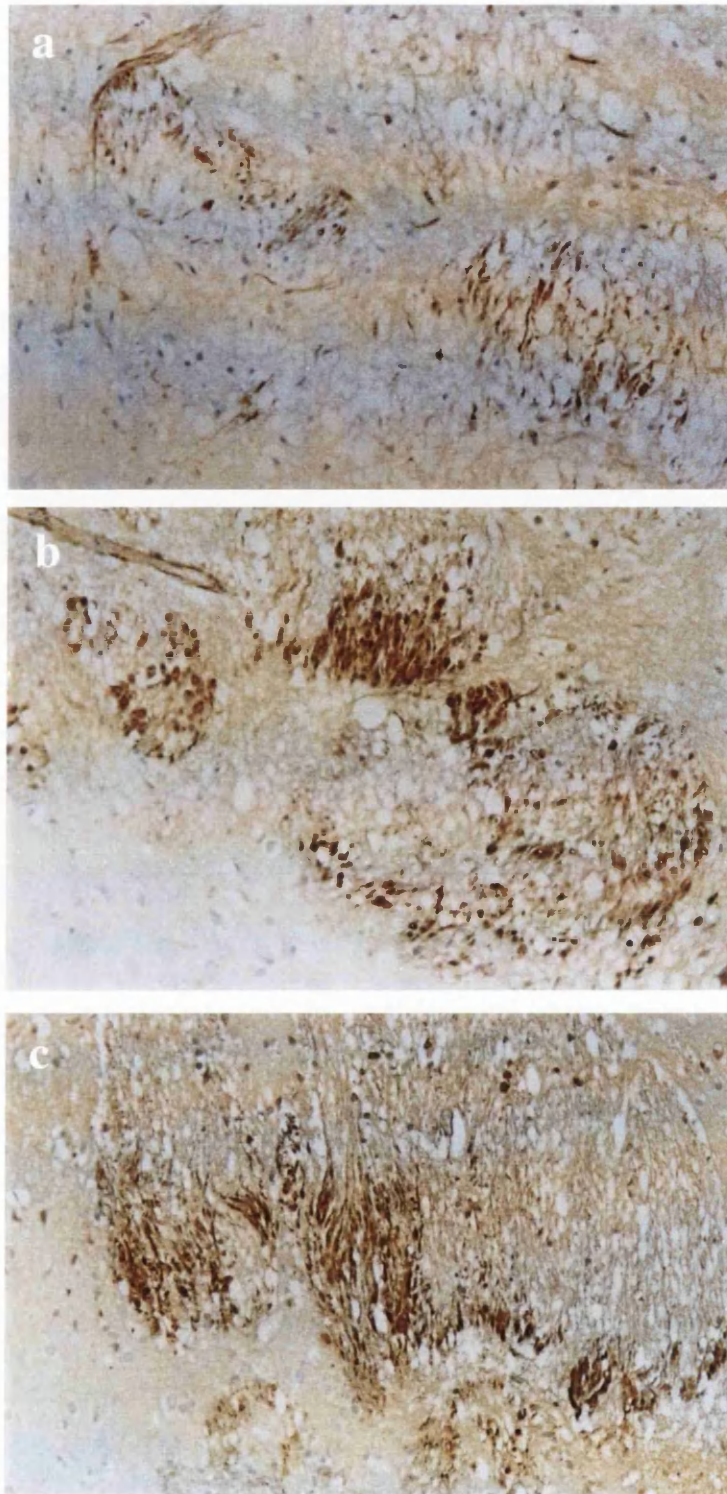
Figure 6.5   APP immunoreactivity: method of scoring.

Representative examples (x200) of a) low level of APP accumulation - allocated score of 1; b) moderate APP accumulation - score of 2; c) dense APP accumulation - score of 3.
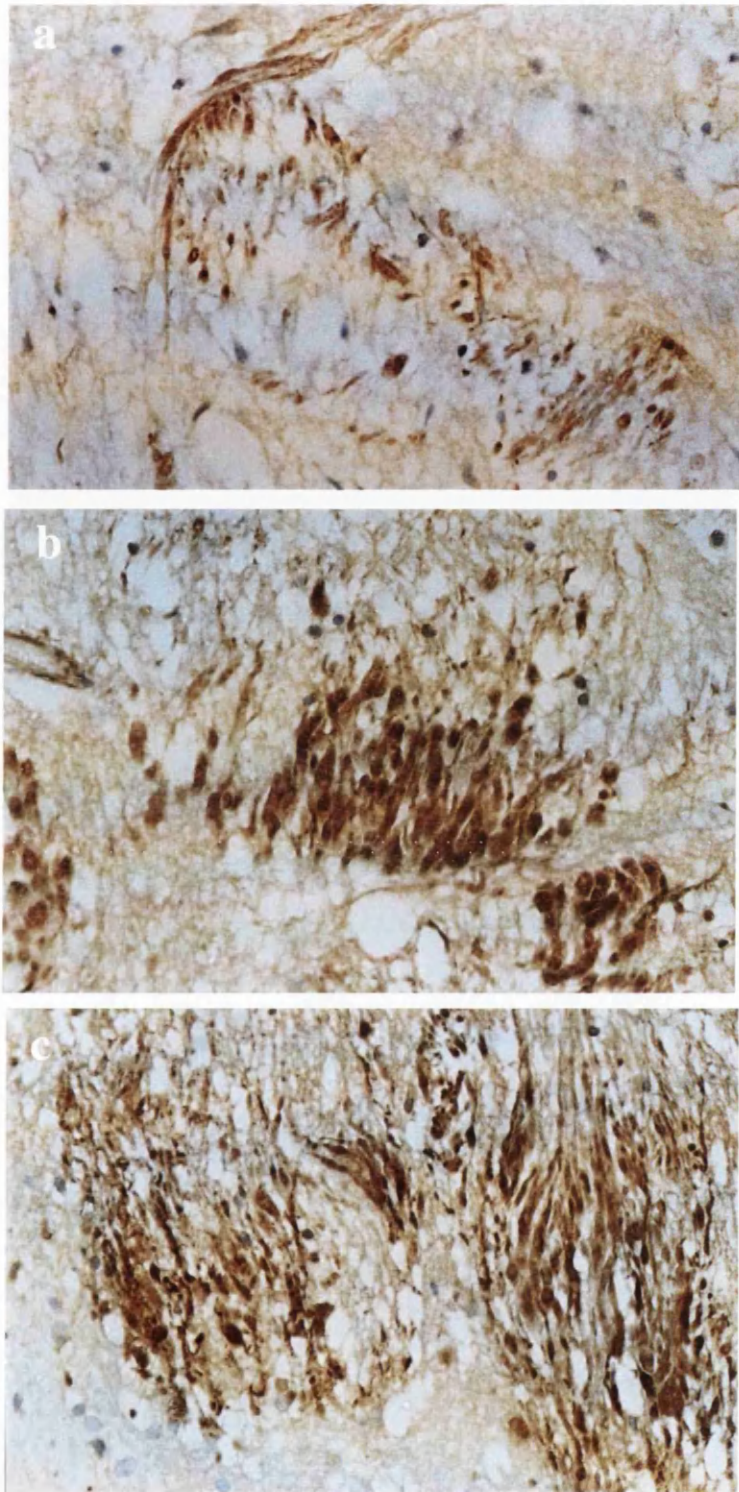
Figure 6.6   APP immunoreactivity: method of scoring.

Representative examples (x400) of a) low level of APP scoring; b) moderate APP accumulation; c) dense APP accumulation.
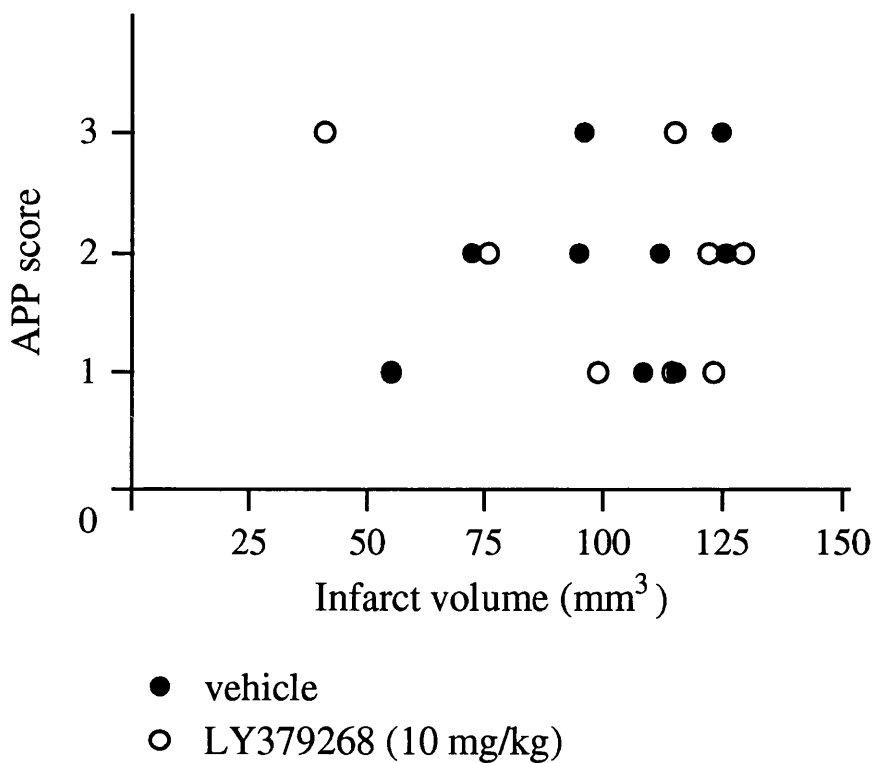
Figure 6.7 **No relationship between the volume of infarction (mm^3) and the level of APP accumulation in vehicle and LY379268 treated animals.**

APP scoring was only taken at one stereotaxic level (anterior 7.19 mm). The solid line corresponds to vehicle treated control group, while the dashed line corresponds to the LY379268 treatment group.

the ischaemic tissue (table 6.4). Cell counts taken outwith the border of the ischaemia show an apparent reduction in the number of positively labelled cells following LY379268. This reduction just failed to reach statistical significance (t = 1.763). However, at the boundary and at the core of the ischaemic lesion, significant reductions in the number of TdT labelled cells were demonstrated. At the boundary of the lesion, LY379268 treated animals displayed a 41% reduction in TdT labelled cells, while at the core a 28% reduction in labelled cells was seen. Figure 6.8 illustrates representative TdT labelled sections at the boundary and core of the lesion.

TGF-β1

Immunohistochemical labelling for TGF-β1 produced widespread staining throughout the tissue. Cells were also counted in the contralateral hemisphere in one area that approximated to the boundary of the ischaemic tissue in the ipsilateral hemisphere. This area was included in order to gauge the level of TGF-β1-positive cells present in undamaged tissue (previous histology for the quantification of infarct volume confirmed that the morphology cells in the contralateral hemisphere to be undamaged) and therefore act as an internal control. Table 6.4 shows that there were no differences in the number of TGF-β1-positive cells between the vehicle treated control and LY379268 treated groups in the contralateral hemisphere. No differences in the number of immunoreactive cells were seen between counts taken in the area outwith the boundary of the ischaemia and the contralateral hemisphere. Both treatment groups also display a general reduction in the number of cells positively stained for TGF-β1, with increasing progression into the ischaemic tissue. Animals treated with LY379268 appear to contain marginally less stained cells than the vehicle treated controls (not statistically significant). Cell counts taken within

the core of the infarct show that the number of TGF-β1-positive cells following LY379268 was significantly reduced (-18%).

TGF-β2

TGF-β2 immunoreactivity was evident throughout both hemispheres. Again, TGF-β2-positive cells in the contralateral hemisphere were counted at a level approximating the boundary of the ischaemic lesion. Table 6.4 shows that no differences were observed in the number of immunoreactive cells on the contralateral hemisphere. However, in the ipsilateral hemisphere, cell counts taken outwith the boundary of ischaemic damage revealed TGF-β2 immunoreactivity to be increased by 25% following LY379268 treatment (just failed to reach statistical significance). With both the vehicle treated controls and the LY379268 treated groups, the number of TGF-β2-positive cells decreased with further progression into the area of ischaemic tissue. In addition, tissue from LY379268 treated animals showed higher counts of immunoreactivity than vehicle treated controls. TGF-β2 immunoreactivity is presented in figure 6.9.

mGluR2/3

Immunohistochemical labelling for mGluR2 and mGluR3 in this study showed widespread immunoreactivity throughout both hemispheres. The number of immunoreactive cells in the contralateral hemisphere did not differ significantly in either the vehicle treated or LY379268 treated groups. Also, numbers of mGluR2/3-immunoreactive cells in the ipsilateral hemisphere outwith the boundary of the ischaemia were not significantly altered from the counts obtained from the contralateral hemisphere. In contrast to the results obtained with fragment end labelling of DNA and TGFβ-1 and -2 immunoreactivity, cell counts of immunoreactivity taken within the area of ischaemic damage did not differ

Table 6.4   Quantification of TdT, TGFβ-1, TGFβ-2 and mGluR2/3 immunoreactive cells following 24 hour permanent focal ischaemia.

AREA	DNA FRAGMENTATION		TGFβ-1		TGFβ-2		mGluR2/3	
	Vehicle	LY379268	Vehicle	LY379268	Vehicle	LY379268	Vehicle	LY379268
Contralateral	-	-	101 ± 8	93 ± 8	86 ± 4	83 ± 7	80 ± 4	67 ± 8
area 1 (outwith boundary)	25 ± 9	7 ± 2	98 ± 5	94 ± 7	81 ± 5	101 ± 10	69 ± 7	63 ± 7
area 2 (boundary)	62 ± 8	36 ± 6*	98 ± 7	89 ± 7	85 ± 5	97 ± 10	72 ± 6	76 ± 7
area 3 (core)	76 ± 10	51 ± 8	80 ± 6	69 ± 5	66 ± 6	77 ± 8	65 ± 4	60 ± 4
area 4 (core)	92 ± 4	67 ± 6**	73 ± 4	60 ± 3**	63 ± 4	66 ± 5	61 ± 5	50 ± 3

The method by which the cell counts were obtained is described in the text and also illustrated in figure 6.1. Data are presented as mean ± SEM. *P<0.05 **P<0.01 for statistical comparison between the vehicle and LY379268 treated groups at the corresponding area (Student's unpaired t-test).
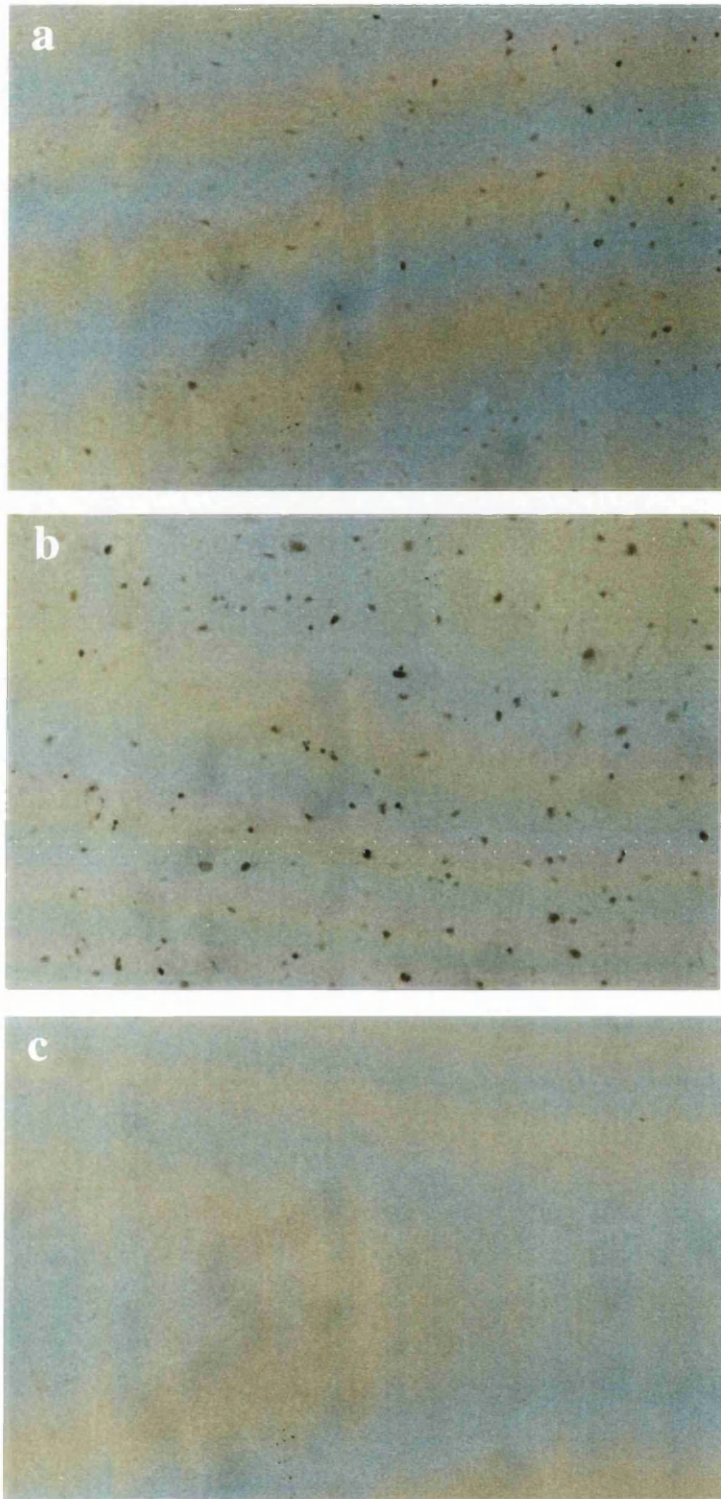
Figure 6.8   Fragment end labelling of DNA by TdT: reduction in the number of immunoreactive cells.

Representative photographs (x200) illustrating the changes in cell immunoreactivity a) the boundary of the ischaemic lesion and b) the core of the lesion. Contralateral staining is also illustrated c).
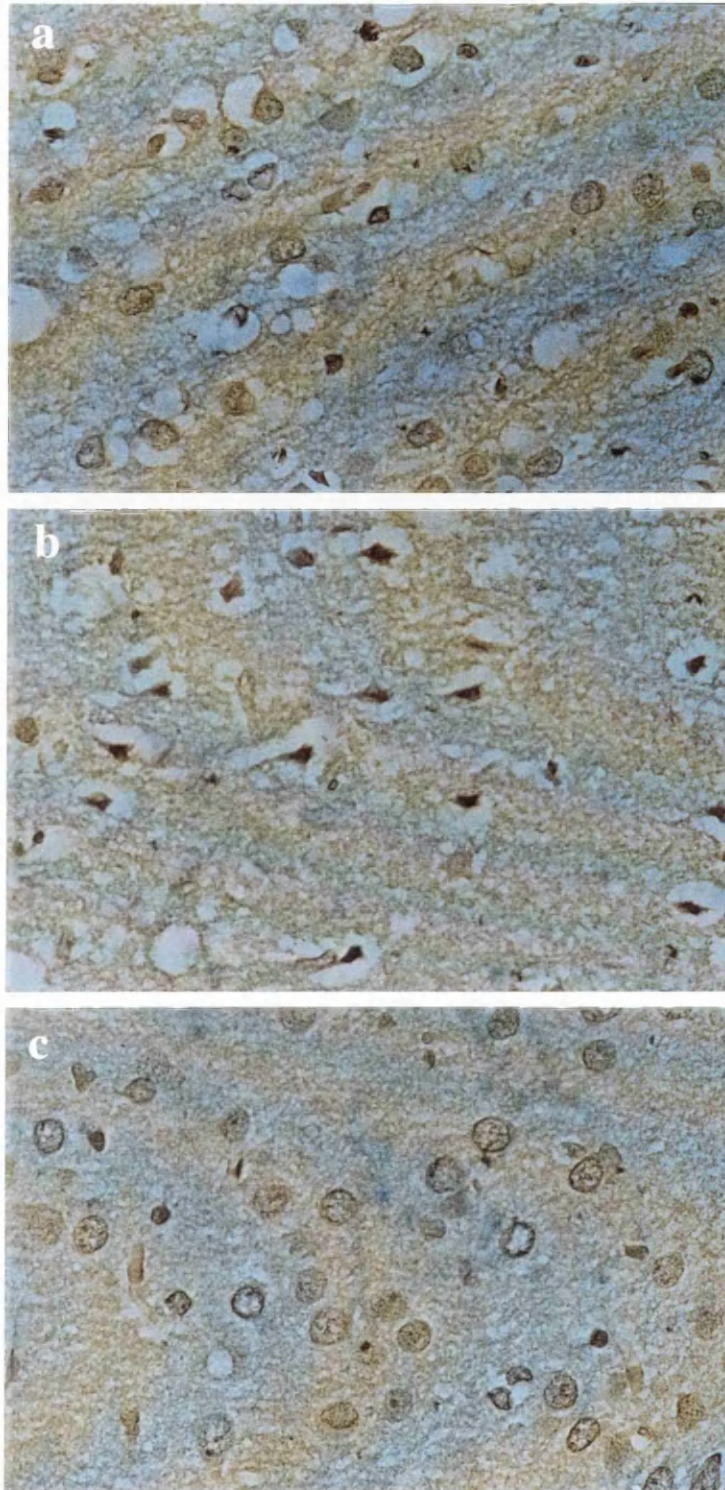
Figure 6.9   Cell immunoreactivity for TGF-β2 : alterations in the number of immunoreactive cells.

Representative photographs illustrating the changes in cell immunoreactivity a) outwith the ischaemic lesion and b) at the core of the lesion.   c) represents TGF-β2 immunoreactivity in the contralateral hemisphere.
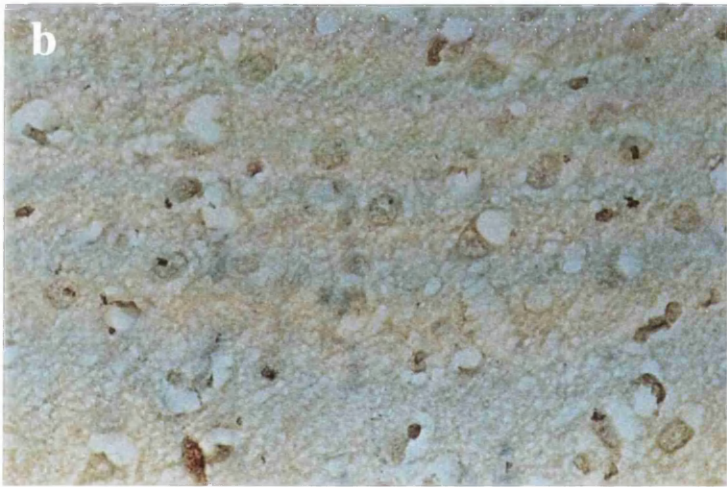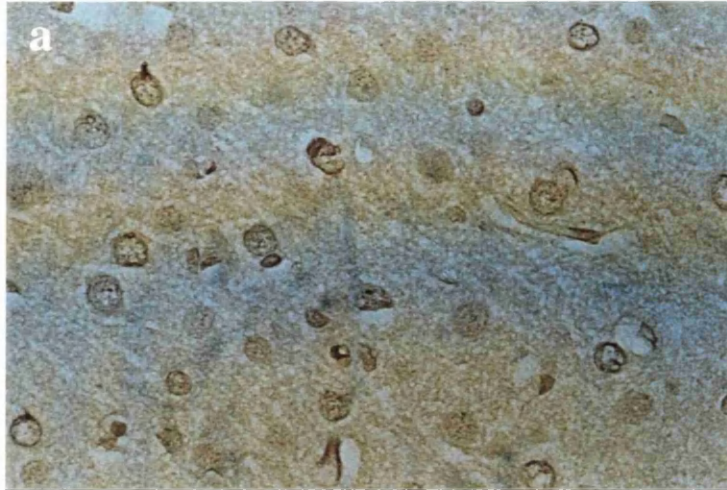
Figure 6.10   mGluR2/3 immunoreactivity.

Representative photographs showing immunoreactivity in the a) contralateral hemisphere and b) ipsilateral hemisphere following 24 hour permanent focal ischaemia. Note the less intense staining of the ipsilateral hemisphere.

markedly from the contralateral hemisphere (table 6.4) following either vehicle or LY379268 treatment. Although the number of positively stained cells did not differ, mGluR2/3 immunoreactivity appeared more faint in the ischaemic ipsilateral hemisphere than the non-ischaemic contralateral hemisphere (figure 6.10).

6.4   Summary and technical considerations

From a histological neuroprotection viewpoint, LY379268 (10mg/kg) failed to reduce ischaemic damage in the brain following 24 hour permanent MCA occlusion model of cerebral ischaemia. Again, questions that address the adequacy of the dosing regimen must be answered. At 10mg/kg (s.c.), LY379268 has been demonstrated to provide effective brain levels for the activation of mGluR2 and mGluR3 for greater than 3 hours (Dr. D. Schoepp, personal communication - see chapter 8, figure 8.1). Also, the results from autoradiographic studies in chapter 3 clearly demonstrate that LY379268, at the same dose, was able to effect selective changes in brain function. *Post hoc* power calculations indicated that for this study, the sample sizes used and the variance would have been capable of detecting changes of approximately 20% (α=5%, β=80%). Consequently, it is unlikely that the inability of LY379268 to reduce tissue damage can be attributed to the dosing regimen, or inadequate power of the study.

Although the use of histological endpoints alone has not provided any evidence to suggest that LY379268 is neuroprotective (reduction in volume of ischaemia) in this rat model of permanent focal ischaemia, the use of immunohistochemical markers in this study may hint at the neuroprotective effects of LY379268, as analysis of the tissue resulted in some interesting data. In this study, 24 hour permanent focal cerebral ischaemia has revealed that the number of TGFβ-1 immunoreactive cells in the ipsilateral hemisphere in both groups is similar to that seen in undamaged contralateral hemisphere, and following

LY379268, a significant reduction in the number of immunoreactive cells is observed in the core of the damaged tissue. In contrast, treatment with LY379268 resulted in an apparent increase in the number of cells displaying TGFβ-2 immunoreactivity in a circumscribed area just outwith the boundary of the ischaemia. This increase in the number of immunoreactive cells is not seen in any of the other areas investigated. The data obtained from fragment end labelling of DNA with the TdT enzyme also displayed significant changes in the number of immunoreactive cells in the drug treated groups. LY379268 treated animals showed marked reductions in the number of positive TdT stained cells in and around the boundary of the ischaemic lesion, with reductions also evident in the core. Staining for immunoreactive mGluR2/3 cells in this study demonstrated that there are no changes in the number of immunoreactive cells, but there may be a reduction in the intensity of the stain in immunoreactive mGluR2/3 cells.

The method of analysis used in this study differed from that used for the quantification of ischaemic damage described in chapter 5 with LY354740. Because of the study's requirements for immunohistochemical analysis of the tissue, the brain material had to be fixed and paraffin embedded. This however, raises problems such as shrinkage of tissue as a result of fixation and the subsequent re-hydration of the tissue, all processes that are uncontrollable and inconsistent (Stowell, 1941). Such changes were clearly evident in the brain tissue used in this study, and are discussed further in appendix 6. Therefore, the method used to measure infarct size excludes the contribution of swelling that could lead to an overestimation of the size of the lesion (Osborne et al., 1987). This method requires the delineation of the area of ischaemia at the pre-determined levels which is then transcribed onto coronal scale diagrams (4x actual size) drawn from the atlas of König & Klippel (1963).

The method by which APP accumulation was assessed was straightforward but not without its limitations. A major problem is the narrow range of the scoring system from 1 to 3 which places constraints upon the staining observed. For example APP accumulation could have been seen diffusely but extensively along the boundary of the ischaemia, and may have been allocated a low score compared to a dense accumulation of APP in circumscribed zones along the boundary. In addition, because only one level was assessed in this instance, a maximum score of 3 is only possible in each group. Although analysis of all 8 levels may have provided more insight into the distribution of APP, the limitation associated with the fixed maximum score still holds true. In theory, one could arbitrarily produce a scoring system ranging from 1-5 or 1-10 *etc.* to assess levels of staining. However, this would introduce the added problem of subjectivity and reproducibility; the use of scores from 1-3 limits this problem and the method is reproducible. In addition, the small variance in lesion sizes in rats and the small number of levels assessed makes the separation of APP scores between different treatment groups difficult. This has led to the development of APP quantification using stereological methods (Yam *et al.*, in preparation). This involves using a transparent fine, regular square array point-grid system. The grid is placed over an image of the section and the number of points overlying areas of APP immunoreactivity are counted. The advantage of this technique is that it is totally quantitative and sensitive. The authors were able to measure APP scores between coronal levels ranging from 1-177.

The use of immunohistochemistry is notoriously subjective, and unless the immunoreactive response is very selective and intense, changes in staining are difficult to discern objectively. Therefore whether the difference between the intensity of mGluR2/3 staining observed in ischaemic tissue following LY379268 compared with vehicle treated controls is a 'real' observation is not known. However, the staining pattern observed should not be interpreted purely on face value. It is known that immunohistochemical staining

carried out at in different batches at different times will produce variable responses in the intensity of staining depending on the length of time the tissue has been exposed to the chromogen. Thus, interpretation of such data is always carried out in blocks so that tissue samples stained at the same time are also analysed together. Needless to say, within any batch of tissue stained, one cannot definitively say that each sample was exposed to the chromogen for exactly the same time. An interesting study to carry out would be to use Western blotting analysis to compare the levels of the mGluR2/3 protein in ischaemic tissue from vehicle and LY379268 treated animals.

The results of this study are discussed in detail in chapter 8, section 8.4.

CHAPTER 7

PROTECTIVE MECHANISMS OF LY354740 & LY379268

FOLLOWING *IN VITRO* NEUROTOXICITY?

7.1 Introduction

In vivo neuroprotection studies are limited in one respect in that they provide, on the whole, observational data. Thus, the *in vivo* studies carried out in chapters 5 and 6 demonstrated that the administration of LY354740 and LY379268 were not capable of reducing the size of the ischaemic lesion. *In vitro* models of cerebral ischaemia may provide valuable information about the cellular mechanisms of injury not possible *in vivo*. For example, the systems allow the possibility of selecting the type of cells cultured (e.g. neurone enriched cultures, astrocytes, oligodendrocytes, endothelial cells), and also cells from specific brain regions. Cell culture systems have been used extensively, and recent work has shown that the activation of group II or group III metabotropic receptors is neuroprotective against a variety of insults such as NMDA-induced excitotoxicity (Bruno *et al.*, 1994, 1995a; Buisson *et al.*, 1996), hypoxia/hypoglycaemia (Buisson & Choi, 1995), nitric oxide (Maiese *et al.*, 1995) and staurosporine (Koh *et al.*, 1994).

The aims of this study were to assess the neuroprotective actions of LY354740 and LY379268 in *in vitro* models of neuronal cell death. By using different models of neurotoxicity together with Western blot analysis of astrocyte cultures to investigate the production of neurotrophic factors, the issues of the possible protective mechanisms of LY354740 and LY379268 were addressed. Neurotoxicity was induced by the deprivation of glucose and oxygen, and by the application of staurosporine.

7.2 Methods

Part of the work described in this chapter (neurotoxicity studies) was carried out over 8 weeks at Eli Lilly, Windlesham, Surrey. The neurotoxicity studies described use both staurosporine and hypoxia/hypoglycaemia models of cell death, neither of which were in use at the laboratories at Eli Lilly. Therefore, initial experiments were carried out in order to optimise the conditions for neurotoxicity. However, because of time constraints, only a limited number of experiments could be carried out. So, although the majority of the experiments carried out in this study were performed by myself, Dr. Ann Kingston (Eli Lilly), kindly agreed to generate additional material on the basis of the initial optimisation experiments. These results are included in this chapter.

7.2.1 Cell culture

Neurone-enriched cultures

Neurone-enriched cultures were prepared from embryonic rat neocortex according to the method of Rose *et al.* (1993). Briefly, neocortices from embryonic rats at day 18 of gestation were dissociated using trypsin and mechanical disruption. Cells were plated in Neurobasal medium (containing 10% heat inactivated FCS and glutamine 1mM) and plated in 15mm 24 well plates previously treated with poly-D-lysine, at a density of 3×10^5 cells per well and kept at 37°C in a humidified 5% CO_2 atmosphere. Non-neuronal cell division was halted after 2 days in culture, by exposure to cytosine arabinoside (5µm) for 3 days. The medium was part-replaced at 3-5 day intervals and the cells used after 10-14 days in culture.

Pure astrocyte cultures

Astrocytes were cultured from the cortices of day 0-3 rat neonates as described in chapter 2, section 2.4.1. Cortices were enzymatically and mechanically dissociated and cells were plated down in DMEM containing 20% FCS and 1mM glutamine at a final density of 1.5×10^6 cells/ml (2×10^5 cells/cm^2) into 75 cm^2 flasks (total volume 10mls). The medium was exchanged after 3 days (DMEM with 10% FCS) and subsequent changes made twice a week. Once the cells reached confluence after 10-12 days in culture, they were purified according to the method of McCarthy & de Vellis (1980). Experiments were performed on cultures after 21 days *in vitro*.

Mixed neuronal-astrocyte cortical cultures

Mixed cultures of neurones and astrocytes were obtained by plating the neocortical cell suspension on a previously established monolayer of type I cortical astrocytes (established *in vitro* for 2 weeks). Astrocytes were prepared and maintained as above and plated at a final density of 15×10^4 cells/well into poly-D-lysine treated 24 well plates. Dissociated cortical neuronal cells were then added (3×10^5 cells/well) directly onto the astrocytes and treated with cytosine arabinoside from day 0 of culture. Cultures were again used after 10-14 days *in vitro* (with respect to neuronal cultures).

7.2.2 Induction of staurosporine-induced neurotoxicity

For staurosporine-induced neurotoxicity, cells were incubated with Neurobasal medium (serum and glucose free with 1% HEPES, 1% glutamine and $10\mu M$ glycine) and staurosporine for 24 hours. Supernatants from the cultures were then collected for the assessment of neurotoxicity. The data were analysed for statistical significance using two-tailed Student's *t*-test.

7.2.3 Glucose and oxygen deprivation

Glucose and oxygen deprivation was induced in 24 well cultures by incubating the cultures in deoxygenated balanced salt solution (glucose free) containing 1% HEPES in a 5% O_2/5% CO_2 environment. Following the incubation, the medium was exchanged with serum free Neurobasal medium and incubated in a 5% CO_2/90% air atmosphere for the remainder of the 24 hour incubation before the evaluation of cell damage and death. The data were not analysed for statistical significance because of the small number of experiments carried out.

7.2.4 Drug administration

LY354740 and LY379268 were prepared as 0.1M stock solutions in 0.1M NaOH. Working concentrations of the two agonists were prepared at 100X the final concentration just before use at various doses. Treatment of the cultures used in the different models of neurotoxicity are described below.

Staurosporine induced neurotoxicity: Cells were pre-incubated with LY354740 or LY379268 for 15 minutes before the addition of staurosporine to the cultures.

Glucose and oxygen deprivation: LY354740 and LY379268 were added to the cultures for the duration of the insult and additionally for the post-insult normoxic incubation.

7.2.5 Assessment of neuronal cell injury

Lactate dehydrogenase efflux assay

Cell death was assessed 24 hours after the insults using the measurement of lactate dehydrogenase (LDH) release from damaged or dead cells. Supernatants were harvested

from the cultures in duplicate (see chapter 2, section 2.6.1), and LDH was measured using a spectrophotometric assay (Cytotoxicity detection kit, Boehringer-Mannheim).

DNA fragmentation

DNA fragmentation was quantified by using an immunoassay kit for measurement of mono- and oligo-nucleosome formation (Calbiochem/Novabiochem). The protocol is described in detail in chapter 2, section 2.6.2.

7.2.6 Characterisation of astrocytes by immunofluorescence and Western blot analysis

Astrocytes cultured in $75cm^2$ flasks were incubated with LY354740 or LY379268 overnight. Following the incubation, the drugs were washed out, the media replaced with fresh DMEM (high glucose) and incubated for the remainder of 24 hours. The cells were harvested in lysis buffer (appendix 2) and the medium from each flask was collected and concentrated into a smaller volume (refer to section 2.7). All the samples were homogenised and loaded onto gels ($25\mu g$/lane). Proteins were separated on 8% SDS-PAGE overnight at 11mA. Proteins were then transferred to PVDF membranes and incubated with 5% Marvel in TBS-T for 1 hour. Membranes were incubated overnight with a primary antibody. On the basis of the results in chapter 6, antibodies used in this study were:

mouse Anti-GFAP, 1:30 000

rabbit Anti-mGluR2/3, 1:1000

goat Anti-TGF-β2, 1:500

All the primary antibodies had been previously titrated at a variety of dilutions to obtain the optimised working solution. Following incubation with the appropriate horseradish peroxidase conjugated secondary antibody (Promega peroxidase coupled anti-mouse and

anti-rabbit IgGs were used at 1:5000; Vector peroxidase coupled anti-goat IgG was used at 1:1000) for 1 hour, detection was performed using ECL. Depending on the amount of target protein on the membrane, exposure of the membrane to the autoradiography film varied from 15 seconds to 1 hour. In this study, the membranes labelled for the different proteins were exposed to the film for:

GFAP - 15 seconds

mGluR2/3 - 1 hour

TGF-β2 - 15 seconds

For the detection of the remaining antibodies, the PVDF membranes were stripped of the bound antibodies and reprobed according to the method described in section 2.7.

As glial cultures had never been cultured before in our laboratory, astrocytes were characterised and assessed for their purity by immunofluorescence. Astrocytes were fixed and permeabilised using 4% paraformaldehyde followed by incubation with -20°C methanol. Cells were washed, blocked with serum and BSA, and incubated with the primary antibody overnight at 4°C. Cells were washed three times and the secondary antibody was added (Vector fluorescein- or Texas red- conjugated secondary antibodies were used at 1:100) and incubated for 1 hour in the dark. The coverslips were rinsed in PBS and water and mounted onto microscope slides using an aqueous polyvinyl alcohol-based mountant.

7.3   Results

7.3.1 Establishing staurosporine-induced neurotoxicity

Initial experiments were carried out to assess the optimal dose of staurosporine to be used to cause neuronal death. Staurosporine (5μl) was added to neurone-enriched cultures in log-doses ranging from 10nM to 10μM for 24 hours. Control groups were given 5μl of the culture medium. Supernatants were removed for quantification of LDH levels
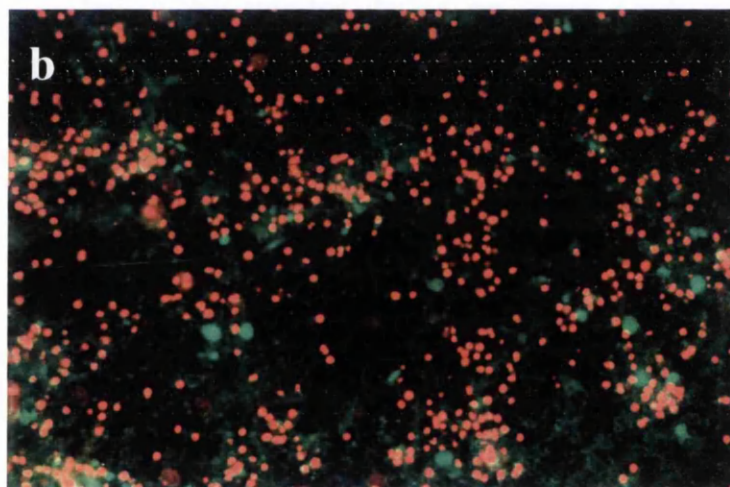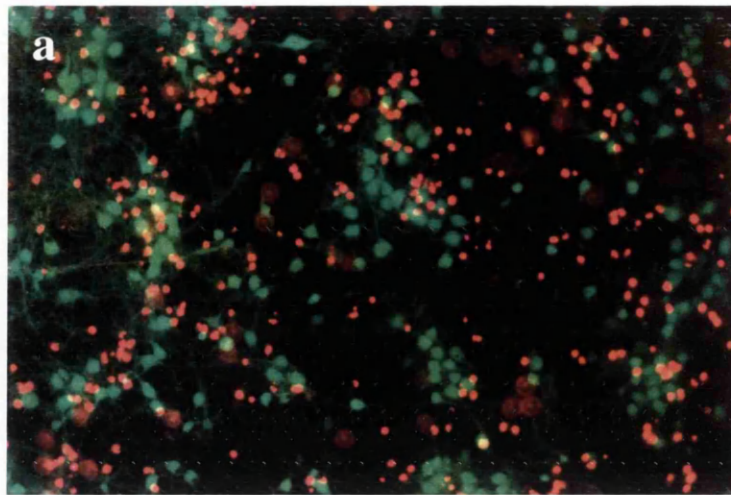
Figure 7.1   Assessment of neuronal cell injury.

Neuronal cell death was assessed by measuring levels of LDH efflux. Cell viability can also be visualised with fluorescent techniques. (a) control neuronal cultures, and (b) non-viable neurones following an excitotoxic insult of NMDA. The green fluorescence (fluorescein) denotes viable cells. Fluorescein diacetate is taken up into healthy cells and becomes hydrolysed by esterases to generate free fluorescein. The red fluorescence corresponds to propidium iodide staining of DNA in dead cells. Note the substantial increase in propidium iodide staining in cells treated with NMDA.

(Courtesy of Dr Ann Kingston; Eli Lilly)
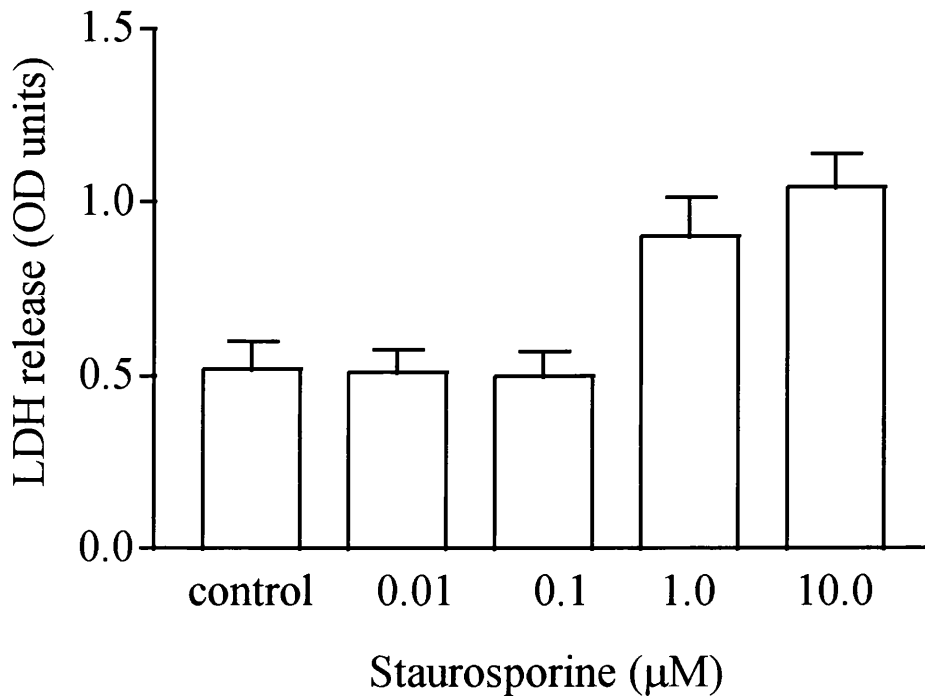
Figure 7.2a.   Effect of staurosporine on LDH release.

Staurosporine-induced neurotoxicity was induced in cortical neurone-enriched cultures (12 days in culture) at a variety of doses for 24 hours. Results represent the LDH release in OD units (mean ± SEM of 1 experiment using quadruplicate culture replication). Maximal LDH release were similarly demonstrated by 1 and 10µM staurosporine.
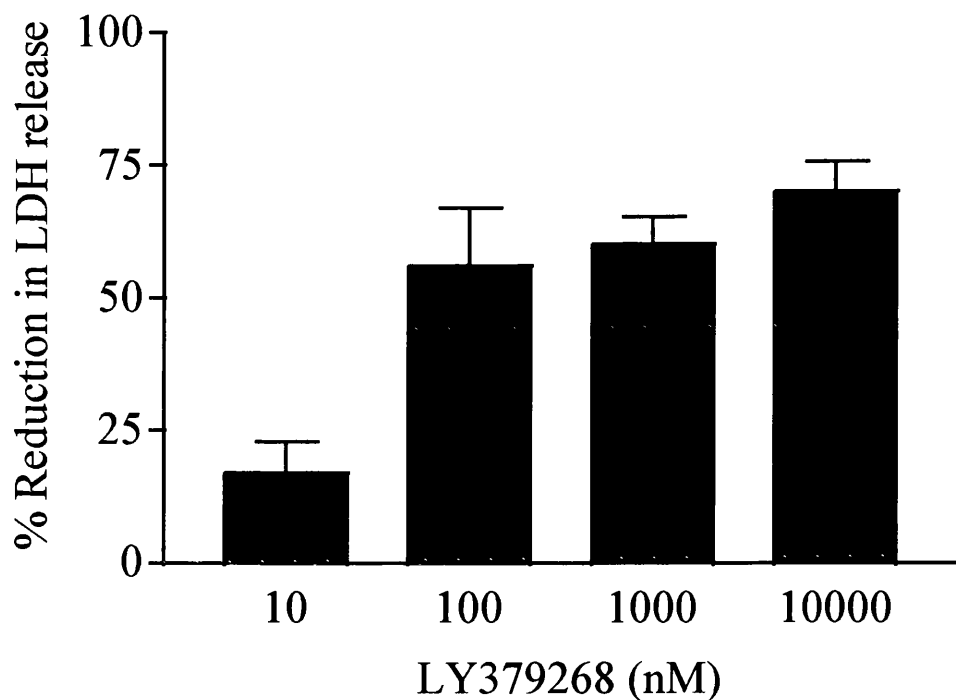
Figure 7.2b   Neuroprotective effects of LY379268 on staurosporine-induced neurotoxicity.

LY379268 is effective at reducing LDH release in staurosporine treated cultures (1µM). LY379268 was added to the cultures and incubated for 15 minutes prior to the addition of staurosporine to the cultures. Results represent the % reduction in LDH release (mean ± SEM of 3 experiments using quadruplicate culture replication).

Table 7.1   **LY354740 and LY379268 protect against staurosporine-induced LDH release.**

COMPOUND (1μM)	% NEUROPROTECTION AGAINST STAUROSPORINE TREATMENT
LY354740	69 ± 9 ***
LY379268	60 ± 4 ***

E18 cortical neuronal cells (days *in vitro* = 12) were pre-incubated with the agonists for 15 minutes prior to the addition of staurosporine (1μM). Cultures were incubated for 24 hours before the assessment of neuronal damage by measurement of LDH release from cells. Results represent % reduction in LDH release (mean ± SEM of 3-4 experiments using quadruplicate culture replication.

***$P<0.001$ for statistical comparison between agonist and staurosporine treated cultures (two-tailed Student's unpaired *t*-test).

% Neuroprotection = 100 X [1 - (OD test - OD control)/OD staurosporine treated - OD control)]

released from the cells (fluorescent visualisation of damaged neurones following an excitotoxic insult is shown in figure 7.1). LDH release into the culture medium was seen to increase with an increasing dose of staurosporine (figure 7.2a). Staurosporine had little effect at 10 and 100nM, with LDH release at levels comparable with control groups. At the highest doses of staurosporine, LDH release was twice that seen in control cultures. As minimal differences in LDH response were observed between 1μM and 10μM staurosporine, 1μM staurosporine was chosen for all the subsequent neurotoxicity experiments.

7.3.2 Effects of LY354740 and LY379268 on staurosporine-induced neurotoxicity

Figure 7.2b presents the effects of various doses of LY379268 (log-doses from 10nM to 10μM) on 1μM staurosporine induced LDH release from enriched cortical neuronal cultures. It is clear that with an increasing dose of LY379268, the greater the reduction in neuronal toxicity. A maximum 70% reduction in LDH release was seen following 10μM LY379268. From these results, the near-maximal dose of 1μM was chosen for subsequent studies. A dose of 1μM was also chosen for LY354740 on the basisof previous studies with NMDA excitotoxicity in which LY354740 demonstrated a similar profile of neuroprotection to LY379268 (Kingston *et al.*, in press).

In rat cortical neuronal cultures (days in vitro = 12), LY354740 and LY379268 (1 μM) significantly reduced neuronal toxicity against cell damage and death, as measured by LDH efflux, caused by staurosporine (1 μM). Table 7.1 shows that both agonists can protect against staurosporine-induced neurotoxicity with similar potencies of effects.

Preliminary experiments investigating DNA fragmentation was also assessed in cultures following exposure to staurosporine-induced neurotoxicity. Due to lack of time, the results shown below were assessed in neuronal cultures used for an optimisation

experiment, which accounts for the difference in the dose of staurosporine used and the time of incubation. The results on nucleosome formation are shown in table 7.2. Both LY354740 and LY379268 demonstrated reductions in the production of DNA fragmentation in the mixed glial-neuronal cultures. The percentage reductions of nucleosome formation were 32% and 50% for LY379268 and LY354740, respectively. However, these results were not statistically significant. No substantial changes in nucleosome formation were noted in neurone-enriched cultures. However, it should be noted that prior to staurosporine treatment, the neurone-enriched cultures did not appear entirely healthy morphologically. The cells did not plate down well during the initial culture and the resulting density of the neurones appeared very low compared with normal cultures. This finding is perhaps reflected in the increased nucleosome formation in the control cultures of neuronal cultures compared to the low level seen in the mixed glia-neuronal cultures.

7.3.3 Establishing glucose and oxygen deprivation

Initial experiments were carried out to determine the time required to cause neuronal death following glucose/oxygen deprivation. Cultures were exposed to a glucose/oxygen-deprived environment for 1 hour and 6 hours. Following the incubation in HBSS, the culture medium was replaced with Neurobasal medium for the remainder of the24 hours. The next set of experiments used the same time points, but in order to remove any dissolved oxygen in the medium prior to incubation in the 5% O_2 incubator, the medium was ultrasonicated for 10 minutes followed by direct gassing with N_2 for at least an hour. The resulting measurements of LDH are presented in figure 7.3. These results indicate that neuronal cell death is greatly enhanced following a 6 hour insult compared with a 1 hour insult. Also, the physical removal of dissolved O_2 from the medium prior to the insult further increased the neurotoxicity of the insult. Additional experiments were carried out in

Table 7.2   LY354740 and LY379268 and staurosporine-induced nucleosome formation.

	NUCLEOSOME FORMATION (U/ml)			
	CONTROL	STAUROSPORINE CONTROL	LY379268	LY354740
Neuronal culture	5.6 ± 1.3	10.8 ± 0.4	9.53 ± 2.1	8.9 ± 0.6
Mixed glial-neuronal cultures	1.5 ± 0.03	7.4 ± 1.5	5.5 ± 0.1	4.5 ± 0.7

E18 cortical neuronal cells (days in vitro = 12) and mixed glial-neuronal cultures were pre-incubated with the agonists for 15 minutes prior to the addition of staurosporine (10 μM). Cultures were incubated for 48 hours before the assessment of nucleosome formation by measurement of DNA fragmentation.

Results represent mean nucleosome formation ± SEM (U/ml) of 2 experiments using triplicate culture replication.

mixed glial-neuronal cultures using N_2-gassed PBS Dulbecco's balanced salt solution, as it was noticed that the HBSS contained a low level of glucose (1000mg/l). Figure 7.3 shows that there appears to be no difference between cultures exposed to glucose/oxygen deprivation in HBSS or PBS Dulbecco's at 6 hours. However, this data should be interpreted with caution because of the different types of cultures used. Unfortunately, neurone-enriched cultures exposed to glucose/oxygen deprivation in PBS Dulbecco's medium were not carried out due to the poor nature of the cultures obtained.

Experiments investigating the neuroprotective effects of LY354740 following glucose/oxygen deprivation were not carried out due to the lack of time. The neuroprotective effects of LY379268 on glucose and oxygen deprived cultures were tested only at each of the time points used for the glucose/oxygen time deprivation course investigation. Unfortunately, LY354740 was not assessed. The results are presented in table 7.3. These preliminary data suggest that LY379268 may reduce LDH release from cultures subjected to glucose/oxygen deprivation of 6 hours. Without considering the background LDH release expected from normal neuronal cultures, a maximal 25% reduction in LDH release was measured in cultures exposed to a 6 hour insult.

7.3.4 Characterisation and purity of astrocytes cultures

Using the most commonly used and widely accepted marker for astroglia, glial fibrillary acidic protein (monoclonal anti-GFAP, 1:15 000), cells cultured from the cortices of day 0-3 neonates were established as astroglia (figure 7.4). In addition to the expression of GFAP, morphologically they appeared to represent type 1 astrocytes as defined by their irregular morphology with one or more thick processes. This contrasts to type 2 astroglia which are defined as process-bearing, like neurones. This was further established through the use of the monoclonal antibody A2B5, which distinguishes between the two types of
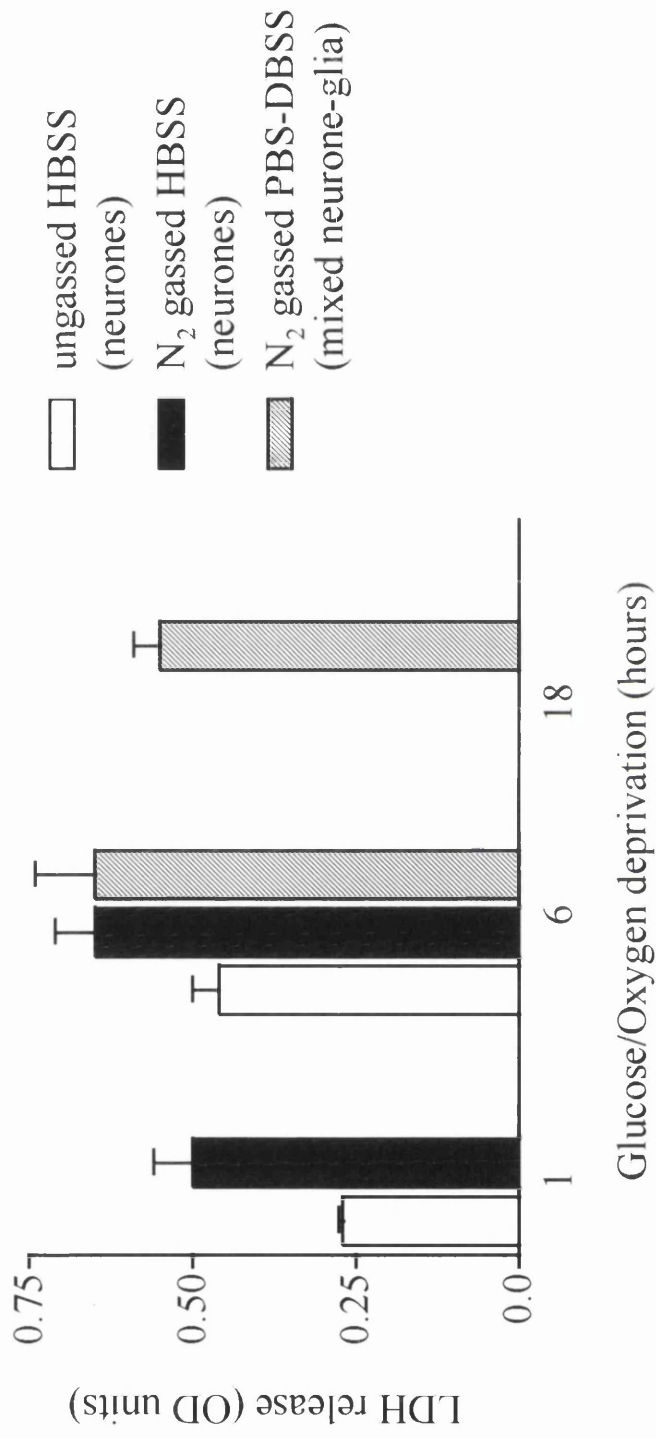
Figure 7.3   Effect of hypoxia and hypoglycaemia on neuronal death.

Glucose and oxygen deprivation was induced in neurone-enriched cultures at a variety of time points. Results represent the LDH release in OD units (mean ± SEM of 2 experiments using quadruplicate/triplicate culture replication). Concurrent control cultures (i.e. cultured under normoxic conditions with glucose) were not possible.

HBSS = Hank's Balanced Salt Solution

PBS-DBSS = PBS Dulbecco's Balanced Salt Solution

Table 7.3   Effect of LY379268 on neuronal cultures subjected to glucose and oxygen deprivation.

	LDH RELEASE (OD UNITS)					
	NEURONE ENRICHED CULTURES (in HBSS)				MIXED NEURONAL-ASTROCYTE CULTURES (in PBS Dulbecco's)	
	NON-DEOXYGENATED MEDIA		DEOXYGENATED MEDIA		DEOXYGENATED MEDIA	
	1 hour	6 hours	1 hour	6 hours	6 hours	18 hours
G. O. D.	0.27 ± 0.006	0.46 ± 0.04	0.50 ± 0.06	0.65 ± 0.06	0.65 ± 0.09	0.55 ± 0.04
LY379268	0.24 ± 0.01	0.40 ± 0.08	0.48 ± 0.11	0.49 ± 0.06	0.50 ± 0.04	0.47 ± 0.004

E18 cortical neuronal cells (days in culture = 12) and mixed cultures were incubated with LY379268 for the various times indicated in the table. Twenty-four hours after the initial insult LDH levels were measured.

Results represent mean ± SEM (OD units). For G.O.D.(glucose-oxygen deprivation) control data, n = 2 using quadruplicate or triplicate culture replication.

For LY379268 data, n = 1 using quadruplicate or triplicate culture replication.

204

astroglia. Figure 7.6 illustrates that the astrocytes cultured in this study were GFAP positive and A2B5 negative, indicative of cerebral type 1 astrocytes. Astrocytes were also assessed for the presence of mGluR2/3 (1:75) using double-labelling immunofluorescence. A low level of autofluorescence was seen, but no detectable mGluR2/3-specific fluorescence was observed in the cultured cells.

The purity of the astrocytes was assessed by labelling the cells for markers of other contaminating cell types commonly seen. Cultures were labelled against two other cell markers, ox42 (1:1000) for the presence of microglia, and galactocerebroside (1:200) for the presence of oligodendrocytes. As figures 7.5 and 7.6 show, cultures were composed primarily of astrocytes, with no detectable presence of oligodendrocytes and only a small proportion of microglial contamination. Astrocytes were not counted to assess the % purity of the cultures, as the purification step via the shaking procedure eliminated the majority of the contaminating cell types. However, it has been previously documented that microglia may represent up to 5% of the total cells in purified cultures of astrocytes (Giulian & Baker, 1986).

7.3.5 Expression of TGF-β in astrocytes following treatment with Group II mGluR agonists

Astrocytes previously treated with LY354740 or LY379268 at doses of 1 μM and 10 μM were used for Western blot analysis. Protein extracts from treated astrocyte cultures together with their supernatants were characterised initially with an antibody against GFAP and mGluR2/3. Figure 7.7 illustrates that an intense 50kDa band corresponding to GFAP was detected at a high level in all the cellular protein extracts, confirming the identity of the cultures. As expected, no GFAP stained bands were seen to be expressed in the culture medium of the corresponding cell extracts. In agreement with the immunofluorescence
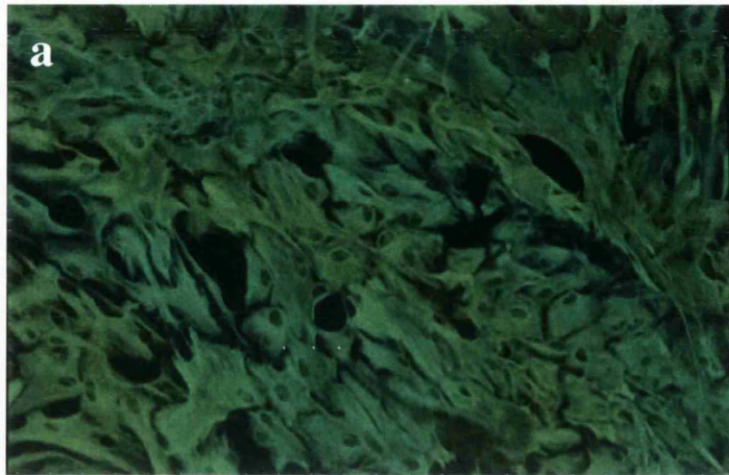
Figure 7.4   Characterisation of primary astrocyte cultures.

Representative photographs of astrocyte cultures (3 weeks in culture) immunolabelled with a monoclonal antibody against GFAP, 1:15000 (a) x200 magnification (b) x 400 magnification. GFAP positive astrocytes visualised using fluorescein.
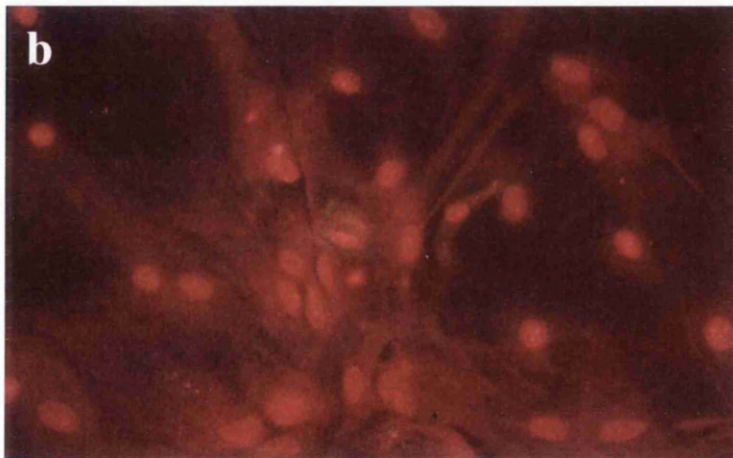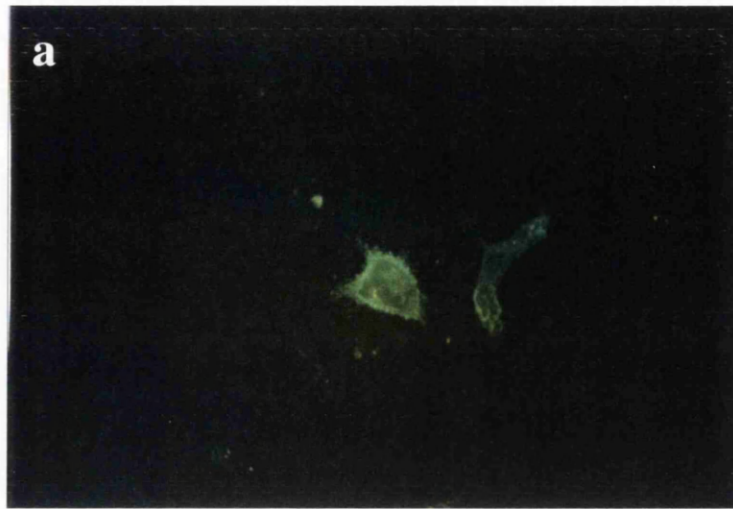
Figure 7.5   Contamination of astrocytes with other cell types: microglia.

Representative photographs (x400) of astrocyte cultures (polyclonal GFAP, 1:500, visualised with texas red). a) antibodies against ox42 stain microglia (fluorescein), but do not stain astrocytes, b) simultaneous localisation of astocytes and microglia in primary astrocyte cultures.
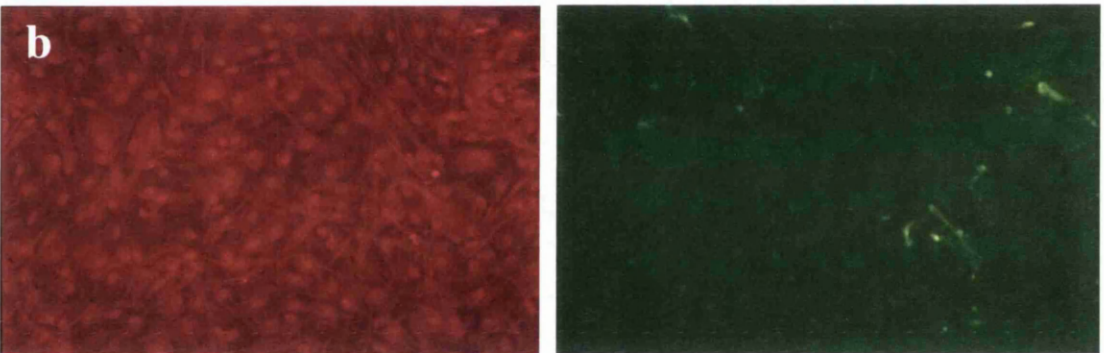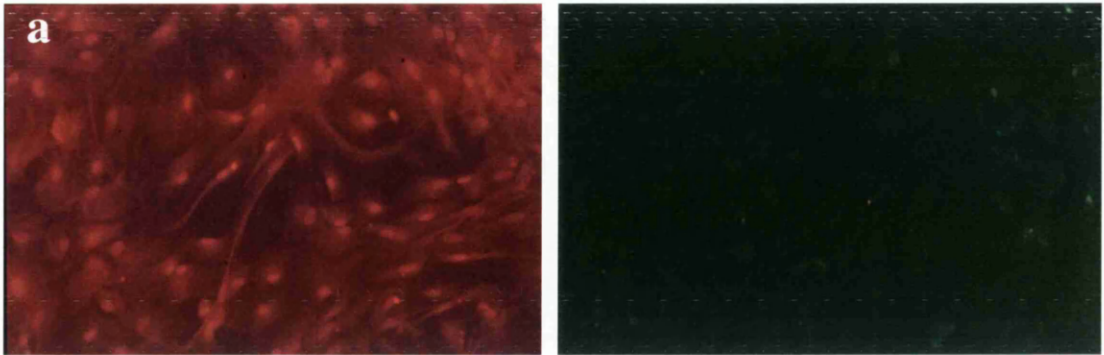
Figure 7.6   No contamination of astrocytes with type 2 astrocytes or oligodendroglia.

Representative photographs of astrocyte cultures visualised with a polyclonal antibody against GFAP together with (a) an antibody against A2B5 selective for type 2 astrocytes (b) an antibody against galactocerebroside selective for oligodendrocytes. Only non-specific autofluorescence can be seen with these two antibodies.

experiments, no protein bands corresponding to mGluR2/3 were detected in any of the samples (figure 7.8). The continued presence of the prestained protein standards on the membranes demonstrated that this observation was not due to a reduction in protein levels. Western blot analysis with an antibody directed against TGF-β2 resulted in the detection of a 25kDa band corresponding to the molecular weight of TGF-β2. This signal was easily detected both in the cell culture media of the control and drug treated astrocytes and also faintly in the astrocytic cellular extract (figure 7.8).

In order to ascertain whether this TGF-β2 response was due to the direct activation of mGluR2/3, astrocyte cultures were incubated simultaneously with either the agonists LY354740 or LY379268, together with the selective mGluR2/3 antagonist LY341495. Figure 7.8 illustrates that despite the absence of a protein band corresponding to mGluR2/3 in cultured astrocytes treated with mGluR2/3 agonists, the secretion of TGF-β2 into the culture medium from astrocytes is abolished following concomitant treatment with the selective antagonist LY341495. Therefore, TGF-β2 production and secretion from astrocytes is selectively mediated through mGluR2/3. To ensure that the reduction in the TGF-β2 signal was not due to the toxic effects of LY341495, the antagonist was also tested for neurotoxic effects by measurement of LDH efflux. LDH efflux was measured using the method of Wroblewski & La Due (1955). Table 7.4 demonstrates that the doses of LY341495 used in this study were not toxic to astrocytes.

7.4   Summary and technical considerations

In vitro model systems provide an environment to examine the mechanisms of neuronal injury in a controlled setting without the complex biological processes associated with whole animal studies. However, the limitations of *in vitro* systems are widely recognised as the experimentally advantageous simplicity of these systems also reflect their
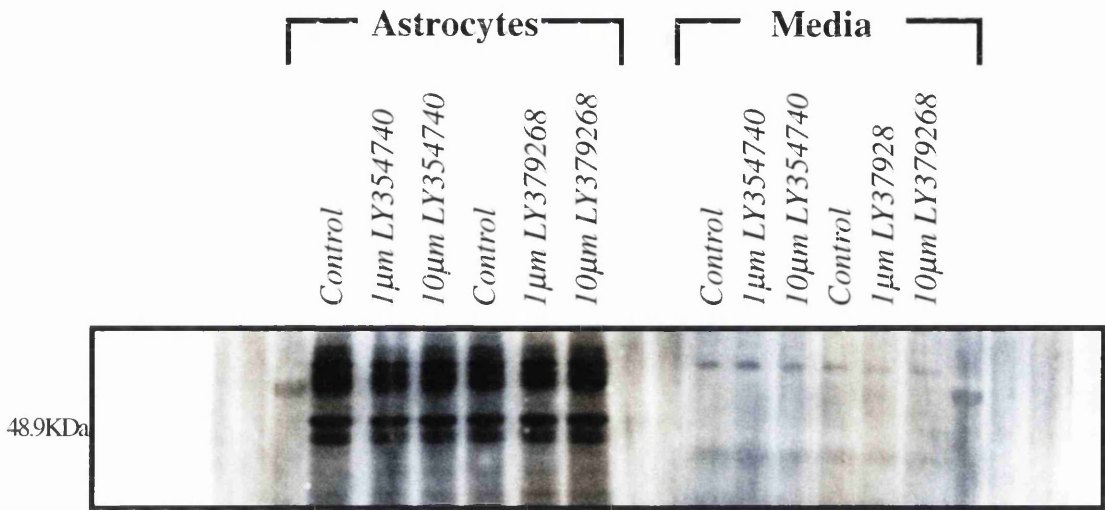
Figure 7.7   Western blot analysis with cultured rat cortical astrocytes treated with LY354740 and LY379268.

Cells were incubated with either LY354740 or LY379268 overnight. The drugs were washed out and the cells returned to the incubator for the remainder of the 24 hour incubation. Supernatants from each of the cultures were also concentrated down and used to investigate the possible secretion of proteins into the medium from the astrocytes. The intense 50KDa protein band which corresponds to the deduced weight of GFAP was detected after a very short exposure to autoradiographic film. GFAP is seen selectively in the cellular extract, with no detectable signal in the medium.
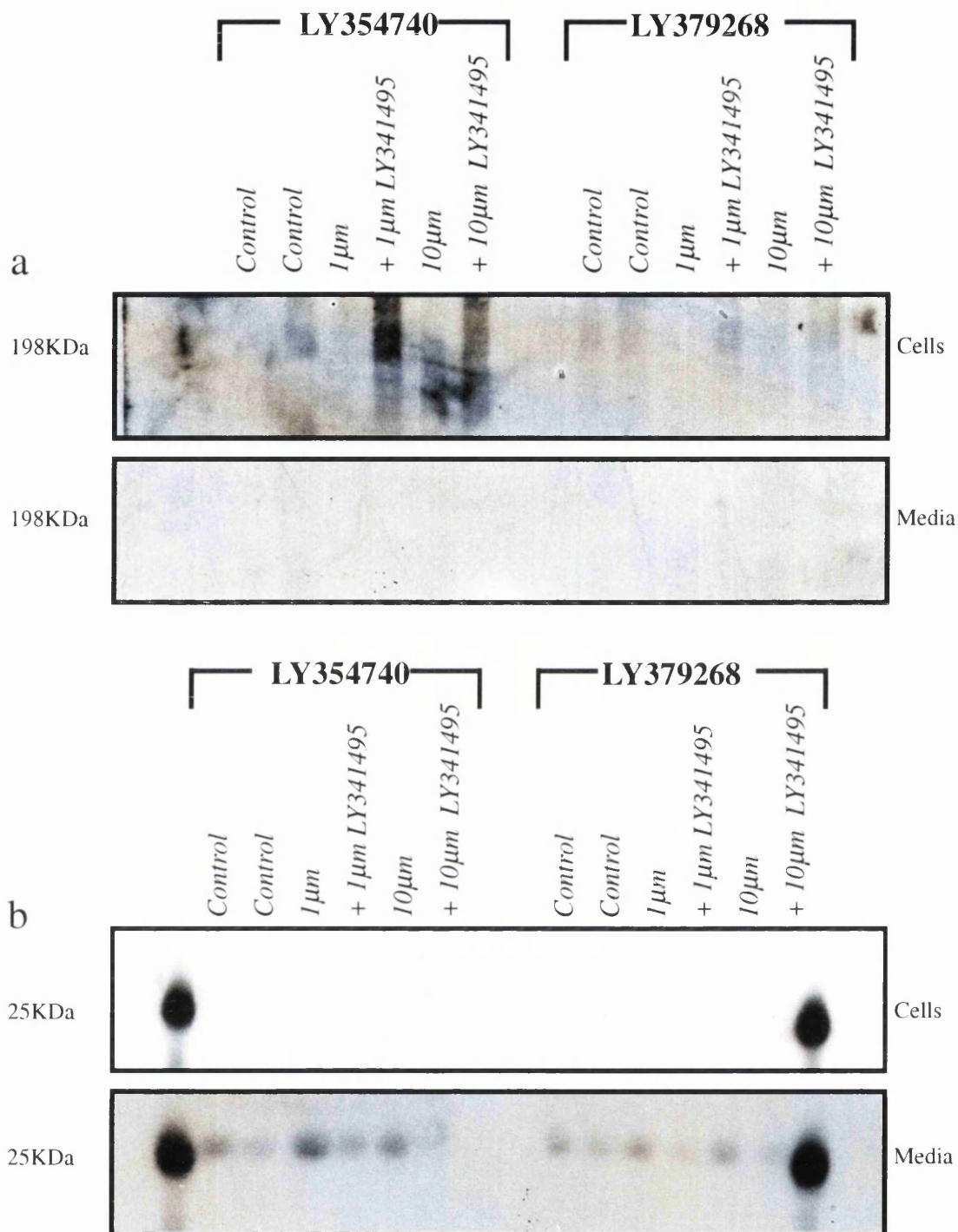
Figure 7.8 **Western blot analysis with cultured cortical astrocytes; Secretion of TGFB2 by astrocytes is an mGluR2/3 mediated event.**

a) Protein bands corresponding to mGluR2/3 were not detected in cortical astrocyte cultures. b) A 25KDa protein band corresponding to the deduced weight of TGF-β2 was detected in the culture medium following treatment with the agonists LY354740 and LY379268. The presence of the TGF-β2 protein band is reduced/abolished following the simultaneous incubation with LY341495. This suggest that TGF-β2 secretion results from mGluR2 or mGluR3 activation.

Table 7.4   **The selective mGluR2/3 antagonist LY341495 is not toxic to astrocytes at the doses used.**

TREATMENT	LDH RELEASE (U/ml)
Control (no treatment)	51.0
LY341495 3μM	47.6
LY341495 10μM	63.8
LY341495 30μM	55.1
LY341495 100μM	26.0

The antagonist LY341495 was incubated with astrocyte cultures for 6 hours at 37°C in a 5% CO_2/air atmosphere. Following the incubation, the antagonist was washed out and replaced with DMEM. LDH release from cells was measured in the supernatants of the cultures 24 hours after the initial incubation.

Results represent the mean LDH released (U/ml) from one experiment carried out in triplicate. LDH was calculated using the equation: ΔA per minute x 20,000 x temperature correction factor (1 at 25°C).

differences from the intact brain. For example, *in vitro* systems lack most obviously the three-dimensional architecture of the intact brain. Other major differences include the absence of the cerebral vasculature which has a central role in cerebral function and the phenotype of cells removed from embryos and postnatal rats may be different to the adult counterparts in the brain *in vivo*.

In this study, the effects of the group II mGluR agonists LY354740 and LY379268 were investigated in two models of neurotoxicity. Staurosporine-induced neuronal death is considered to be mediated primarily through the activation of apoptotic pathways (Koh *et al.*, 1995). In direct contrast, neuronal cultures subjected to glucose and oxygen deprivation are generally considered to die by necrosis (Goldberg *et al.*, 1997). Both LY354740 and LY379268 were similarly demonstrated to significantly reduce neuronal cell death caused by staurosporine and reduced nucleosome formation in mixed neuronal-astrocytic cultures. Preliminary experiments investigating the effects of group II mGluR agonists following glucose/oxygen deprivation indicate that LY379268 at least, may reduce neuronal cell death. However, this requires further investigation. Given more time, a comprehensive and systematic time-course study on the effects of glucose and oxygen deprivation on neuronal LDH release would have been undertaken using neurone-enriched cortical cultures. Once the conditions were optimised, a direct comparison could then be made with mixed neuronal-astrocytic cultures.

Characterisation of the glial cultures using GFAP established the cells as astrocytes, with little or no contamination with microglia or oligodendrocytes. To investigate the presence of group II mGluRs in astrocytes, immunofluorescence and Western blot analysis were performed using a commercially available polyclonal antibody against mGluR2/3. mGluR2/3-specific fluorescence was not detected in the cultures. In addition Western blot analysis of purified cortical astrocyte cultures did not reveal any immunoreactive band in

protein extracts. This finding has been shown by others (Bruno *et al.*, 1997). They found no detection of mGluR2/3 in protein extracts from either rat or mouse cortical astrocytes, while mGluR3 mRNA levels were only detectable in cultured rat astrocytes following RT-PCR. This suggests that the amount of mGluR2/3 protein expressed by cultured astrocytes is below detection level either by Western blot analysis or by immunofluorescence. These negative findings in this study also raises the possible issue of lack of specificity of the mGluR2/3 antibody. However, the same antibody was used successfully in chapter 6 to detect mGluR2/3-immunoreactive cells in rat brain sections using immunohistochemistry. In order to determine the use of this antibody in immunofluorescence, the staining procedure carried out on the astrocyte cultures was repeated with fresh frozen sections of rat brain (fluorescein as fluorochrome). Controls were also generated by omitting the incubation with the mGluR2/3 antibody in order to gauge the level of background autofluorescence. Differences in fluorescence was observed between the control sections and sections treated with the mGluR2/3 antibody. Specifically, the control sections emitted a pale yellow-green autofluorescence while treated sections gave a much stronger green signal. The strongest signal was noted in the corpus callosum. However, photographs have not been included due to the rapid photobleaching of the fluorescence, with the signal fading within seconds. Thus it appears likely the levels of mGluR2/3 in astrocyte cultures were below levels detectable by immunofluorescence or by Western blot analysis.

The findings from this study are discussed in chapter 8, section 8.4.

CHAPTER 8

DISCUSSION

8.1   LY354740 and LY379268 are selective agonists for mGluR2/3

Previous studies have shown that the two agonists LY354740 and LY379268 are highly potent and selective for group II mGluRs (mGluR2 and mGluR3). By using recombinant mGluRs expressed in non-neuronal cells, Monn *et al.* (in press) demonstrated that LY354740 suppressed forskolin-stimulated cAMP with nanomolar potency (mGluR2 EC_{50} = 11nM; mGluR3 EC_{50} = 38nM) and displaced the high affinity binding of [^{3}H]LY341495 at low concentrations (mGluR2 K_i = 75nM; mGluR3 K_i = 93nM). LY379268 showed even greater agonist potency on the mGluR2 (EC_{50} = 3nM) and mGluR3 (EC_{50} = 5nM) cloned receptors together with a higher affinity to the receptors (mGluR2 K_i = 14nM; mGluR3 K_i = 6nM).

Further *in vitro* studies using recombinant human mGluRs have demonstrated that LY354740 has no activity at group III receptors (mGluR4 and mGluR7) up to 100 μM, or at group I (mGluR1 and mGluR5) receptors at 300 μM or more. However, agonist responses have been demonstrable at mGluR6 and mGluR8 at the low μM dose range (Monn *et al.*, in press). In addition, the application of 100 μM of LY354740 alone on recombinant AMPA and kainate receptors produced only negligible currents, while binding assays confirmed that the agonist (up to 100 μM) did not have any NMDA activity (Monn *et al.*, 1997). Similarly, LY379268 did not produce any effects (agonist or antagonist) in cells expressing recombinant mGluR1, mGluR5 or mGluR7 at concentrations up to 100 μM, and again no NMDA activity was measured at concentrations up to 100 μM. In contrast to LY354740, LY379268 has been shown to have higher affinity at mGluR6 (inhibition of forskolin stimulated cAMP EC_{50} = 0.04 μM), mGluR4 (21 μM) and mGluR8 (2 μM) (Monn *et al.*, in press). In rat cortical slices, LY354740 has also demonstrated the inhibition of forskolin-stimulated cAMP formation (EC_{50} = 55nM) with no phosphoinositide stimulation (Monn *et al.*, 1997), which indicates that it has similar group II mGluR

selectivity in rat tissue as in recombinant cells. *In vitro* binding of [³H]LY354740 in rat brain has also confirmed the selectivity of this agonist to group II mGluRs (Schaffhauser *et al.*, 1998). In agreement with the previous findings, NMDA, AMPA/KA and a group I mGluR selective agonist did not inhibit [³H]LY354740 binding in cortical membranes. It binds to at least two populations of receptors that are thought to correspond to mGluR2 and mGluR3 on the basis of the reported affinity of LY354740 on cloned receptors.

8.2 Functional consequences of mGluR2/3 activation

The [¹⁴C]2-deoxyglucose autoradiographic technique provides a reliable method in which the functional events of the brain can be mapped simultaneously following specific receptor manipulations. In the past, this technique has been used successfully in revealing the anatomical pathways associated with the manipulation of specific receptor populations (McCulloch, 1982). Until now, the functional events in the brain resulting from group II mGluR activation have not been documented because of the lack of good pharmacological tools. In this thesis, [¹⁴C]2-deoxyglucose autoradiography was employed to assess the effects of two recently developed mGluR2 and mGluR3 receptor agonists, LY354740 and LY379268.

LY354740 and LY379268 are structurally similar and are constrained analogues of glutamate (chapter 1, figure 1.5). While LY354740 is approximately equipotent at mGluR2 and mGluR3, LY379268, although more potent than its heterobicyclic analogue for both receptors (16X at mGluR3, 5X at mGluR2), has a higher affinity for mGluR3 (Monn *et al.*, in press). This may explain both the different responses measured in the brain regions and the contrasting behaviour elicited following the administration of the two drugs. At the levels of LY354740 and LY379268 used in this study, the concentration of both compounds in the brain would definitely have been sufficient to activate the group II

Table 8.1 Effects of LY354740 and LY379268 on second messenger responses in a stable mammalian cell line co-transfected with a glutamate transporter (RGT cells) expressing recombinant human mGluR subtypes.

Compound	mGluR1a	mGluR2	mGluR3	mGluR4a	mGluR5a	mGluR6	mGluR7a	mGluR8
				EC_{50} (nM) ± SEM				
LY354740	>100 000	11.08 ± 2.53	38.0 ± 3.07	>100 000	>100 000	2 990 ± 120	>100 000	11 470 ± 207
LY379268	>100 000	2.69 ± 0.26	4.58 ± 0.04	21 100 ± 8 600	>100 000	39.0 ± 5.0	>100 000	1 690 ± 130

(Drs. J Monn & D Schoepp, personal communication).

Table 8.2 Effects of LY354740 and LY379268 on radioligand binding to mGluR receptors in the rat brain and to recombinant mGluR2 and mGluR3 expressed in RGT cells.

Compound	IC_{50} (nM) ± SEM	K_i (nM) ± SEM	
	[3H]-LY341495	[3H]-LY341495	[3H]-LY341495
	rat brain	mGluR2	mGluR3
LY354740	254 ± 86	74.9 ± 9.1	93.3 ± 2.6
LY379268	15 ± 4	14.1 ± 1.4	5.8 ± 0.6

(Drs. J Monn & D Schoepp, personal communication)
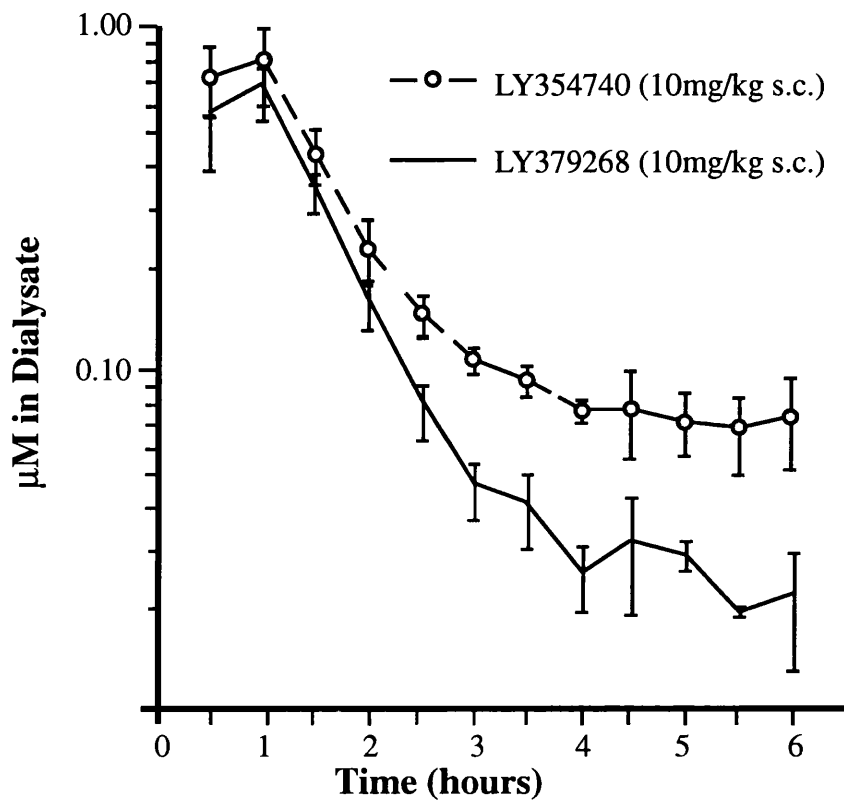
Figure 8.1   Brain levels of LY354740 and LY379268.

(Figure courtesy of Dr. D Schoepp, Eli Lilly)

mGluRs in the brain (figure 8.1). However, LY379268 (10 mg/kg) could possibly have produced non-selective effects due to mGluR6 or mGluR8 activation, which are thought to be implicated in sensory function (Schoepp *et al.*, unpublished data). The behavioural changes elicited following the administration of LY354740 and LY379268 may reflect this difference in receptor selectivity. While the acute administration LY354740 (10mg/kg) did not produce any notable changes in behaviour, LY379268 (10mg/kg) produced a substantial hypersensitivity reaction to auditory stimuli. This response was not observable at LY379268 (1mg/kg). The sensitivity of the locus coeruleus to LY379268, as demonstrated by the substantial changes in glucose utilisation, appears to substantiate this behavioural response.

The additional use of the ranking function f illustrates that although a number of similarities in function-related glucose utilisation were apparent following both agonists, the regional responses of local glucose use to the agonists were dissimilar. Similar responses in glucose use were identified in a number of anatomically interconnected regions of the limbic system; the anteroventral thalamic nucleus, mammillary body and the lateral habenular nucleus. Glucose use in the superior colliculus (superficial layer) was also increased by both metabotropic agonists. In contrast, LY354740 provoked anatomically widespread reductions in glucose use, notably in the cerebral cortex and visual system, whereas LY379268 elicited circumscribed increases in glucose use in the auditory relay nuclei and locus coeruleus. However, the f rank function fails to address alterations in cerebral function in discrete nuclei where they are masked by the more global changes in the brain. For example, following LY354740, reductions in glucose use were affected in visual regions with the majority of brain regions assessed in this system significantly affected. In fact, the only regions seemingly unaffected were the lateral geniculate bodies. This is also reflected in the hierarchy of responsiveness where the lateral geniculate bodies have been placed at the

bottom end of the responsiveness scale. However, visual inspection of the autoradiograms in animals treated with LY354740 (30mg/kg) showed that although the majority of the brain displayed a general depression in function, the lateral geniculate bodies were clearly evident and glucose levels were relatively unchanged across the treatment groups. This suggests that the lateral geniculate bodies are trying to compensate the reduction in activity in the visual system by 'switching on'. However, this response cannot be demonstrated because of the general reduction in metabolism in the rest of the brain.

The patterns of glucose alterations seen in this study could simply reflect the distribution of mGluR2 and mGluR3 in the CNS. *In situ* hybridisation, immunohistochemical and *in vitro* binding studies have been carried out to examine the distribution of these receptors in the rat brain (Ohishi *et al.*, 1993a & b, 1994; Neki *et al.*, 1996a & b; Petralia *et al.*, 1996; Schaffhauser *et al.*, 1998). These studies demonstrated the differential distribution of the receptors, illustrating that even though mGluR2 and mGluR3 are seen throughout the rat brain, mGluR3 are distributed more widely in forebrain neurones, glia and white matter. The elevation in local cerebral glucose utilisation in the genu of the corpus callosum following LY379268 administration, which is more selective for mGluR3, substantiates this difference. The sensitivity of the superficial layer of the superior colliculus to LY354740 and LY379268 can most probably be the result of the direct actions of these agonist on the neuronal pathways associated with vision. As already mentioned, LY379268 appears to have a strong agonist activity at mGluR6, which are located in the retina. Recent evidence also shows that mGluR2 are present in subsets of amacrine cells located at the border of the plexiform layer of the retina (Hartveit *et al.*, 1995). While the distribution of local cerebral glucose utilisation changes following the administration of the drugs displayed a general relationship to the topography of group II mGluR localisation, discrepancies were also evident. Substantial alterations in glucose use

were measured in the red nuclei and the inferior colliculus with LY354740 and LY379268 respectively, but the presence of mGluR2 and mGluR3 in these brain areas are not substantial. The brain regions demonstrating substantial alterations in glucose use also do not appear to be randomly distributed. As dynamic alterations in glucose use appear to reflect mostly the activity in axonal terminals of neuronal pathways (Schwartz *et al.*, 1979), alterations in local rates of glucose use are not restricted to the regions rich in group II mGluRs, but also in neuronal pathways connected to the receptor-rich areas.

The [^{14}C]2-deoxyglucose autoradiographic technique has been widely employed to investigate changes after a wide range of neuropharmacological manipulations (for review, see McCulloch, 1982). The anatomical patterns of response to the two metabotropic agonists in the present study do not resemble those described previously for glutamate receptor blockade (NMDA), or modulators of presynaptic glutamate release, such as κ receptor agonists (Mackay & McCulloch, 1994). NMDA receptor blockade using the non-competitive and use dependent antagonist MK-801 (Nehls *et al.*, 1988) produced widespread increases throughout the limbic system, with the greatest changes (greater than 50%) effected in the Papez circuit (posterior cingulate cortex, entorhinal cortex, hippocampus, mammillary body). CPP, a competitive NMDA antagonist however, evoked minimal alterations in glucose use in the limbic system (Nehls *et al.*, 1988). Previous work has revealed that the κ-opioid agonist CI-977 results in relatively homogeneous reductions in cerebral glucose utilisation (Mackay & McCulloch 1994). The findings from these studies contrast with the reductions observed in these similar brain areas following LY354740 and LY379268. The patterns of response to mGluR2/3 activation are also very different to those reported following AMPA antagonism. By using NBQX and LY293558, Browne & McCulloch (1994) demonstrated widespread reductions in glucose use in nearly all brain regions examined. In contrast to this study, the superficial layer of the superior colliculus

Table 8.3   Changes in glucose utilisation in components of the limbic system following glutamatergic manipulation: comparison between NMDA, AMPA and group II mGluR systems.

| BRAIN REGION | GLUCOSE UTILISATION (% CHANGE FROM CONTROLS) | | | | | | |
| | NMDA[a] | | AMPA[b] | | | mGluR2/3 | |
	CPP (30mg/kg)	MK-801 (5mg/kg)	NBQX (100mg/kg)	LY293558 (100mg/kg)	LY354740 (30mg/kg)	LY379268 (10mg/kg)
Mammillary body	+8%	+64%	-46%	-44%	-43%	-34%
Anteroventral thalamic nucleus	-14%	+53%	-54%	-57%	-46%	-28%
Hippocampus (molecular layer)	+40%	+53%	-48%	-44%	-19%	0%
Dentate gyrus	+25%	+56%	-52%	-40%	-15%	-2%

Glucose use changes in components of limbic system following the systemic administration of CPP, a competitive NMDA antagonist; the non-competitive NMDA antagonist MK-801; two selective AMPA antagonists and the two selective group II mGluR agonists used in this thesis. The data in each case is from the highest dose group used.

[a]Nehls *et al.*, 1988.
[b]Browne & McCulloch, 1994.

was minimally affected following the AMPA antagonists. The findings demonstrated in the limbic system following the systemic manipulation of NMDA, AMPA and mGluR2 and mGluR3 receptor systems are presented in table 8.3.

The group II mGluRs are known to have a modulatory role pre- and peri-synaptically (Forsythe & Barnes-Davies, 1997). Here they can exist either as autoreceptors at glutamatergic synapses, or as heteroreceptors at GABAergic synapses. Previous [^{14}C]2-DG studies (Kelly & McCulloch, 1982; Ableitner et al., 1985; Kelly et al., 1986) using GABAergic agonists (muscimol and THIP) and the benzodiazepine receptor agonist diazepam elicited reductions in glucose use. While nearly all brain regions were seen to be affected following diazepam, a more heterogeneous response was observed following GABA agonists, with anterior thalamic and cortical areas, extrapyramidal and limbic systems predominantly affected. Similar reductions in glucose use were also observed in these areas with LY354740 (albeit with greater heterogeneity), and to a lesser extent with LY379268. It may be that the observed changes result from the activation of presynaptic heteroreceptors. In addition, the activation of presynaptic autoreceptors that function as negative feedback receptors would inhibit any further release of glutamate onto postsynaptic receptors, leading to a decrease in glucose use. Indeed, evidence that LY354740 plays a role in the presynaptic negative modulation of glutamate release has been reported. Battaglia et al. (1997) recently demonstrated that LY354740 completely prevented veratridine-evoked release of glutamate and aspartate in the striatum. Furthermore, recent electrophysiological studies have shown the presynaptic inhibitory action of LY354740 in the medial and lateral perforant pathway of the hippocampal dentate gyrus (Kilbride et al., 1998). Thus, the reductions in glucose utilisation observed following LY354740 may be due to its preferential action on pre-synaptically located mGluR2 receptors. From a more general standpoint, the reductions in glucose use could also be a

direct result of the possible negative modulation of group II mGluRs on VSCCs and K^+ channels. It is thought that this mechanism results from the activation of mGluR2 (Kilbride *et al.*, 1998).The tendency for elevations in glucose utilisation following LY379268 could be attributed to the possible action of the ligand on post-synaptic receptors or non-selective cation channels.

There is recent evidence to suggest that mGluR2 are localised in perisynaptic areas which could permit activity-dependent receptor activation (Scanziani *et al.*, 1997), suggesting their involvement in the suppression of over-excited systems. While this study has demonstrated more general reductions in glucose utilisation following LY354740 (but not LY379268), the exact sites of action of this agonist in the brain could be more fully exploited. By increasing glucose metabolism (i.e. exciting neuronal systems), one may well observe clear and specific reductions in brain metabolism directly related to the activation of mGluR2 as a direct result of their modulatory role peri-synaptically. In fact, behavioural evidence for the involvement of mGluR2 in suppressing glutamatergic disruptions was demonstrated recently (Modghaddam & Adams 1998). They presented evidence to suggest that LY354740 was capable of suppressing PCP-induced behaviours. A recent study by Schoepp *et al.* (personal communication) have also indicated LY379268 acts similarly.

Glutamate is the major excitatory neurotransmitter of the perforant pathway which projects from the entorhinal cortex and terminates in the hippocampus and dentate gyrus. Petralia *et al.* (1996) demonstrated that the hippocampus, and in particular, the terminals of axons located in the hippocampus originating from the entorhinal cortex, was the region richest in mGluR2 and mGluR3. In this study, the molecular layer of the hippocampus was substantially affected with both compounds, but did not show the most significant changes in local cerebral glucose use. However, this would be an expected finding, since the metabolic effect of the activation of these receptors would be expected downstream at the

next synapse of that pathway. The mammillary body is an important efferent area of the hippocampal region, while the mammillary body in turn projects onto the anterior thalamus via the mammillothalamic projection. These structures form the main components of the circuit described by Papez (1937); entorhinal cortex → hippocampus → mammillary body → anterior thalamus → cingulate cortex. Local rates of glucose utilisation were substantially altered in the majority of these structures in this study.

In summary, this present study has demonstrated utility of the [^{14}C]2-deoxyglucose technique in discerning the responses of the two selective agonists in the brain. The actions of LY354740 and LY379268 in the brain do not resemble the responses previously demonstrated with other glutamate receptor ligands, and their sites of action are selectively mediated by the mGluRs. The findings from this study reveal the important functional involvement of the limbic system in response to the activation of mGluR2 and mGluR3 with LY354740 and LY379268. Aside from the mutual change produced in the limbic system, the two agonists produce essentially different CNS effects following systemic administration. These central effects shown following systemic administration demonstrate their usefulness as pharmacological tools, especially with their different affinities to the two receptor subtypes, and that they may be of potential therapeutic use in conditions where there is an apparent overactivity of the limbic system.

8.3   The significance of limbic system manipulation

The [^{14}C]2-DG autoradiographic technique has been used successfully in the past to map the functional changes following local intracerebral administration of various agents (Kelly & McCulloch, 1984; Lothman *et al.*, 1985). With respect to glutamatergic hippocampal manipulations, studies have previously examined the functional consequences following the NMDA receptor antagonist MK-801, but no such studies have been

225

performed with AMPA receptors or mGluRs. This present study was performed in order to investigate the functional consequences in the CNS during and following local bilateral intrahippocampal administration of LY326325.

In this thesis, reductions in glucose utilisation were restricted to the hippocampus. Reductions in glucose use were more predominant in the dorsal aspect of the hippocampus over the ventral hippocampus. An unexpected surprise was the very subtle nature of the changes in glucose utilisation seen following the intrahippocampal injections of LY326325. No significant changes in glucose metabolism were observed in any other regions directly connected with the hippocampus, and no diffusion effects of the drug were detected. A similar study using MK-801 injected directly into the hippocampus demonstrated that alterations in glucose metabolism were also restricted to the hippocampus (albeit increases in glucose utilisation) with no significant changes noted in regions connected with the hippocampus (Kurumaji & McCulloch, 1990). However, the alterations were found in the ventral portion of the hippocampus rather than the dorsal hippocampus. A comparison of the consequences in brain function following MK-801 and LY326325 is presented in table 8.4.

The most important and novel finding from this present study is the nature of the inactivation. The reductions in glucose utilisation of the hippocampus are reversible as levels of glucose metabolism following the infusion of the drug return to levels comparable with aCSF treated animals. In essence, infusions of LY326325 is able to selectively 'switch off' the dorsal hippocampus for the duration of the infusion period, and then 'switch on' again. The reduction in function of the hippocampus as demonstrated with [^{14}C]2-DG was also demonstrated electrophysiologically (figure 8.2). Dentate gyrus field-potentials to perforant path stimulation were monitored daily over a period of over two weeks. The data revealed an abrupt decrease in fast synaptic transmission which remained throughout the

Table 8.4   Changes in glucose utilisation in the CNS following intrahippocampal glutamatergic manipulation: comparison between NMDA and AMPA receptor systems.

BRAIN REGION	GLUCOSE UTILISATION (% CHANGE FROM CONTROLS)	
	MK-801[a]	LY326325
Entorhinal cortex	+19%	+14%
Ventral hippocampus (molecular layer)	+31%	+5%
Ventral dentate gyrus	+44%	+13%
Posterior cingulate cortex	+8%	-17%
Sensorimotor cortex	0%	+12%

Glucose use changes in selected brain regions following the intrahippocampal administration of the non-competitive NMDA antagonist MK-801 and the selective AMPA antagonist LY326325, used in this thesis.
[a]Kurumaji & McCulloch, 1990.
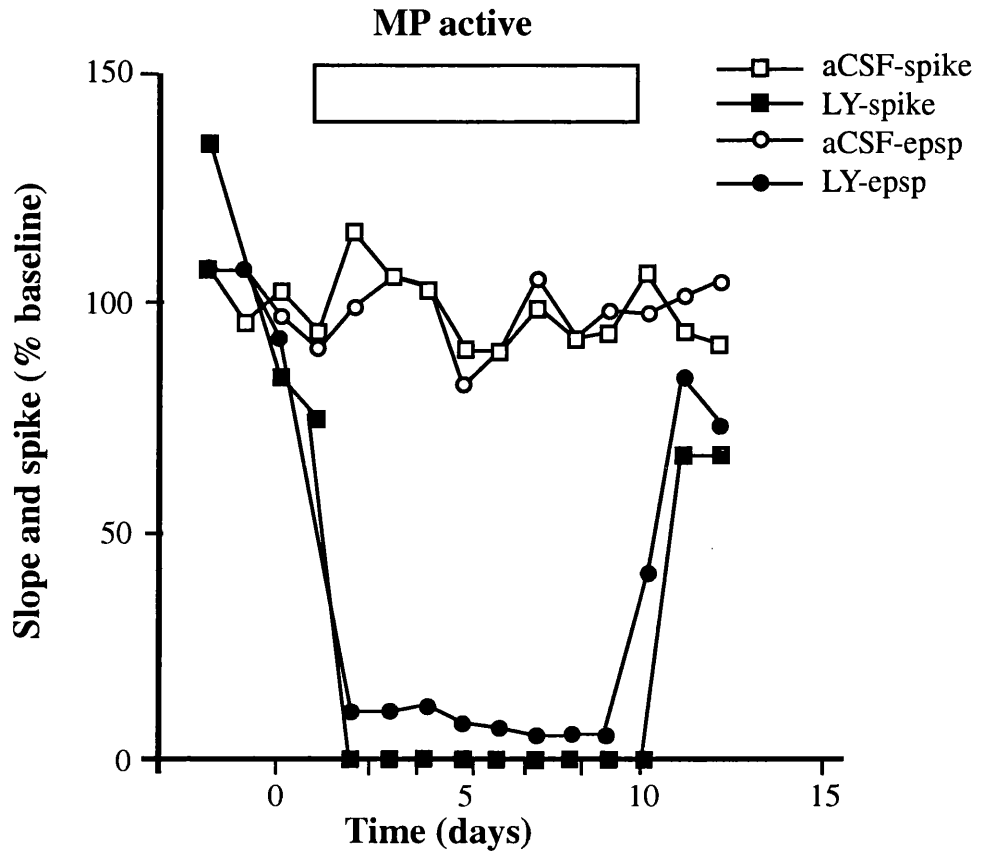
Figure 8.2   The AMPA receptor antagonist LY326325 blocks fast synaptic transmission at perforant path/granule cell synapses.

Representative aCSF and LY326325 micropump-implanted animals show a reduction in fast synaptic transmission during 7 days of infusion and no change in the aCSF control. Means for slope and population spike.
MP = minipump

(From Riedel *et al.*, submitted)

infusion period of LY326325, which suddenly returned to baseline levels within one day of the exhaustion of LY326325 from the minipumps (Riedel *et al.*, submitted). In this study, the level of glucose utilisation in the dorsal hippocampus during LY326325 infusion was similar to that after the suppression of synaptic transmission (flat EEG) induced by pentobarbital (Crane *et al.*, 1978; Astrup *et al.*, 1981). Increasing the dose of LY326325 may have reduced function-related glucose metabolism in the hippocampus even further, but this is associated with the risk of increasing extra-hippocampal diffusion and functional changes elsewhere.

Reversible infusions of this kind that selectively inactivate the hippocampus may provide invaluable insight into memory processes. Studies of brain dysfunction have provided substantial evidence for the involvement of glutamate receptors and the hippocampus in various types of learning and memory (Squire, 1992; Gaffan, 1994; Vargha-Khadem *et al.*, 1997; Riedel *et al.*, 1994; Ohno & Watanabe, 1996). In addition, the involvement of the dorsal hippocampus, but not the ventral hippocampus, has been shown to be important in various types of learning (Moser *et al.*, 1995).

Each of these types of memory is thought to consist of a series of interdependent memory processes, namely encoding, storage, consolidation and retrieval. The conventional neurotoxic lesions used at present cannot categorically dissociate between these different processes due to their permanent nature. For example, lesions made prior to the training (learning the task) would affect the later retrieval of the task were they to disrupt any of the memory processes. Similarly, lesions made after the training period could disrupt the storage of the information or processes associated with consolidation processes and retrieval. Thus, using this method of reversible inactivation of the hippocampus would enable the contribution of the hippocampus to the different memory processes to be independently studied. This novel method of synaptic inactivation has been put to use for

the study of memory processes recently. Seminal studies by Morris and colleagues (submitted) have provided the first direct evidence for the involvement of the hippocampus in the distinct memory processes of one type of memory, spatial memory. Rats were trained using a variant of the open-field watermaze in which an escape platform is raised only if the animal searches at the correct location persistently (Morris, 1981; Spooner, 1994). Inactivation and reactivation of the hippocampus by LY326325 at different times made it possible to investigate the involvement of the hippocampus in these processes. The studies revealed a marked deficit in spatial learning during the training period (encoding) in animals with abnormal hippocampal neural activity. In the same set of experiments, retrieval of spatial memory following training was also revealed to be affected following manipulation of hippocampal function. Animals treated with LY326325 during training not only failed to learn where the platform was located but also failed to acquire the 'search and dwell' strategy needed for this type of test. In contrast, animals trained under aCSF were able to learn the strategy, but when tested later at the retrieval stage with LY326325 could not recall where to search for the platform and were demonstrated to search and dwell in the inappropriate quadrant. Subsequent studies showed that the hippocampus is also involved in maintaining storage of certain memory traces or consolidation processes in circuits elsewhere in the brain.

Although the group II mGluR ligands were not used in this study, the use of selective mGluR ligands to produce this type of reversible inactivation of the hippocampus would provide great insight into the involvement of these G-protein coupled receptors in memory and learning. Recent electrophysiological studies and studies using trangenic animals have provided much evidence for the important role of mGluRs, particularly of group I mGluRs in LTP (O'Connor et al., 1995; Zheng & Gallagher, 1992) and behaviourally in spatial learning (Balschun & Wetzel, 1998). It would be of great interest to

start to look at their potential role in the different processes involved in memory. Together with other technologies used for the study of memory, such as functional imaging approaches, this type of temporary inactivation of synaptic transmission will undoubtedly help unravel and increase our understanding of the complexities of cognitive function.

8.4   mGluR agonists as potential neuroprotective agents?

Various problems have been associated with the use of ionotropic glutamate receptor antagonists as neuroprotective agents. For example, inhibition of these receptors can compromise fast excitatory synaptic transmission and can have serious side effects. The most obvious problem associated with ionotropic glutamate receptor antagonists in recent years has been the realisation that these agents show no therapeutic benefit in human stroke. None of the agents selected for clinical trials have proved successful. This has paved the way for exploring the potential of mGluRs for the therapy of neurodegenerative disorders. The mGluRs are similarly distributed throughout the CNS, but because they have more subtle effects on neurotransmission at synapses, it is believed that they will have fewer side effects than the antagonists developed for the ionotropic glutamate receptors.

In this thesis, contrary to the evidence in the literature that group II mGluR agonists are neuroprotective, LY354740 and LY379268 failed to demonstrate a reduction in the size of the infarct volume following 24 hour permanent cerebral ischaemia in the rat. Unlike the existing ligands for group II receptors, LY354740 and LY379268 are both orally active, and are currently the most potent agonists (in terms of the inhibition of forskolin-stimulated cyclic AMP formation) available for mGluR2 and mGluR3.

Various factors have to be taken into consideration in order to understand the possible neuroprotective role of group II metabotropic glutamate receptors in cerebral ischaemia. Firstly, it has been demonstrated that the choice of ischaemia model determines

231

the severity of damage. Secondly, the mechanisms participating in the evolving damage in the different models are different (Macrae *et al.*, 1992). Interestingly, Bruno *et al.* (1997) recently proposed that neuroprotection mediated by group II mGluRs *in vitro* requires new protein synthesis and involves an interaction between neurones and astrocytes, an event distinct from their actions on reducing synaptic activity. It may be possible that studies using focal models of permanent ischaemia will not protect against neuronal damage due to the rapid evolvement of damaged tissue, but a more slowly progressing infarct would allow this neuroprotective mechanism to take place.

APP

In addition to protecting neuronal elements, the protection of myelinated white matter tracts should also be considered. Recently, APP has been used a marker for assessing axonal damage after an ischaemic insult. Previous studies have demonstrated the larger the volume of the ischaemic lesion, the greater the extent of increased APP immunoreactivity (Yam *et al.*, 1998b). A marker for APP was used in this thesis to investigate any changes in APP accumulation following focal cerebral ischaemia and intervention with LY379268. No positive correlation between APP and infarct size was revealed; in fact infarct size and APP in the LY379268 treated group appeared slightly negatively correlated. No firm conclusions can be drawn from this data, as only one level out of the possible 8 was investigated. However, it may suggest that LY379268 may protect axons against cerebral ischaemia using a non-synaptic mechanism. This contrasts with the neuroprotective agent MK-801, which failed to protect axons even though a 30% reduction in ischaemia was demonstrated (Yam *et al.*, 1998).

TGFβ

The subsequent studies of Bruno *et al.* (1998) claim that the neuroprotection is in fact mediated by TGF-β, as antibodies that selectively neutralised the actions of TGFβ–1 or TGFβ–2 prevented any neuroprotective activity. TGF-βs form a group of homodimeric proteins of 25 kDa that are secreted in latent forms made up of a TGF-β active dimer associated with a set of proteins that need to be activated in order to become functional. They exert their effects by binding to one of three cell surface receptors - TβR-I, -II or -III. Activation of the receptors leads to the phosphorylation of effectors (SMAD proteins) eventually resulting in changes in transcriptional responses such as modulation of genes in the cell cycle (Vivien *et al.*, 1998). From the immunohistochemistry studies carried out in this thesis, the results provide tentative evidence to substantiate the findings of Bruno and colleagues (although only one stereotaxic level was assessed).The pattern of the changes seen following TGFβ2 and TdT immunohistochemistry confirm that the area at the periphery of the infarcted tissue is salvageable unlike the ischaemic core, and that the vulnerable cells in this area may be promoting cell survival. The reduction in TdT labelled cells displayed following LY379268 in and around the boundary of the ischaemic lesion may result from the activation of mGluR2 and mGluR3 in the penumbra which activate intracellular signalling pathways, such as the production of trophic factors such as TGFβ-2 to prevent further cell death. An increase in the number of cells displaying TGF-β1 immunoreactivity following LY379268 however, was not demonstrated in this thesis. TGF-β1 mRNA immunoreactivity in the normal rat brain has been shown previously to be confined to the meninges and choroid plexus only (Unsicker *et al.*, 1991). This may explain the low level TGF-β1 response observed in this thesis. However, TGF-β1 and TGF-β2 mRNA has been previously demonstrated to be dramatically increased at 24 hours and 3 days after focal ischaemia in the mouse (Vivien *et al.*, 1998). It may be possible that an

increased TGF-β1 immunoreactive response would have been observed in this thesis at a later time point than 24 hours.

Group II mGluRs: neuroprotection against delayed neuronal death?

It has been recognised that neuroprotection by new protein synthesis and neuronal-glial signalling may not be efficient against all types of excitotoxic insults *in vitro*. For example, the activation of group II mGluRs has not been shown to protect mixed cortical cultures exposed to AMPA (Buisson *et al.*, 1996). This 'selective' protective mechanism appears also to extend to *in vivo* paradigms. In this thesis, LY354740 and LY379268 did not demonstrate a reduction in the size of the ischaemic lesion following a 24 hour model of focal cerebral ischaemia. Interestingly, a similar finding is demonstrated with LY354740 following the endothelin-1 model of focal cerebral ischaemia (O'Neill, unpublished observations). In contrast, studies using the gerbil model of global ischaemia have indicated that LY354740 is effective in significantly reducing the damage to CA1 hippocampal neurones, which is seen to develop over several days (Bond *et al.*, 1998; Kingston *et al.*, in press). However, this neuroprotective effect was temporally dependent. A mild three minute insult reduced the damage to the CA1 neurones significantly, while a more severe insult attenuated the neuroprotection.

In view of the delayed nature of the neuronal cell death observed following global ischaemia and the idea that cell death pathways are dependent upon the insult severity and $[Ca^{2+}]_i$ (Choi, 1995), it may be that global ischaemia is associated with an apoptotic component of cell death. In contrast to the cell swelling and disintegration of cell architecture seen in necrosis, apoptosis is recognised to result from the execution of finely regulated genetic programs. Apoptosis leads to chromatin aggregation and compaction, a progressive loss of cell volume and the extrusion of membrane-bound cytoplasmic

fragments known as apoptotic bodies. However, the criteria for defining apoptosis are still not absolute. In recent years, it has been popular to use DNA breakdown, such as agarose DNA ladders, as a marker for apoptosis. However, it should be mentioned that the detection of DNA breakdown by TdT-mediated end labelling can also occur in cells undergoing necrosis (as in cases of incomplete triggering of apoptosis).

In comparison to the slowly evolving cell death seen after global ischaemia, the severe regional cell death associated following focal ischaemic insults seems an unlikely setting for apoptosis. Apoptosis may follow focal ischaemia as an event distinct from ischaemia induced excitotoxicity. Thus it has been estimated that around 4% of cells are thought to become apoptotic following focal ischaemia, and that the number reaches a maximum at 24-48 hours after the insult (Linnik, 1996). Studies have demonstrated DNA laddering (Linnik *et al.*, 1993) while other studies have revealed that the molecular systems linked to the generation of apoptosis can be manipulated, e.g. *bcl-2*, *bax* genes, which can alter the outcome of focal ischaemia (Martinou *et al.*, 1994; Linnik *et al.*, 1995). Consistent with these observations, the use of fragment end labelling of DNA by TdT in this thesis has revealed that there is substantial reduction in the number of apoptotic-like cells in the area of the ischaemic lesion following LY379268 compared with vehicle treated controls.

Chopp & Li (1996) have previously characterised the cell types exhibiting apoptotic morphology following two hours MCA occlusion and 24 hours reperfusion. They claim that 90-95% of the cells displaying apoptotic morphology were neurones with astrocytes comprising around 5-10% and endothelial cells less than 1%. Interestingly, comparable to the distribution seen for APP in this thesis, they found the vast majority of the apoptotic cells were located along the inner boundary of the ischaemic lesion (Chopp & Li, 1996). The finding that the number of TdT immunolabelled cells is reduced following permanent MCA occlusion suggests an important intracellular event involved in the cascade of

apoptotic cell death is being selectively targeted following the activation of group II mGluRs by LY379268 - possibly through the actions of the less vulnerable astrocytes. Despite the absence of a reduction in the size of the ischaemic lesion following LY379268, this study supports the view that a broad range of insults, even those that strongly favour membrane failure and necrosis, have the potential to cause cells to initiate apoptosis.

Gene Expression

Ischaemia modifies gene expression (for reviews see Koistinaho & Hokfelt, 1997; MacManus & Linnik, 1997). Studies relevant to this thesis include previous investigations of changes in mGluR mRNA levels following global ischaemia. Using *in situ* hybridisation, levels of mRNA were measured 24 hours after the transient global insult - a time point when no neuronal damage can yet be seen morphologically. Iversen and colleagues (1994) demonstrated that while mGluR3 mRNA levels were not changed, the mRNA levels for mGluR2 were decreased. Whether their eventual translation to protein is reduced too is not known. These findings are consistent with previous studies which have shown that mRNA encoding the ionotropic glutamate receptors are downregulated following ischaemia (Pellegrini-Giampietro *et al.*, 1992; Frank *et al.*, 1995). Interestingly, it has recently been observed that protein levels of mGluR2/3 in animals subjected to hypoxia are substantially reduced. These animals were subjected to hypoxic and hypobaric conditions for two weeks (MacLean *et al.*, 1995) and cortical levels of mGluR2/3 protein were reduced by up to 80% (Dr I Mullaney, unpublished observations). Moreover, there was a concurrent reduction in the levels of G_{i2} and G_s type G-proteins.

No notable changes in mGluR2/3 immunoreactive cells were demonstrated following permanent focal ischaemia in this thesis, which further serves to highlight the differences in the mechanistic events following different central insults. Focal cerebral

ischaemia has been traditionally viewed as producing severe cell damage rapidly; changes can be seen in cells as early as 30 minutes after the insult (Garcia *et al.*, 1993). This contrasts to the delayed neuronal death seen after transient global ischaemia where cells die over the following 48-72 hours and the graduated and milder insult of hypoxia.

Actions of LY354740 and LY379268 following in vitro neurotoxicity

From the speculative *in vivo* findings observed in this thesis together with the existing evidence for the involvement of mGluR2 and mGluR3 in neuroprotection in the literature, the idea that mGluR2 and mGluR3 activation are protective in instances where the evolving damage is protracted to allow defensive intracellular events to take place appears possible. Using *in vitro* cell culture studies, the actions of LY354740 and LY379268 on cell death were explored using two different models of neurotoxicity with different mechanisms of damage. Previous studies have demonstrated that LY354740 and LY379268 can preserve the viability of cortical neuronal cells under conditions of NMDA-induced excitotoxicty in a dose-dependent manner (Kingston *et al.*, *in press*). This neuroprotective response was demonstrated to be specifically mediated through mGluR2/3 activation, as the addition of the selective group II antagonist, LY341495 (Kingston *et al.*, 1998) caused a reversal in the neuroprotective response. Neuronal death induced by NMDA exposure has been reported to occur predominantly by necrosis (Gwag *et al.*, 1997). However, NMDA-treated cortical cells exhibit an increase in nucleosome formation, which is effectively reduced following the administration of LY354740 and LY379268 to cultures. This response was demonstrated at low nM concentrations (observed at a much lower concentration than that required for LDH release) at doses in accordance with their measured receptor affinities in clonal lines (Kingston *et al.*, in press). The authors propose that the difference in the ability of the agonists to produce these effects is due to the ligands

differentiating a population of apoptotic cells within an overall population of dying neurones.

Additional evidence to support this anti-apoptotic effect is provided in this thesis by the ability of LY354740 and LY379268 to protect against staurosporine-induced cell death. Nucleosome formation in cultures following the hypoxic-hypoglycaemic insult were not measured unfortunately. In view of the hypothesis put forward by Kingston *et al.*, one would expect that the application of LY354740 and LY379268 to cultures subjected to glucose and oxygen deprivation would lead to a similar reduction in nucleosome formation. In addition, the activity of the agonists against staurosporine-induced neurotoxicity also appeared to be enhanced in the mixed cultures compared with the neurone-enriched cultures. Therefore, this may indicate that glial cells have an important role in the neuroprotective mechanism and further supports the findings of Bruno *et al.* (1997). Although no firm conclusions can be drawn from the glucose and oxygen deprivation studies due to the inadequate number of experiments performed, the data suggest that activation of mGluR2/3 may lead to actions on an apoptotic pathway.

Astroglial involvement in neuroprotection?

Western blot analysis in astrocytes carried out in this thesis corroborate the existing evidence that astrocytes are crucial to the mGluR2/3 neuroprotective mechanism and are involved in producing neurotrophic factors for neurones. While an immunoreactive protein band was not detected for mGluR2/3, a TGF-β2-specific protein band was detected both in the astrocyte homogenates and in the cell culture medium, which suggests the expression and secretion of TGF-β2 from cultured rat cortical astrocytes. This response was demonstrated to be mediated through mGluR2/3 as concomitant treatment of astrocytes with the selective antagonist LY341495 reversed this response. Astrocytes *in vitro* have

been shown to secrete TGF-β2 and to express TGF-β1 and TGF-β3 mRNAs, while cortical neurones only express TGF-β2 mRNA (Constam *et al.*, 1992; Vivien *et al.*, 1998). The recent demonstration that neurones and astrocytes are able to express TGF-β receptors (Vivien *et al*, 1998), which are necessary for the signal transduction of the TGF-βs, suggest that these cytokines play a critical role in the biology of neurones and astrocytes. Again, the findings of this study provide further support that neuroprotection by the group II mGluR agonists LY354740 and LY379268 requires the involvement of astrocytes and new protein synthesis. It is possible that while cells may be undergoing cell death by necrosis, the activation of group II mGluRs can also trigger a specific intracellular pathway that opposes the execution of programmed cell death. Investigations should be continued to assess the involvement of mGluR2/3 with the intracellular cascades.

Neuroprotective therapy

Neuroprotective drugs of many classes that target various steps of the excitotoxic cascade have undergone clinical trials, and none have yet proved successful. The failure of these trials has led to a rethink of trial designs for future protocols. Some common themes can be seen to underlie trial failures, such as patient recruitment, drug tolerability, and systemic toxicity. Some agents may have been simply launched prematurely into clinical trials. For example, the mechanism of action of Lubeluzole, an agent entered into clinical testing, is still unknown. In light of the negative findings from clinical trials in stroke, the predictive value of the animal models used in ischaemia research has also been questioned (Hunter *et al.*, 1995). However, the negative results clinically following positive animal data should not be regarded as damaging to the usefulness of these models, only indicating that certain criteria may have to change. For example, despite the fact that stroke primarily affects those of middle or later life, the animals used preclinically are invariably young rather

than aged. Additionally, one of the most important factors to take into consideration is the timing of the treatment in cerebral ischaemia. Agents therefore should be efficacious when given after the ischaemic insult and not before to mimic the clinical situation.

The way in which the ischaemia is analysed also needs to be changed. The most common method used at present for the assessment of damage following an experimental ischaemic insult is usually by histopathological measures of neurodegeneration. However, this is not an appropriate option in the clinical setting where measures of functional impairment and neurological outcome are measured. Therefore, measures of functional impairment and improvement should also be used in experimental stroke models. Various types of tasks have been developed to evaluate the functional performance in rats subjected to ischaemic insults. Because of the nature of the animal models of ischaemia, functional tests have been restricted to sensorimotor and cognitive performance (for review see Hunter *et al.*, 1998). The use of functional performance appears to be increasingly important since a variety of evidence indicates that neurological deficits and lesion size do not automatically correlate (Rogers *et al.*, 1992). The failure of clinical trials show that neuroprotective therapies using glutamatatergic agents alone do not appear likely treatments for stroke. Future successful treatment of stroke may emerge from a polypharmacy approach as reducing infarct volume in the absence of any functional benefit will have little impact on the quality of life of the patient. Moreover, it is of paramount importance to protect not just grey matter, but white matter also, as it is crucial to the fundamental architecture of the brain. Thus agents that can limit the spread of acute damage in the brain, for example, such as that seen at the level of the glutamate receptors, together with agents that improve long term functional recovery, e.g. anti-inflammatory agents, may result in promising therapeutic candidates for stroke.

8.5 The future of group II mGluRs in therapy...

There is currently much interest in the potential use of mGluR ligands in the therapy of neurologic disorders. Aside from their emerging role in neuroprotection following ischaemia, agonists acting at group II receptors have also been shown to reverse glutamatergic disruptions in an animal model of schizophrenia. Thus, the mGluRs present an alternative non-dopaminergic therapeutic strategy for the treatment in schizophrenia (Moghaddam & Adams, 1998).

Activation of group I mGluRs in the hippocampus has been shown to facilitate the generation of limbic seizures. Consistent with this, various studies have shown that seizure activity can be attenuated either by antagonists for group I receptors or by selective agonists of group II or group III receptors. For example, a study using (S)-4C3HPG (antagonist at group I and agonist at group II mGluRs) demonstrated anticonvulsant effects in mice (Thomsen et al., 1994; Dalby & Thomsen, 1996). mGluRs may serve as important new targets for development of novel anticonvulsant agents.

In addition to their involvement in memory, mGluRs also elicit physiologic effects in the hippocampus that may enhance cognitive function thus suggesting that mGluR ligands may be useful as cognitive enhancing agents. This would be of particular benefit to those suffering from memory impairments. Recent work has also implicated the involvement of mGluRs in Huntington disease (Cha et al., 1998). By using transgenic mice expressing a portion of an abnormal human HD gene, the mutant mice were found to have a reduction in mGluR1, mGluR2 and mGluR3. These changes were observed in association with decreases in ionotropic glutamate and dopamine receptors, which are thought to be pathologic hallmarks of Huntingdon disease. Studies have also implicated group I and II mGluRs in transmitting noxious sensory information to the thalamus (Salt & Eaton 1994; Eaton et al.,

1993).Thus, development of selective ligands for the mGluRs involved in the transmission of these signals could potentially be useful in the treatment of acute and chronic pain.

As already mentioned, LY354740 is currently under clinical development. A potential clinical use of LY354740 could be for the treatment of anxiety (Helton *et al.*, 1998b). The anxiolytic effects of LY354740 were tested in the fear potentiated startle procedure and the elevated plus maze models (Davies, 1979; Lister, 1987), both of which have been used for clinically proven anxiolytics such as the benzodiazepine, diazepam and the $5HT_{1a}$ agonist, buspirone (Helton *et al.*, 1998b). The study indicates that LY354740 produces benzodiazepine-like efficacy, but is devoid of benzodiazepine-like side effects at anxiolytic doses. Moreover, the $[^{14}C]2$-DG study carried out in this thesis demonstrated that LY354740 reduced function-related glucose metabolism in the perforant pathway, which is known to be important for producing anxiolytic effects (Pratt, 1992). Given the anxiolytic profile of LY354740, this agent also appears to be efficacious in reducing the symptoms associated with nicotine withdrawal during smoking cessation (Helton *et al.*, 1998a). The effects of nicotine withdrawal were assessed by measuring the sensorimotor reactivity to an auditory startle reflex in rats. The discontinuation of chronic exposure to nicotine in rats results in a marked increase in the auditory startle reflex. The administration of LY354740 (6 mg/kg for 12 days) resulted in an attenuation of the withdrawal-enhanced startle responses. How it affects nicotine withdrawal however, is not known. The potential of LY354740 in smoking cessation in humans has yet to be tested. Similarly, LY354740 has indicated a promising role in attenuating morphine withdrawal symptoms and may be of therapeutic benefit in man for the treatment of opiate withdrawal (Vandergriff & Rasmussen, 1999). At the time of writing this thesis, LY379268 is also undergoing clinical development. However, as many aspects of the work carried out with LY379268 have not been disclosed, they cannot be discussed here. Nonetheless, because of its different central

profile and selectivity for the group II mGluRs, its use in the clinical setting will most probably be different from LY354740.

Because of the fundamental roles of mGluRs in the brain, the development of agonists and antagonists selective for specific mGluR subtypes will provide invaluable tools for increasing our understanding of mGluRs. The variety of mGluRs and the differences in their localisation suggests that they specialise in their functions. Because of the heterogeneity of the subtypes, the potential to develop drugs that are selective for mGluRs in specific brain regions for neurologic and psychiatric disorders is great. Much has been learnt about the mGluRs in the last decade, and the continuing effort to produce better ligands will help us proceed in unravelling the complexity and functional importance of these receptors.

References

Abe, T., Sugihara, H., Nawa, H., Shigemoto, R., Mizuno, N. & Nakanishi, S. (1992) Molecular characterization of a novel metabotropic glutamate receptor mGluR5 coupled to inositol phosphate/Ca^{2+} signal transduction. *Journal of Biological Chemistry*, **267**, 13361-13368.

Abe, A., Aoki, M., Kawagoe, J., Yoshida, T., Hattori, A., Kogure, K. & Itoyama, Y. (1995) Ischemic delayed neuronal death: a mitochondrial hypothesis. *Stroke*, **26**, 1478-1489.

Ableitner, A., Wuster, M. & Herz, A. (1985) Specific changes in local cerebral glucose utilization in the rat brain induced by acute and chronic diazepam. *Brain Research*, **359**, 49-56.

Adams, H.P., Brott, T.G., Furlan, A.J., Gomez, C.R., Grotta, J., Helgason, C.M., Kwiatkowski, T., Lyden, P.D., Marler, J.R., Troner, J., Feinberg, W., Mayberg, M. & Theis, W. (1996) Guidelines for thrombolytic therapy for acute stroke. A supplement to the guidelines for the management of patients with acute ischaemia stroke. A statement for healthcare professionals from a special writing group of the Stroke Council, American Heart Association. *Stroke*, **27**, 1711-1718.

Adler, C.M., Goldberg, T.E., Malhotra, A.K., Pickar, D. & Breier, A. (1998) Effects of ketamine on thought disorder, working memory, and semantic memory in healthy volunteers. *Biological Psychiatry*, **43**, 811-816.

Aiba, A., Chen, C., Herrup, K., Rosenmund, C., Stevens, C.F. & Tonegawa, S. (1994) Reduced hippocampal long-term potentiation and context-specific deficit in associative learning in mGluR1 mutant mice. *Cell*, **79**, 365-375.

Alps, B.J., Calder C., Hass, W.K. & Wilson, A.D. (1988) Comparative protective effects of nicardipine, flunarizine, lidoflazine and nimodipine against ischaemic injury in the hippocampus of the Mongolian gerbil. *British Journal of Pharmacology*, **93**, 877-883.

Andine, P., Otwar, O., Jacobson, I., Sandberg, M. & Hagberg, H. (1991) Changes in extracellular amino acids and spontaneous neuronal activity during ischaemia and extended reflow in the CA1 of the rat hippocampus. *Journal of Neuroscience*, **57**, 222-239.

Aramori, I. & Nakanishi, S. (1992) Signal transduction and pharmacological characteristics of a metabotropic glutamate receptor, mGluR1, in transfected CHO cells. *Neuron*, **8**, 757-765.

Astrup, J., Sørensen, P.M. & Sørensen, H.R. (1981) Oxygen and glucose consumption related to Na^+-K^+ transport in canine brain. *Stroke*, **12**, 726-730.

Attwell, D. & Mobbs, P. (1994) Neurotransmitter transporters. *Current Opinion in Neurobiology*, **4**, 353-359.

Auer, R., Wieloch, T., Olsson, Y. & Siesjö, B.K. (1984) The distribution of hypoglycemic brain damage. *Acta Neuropathologica*, **64**, 177-191.

Bahn, S., Volk, B. & Wisden, W. (1994) Kainate receptor gene expression in the developing rat brain. *Journal of Neuroscience*, **14**, 5525-5547.

Balschun, D. & Wetzel, W. (1998) Inhibition of group I metabotropic glutamate receptors blocks spatial learning in rats. *Neuroscience Letters*, **249**, 41-44.

Barbour, B., Keller, B.U., Llano, I. & Marty, A. (1994) Prolonged presence of glutamate during excitatory synaptic transmission to cerebellar Purkinje cells. *Neuron*, **12**, 1331-1343.

Barnard, E.A. (1997) Ionotropic glutamate receptors: new types and new concepts. *Trends in Pharmacological Sciences*, **18**, 141-148.

Barone, F.C., Lysko, P.G., Price, W.J., Feuerstein, G., Al-Baracanji, K.A., Benham, C.D., Harrison, D.C., Harries, M.H., Bailey, S.J. & Hunter, A.J. (1995) SB201823-A antagonises calcium currents in central neurons and reduces the effects of focal ischaemia in rats and mice. *Stroke*, **26**, 1683-1690.

Barrionuevo, G., Schottler, F. & Lynch, G. (1980) The effects of repetitive low frequency stimulation on control and "potentiated" synaptic responses in the hippocampus. *Life Sciences*, **27**, 2385-2391.

Bashir, Z.I., Bortolotto, Z.A., Davies, C.H., Berreta, N., Irving, A.J., Seal, A.J., Henley, J.M., Jane, D.E., Watkins, J.C. & Collingridge, G.L. (1993) Induction of LTP in the hippocampus needs synaptic activation of glutamate metabotropic receptors. *Nature*, **363**, 347-350.

Battaglia, G., Monn, J.A. & Schoepp, D.D. (1997) *In vivo* inhibition of veratridine-evoked release of striatal excitatory amino acids by the group II metabotropic glutamate receptor agonist LY354740 in rats. *Neuroscience Letters*, **229**, 161-164.

Baude, A., Nusser, Z., Roberts, J.D.B., Mulvihill, E., McIlhinney, R.A.J. & Somogyi, P. (1993) The metabotropic glutamate receptor (mGluR1α) is concentrated at perisynaptic membrane of neuronal subpopulations as detected by immunogold reaction. *Neuron*, **11**, 771-787.

Beal, M.F. (1992) Does impairment of energy metabolism result in excitotoxic neuronal death in neurodegenerative illnesses? *Annals of Neurology*, **31**, 119-130.

Beckman, J.S. (1991) The double-edged role of nitric oxide in brain function and superoxide-mediated injury. *Journal of Developmental Physiology*, **15**, 53-59.

Behnisch, T., Wilsch, V.W., Balschun, D. & Reymann, K.G. (1998) The role of group II metabotropic glutamate receptors in hippocampal CA1 long-term potentiation *in vitro*. *European Journal of Pharmacology*, **356**, 159-165.

Benveniste, H., Drejer, J., Schousboe, A. & Diemer, N.H. (1984) Elevation of the extracellular concentrations of glutamate and aspartate in rat hippocampus during transient cerebral ischaemia monitored by intracerebral microdialysis. *Journal of Neurochemistry*, **43**, 1369-1374.

Bernardi, P. & Petronilli, V. (1996) The permeability transition pore as a mitochondrial calcium release channel: a critical appraisal. *Journal of Bioenergetics and Biomembranes*, **28**, 131-137.

Bettler, B., Egebjerg, J., Sharma, G., Pecht, G., Hermans-Borgmeyer, I., Moll, C., Stevens, C.F. & Heinemann, S. (1992) Cloning of a putative glutamate receptor: a low affinity kainate-binding subunit. *Neuron*, **8**, 257-265.

Bettler, B. & Mulle, C. (1995) AMPA and kainate receptors. *Neuropharmacology*, **34**, 123-139.

Bielenberg, G.W., Burniol, M., Rosen, R. & Klaus, W. (1990) Effects of nimodipine on infarct size and cerebral acidosis after middle cerebral artery in the rat. *Stroke*, **21** (Supp IV), IV90-IV92.

Birse, E.F., Eaton, S.A., Jane, D.E., Jones, P.L., Porter, R.H., Pook, P.C., Sunter, D.C., Udvarhelyi, P.M., Wharton, B., Roberts, P.J., Salt, T.E. & Watkins, J.C. (1993) Phenylglycine derivatives as new pharmacological tools for investigating the role of metabotropic glutamate receptors in the central nervous system. *Neuroscience*, **52**, 481-488.

Bischoff, S., Barhanin, J., Bettler, B., Mulle, C. & Heinemann, S. (1997) Spatial distribution of kainate receptor subunit mRNA in the mouse basal ganglia and ventral mesencephalon. *Journal of Comparative Neurology*, **379**, 541-562.

Blaschke, M., Keller, B.U., Rivosecchi, R., Hollman, M., Heinemann, S. & Konnerth, A. (1993) A single amino acid determines the subunit-specific spider toxin block of alpha-amino-3-hydroxy-methyl-5-methylisoxazole-4-proprionate/kainate receptor channels. *Proceedings of the National Academy of Sciences USA*, **90**, 6528-6532.

Blaustein, M. (1988) Calcium transport and buffering in neurons. *Trends in Neurosciences*, **11**, 438-443.

Bleakman, D., Rusin, K.I., Chard, P.S., Glaum, S.R. & Miller, R.J. (1992) Metabotropic glutamate receptors potentiate ionotropic glutamate responses in the rat dorsal horn. *Molecular Pharmacology*, **42**, 192-196.

Bliss, T.V.P. & Collingridge, G. (1993) A synaptic model of memory: long-term potentiation in the hippocampus. *Nature*, **361**, 31-39.

Bliss, T.V.P. & Lømo, T. (1973) Long-lasting potentiation of synaptic transmission in the dentate area of the unanesthetized rabbit following stimulation of the perforant path. *Journal of Physiology (London)*, **232**, 331-356.

Blitzer, R.D., Wong, T., Nouranifar, R., Iyengar, R. & Landau, E.M. (1995) Postsynaptic cAMP pathway gates early LTP in hippocampal CA1 region. *Neuron*, **15**, 1403-1414.

Blumbergs, P.C., Scott, G., Manavis, J., Wainwright, H., Simpson, D.A. & McLean, A.J. (1994) Staining of amyloid precursor protein to study axonal damage in mild head injury. *Lancet*, **344**, 1055-1056.

Boast, C.A., Gerhardt, S.C., Pastor, G., Lehmann, J., Etienne, P.E. & Liebman, J.M. (1988) The N-methyl-D-aspartate antagonists CGS 19755 and CPP reduce ischaemic brain damage in gerbils. *Brain Research*, **442**, 345-348.

Bochet, P., Audinat, E., Lambolez, B., Crepel, F., Rossier, J., Iino, M., Tsuzuki, K. & Ozawa, S. (1994) Subunit composition at the single-cell level explains functional properties of a glutamate-gated channel, *Neuron*, **12**, 383-388.

Bond, A., Monn, J.A. & Lodge, D. (1997) A novel orally active group 2 metabotropic glutamate receptor agonist: LY354740. *NeuroReport*, **8**, 1463-1466.

Bond, A. O'Neill, M.J. Hicks, C.A. Monn, J.A. & Lodge, D. (1998) Neuroprotective effects of a systemically active Group II metabotropic glutamate receptor agonist LY354740 in a gerbil model of global ischaemia. *NeuroReport*, **9**, 1191-1193.

Boss, V., Nutt, K.M. & Conn, P.J. (1994) L-cysteine sulfinic acid as an endogenous agonist of a novel metabotropic receptor coupled to stimulation of phospholipase D activity. *Molecular Pharmacology*, **45**, 1177-1182.

Boulter, J., Hollman, M., O'Shea-Greenfield, A., Hartley, M., Deneris, E.S. & Heinemann, S. (1990) Molecular cloning and functional expression of glutamate receptor subunit genes. *Science*, **249**, 1033-1037.

Bowman, C.L. & Kimelberg, H.K. (1984) Excitatory amino acids directly depolarize rat brain astrocytes in primary culture. *Nature*, **311**, 656-659.

Brown, E.M., Gamba, G., Riccard, D., Lombardi, M., Butters, R., Kifor, O., Sun, A., Hediger, M.A., Lytton, J. & Hebert, S.C. (1993) Cloning and characterization of an extracellular Ca^{2+}-sensing receptor from bovine parathyroid. *Nature*, **366**, 575-580.

Browne, S.E. & McCulloch, J. (1994) AMPA receptor antagonists and local cerebral glucose utilization in the rat. *Brain Research*, **641**, 10-20.

Bruno, V., Copani, A., Battaglia, G., Raffale, R., Shinozaki, H. & Nicoletti, F. (1994) Protective effect of the metabotropic glutamate receptor agonist, DCG-IV, against excitotoxic neuronal death. *European Journal of Pharmacology*, **256**, 109-112.

Bruno, V., Battaglia, G., Copani, A., Giffard, R.G., Raciti, G., Raffaele, R., Shinozaki, H. & Nicoletti, F. (1995a) Activation of class II or III metabotropic glutamate receptors protects cultured cortical neurons against excitotoxic degeneration. *European Journal of Neuroscience*, **7**, 1906-1913.

Bruno, V., Copani, A., Knöpfel, T., Kuhn, R., Casabona, G., Dell' Albani, P., Condorelli, D. & Nicoletti, F. (1995b) Activation of metabotropic glutamate receptors coupled to inositol phospholipid hydrolysis amplifies NMDA-induced neuronal degeneration in cultured cortical cells. *Neuropharmacology*, **34**, 1089-1098.

Bruno, V., Copani, A., Bonanno, L., Knöpfel, T., Kuhn, R., Roberts, P.J. & Nicoletti, F. (1996) Activation of group III metabotropic glutamate receptors is neuroprotective in cortical cultures. *European Journal of Pharmacology*, **310**, 61-66.

Bruno, V., Sureda, F.X., Storto, M., Casabona, G., Caruso, A., Knöpfel, T., Kuhn, R. & Nicoletti, F. (1997) The neuroprotective activity of group II metabotropic glutamate receptors requires new protein synthesis and involves a glial-neuronal signaling. *Journal of Neuroscience*, **17**, 1891-1897.

Bruno, V., Battaglia, G., Casabona, G., Copani, A., Caciagli, F. & Nicoletti, F. (1998) Neuroprotection by glial metabotropic glutamate receptors is mediated by transforming growth factor-beta. *The Journal of Neuroscience*, **18**, 9594-9600.

Bruno, V., Battaglia, G., Kingston, A., O'Neill, M.J., Catania, M.V., Di Grezia, R. & Nicoletti, F. (1999) Neuroprotective activity of the potent and selective mGlu1a metabotropic glutamate receptor antagonist, (+)-2-methyl-4-carboxyphenylglycine (LY367385): comparison with LY357366, a broader spectrum antagonist with equal affinity for mGlu1a and mGlu5 receptors. *Neuropharmacology*, **38**, 199-207.

Buchan, A.M., Li, H., Cho, S. & Pulsinelli, W.A. (1991a) Blockade of the AMPA receptor prevents CA1 hippocampal injury following severe but transient forebrain ischemia in adult rats. *Neuroscience Letters*, **132**, 255-258.

Buchan, A.M., Xue, D., Huang, Z-G., Smith, K.H. & Lesiuk, H. (1991b) Delayed AMPA receptor blockade reduces cerebral infarction induced by focal ischemia. *NeuroReport*, **2**, 473-476.

Buisson, A. & Choi, D.W. (1995) The inhibitory mGluR agonist, S-4-carboxy-3-hydroxy-phenylglycine selectively attenuates NMDA neurotoxicity and oxygen-glucose deprivation-induced neuronal death. *Neuropharmacology*, **34**, 1081-1087.

Buisson, A., Yu, S.P. & Choi, D.W. (1996) DCG-IV selectively attenuates rapidly triggered NMDA-induced neurotoxicity in cortical neurons. *European Journal of Neuroscience*, **8**, 138-143.

Buller, A.L., Larson, H.C., Schneider, B.E., Beaton, J.A., Morrisett, R.A. & Monaghan, D.T. (1994) The molecular basis of NMDA receptor subtypes: Native receptor diversity is predicted by subunit composition. *Journal of Neuroscience*, **14**, 5471-5484.

Bullock, R., Graham, D.I., Swanson, S. & McCulloch, J. (1994) Neuroprotective effect of the AMPA receptor antagonist LY-293558 in focal cerebral ischaemia in the cat. *Journal of Cerebral Blood Flow and Metabolism*, **14**, 466-471.

Burnashev, N., Khodorova, A., Jonas, P., Helm, P.J., Wisden, W., Monyer, H., Seeburg, P.H. & Sakmann, B. (1992) Calcium permeable AMPA-kainate receptors in fusiform cerebellar glial cells. *Science*, **256**, 1566-1570.

Carafoli, E. (1987) Intracellular calcium homeostasis. *Annual Review of Biochemistry*, **56**, 395-433.

Carney, J.M. & Floyd, R.A. (1991) Protection against oxidative damage to CNS by α-phenyl-tert-butyl-nitrone (PBN) and other spin-trapping agents: A novel series of nonlipid free radical scavengers. *Journal of Molecular Neuroscience*, **3**, 47-57.

Castillo, P.E., Malenka, R.C. & Nicoll, R.A. (1997) Kainate receptors mediate a slow postsynaptic current in hippocampal CA3 neurons. *Nature*, **388**, 182-186.

Cerne, R. & Randic, M. (1992) Modulation of AMPA and NMDA responses in rat spinal dorsal horn neurons by trans-1-aminocyclopentane-1, 3-dicarboxylic acid. *Neuroscience Letters*, **144**, 180-184.

Cha, J.H., Kosinski, C.M., Kerner, J.A., Alsdorf, S.A., Mangiarini, L., Davies, S.W., Penney, J.B., Bates, G.P. & Young, A.B. (1998) Altered brain neurotransmitter receptors in transgenic mice expressing a portion of an abnormal human huntington disease gene. *Proceedings of the National Academy of Sciences USA*, **26**, 6480-6485.

Chavis, P., Fagni, L., Bockaert, J. & Lansman, J.B. (1995) Modulation of calcium channels by metabotropic glutamate receptors in cerebellar granule cells. *Neuropharmacology*, **34**, 929-937.

Chiamulera, C., Albertini, P., Valerio, E. & Reggiani, A. (1992) Activation of metabotropic receptors has a neuroprotective effect in a rodent model of focal ischaemia. *European Journal of Pharmacology*, **216**, 335-336.

Chinestra, P., Aniksztejn, L., Diabira, D. & Ben-Ari, Y. (1993) (RS)-α-methyl-4-carboxyphenylglycine neither prevents induction of LTP nor antagonizes metabotropic glutamate receptors in CA1 hippocampal neurons. *Journal of Neurophysiology*, **70**, 2684-2689.

Choi, D.W. (1987) Ionic dependence of glutamate neurotoxicity. *Journal of Neuroscience*, **7**, 369-379.

Choi, D.W. (1988) Glutamate neurotoxicity and diseases of the nervous system. *Neuron*, **1**, 623-634.

Choi, D.W. (1995) Calcium: still center-stage in hypoxic-ischemic neuronal death. *Trends in Neurosciences*, **18**, 58-60.

Choi, S. & Lovinger, D.M. (1996) Metabotropic glutamate receptor modulation of voltage-gated Ca^{2+} channels involves multiple receptor subtypes in cortical neurons. *Journal of Neuroscience*, **16**, 36-45.

Chopp, M. & Li, Y. (1996) Apoptosis in focal cerebral ischemia. *Acta Neurochir.*, **66**(Suppl), 21-26.

Chung, D.S., Traynelis, S.F., Murphy, T.J. & Conn, P.J. (1997) 4-Methylhomoibotenic acid activates a novel metabotropic glutamate receptor coupled to phosphotidylinositol hydrolysis. *Journal of Pharmacology and Experimental Therapeutics*, **283**, 742-749.

Clarke, V.R.J., Ballyk, B.A., Hoo, K.H., Mandelzys, A., Pellizari, A., Bath, C.P., Thomas, J., Sharpe, E.F., Davies, C.H., Ornstein, P.L., Schoepp, D.D., Kamboj, R.K., Collingridge, G.L., Lodge, D. & Bleakman, D. (1997) A hippocampal GluR5 kainate receptor regulating inhibitory synaptic transmission. *Nature*, **389**, 599-602.

Cline, H.T., Debski, E. & Constantine-Paton, M. (1987) NMDA receptor antagonist desegregates eye specific stripes. *Proceedings of the National Academy of Sciences USA*, **84**, 4342-4345.

Clineschmidt, B.V., Martin, G.E. & Bunting, P.R. (1982) Anticonvulsant activity of (+)-5-methyl-10,11-dihydro-5H-dibenzo[a,d]cyclohepten-5,10-imine maleate (MK-801), a substance with potent anticonvulsant central sympathomimetic and apparent anxiolytic properties. *Drug Development Research*, **2**, 123-134.

Collingridge, G.L. & Bliss, T.V.P. (1987) NMDA receptors-their role in long-term potentiation. *Trends in Neurosciences*, **10**, 288-294.

Collingridge, G.L. & Bliss, T.V.P (1995) Memories of NMDA receptors and LTP. *Trends in Neurosciences*, **18**, 54-62.

Collins, D.R. & Davies, S.N. (1993) Co-administration of (1S,3R)-1-aminocyclo-pentane-1,3-dicarboxylic acid and arachidonic acid potentiates synaptic transmission in rat hippocampal slices. *European Journal of Pharmacology*, **240**, 325-326.

Colwell, C.S. & Levine, M.S. (1994) Metabotropic glutamate receptors modulate N-methyl-D-aspartate receptor function in neostriatal neurons. *Neuroscience*, **61**, 497-507.

Conn, P.J., Winder, D.G. & Gereau IV, R.W. (1995) Regulation of neuronal circuits and animal behaviour by metabotropic glutamate receptors. *In The Metabotropic Glutamate Receptors*, ed. Conn, P.J. & Platel, J. pp 195-229. Totowa: Humana Press.

Conn, P.J. & Pin, J-P. (1997) Pharmacology and functions of metabotropic glutamate receptors. *Annual Review of Pharmacology and Toxicology*, **37**, 205-37.

Conquet, F., Bashir, Z.I., Davies, C.H., Daniel, H., Ferraguti, F., Bordi, F., Franz-Bacon, K., Reggiani, A., Matarese, V., Condé, F. Collingridge, G.L. & Crepel, F. (1994) Motor deficit and impairment of synaptic plasticity in mice lacking mGluR1. *Nature*, **372**, 237-243.

Constam, D.B., Philipp, J., Malipiero, U.V., ten Dijke, P., Schachner, M. & Fontana, A. (1992) Differential expression of transforming growth factor-beta 1, -beta 2 and -beta 3 by glioblastoma cells, astrocytes and microglia. *Journal of Immunology*, **148**, 1404-1410.

Copani, A., Bruno, V., Battaglia, G., Leanza, G., Pellitteri, R., Russo, A., Stanzani, S. & Nicoletti, F. (1995) Activation of metabotropic glutamate receptors protects cultured neurons against apoptosis induced by β-amyloid peptide. *Molecular Pharmacology*, **47**, 890-897.

Crane, P.D., Braun, L.D., Cornford, E.M., Cremer, J.E., Glass, J.M. & Oldendorf, W.H. (1978) Dose dependent reduction of glucose utilization by pentobarbital in rat brain. *Stroke*, **9**, 12-18.

Crépel, V., Aniksztejn, L., Ben-Ari, Y. & Hammond, C. (1994) Glutamate metabotropic receptors increase a Ca^{2+}-activated non-specific cationic current in CA1 hippocampal neurons. *Journal of Neurophysiology*, **72**, 1561-1569.

Crompton, M., Ellinger, H. & Costi, A. (1988) Inhibition by cyclosporin A of a CsA dependent pore in heart mitochondria activated by inorganic phosphate and oxidative stress. *Biochemical Journal*, **255**, 357-360.

Curtis, D.R. & Watkins, J.C. (1963) Acidic amino acids with strong excitatory actions on mammalian neurones. *Journal of Physiology (London)*, **166**, 1-14.

Daggett, L.P., Sacaan, A.I., Akong, M., Rao, S.P., Hess, S.D., Liaw, C., Urratia, A., Jachec, C., Ellis, S.B., Dreessen, J., Knöpfel, T., Landwehrmeyer, G.B., Testa, C.M., Young, A.B., Varney, M., Johnson, E.C. & Veliçelebi, G. (1995) Molecular and functional characterization of recombinant human metabotropic glutamate receptor subtype 5. *Neuropharmacology*, **34**, 871-886.

Dalby, N.O. & Thomsen, C. (1996) Modulation of seizure activity in mice by metabotropic glutamate receptor ligands. *Journal of Pharmacology and Experimental Therapeutics*, **276**, 516-522.

Davies, J. & Watkins, J.C. (1973) Antagonism of synaptic and amino acid induced excitation in the cuneate nucleus of the cat by HA-966. *Neuropharmacology*, **12**, 637-640.

Davies, M. (1979) Diazepam and flurazepam: Effects on conditioned fear as measured with the potentiated startle paradigm. *Psychopharmacology*, **62**, 1-7.

Davies, S.N., Lester, R.A., Reymann, K.G. & Collingridge, G.L. (1989) Temporally distinct pre- and post-synaptic mechanisms maintain long-term potentiation. *Nature*, **338**, 500-503.

Davies, C.H., Clarke, V.R.J., Jane, D.E. & Collingridge, G.L. (1995) Pharmacology of postsynaptic metabotropic glutamate receptors in rat hippocampal CA1 pyramidal neurons. *British Journal of Pharmacology*, **116**, 1859-1869.

Dawson, T.M., Dawson, V.L. & Synder, S.H. (1992) A novel neuronal messenger in brain: the free radical, nitric oxide. *Annals of Neurology*, **32**, 297-311.

Degraba, T.J., Ostrow, P., Hanson, S. & Grotta, J.C. (1994) Motor performance, histologic damage, and calcium influx in rats treated with NBQX after focal ischaemia. *Journal of Cerebral Blood Flow and Metabolism*, **14**, 262-268.

Demerle-Pallardy, C., Lonchampt, M.O., Chabrier, P.E. & Braquet, P. (1991) Absence of implication of L-arginine/nitric oxide pathway on neuronal cell injury induced by L-glutamate or hypoxia. *Biochemical and Biophysical Research Communications*, **181**, 456-464.

De Ryck, M., Keersmaekers, R., Clincke, G., Janssen, M. & Van Reet, S. (1994) Lubeluzole, a novel benzothiazole, protects neurologic function after cerebral thrombotic stroke in rats: an apparent stereospecific effect. *Society for Neuroscience Abstracts*, **20**, 185.

Desai, M.A., Burnett, J.P., Mayne, N.G. & Schoepp, D.D. (1995) Cloning and expression of a human metabotropic glutamate receptor 1α: enhanced coupling on co-transfection with a glutamate transporter. *Molecular Pharmacology*, **48**, 648-657.

Deshpande, J.K., Siesjö, B.K. & Wieloch, T. (1987) Accumulation and neuronal damage in the rat hippocampus following cerebral ischemia. *Journal of Cerebral Blood Flow and Metabolism*, **7**, 89-95.

Doherty, A.J., Palmer, M.J., Henley, J.M., Collingridge, G.L. & Jane, D.E. (1997) (RS)-2-chloro-5-hydroxyphenylglycine (CHPG) activates mGlu5, but not mGlu1 receptors expressed in CHO cells and potentiates NMDA responses in the hippocampus. *Neuropharmacology*, **36**, 265-267.

Duchen, M.R., McGuinness, O., Brown, L.A. & Crompton, M. (1993) On the involvement of a cyclosporin A sensitive mitochondrial pore in myocardial reperfusion injury. *Cardiovascular Research*, **27**, 1790-1794.

Dudek, S.M. & Bear, M.F. (1992) Homosynaptic long-term depression in area CA1 of the hippocampus and the effects of NMDA receptor blockade. *Proceedings of the National Academy of Sciences USA*. **89**, 4363-4367.

Duverger, D. & Mackenzie, E.T (1988) The quantification of cerebral infarction following focal ischemia in the rat: influence of strain, arterial pressure, blood glucose concentration, and age. *Journal of Cerebral Blood Flow and Metabolism*, **8**, 449-461.

Eaton, S.A., Birse, E.F., Wharton, B., Sunter, D.C., Udvarhelyi, P.M., Watkins, J.C. & Salt, T.E. (1993) Mediation of the thalamic sensory responses in vivo by ACPD-activated excitatory amino acid receptors. *European Journal of Neuroscience*, **5**, 186-189.

Elford, P.R., Heng, R., Révész, L. & MacKenzie, A.R. (1995) Reduction of inflammation and pyrexia in the rat by oral administration of SDZ 224-015, an inhibitor of the interleukin-1β converting enzyme. *British Journal of Pharmacology*, **115**, 601-606.

Emile, L., Mercken, L., Apiou, F., Pradier, L., Bock, M-D. Menager, J., Clot, J., Doble, A. & Blanchard, J.C. (1996) Molecular cloning, functional expression, pharmacological characterization and chromosomal localisation of the human metabotropic glutamate receptor type 3. *Neuropharmacology*, **35**, 523-530.

Erecinska, M. & Silver, I. (1994) Ions and energy in mammalian brain. *Progress in Neurobiology*, **43**, 37-71.

Ferraguti, F., Pietra, C., Valerio, E., Corti, C., Chiamulera, C. & Conquet, F. (1997) Evidence against a permissive role of the metabotropic glutamate receptor 1 in acute excitotoxicity. *Neuroscience*, **79**, 1-5.

Feuerstein, G.Z., Wang, X., Lue, T-L. & Barone, F.C. (1996) Inflammatory cytokines and stroke: Emerging new strategies for stroke therapies. In *19th Princeton Stroke Conference*, ed. Moskowitz, M.A. & Caplan, L.R. pp 75-91. Boston: Butterworth-Heinemann.

Flor, P.J., Lindauer, K., Püttner, I., Rüegg, D., Lukic, S., Knöpfel, T. & Kuhn, R. (1995a) Molecular cloning, functional expression and pharmacological characterization of the human metabotropic glutamate receptor type 2. *European Journal of Neuroscience*, **7**, 622-629.

Flor, P.J., Lukic, S., Rüegg, D., Leonhardt, T., Knöpfel, T. & Kuhn, R. (1995b) Molecular cloning, functional expression and pharmacological characterization of the human metabotropic glutamate receptor type 4. *Neuropharmacology*, **34**, 149-155.

Floyd, R.A. & Carney, J.M. (1992) Free radical damage to protein and DNA: mechanisms involved and relevant observations on brain undergoing oxidative stress. *Annals of Neurology*, **32**, S22-S27.

Ford, I., Kelly, P.A.T. & McCulloch, J. (1985) Fingerprinting neuropharmacological profiles: A systematic approach to handling data from 2-deoxyglucose autoradiography. *Journal of Cerebral Blood Flow and Metabolism*, **5**(suppl. 1), S647-S648.

Forsythe, I.D. & Barnes-Davies, M. (1997) Synaptic transmission: Well-placed modulators. *Current Biology*, **7**, R362-R365.

Foster, A.C. & Fagg, G.E. (1984) Acidic amino acid binding sites in mammalian neuronal membranes: their characteristics and relationship to synaptic receptors. *Brain Research Reviews*, 7, 103-164.

Frank, L., Diemer, N.H., Kaiser, F., Sheardown, M., Rasmussen, J.S. & Kristensen, P. (1995) Unchanged balance between levels of mRNA encoding AMPA glutamate receptor subtypes following global cerebral ischemia in the rat. *Acta Neurologica Scandinavica*, 92, 337-343.

Frey, U. & Morris, R.G.M. (1998) Synaptic tagging: implications for late maintenance of hippocampal long-term potentiation. *Trends in Neurosciences*, 21, 181-188.

Funahashi, S., Bruce, C.J. & Goldman-Rakic, P.J. (1989) Mnemonic coding of visual space in the monkey's dorsolateral prefrontal cortex. *Journal of Neurophysiology*, 61, 331-349.

Gabuzda, D., Busciglio, J. & Yankner, B.A. (1993) Inhibition of β-amyloid production by activation of protein kinase C. *Journal of Neurochemistry*, 61, 2326-2329.

Gaffan, D. (1994) Scene-specific memory for objects: A model of episodic memory impairment in monkeys with fornix transection. *Journal of Cognitive Neuroscience*, 6, 305-320.

Garcia, J.H., Yoshida, Y., Chen, H., Li, Y., Zhang, Z.G., Lian, J., Chen, S. & Chopp, M. (1993) Progression from ischemic injury to infarct following middle cerebral artery occlusion in the rat. *American Journal of Pathology*, 142, 623-635.

Gasic, G.P. & Hollman, M. (1992) Molecular neurobiology of glutamate receptors. *Annual Review of Physiology*, 54, 507-536.

Gentleman, S.M., Roberts, G.W., Gennarelli, T.A., Maxwell, W.L., Adams, J.H., Kerr, S. & Graham, D.I. (1995) Axonal injury: a universal consequence of fatal closed head injury. *Acta Neuropathologica Berl.*, 89, 537-543.

Gereau, R.W. & Conn, P.J. (1995a) Multiple presynaptic metabotropic glutamate receptors modulate excitatory and inhibitory synaptic transmission in hippocampal area CA1. *Journal of Neuroscience*, 15, 6879-6889.

Gereau, R.W. & Conn, P.J. (1995b) Roles of specific metabotropic glutamate receptor subtypes in regulation of hippocampal CA1 pyramidal cell excitability. *Journal of Neurophysiology*, 74, 122-129.

Gill, R. & Lodge, D. (1991) The neuroprotective action of 2,3-dihydroxy-6-nitro-7-sulfamoyl-benzo(F)quinoxaline (NBQX) in a rat focal ischaemia model. *British Journal of Pharmacology (Proc. Suppl)*, 102, 61P.

Gill, R., Nordholm, L. & Lodge, D. (1992) The neuroprotective actions of 2,3-dihydroxy-6-nitro-7-sulfamoyl-benzo(F)quinoxaline (NBQX) in a rat focal ischaemia model. *Brain Research*, 580, 35-43.

Gill, R. & Lodge, D. (1997) Pharmacology of AMPA antagonists and their role in neuroprotection. In *International Review of Neurobiology*, ed. Bradley, R.J., Harris, R.A. & Jenner, P. Vol 40. Ch. 9. pp 197-232.

Ginsberg, M.D. & Pulsinelli, W.A. (1994) Editorial: The ischemic penumbra, injury thresholds, and the therapeutic window for acute stroke. *Annals of Neurology*, **36**, 553-554.

Ginsberg, M.D. (1995) Neuroprotection in brain ischaemia: An update (part I). *The Neuroscientist*, **1**, 95-103.

Giulian, D. & Baker, T.J. (1986) Characterization of ameboid microglia isolated from developing mammalian brain. *The Journal of Neuroscience*, **6**, 2163-2178.

Glaum, S.R. & Miller, R.J. (1993) Zinc protoporphyrin-1X blocks the effects of metabotropic glutamate receptor activation in the rat nucleus tractus solitarius. *Molecular Pharmacology*, **43**, 965-969.

Globus, M.Y-T., Busto, R., Dietrich, W.D., Martinez, E., Valdes, I. & Ginsberg, M.D. (1988) Effect of ischemia on the *in vivo* release of striatal dopamine, glutamate and γ-amino butyric acid studied by intracerebral microdialysis. *Journal of Neurochemistry*, **51**, 1455-1464.

Goldberg, M.P., Strasser, U. & Dugan, L.L. (1997) Techniques for assessing neuroprotective drugs *in vitro*. In *International Review of Neurobiology*, vol. 42, ed. Bradley, R.J., Harris, R.A. & Jenner, P. pp 69-93. London: Academic Press.

Gomeza, J., Joly, C., Kuhn, R., Knöpfel, T., Bockaert, J. & Pin, J-P. (1996) The second intracellular loop of metabotropic glutamate receptor 1 cooperates with the other intracellular domains to control coupling to G-proteins. *Journal of Biological Chemistry*, **271**, 2199-2205.

Gotti, B., Duverger, D., Bertin, J., Carter, C., Dupont, R., Frost, J., Gaudilliere, B., MacKenzie, E.T. , Rousseau, J., Scatton, B. & Wick, A. (1988) Ifenprodil and SL82.0715 as cerebral anti-ischaemic agents. I. Evidence for efficacy in models of focal cerebral ischaemia. *Journal of Pharmacology and Experimental Therapeutics*, **247**, 1211-1221.

Greenamyre, J.T. & O'Brien, C.F. (1991) N-methyl-D-aspartate antagonists in the treatment of Parkinson's disease. *Archives of Neurology*, **48**, 977-981.

Greenamyre, J.T., Eller, R.V., Zhang, Z., Ovadia, A., Kurlan, R. & Gash, D.M. (1994) Antiparkinsonian effects of remacemide hydrochloride, a glutamate antagonist, in rodent and primate models of Parkinson's disease. *Annals of Neurology*, **35**, 639-661.

Gunter, T. & Pfeiffer, D. (1990) Mechanisms by which mitochondria transport calcium. *American Journal of Physiology*, **258**, C755-C786

Gwag, B.J., Koh, J.Y., Demaro, J.A., Ying, H.S., Jacquin, M. & Choi, D.W. (1997) Slowly triggered excitotoxicity occurs by necrosis in cortical cultures. *Neuroscience*, **77**, 393-401.

Haldemann, S. & McLennan, H. (1972) The antagonistic action of glutamic acid diethylester towards amino acid-induced and synaptic excitations of central neurones. *Brain Research*, **45**, 393-400.

Hall, E.D., McCall, J.M. & Means, E.D. (1994) Therapeutic potential of the lazaroids (21-aminosteroids) in acute central nervous system trauma, ischaemia and subarachnoid hemorrhage. *Advances in Pharmacology*, **28**, 221-267.

Hargreaves, R.J., Rigby, M., Smith, D., Hill, R.G. & Iversen, L.L. (1993) Competitive as well as uncompetitive N-methyl-D-aspartate receptor antagonists affect cortical neuronal morphology and cerebral glucose metabolism. *Neurochemical Research*, **18**, 1263-1269.

Hartveit, E., Brandstätter, J.H., Enz, R. & Wässle, H. (1995) Expression of the mRNA of seven metabotropic glutamate receptors (mGluR1 to 7) in the rat retina. An *in situ* hybridization study on tissue sections and isolated cells. *European Journal of Neuroscience*, **7**, 1472-1483.

Hayashi, T. (1954) Effects of sodium glutamate on the nervous system. *Keio Journal of Medicine*, **3**, 183-192.

Hayashi, Y., Momiyama, A., Takahashi, T., Ohishi, H., Ogawa-Meguro, R., Shigemoto, R., Mizuno, N. & Nakanishi, S. (1993) Role of a metabotropic glutamate receptor in synaptic modulation in the accessory olfactory bulb. *Nature*, **366**, 687-690.

Headley, P.M. & Grillner, S. (1990) Excitatory amino acids and synaptic transmission: The evidence for a physiological function. *Trends in Pharmacological Sciences*, **11**, 205-211.

Helton, D.R., Tizzano, P., Monn, J.A., Schoepp, D.D. & Kallman, M.J. (1998a) LY354740: a metabotropic glutamate receptor agonist which ameliorates symptoms of nicotine withdrawal in rats. *Neuropharmacology*, **36**, 1511-1516.

Helton, D.R., Tizzano, J.P., Monn, J.A., Schoepp, D.D. & Kallman, M.J. (1998b) Anxiolytic and side-effect profile of LY354740: A potent, highly selective, orally active agonist for group II metabotropic glutamate receptors. *Journal of Pharmacology and Experimental Therapeutics*, **284**, 651-660.

Henley, J.M., Ambrosini, A., Rodriguez-Ithurralde, D., Sudan, H., Brackley, P., Kerry, C., Mellor, I., Abutidze, K., Usherwood, P.N. & Barnard, E.A. (1992) Purified unitary kainate/alpha-amino-3-hydroxy-5-methylisooxazole-proprionate (AMPA) and KA/AMPA/N-methyl-D-aspartate receptors with interchangeable subunits. *Proceedings of the National Academy of Sciences*, **89**, 4806-4810.

Hensley, K., Carney, J.M., Stewart, C.A., Tabatabaie, T., Pye, Q. & Floyd, R.A. (1997) Nitrone-based free radical traps as neuroprotective agents in cerebral ischaemia and other pathologies. In *International Review of Neurobiology*, ed. Bradley, R.J., Harris, R.A. & Jenner, P. Vol 40. Ch.13. pp 299-317. London: Academic Press.

Herb, A., Burnashev, N., Werner, W., Sakmann, B., Wisden, W. & Seeburg, P.H. (1992) The KA-2 subunit of excitatory amino acid receptors shows widespread expression in brain and forms ion channels with distinctly related subunits. *Neuron*, **8**, 775-785.

Herrero, I., Miras-Portugal, M.T. & Sánchez-Prieto, J. (1992) Positive feedback of glutamate exocytosis by metabotropic presynaptic receptor stimulation. *Nature*, **360**, 163-166.

Holler, T., Cappel, E., Klein, J. & Loffelholz, K. (1993) Glutamate activates phospholipase D in hippocampal slices of newborn and adult rats. *Journal of Neurochemistry*, **61**, 1569-1572.

Hollman, M., O'Shea-Greenfield, A., Rogers, S.W. & Heinemann, S.F. (1989) Cloning by functional expression of a member of the glutamate family. *Nature*, **342**, 643-648.

Hollman, M., Hartley, M. & Heinemann, S.F. (1991) Ca^{2+} permeability of KA-AMPA gated glutamate receptor channels depends on subunit composition. *Science*, **252**, 851-853.

Hollman, M., Maron, C. & Heinemann, S. (1994) N-glycosylation site tagging suggests a three transmembrane domain topology for the glutamate receptor GluR1. *Neuron*, **13**, 1331-1343.

Hossman, K.A. (1994) Viability thresholds and the penumbra of focal ischemia. *Annals of Neurology*, **36**, 557-565.

Houamed, K.M., Kuijper, J.L.,Gilbert, T.L., Haldeman, B.A., O'Hara, P.J., Mulvihill, E.R., Almers, W. & Hagen, F.S. (1991) Cloning, expression, and gene structure of a G protein-coupled glutamate receptor from rat brain. *Science*, **252**, 1318-1321.

Huang, Z., Huang, P.L., Ma, J., Panahian, N., Dalkara, T., Fishman, M.C. & Moskowitz, M.A. (1996) Effects of cerebral ischaemia in mice deficient in neuronal nitric oxide synthase. *Science*, **265**, 1883-1885.

Huettner, J.E. (1990) Glutamate receptor channels in rat dorsal root ganglion neurons: activation by kainate and quisqualate, and blockade of desensitization by concanavalin A. *Neuron*, **5**, 255-266.

Hume, R.I. Dingledine, R. & Heinemann, S.F. (1991) Identification of a site in glutamate receptor subunits that controls calcium permeability. *Science*, **253**, 1028-1031.

Hunter, A.J., Green, A.R. & Cross, A.J. (1995) Animal models of acute ischaemic stroke: can they predict clinically successful neuroprotective drugs? *Trends in Pharmacological Sciences*, **16**, 123-128.

Hunter, A.J., Mackay, K.B. & Rogers, D.C. (1998) To what extent have functional studies of ischaemia in animals been useful in the assessment of potential neuroprotective agents? *Trends in Pharmacological Sciences*, **19**, 59-66.

Iadorola, M.J., Nicoletti, F., Naranjo, J.R., Putnam, F. & Costa, E. (1986) Kindling enhances the stimulation of inositol phospholipid hydrolysis elicited by ibotenic acid in rat hippocampal slices. *Brain Research*, **374**,174-178.

Ikeda, S.R., Lovinger, D.M., McCool, B.A. & Lewis, D.L. (1995) Heterologous expression of metabotropic glutamate receptors in adult rat sympathetic neurons: subtype-specific coupling to ion channels. *Neuron*, **14**, 1029-1038.

Ishimaru, H., Kamboj, R., Ambrosini, A., Henley, J.M., Soloviev, M.M., Sudan, H., Rossier, J., Abutidze, K., Rampersad, V., Usherwood, P.N., Bateson, A.N. & Barnard, E.A. (1996) A unitary non-NMDA receptor short subunit from *Xenopus*: DNA cloning and expression. *Receptor Channels*, **4**, 31-49.

Ito, I., Kohda, A., Tanabe, S., Hirose, E., Hayashi, M., Mitsunaga, S. & Sugiyama, H. (1992) 3,5-dihydroxyphenylglycine: a potent agonist of metabotropic glutamate receptors. *NeuroReport*, **3**, 1013-1016.

Iversen, L., Mulvihill, E., Haldeman, B., Diemer, N.H., Kaiser, F., Sheardown, M. & Kristensen, P. (1994) Changes in metabotropic glutamate receptor mRNA levels following

global ischemia: Increase of a putative presynaptic subtype (mGluR4) in highly vulnerable rat brain areas. *Journal of Neurochemistry*, **63**, 625-633.

Jackson, P. & Blythe, D. (1993) Immunolabelling techniques for light microscopy. In: *Immunocytochemistry*, ed. Beesley, J.E. Ch.3. pp 15-41. Oxford: IRL Press at Oxford University Press.

Jane, D.E., Jones, P.L., Pook, P.C., Tse, H.W. & Watkins, J.C. (1994) Actions of two new subtype-selective metabotropic glutamate receptor antagonists in the neonatal rat spinal cord. *British Journal of Pharmacology*, **112**, 809-816.

Jane, D.E., Thomas, N.K., Tse, H.W. & Watkins, J.C. (1996) Potent antagonists at L-AP4 and (1S,3S)-ACPD-sensitive presynaptic metabotropic glutamate receptors in neonatal rat spinal cord. *Neuropharmacology*, **35**, 1029-1035.

Jones, K.A. & Baughman, R.W. (1991) Both NMDA and non-NMDA subtypes of glutamate receptors are concentrated at synapses on cerebral cortical neurons in culture. *Neuron*, **7**, 593-603.

Kaba, H, Hayashi, Y., Higuchi, T. & Nakanishi, S. (1994) Induction of an olfactory memory by the activation of a metabotropic glutamate receptor. *Science*, **265**, 262-264.

Kaku, D.A., Goldberg, M.P. & Choi, D.W. (1991) Antagonism of non-NMDA receptors augment the neuroprotective effect of NMDA receptor blockade in cortical cultures subjected to prolonged deprivation of oxygen and glucose. *Brain Research*, **554**, 344-347.

Kalaria, R.N., Bhatti, S.U., Palatinsky, E.A., Pennington, D.H., Shelton, E.R., Chan, H.W., Perry, G. & Lust, W.D. (1993) Accumulation of the β amyloid precursor protein at sites of ischemic injury in rat brain. *NeuroReport*, **4**, 211-214.

Kaupmann, K., Huggel, K., Heid, J., Flor, P.J., Bischoff, S., Mickel, S.J., McMaster, G., Angst, C., Bittiger, H., Froestl, W. & Bettler, B. (1997) Expression cloning of GABA(B) receptor uncovers similarity to metabotropic glutamate receptors. *Nature*, **386**, 239-246.

Kawabata, S., Tsutsumi, R., Kohara, A., Yamaguchi, T., Nakanishi, S. & Okada, M. (1996) Control of calcium oscillations by phosphorylation of metabotropic glutamate receptors. *Nature*, **383**, 89-92.

Keinänen, K., Wisden, W., Sommer, B., Werner, P., Herb, A., Verdoorn, T.A., Sakmann, B. & Seeburg, P.H. (1990) A family of AMPA-selective glutamate receptors. *Science*, **249**, 556-560.

Kelly, P.A.T., Graham, D.I. & McCulloch, J. (1982) Specific alterations in local cerebral glucose utilisation following striatal lesions. *Brain Research*, **233**, 157-172.

Kelly, P.A.T. & McCulloch, J. (1982) The effects of the putative GABAergic agonists, muscimol and THIP upon local cerebral glucose utilisations. *Journal of Neurochemistry*, **39**, 613-624.

Kelly, P.A.T. & McCulloch, J. (1984) Extrastriatal circuits activated by intrastriatal muscimol: a [^{14}C]2-deoxyglucose investigation. *Brain Research*, **292**, 357-366.

Kelly, P.A.T., Ford, I. & McCulloch, J. (1986) The effect of diazepam upon local cerebral glucose use in the conscious rat. *Neuroscience*, **19**, 257-265.

Kemp, J.A., Foster, A.C. & Wong, E.H.F. (1987) Non competitive antagonists of excitatory amino acid receptors. *Trends in Neurosciences*, **10**, 294-298.

Kennedy, M. (1989) Regulation of neuronal function by calcium. *Trends in Neuroscience*, **12**, 417-424.

Kilbride, J., Huang, L.Q., Rowan, M.J. & Anwyl, R. (1998) Presynaptic inhibitory action of the group II metabotropic glutamate receptor agonists, LY354740 and DCG-IV. *European Journal of Pharmacology*, **356**, 149-157.

Kingston, A.E., Ornstein, P.L., Wright, R.A., Johnson, B.G., Mayne, N.G., Burnett, J.P., Belagaje, R., Wu, S. & Schoepp, D.D (1998) LY341495 is a nanomolar potent and selective antagonist of group II metabotropic glutamate receptors. *Neuropharmacology*, **37**, 1-12.

Kingston, A.E., O'Neill, M.J., Lam, A., Bales, K.R., Monn, J.A. & Schoepp, D.D (in press) Neuroprotective actions of novel and highly potent group II mGluR agonists: LY354740, LY379268 and LY389795 in cortical neurons. *European Journal of Pharmacology*.

Kinoshita, A., Ohishi, H., Neki, A., Nomura, S., Shigemoto, R., Takada, M., Nakanishi, S. & Mizuno, N. (1996a) Presynaptic localization of a metabotropic glutamate receptor, mGluR8, in the rhinencephalic areas: a light and electron microscope study in the rat. *Neuroscience Letters*, **207**, 61-64.

Kinoshita, A., Ohishi, H., Nomura, S., Shigemoto, R., Nakanishi, S. & Mizuno, N. (1996b) Presynaptic localization of a metabotropic glutamate receptor, mGluR4a, in the cerebellar cortex: a light and electron microscope study in the rat. *Neuroscience Letters*, **207**, 199-202.

Knöpfel, T., Lukic, S., Leonard, T., Flor, P.J., Kuhn, R. & Gasparini, F. (1995) Pharmacological characterization of MCCG and MAP4 at the mGluR$_{1b}$, mGluR$_2$, and mGluR$_{4a}$ human metabotropic receptor subtypes. *Neuropharmacology*, **34**, 1099-1102.

Koerner, J.F. & Johnson, R.L. (1992) L-AP4 receptor ligands. *In Excitatory amino acid receptors; Design of agonists and antagonists*, ed. Krogsgaard-Larsen, P. & Hansen, J.J. pp 308-330. West Sussex: Ellis Horwood Limited.

Koh, J. & Choi, D.W. (1988) Vulnerability of cultured cortical neurones to damage by excitotoxins: differential susceptibility of neurones containing NADPH-diaphorase. *Journal of Neuroscience*, **8**, 2153-2163.

Koh, J-Y., Palmer, E. & Cotman, C.W. (1991) Activation of the metabotropic glutamate receptor attenuates N-methyl-D-aspartate neurotoxicity in cortical cultures. *Proceedings of the National Academy of Sciences USA*, **88**, 9431-9435.

Koh, J-Y., Wie, M.B., Gwag, B.J., Sensi, S.L., Canzoniero, L.M.T. & Choi, D.W. (1994) Staurosporine induces apoptosis in cultured cortical neurons. *Society for Neuroscience Abstracts*, **20**, 113.11.

Koh, J-Y., Wie, M.B., Gwag, B.J., Sensi, S.L., Canzoniero, L.M.T., Demaro, J., Csernansky, C. & Choi, D.W. (1995) Staurosporine-induced neuronal apoptosis. *Experimental Neurology*, **135**, 153-159.

Köhler, M., Burnashev, N., Sakmann, B. & Seeburg, P.H. (1993) Determinants of Ca^{2+} permeability in both TM1 and TM2 of high affinity kainate receptor channels: diversity by RNA editing. *Neuron*, **10**, 491-500.

Koistinaho, J. & Hökfelt, T. (1997) Altered gene expression in brain ischemia. *NeuroReport*, **8**, 1-8.

König, J.F.R. & Klippel, R.A. (1963) In *The rat brain: a stereotaxic atlas of the forebrain and lower parts of the brain stem*. New York: Krieger.

Koppenol, W.H., Moreno, J.J., Pryor, W.A., Ischiropoulos, H. & Beckman, J.S. (1992) Peroxynitrite, a cloaked oxidant formed by nitric oxide and superoxide. *Chemical Research in Toxicology*, **5**, 834-842.

Kristián, T. & Siesjö, B.K. (1998) Calcium in ischemic cell death. *Stroke*, **29**, 705-718.

Krogsgaard-Larsen, P, Honoré, T., Hansen, J.J., Curtis, D.R. & Lodge, D. (1980) New class of glutamate agonist structurally related to ibotenic acid. *Nature*, **284**, 64-66.

Kulagowski, J.J., Baker, J.R., Curtis, N.R., Leeson, P.D., Mawer, I.M., Moseley, A.M. Ridgill, M.P., Rowley, M., Stansfield, I., Foster, A.C. Grimwood, S., Hill, R.G., Kemp, J.A., Marshall, G.R., Saywell, K.L. & Tricklebank, M.D. (1994) 3'-(arylmethyl)- and 3'(aryloxy)-3-phenyl-4-hydroxyquinolin-2(1H)-ones: orally active antagonists of the glycine site on the NMDA receptor. *Journal of Medicinal Chemistry*, **37**, 1402-1405.

Kurumaji, A. & McCulloch, J. (1990) Effects of unilateral intrahippocampal injection of MK-801 upon local cerebral glucose utilisation in conscious rats. *Brain Research*, **518**, 342-346.

Kuryatov, A., Laube, B., Betz, H. & Kuhse, J. (1994) Mutational analysis of the glycine-binding site of the NMDA receptor: Structural similarity with bacterial amino acid-binding proteins. *Neuron*, **12**, 1291-1300.

Kwon, N.S., Stuehr, D.J. & Nathan, C.F. (1991) Inhibition of tumour cell ribonucleotide reductase by macrophage-derived nitric oxide. *Journal of Experimental Medicine*, **174**, 761-767.

Laurie, D.J., Boddeke, H.W.G.M., Hiltscher, R. & Sommer, B. (1996) $HmGlu_{1d}$, a novel splice variant of the human type I metabotropic glutamate receptor. *European Journal of Pharmacology*, **296**, R1-R3.

Lee, R.K.K., Wurtman, R.J., Cox, A.J. & Nitsch, R.M. (1995) Amyloid precursor protein processing is stimulated by metabotropic glutamate receptors. *Proceedings of the National Academy of Sciences USA*, **92**, 8083-8087.

Lerma, J., Paternain, A.V., Naranjo, J.R. & Mellström, B. (1993) Functional kainate selective glutamate receptors in cultured hippocampal neurons. *Proceedings of the National Academy of Sciences USA*, **90**, 11688-11692.

Lerma, J. (1997) Kainate reveals its targets. *Neuron*, **19**, 1155-1158.

Lester, R.A.J., Clements, J.D., Westbrook, G.L. & Jahr, C.E. (1990) Channel kinetics determine the time course of NMDA receptor-mediated synaptic currents. *Nature*, **346**, 565-567.

Levison, S.W. & McCarthy, K.D. (1991) Astroglia in culture. In *Culturing Nerve Cells*, ed. Banker, G. & Goslin, K. pp 309-336. Cambridge, Massachusetts: The MIT Press.

Levy, D.I., Sucher, N.J. & Lipton, S.A. (1990) Redox modulation of NMDA receptor-mediated toxicity in mammalian central neurons. *Neuroscience Letters*, **110**, 291-296.

Li, H. & Buchan, A.M. (1993) Treatment with an AMPA antagonist 12 hours following severe normothermic forebrain ischemia prevents CA1 neuronal injury. *Journal of Cerebral Blood Flow and Metabolism*, **13**, 933-939.

Lincoln, J., Coopersmith, R., Harris, E.W., Cotman, C.W. & Leon, M. (1988) NMDA receptor activation and early olfactory learning. *Developmental Brain Research*, **39**, 309-312.

Linden, D.J. (1994) Long term synaptic depression in the mammalian brain. *Neuron*, **12**, 457-472.

Linnik, M.D., Zobrist, R.H. & Hatfield, M.D. (1993) Evidence supporting a role for programmed cell death in focal cerebral ischemia in rats. *Stroke*, **24**, 2002-2009.

Linnik, M.D., Zahos, P., Geschwind, M.D. & Federoff, H.J. (1995) Expression of bcl-2 from a defective herpes simplex virus-1 vector limits neuronal death in focal cerebral ischemia. *Stroke*, **26**, 1670-1674.

Linnik, M.D. (1996) Role of apoptosis in acute neurodegenerative disorders. *Restorative Neurology and Neuroscience*, **9**, 219-225.

Lipton, S.A., Choi, Y.B., Lei, S.Z., Chen, H.V., Sucher, N.J., Loscalzo, J., Singel, D.J. & Stamler, J.S. (1993) A redox-based mechanism for the neuroprotective and neurodestructive effects of nitric oxide and related nitroso-compounds. *Nature*, **364**, 626-632.

Lisman, J.E., Fellous, J-M. & Wang, X-J. (1998) A role for NMDA-receptor channels in working memory. *Nature Neuroscience*, **1**, 273-275.

Lister, R.G. (1987) The use of a plus-maze to measure anxiety in the mouse. *Psychopharmacology*, **92**, 180-185.

Little, Z., Grover, L.G. & Teyler, T.J. (1995) Metabotropic glutamate receptor antagonist, (R,S)-α-methyl-4-carboxyphenylglycine, blocks two distinct forms of long-term potentiation in area CA1 of rat hippocampus. *Neuroscience Letters*, **201**, 73-76.

Liu, T.H., Beckman, J.S., Freeman, B.A., Hogan, E.L. & Hsu, C.Y. (1989) Polyethylene glycol-conjugated superoxide dismutase and catalase reduce ischaemic brain injury. *American Journal of Physiology*, **256**, H589-H593.

Liu, T., McDonnell, P.C., Young, P.R., White, R.F., Siren, A.L., Hallenbeck, J.M., Barone, F.C. & Feurestein, G.Z. (1993) Interleukin-1 beta mRNA expression in ischaemic rat cortex. *Stroke*, **24**, 1746-1750.

Livsey, C.T. & Vicini, S. (1992) Slower spontaneous excitatory postsynaptic currents in spiny versus aspiny hilar neurons. *Neuron*, **8**, 745-755.

Loddick, S.A. & Rothwell, N.J. (1996) Neuroprotective effects of human recombinant interleukin 1 ra in focal cerebral ischaemia in the rat. *Journal of Cerebral Blood Flow and Metabolism*, **16**, 932-940.

Lomeli, H., Wisden, W., Kohler, M., Keinanen, K., Sommer, B. & Seeburg, P.H. (1992) High-affinity kainate and domoate receptors in rat brain. *FEBS Letters*, **307**, 139-143.

Lomeli, H., Sprengel, R., Laurie, D.J., Kohr, G., Herb, A., Seeburg, P.H. & Wisden, W. (1993) The rat delta-1 and delta-2 subunits extend the excitatory amino acid receptor family. *FEBS Letters*, **315**, 318-322.

Lomeli, H., Mosbacher, J., Melcher, T., Höger, T., Gerger, J.R., Kuner, P., Monyer, H., Higuchi, M., Nach, A. & Seeburg, P.H. (1994) Control of kinetic properties of AMPA receptor channels by nuclear RNA editing. *Science*, **266**, 1709-1713.

Lothman, E.W., Hatlelid, J.M. & Zorumski, C.F. (1985) Functional mapping of limbic seizures originating in the hippocampus: a combined 2-deoxyglucose and electrophysiologic study. *Brain Research*, **360**, 92-100.

Lovinger, D.M. & McCool, B.A. (1995) Metabotropic glutamate receptor-mediated presynaptic depression at corticostriatal synapses involves mGluR2 or 3. *Journal of Neurophysiology*, **73**, 1076-1083.

Lu, Y-M., Jia, Z., Janus, C., Henderson, J.T., Gerlai, R., Wojtowicz, J.M. & Roder, J.C. (1997) Mice lacking metabotropic glutamate receptor 5 show impaired learning and reduced CA1 long-term potentiation (LTP) but normal CA3 LTP. *Journal of Neuroscience*, **17**, 5196-5205.

Lucas, D.R. & Newhouse, J.P. (1957) The toxic effect of sodium L-glutamate on the inner layers of the retina. *AMA Archives of Ophthalmology*, **58**, 193-201.

Mackay, K.B. & McCulloch, J. (1994) Distribution of effects of the κ-opioid agonist CI-977 on cerebral glucose utilization in rat brain. *Brain Research*, **642**, 160-168.

Mackler, S.A. & Eberwine, J.H. (1993) Diversity of glutamate receptor subunit mRNA expression within live hippocampal CA1 neurons. *Molecular Pharmacology*, **44**, 308-315.

MacLean, M.R., McCulloch, K.M. & Baird, M. (1994) Pulmonary arterial ET_A- and ET_B-receptor-mediated vasoconstriction in rat pulmonary arteries and arterioles. *Journal of Cardiovascular Pharmacology*, **26**, 822-830.

MacManus, J.P. & Linnik, M.D. (1997) Gene expression induced by cerebral ischemia: an apoptotic perspective. *Journal of Cerebral Blood Flow and Metabolism*, **17**, 815-832.

Macrae, I.M. (1992) New models of focal cerebral ischaemia. *British Journal of Clinical Pharmacology*, **34**, 302-308.

Maiese, K., Greenberg, R., Boccone, L & Swiriduk, M. (1995) Activation of the metabotropic glutamate receptor is neuroprotective during nitric oxide toxicity in primary hippocampal neurons of rats. *Neuroscience Letters*, **194**, 173-176

Mainen, Z.F., Jia, Z., Roder, J. & Malinow, R. (1998) Use-dependent AMPA receptor block in mice lacking GluR2 suggests postsynaptic site for LTP expression. *Nature Neuroscience*, **1**, 579-586.

Manahan-Vaughan, D., Reiser, M., Pin, J-P., Wilsch, V., Reymann, K.G. & Riedel, G. (1996) Physiological and pharmacological profile of trans-azetidine 2,4-dicarboxylic acid: metabotropic glutamate receptor agonism and effects on long-term potentiation. *Neuroscience*, **72**, 999-1008.

Manahan-Vaughan, D. & Reymann, K.G. (1996) Metabotropic glutamate receptor subtype agonists facilitate LTP within a distinct time window in the dentate gyrus *in vivo*. *Neuroscience*, **74**, 723-731.

Manahan-Vaughan, D., Braunewell, K-H. & Reymann, K.G. (1998) Subtype-specific involvement of metabotropic glutamate receptors in two forms of long-term potentiation in the dentate gyrus of freely moving rats. *Neuroscience*, **86**, 709-721.

Manzoni, O.J., Weisskop, M.G. & Nicoll, R.A. (1994) MCPG antagonizes metabotropic glutamate receptors but not long-term potentiation in the hippocampus. *European Journal of Neuroscience*, **6**, 1050-1054.

Manzoni, O.J., Castillo, P.E. & Nicoll, R.A. (1995) Pharmacology of metabotropic glutamate receptors at the mossy fiber synapses of the guinea pig hippocampus. *Neuropharmacology*, **34**, 965-971.

Manzoni, O. & Bockaert, J. (1995) Metabotropic glutamate receptors inhibiting excitatory synapses in the CA1 area of rat hippocampus. *European Journal of Neuroscience*, **7**, 2518-2523.

Maragos, W.F., Chu, D.C.M., Greenamyre, J.T., Penney, J.B. & Young, A.B. (1986) High correlation between localization of [^{3}H]TCP binding and NMDA receptors. *European Journal of Pharmacology*, **123**, 173-174.

Martin, L.J., Blackstone, C.D., Levey, A.I., Huganir, R.L. & Price, D.L. (1993) AMPA glutamate receptor subunits are differentially distributed in rat brain. *Neuroscience*, **53**, 327-358.

Martinou, J-C., Dubois-Dauphin, M., Staple, J.K., Rodriguez, I., Frankowski, H., Missotten, M., Albertini, P., Talabot, D., Catsicas, S., Pietra, C. & Huarte, J. (1994) Overexpression of BCL-2 in transgenic mice protects neurons from naturally occurring cell death and experimental ischemia. *Neuron*, **13**, 1017-1030.

Martins, E., Inamura, K., Themner, K., Malmqvist, K.G. & Siesjö, B.K. (1988) Accumulation of calcium and loss of potassium in the hippocampus following transient cerebral ischemia: a proton microprobe study. *Journal of Cerebral Blood Flow and Metabolism*, **8**, 531-538.

Masu, M., Tanabe, Y., Tsuchida, K., Shigemoto, R. & Nakanishi, S. (1991) Sequence and expression of a metabotropic glutamate receptor. *Nature*, **349**, 760-765.

McAuley, M.A. (1995) Rodent models of focal ischemia. *Cerebrovascular and Brain Metabolism Reviews*, 7, 153-180.

McBain, C.J., DiChiara, T.J. & Kauer, J.A. (1994) Activation of metabotropic glutamate receptors differentially affects two classes of hippocampal interneurons and potentiates excitatory synaptic transmission. *Journal of Neuroscience*, 14, 4433-4445.

McCarthy, K.D. & de Vellis, J (1980) Preparation of separate astroglial and oligodendroglial cultures from rat cerebral tissue. *Journal of Cell Biology*, 85, 890-902.

McCulloch, J., Savaki, H.E., McCulloch, M.C. & Sokoloff, L. (1980) Retina-dependent activation by apomorphine of metabolic activity in the superficial layer of the superior colliculus. *Science*, 207, 313-315.

McCulloch, J. (1982) Mapping functional alterations in the CNS with [^{14}C] deoxyglucose. In *Handbook of Psychopharmacology*, Vol. 15, ed. Iversen, L.L., Iversen, S.D. & Snyder, S.H. pp 331-410. New York: Plenum.

McCulloch, J. & Iversen, L.L. (1991) Autoradiographic assessment of the effects of N-methyl-D-aspartate (NMDA) receptor antagonists *in vivo*. *Neurochemistry Research*, 16, 897-916.

McDonald, J.W. & Schoepp, D.D. (1992) The metabotropic excitatory amino acid receptor agonist 1S,3R-ACPD selectively potentiates N-methyl-D-aspartate-induced brain injury. *European Journal of Pharmacology*, 215, 353-354.

McHugh, T.J., Blum, K.I., Tsien, J.Z., Tonegawa, S. & Wilson, M.A. (1996) Impaired hippocampal representation of space in CA1-specific NMDAR1 knockout mice. *Cell*, 87, 1339-1349.

McNeill, H., Williams, C., Guan, J., Dragunow, M., Lawlor, P., Sirimanne, E., Nikolics, K. & Gluckman, P. (1994) Neuronal rescue with transforming growth factor beta 1 after hypoxic-ischaemic brain injury. *NeuroReport*, 5, 901-904.

Meibach, R.C., Glick, S.D., Cox, R.L. & Maayani, S. (1979) Localization of phencyclidine induced changes in brain energy metabolism. *Nature*, 282, 625-626.

Meldrum, B. & Garthwaite, J. (1990) Excitatory amino acid neurotoxicity and neurodegenerative disease. *Trends in Pharmacological Sciences*, 11, 79-87.

Minakami, R., Katsuki, F., Yamamoto, T., Nakamura, K. & Sugiyama, H. (1994) Molecular cloning and the functional expression of two isoforms of human metabotropic glutamate receptor subtype 5. *Biochemical and Biophysical Research communications*, 199, 1136-1143.

Mitani, A. & Kataoka, K. (1991) Critical levels of extracellular glutamate mediating gerbil hippocampal delayed neuronal death during hypothermia: Brain microdialysis study. *Neuroscience*, 42, 661-670.

Miyamoto, M., Ishida, M. & Shinozaki, H. (1997) Anticonvulsive and neuroprotective actions of a potent agonist (DCG-IV) for group II metabotropic glutamate receptors against intraventricular kainate in the rat. *Neuroscience*, 77, 131-140.

Moghaddam, B. & Adams, B.W. (1998) Reversal of phencyclidine effects by a group II metabotropic glutamate receptor agonist in rats. *Science*, **281**, 1349-1352.

Mohr, J.P., Gautier, J.C., Hier, D. & Stein, R.W. (1986) Middle cerebral artery. In *Stroke: Pathophysiology, Diagnosis and Management*, ed. Barnett, H.J.M., Stein, B.M., Mohr, J.P. & Yatsu, F.M. Vol 1, pp 377-450. New York: Churchill Livingstone.

Monaghan, D.T. & Cotman, C.W. (1982) Distribution of ^{3}H-kainic acid binding sites in rat CNS as determined by autoradiography. *Brain Research*, **252**, 91-100.

Monaghan, D.T., Yao, D. & Cotman, C.W. (1984) Distribution of ^{3}H-AMPA binding sites in rat brain as determined by quantitative autoradiography. *Brain Research*, **324**, 160-164.

Monaghan, D.T. & Cotman, C.W. (1985) Distribution of N-methyl-D-aspartate-sensitive L-[^{3}H]glutamate-binding sites in rat brain. *Journal of Neuroscience*, **5**, 2909-2919.

Monn, J.A., Valli, M.J., Johnson, B.G., Salhoff, C.R., Wright, R.A., Howe, T., Bond, A., Lodge, D., Spangle, L.A., Paschal, J.W., Campbell, J.B., Griffey, K., Tizzano, J.P. & Schoepp, D.D. (1996) Synthesis of the four isomers of 4-aminopyrrolidine-2, 4-dicarboxylate: identification of a potent, highly selective, and systemically-active agonist for metabotropic glutamate receptors negatively coupled to adenylate cyclase. *Journal of Medicinal Chemistry*, **39**, 2990-3000.

Monn, J.A., Valli, M.J., Massey, S.M., Wright, R.A., Salhoff, C.R., Johnson, B.G., Howe, T., Alt, C.A., Rhodes, G.A., Robey, R.L., Griffey, K.R., Tizzano, J.P., Kallman, M.J., Helton, D.R. & Schoepp, D.D. (1997) Design, synthesis and pharmacological characterization of (+)-2-aminobicyclo[3.1.0]hexane-2,6-dicarboxylic acid (LY354740): A potent, selective, and orally active group 2 metabotropic glutamate receptor agonist possessing anticonvulsant and anxiolytic properties. *Journal of Medicinal Chemistry*, **40**, 528-537.

Monn, J.A., Valli, M.J., Massey, S.M., Hansen, M.M., Kress, T.J., Wepsiec, J.P., Harknes, A.R., Grutsch Jr, J.L., Wright, R.A., Johnson, B.G., Andis, S.L., Kingston, A., Tomlinson, R., Lewis, R., Griffey, K.R., Tizzano, J.P. & Schoepp, D.D. (in press) Synthesis, pharmacological characterization and molecular modeling of heterobicylic amino acids related to LY354740: Identification of LY379268 and LY389795: Two potent, selective and systemically active agonists for group II metabotropic glutamate receptors. *Journal of Medicinal Chemistry*.

Monyer, H., Seeburg, P.H. & Wisden, W. (1991) Glutamate-operated channels-developmentally early and mature forms arise by alternative splicing. *Neuron*, **6**, 799-810/

Monyer, H., Sprengel, R., Schoepfer, R., Herb, A., Higuchi, M., Lomeli, H., Burnashev, N., Sakmann, B. & Seeburg, P.H. (1992) Heteromeric NMDA receptors: molecular and functional distinction of subtypes. *Science*, **256**, 1217-1221.

Monyer, H., Burnashev, N., Laurie, D.J., Sakmann, B. & Seeburg, P.H. (1994) Developmental and regional expression in the rat brain and functional properties of four NMDA receptors. *Neuron*, **12**, 529-540.

Moriyoshi, K., Masu, M., Ishii, T., Shigemoto, R., Mizuno, N. & Nakanishi, S. (1991) Molecular cloning and characterization of the rat NMDA receptor. *Nature*, **354**, 31-37.

Morris, R.G.M. (1981) Spatial localisation does not depend on the presence of local cues. *Learning and Motivation*, **12**, 239-260.

Morris, R.G.M., Anderson, E., Lynch, G.S. & Baudry, M. (1986) Selective impairment of learning and blockade of long-term potentiation by an N-methyl-D-aspartate receptor antagonist, AP5. *Nature*, **319**, 774-776.

Mosbacher, J., Schoepfer, R., Monyer, H., Burnashev, N., Seeburg, P.H. & Ruppersberg, J.P. (1994) A molecular determinant for submillisecond desensitization in glutamate receptors. *Science*, **266**, 1059-1062.

Moser, M.B., Moser, E.I., Forrest, E., Andersen, P. & Morris, R.G.M. (1995) Spatial-learning with a minislab in the dorsal hippocampus. *Proceedings of the National Academy of Sciences USA*, **92**, 9697-9701.

Mosinger, J.L., Price, M.T., Bai, H.Y., Xiao, H., Wozniak, D.F. & Olney, J.W. (1991) Blockade of both NMDA and non-NMDA receptors is required for optimal protection against ischemic neuronal degeneration in the *in vivo* adult mammalian retina. *Experimental Neurology*, **113**, 10-17.

Muir, K.W. & Lees, K.R. (1995) Clinical experience with excitatory amino acid antagonist drugs. *Stroke*, **26**, 503-513.

Mukhin, A., Fan, L. & Faden, A.I. (1996) Activation of metabotropic glutamate receptor subtype mGluR1 contributes to post-traumatic neuronal injury. *Journal of Neuroscience*, **16**, 6012-6020.

Müller, T., Möller, T., Berger, T., Schnitzer, J. & Kettenmann, H. (1992) Calcium entry through kainate receptors and resulting potassium-channel blockade in Bergmann glial cells. *Science*, **256**, 1563-1566.

Nakajima, Y., Iwakabe, H., Akazawa, C., Nawa, H., Shigemoto, R., Mizuno, N. & Nakanishi, S. (1993) Molecular characterization of a novel retinal metabotropic glutamate receptor mGluR6 with a high agonist selectivity for L-2-amino-4-phosphonobutyrate. *Journal of Biological Chemistry*, **268**, 11868-11873.

Nakanishi, N., Schneider, N.A. & Axel, R. (1990) A family of glutamate receptor genes: Evidence for the formation of heteromultimeric receptors with distinct channel properties. *Neuron*, **5**, 569-581.

Nakanishi, S. (1992) Molecular diversity of glutamate receptors and implications for brain function. *Science*, **258**, 597-603.

Nakanishi, S. (1994) Metabotropic glutamate receptors: synaptic transmission, modulation and plasticity. *Neuron*, **13**, 1031-1037.

Nakanishi, S., Nakajima, Y., Masu, M., Ueda, Y., Nakahara, K., Watanabe, D., Yamaguchi, S., Kawabata, S. & Okada, M. (1998) Glutamate receptors: brain function and signal transduction. *Brain Research Reviews*, **26**, 230-235.

Nawy, S. & Jahr, C.E. (1990) Suppression by glutamate of cGMP-activated conductance in retinal bipolar cells. *Nature*, **346**, 269-271.

Nehls, D.G., Kurumaji, A., Park, C.K. & McCulloch, J. (1988) Differential effects of competitive and non-competitive N-methyl-D-aspartate antagonists on glucose use in the limbic system. *Neuroscience Letters*, **91**, 204-210.

Neki, A., Ohishi, H., Kaneko, T., Shigemoto, R., Nakanishi, S. & Mizuno, N. (1996a) Pre- and postsynaptic localization of a metabotropic glutamate receptor, mGluR2, in the rat brain: an immunohistochemical study with a monoclonal antibody. *Neuroscience Letters*, **202**, 197-200.

Neki, A., Ohishi, H., Kaneko, T., Shigemoto, R., Nakanishi, S. & Mizuno, N. (1996b) metabotropic glutamate receptors mGluR2 and mGluR5 are expressed in two non-overlapping populations of Golgi cells in the rat cerebellum. *Neuroscience*, **75**, 815-826.

Nelson, S.R., Howard, R.B., Cross, R.S. & Samson, F. (1980) Ketamine-induced changes in regional glucose utilization in the rat brain. *Anesthesiology*, **52**, 330-334.

Nicholls, D.G. (1985) A role for the mitochondrion in the protection of cells against calcium overload? *Progress in Brain Research*, **63**, 97-106.

Nicholson, C., Bruggencate, G.T., Steinberg, R. & Stockle, H. (1977) Calcium modulation in brain extracellular microenvironment demonstrated with non-selective micropipette. *Proceedings of the National Academy of Sciences USA*, **74**, 1287-1290.

Nicoletti, F., Wroblewski, J.T., Alho, H., Eva, C., Fadda., E. & Costa, E. (1987) Lesions of putative glutaminergic pathways potentiate the increase of inositol phospholipid hydrolysis elicited by excitatory amino acids. *Brain Research*, **436**, 103-112.

Nicoletti, F., Bruno, V., Copani, A., Casabona, G. & Knöpfel, T. (1996) Metabotropic glutamate receptors: a new target for the therapy of neurodegenerative disorders? *Trends in Neurosciences*, **19**, 267-271.

Nomura, A., Shigemoto, R., Nakamura, Y., Okamoto, N, Mizuno, N. & Nakanishi, S. (1994) Developmentally regulated postsynaptic localization of a metabotropic glutamate receptor in rat rod bipolar cells. *Cell*, **77**, 361-369.

O'Connor, J.J., Rowan, M.J. & Anwyl, R. (1995) Tetanus-induced a similar increase in the AMPA and NMDA receptor components of the excitatory postsynaptic current: investigations of the involvement of mGlu receptors. *Journal of Neuroscience*, **15**, 2013-2020.

O'Hara, P.J., Sheppard, P.O., Thögersen, H., Venezia, D., Haldeman, B.A., McGrane, V., Houamed, K.M., Thomsen, C., Gilbert, T.L. & Mulvihill, E.R. (1993) The ligand-binding domain in metabotropic glutamate receptors is related to bacterial periplasmic binding proteins. *Neuron*, **11**, 41-52.

Ohishi, H., Shigemoto, R., Nakanishi, S. & Mizuno, N. (1993a) Distribution of the messenger RNA for a metabotropic glutamate receptor, mGluR2, in the central nervous system of the rat. *Neuroscience*, **53**, 1009-1018.

Ohishi, H., Shigemoto, R., Nakanishi, S. & Mizuno, N. (1993b) Distribution of the mRNA for a metabotropic glutamate receptor (mGluR3) in the rat brain: an *in situ* hybridization study. *Journal of Comparative Neurology*, **335**, 252-266.

Ohishi, H., Ogawa-Meguro, R., Shigemoto, R., Kaneko, T., Nakanishi, S. & Mizuno, N. (1994) Immunohistochemical location of metabotropic glutamate receptors mGluR2 and mGluR3 in rat cerebellar cortex. *Neuron*, **13**, 55-66.

Ohishi, H., Akazawa, C., Shigemoto, R., Nakanishi, S. & Mizuno, N. (1995) Distributions of the mRNAs for L-2-amino-4-phosphonobutyrate-sensitive metabotropic glutamate receptors, mGluR4 and mGluR7, in the rat brain. *Journal of Comparative Neurology*, **360**, 555-570.

Ohno, M. & Watanabe, S. (1996) Concurrent blockade of hippocampal metabotropic glutamate and N-methyl-D-aspartate receptors disrupts working memory in the rat. *Neuroscience*, **70**, 303-311.

Okada, D. (1992) Two pathways of cyclic CMP production through glutamate receptor-mediated nitric oxide synthesis. *Journal of Neurochemistry*, **59**, 1203-1210.

Okamoto, N., Hori, S., Akazawa, C., Hayashi, Y., Shigemoto, R., Mizuno, N. & Nakanishi, S. (1994) Molecular characterization of a new metabotropic glutamate receptor mGluR7 coupled to inhibitory cyclic AMP signal transduction. *Journal of Biological Chemistry*, **269**, 1231-1236.

Olney, J.W. (1969) Brain lesions, obesity, and other disturbances in mice treated with monosodium glutamate. *Science*, **164**, 719-721.

Olney, J.W., Ho, O.L. & Rhee, V. (1971) Cytotoxic effects of acidic and sulphur containing amino acids on the infant mouse central nervous system. *Experimental Brain Research*, **14**, 61-76.

Olney, J.W., Collins, R.C. & Sloviter, R.S. (1986) Excitotoxic mechanisms of epileptic brain damage. *Advances in Neurology*, **44**, 857-877.

Opitz, T., Richter, P. & Reymann, K.G. (1994) The metabotropic glutamate receptor antagonist (+)-α-methyl-4-carboxyphenylglycine protects hippocampal CA1 neurons of the rat from *in vitro* hypoxia/hypoglycemia. *Neuropharmacology*, **33**, 715-717.

Ornstein, P.L., Arnold, M.B., Augenstein, N.K., Lodge, D., Leander, J.D. & Schoepp, D.D. (1993) (3SR,4aRS,6RS,8aRS)-6-[2-(1H-tetrazol-5-yl)ethyl]decahydroisoquinoline-3-carboxylic acid: A structurally novel, systemically active, competitive AMPA receptor antagonist. *Journal of Medicinal Chemistry*, **36**, 2046-2048.

Osborne, K.A. Shigeno, T. Balarsky, A.M. Ford, I. McCulloch, J. Teasdale G.M. & Graham, D.I. (1987) Quantitative assessment of early brain damage in a rat model of focal cerebral ischaemia. *Journal of Neurology, Neurosurgery, and Psychiatry*, **50**, 402-410.

Ozawa, S., Kamiya, H. & Tsuzuki, K. (1998) Glutamate receptors in the mammalian central nervous system. *Progress in Neurobiology*, **54**, 581-618.

Packer, M.A. & Murphy, M.P. (1995) Peroxynitrite formed by simultaneous nitric oxide and superoxide generation causes cyclosporin-A-sensitive mitochondrial calcium efflux and depolarisation. *European Journal of Biochemistry*, **234**, 231-239.

Palmer, A.J. & Lodge, D. (1993) Cyclothiazide reverses AMPA receptor antagonism of the 2,3-benzodiazepine, GYKI 53655. *European Journal of Pharmacology*, **244**, 193-194.

Palmer, E., Monaghan, D.T. & Cotman, C.W. (1989) *Trans*-ACPD, a selective agonist of the phosphoinositide-coupled excitatory amino acid receptor. *European Journal of Pharmacology*, **166**, 585-587.

Palmer, E., Nangel, T.K., Krause, J.D., Roxas, A. & Cotman, C.W. (1990) Changes in excitatory amino acid modulation of phosphoinositide metabolism during development. *Developmental Brain Research*, **51**, 132-134.

Pantoni, L., Garcia, J.H. & Gutierrez, J.A. (1996) Cerebral white matter is highly vulnerable to ischemia. *Stroke*, **27**, 1641-1647.

Papez, J.W. (1937) A proposed mechanism of emotion. *American Medical Association Archives of Neurology and Psychology*, **38**, 725-743.

Park, C.K., Nehls, D.G., Graham, D.I., Teasdale, G.M. & McCulloch, J. (1988*)* The glutamate antagonist MK-801 reduces focal ischaemic brain damage in the rat. *Annals of Neurology*, **24**, 543-551.

Park, C.K., McCulloch, J., Kang, J.K. & Choi, C.R. (1992) Efficacy of D-CPPene, a competitive N-methyl-D-aspartate antagonist in focal cerebral ischaemia in the rat. *Neuroscience Letters*, **147**, 41-44.

Partin, K.N., Patneau, D.K., Winters, C.A., Mayer, M.L. & Buonanno, A. (1993) Selective modulation of desensitization at AMPA versus kainate receptors by cyclothiazide and concanavalin A. *Neuron*, **11**, 1069-1082.

Patneau, D.K., Wright, P.W., Winters, C., Mayer, M.L. & Gallo, V. (1994) Glial cells of the oligodendrocyte lineage express both kainate- and AMPA-preferring subtypes of glutamate receptor. *Neuron*, **12**, 357-371.

Pawloski-Dahm, C. & Gordon, F.J. (1992) Evidence for a kinurenate-insensitive glutamate receptor in the nucleus tractus solitarius. *American Journal of Physiology*, **363**, 1611-1615.

Paxinos, G. & Watson, C. (1986) The rat brain in stereotaxic coordinates, 2nd edition. Sydney: Academic Press.

Pellegrini-Giampietro, D.E., Zukin, R.S., Bennett, M.V.L., Cho, S. & Pulsinelli, W.A. (1992) Switch in glutamate receptor subunit gene expression in CA1 subfield of hippocampus following global ischemia in rats. *Proceedings of the National Academy of Sciences USA*, **89**, 10499-10503.

Pellegrini-Giampietro, D.E., Gorter, J.A., Bennett, M.V.L. & Zukin, R.S. (1997) The GluR2 (GluR-B) hypothesis: Ca^{2+}-permeable AMPA receptors in neurological disorders. *Trends in Neurosciences*, **20**, 464-470.

Pellerin, L. & Magistretti, P.J. (1994) Glutamate uptake into astrocytes stimulates aerobic glycolysis: a mechanism coupling neuronal activity to glucose utilization. *Proceedings of the National Academy of Sciences USA*, 91, 10625-10629.

Pellicciari, R., Luneia, R., Costantino, G., Marinozzi, M., Natalini, B., Jakobsen, P., Kanstrup, A., Lombardi, G., Moroni, F. & Thomsen, C (1995) 1-aminoindan-1,5-dicarboxylic acid: a novel antagonist at phospholipase C-linked metabotropic glutamate receptors. *Journal of Medicinal Chemistry*, **38**, 3717-3719.

Petralia, R.S. & Wenthold, R.J. (1992) Light electron and electron immunocytochemical localization of AMPA-selective glutamate receptors in the rat brain. *Journal of Comparative Neurology*, **318**, 329-354.

Petralia, R.S., Wang, Y-X., Niedzielski, A.S. & Wenthold, R.J. (1996) The metabotropic glutamate receptors, mGluR2 and mGluR3, show unique postsynaptic, presynaptic and glial localisations. *Neuroscience*, **71**, 949-976.

Pettit, H.O., Lutz, D., Gutierrez, C. & Eveleth, D. (1994) I.c.v. infusions of ACPD$_{(1S,3R)}$ attenuate learning in a Morris water maze paradigm. *Neuroscience Letters*, **178**, 43-46.

Philips, R.G. & LeDoux, J.E. (1992) Differential contribution of amygdala and hippocampus to cued and contextual fear conditioning. *Behavioral Neuroscience*, **106**, 274-285.

Pickering, D.S., Thomsen, C., Suzdak, P.D., Fletcher, E.J., Robitaille, R., Salter, M.W., MacDonald, J.F., Huang, X.P. & Hampson, D.R. (1993) A comparison of two alternatively spliced forms of a metabotropic glutamate receptor coupled to phosphoinositide turnover. *Journal of Neurochemistry*, **61**, 85-92,

Pin, J, Weber, C., Prezeau, L, Bockaert, J. & Heinemann, S.F. (1992) Alternative splicing generates metabotropic glutamate receptors inducing different patterns of calcium release in *Xenopus* oocytes. Proceedings of the National Academy of Science USA, 89, 10331-10335.

Pin, J-P., Joly, C., Heinemann, S.F. & Bockaert, J. (1994) Domains involved in the specificity of G protein activation in phospholipase C-coupled metabotropic glutamate receptors. *EMBO Journal*, **13**, 342-348.

Pin, J-P. & Bockaert, J. (1995) Get receptive to metabotropic glutamate receptors. *Current Opinion in Neurobiology*, **5**, 342-349.

Pin, J-P. & Duvoisin, R. (1995) The metabotropic glutamate receptors: structure and functions. *Neuropharmacology*, **34**, 1-26.

Pratt, J.A. (1992) The neuroanatomical basis of anxiety. *Pharmacology & Therapeutics*, **55**, 149-181.

Pratt, J., Rataud, J., Bardot, F., Roux, M., Blanchard, J.-C., Laduron, P.M. & Stutzmann, J.-M. (1992) Neuroprotective actions of riluzole in rodent models of global and focal ischaemia. *Neuroscience Letters*, **140**, 225-230.

Prézeau, L., Gomeza, J., Ahern, S., Mary, S., Galvez, T., Bockaert, J. & Pin, J-P. (1996) Changes in the carboxyl-terminal domain of metabotropic glutamate receptor I by alternative splicing generate receptors with differing agonist-independent activity. *Molecular Pharmacology*, **49**, 422-429.

Rainbow, T.C., Wieczorek, C.M. & Halpain, S. (1984) Quantitative autoradiography of binding sites for ^{3}H-AMPA, a structural analogue of glutamic-acid. *Brain Research*, **309**, 173-177.

Rainnie, D.G., Holmes, K.H. & Shinnick-Gallagher, P. (1994) Activation of postsynaptic metabotropic glutamate receptors by trans-ACPD hyperpolarizes neurons of the basolateral amygdala. *Journal of Neuroscience*, **14**, 7208-7220.

Rami, A. & Krieglstein, J. (1993) Protective effects of calpain inhibitors against neuronal damage caused by cytotoxic hypoxia *in vitro* and *in vivo*. *Brain Research*, **609**, 67-70.

Richter, C., Gogvadze, V., Laffranchi, R., Schlapbach, R., Schweizer, M., Suter, M., Walter, P. & Yaffee, M. (1995) Oxidants in mitochondria: from physiology to diseases. *Biochimica et Biophysica Acta*, **1271**, 67-74.

Riedel, G., Wetzel, W. & Reymann, K.G. (1994) (R,S)-α-methyl-4-carboxyphenylglycine (MCPG) blocks spatial learning in rats and long-term potentiation in the dentate gyrus *in vivo*. *Neuroscience Letters*, **167**, 141-144.

Riedel, G. & Reymann, K.G. (1996) Metabotropic glutamate receptors in hippocampal long-term potentiation and learning and memory. *Acta Physiologica Scandinavica*, **157**, 1-19.

Riedel, G., Micheau, J., de Hoz, L., Roloff, E.v.L., Bridge, H., Lam, A.G.M., McCulloch, J. & Morris, R.G.M. (submitted) Temporary neural inactivation reveals hippocampal participation in several memory processes. *Nature Neuroscience*.

Rodríguez-Moreno, A., Herreras, O. & Lerma, J. (1997) Kainate receptors presynaptically downregulate GABAergic inhibition in the rat hippocampus. *Neuron*, **19**, 893-901.

Rogers, S.W., Hughes, T.E., Hollmann, M., Gasic, G.P., Deneris, E.S. & Heinemann, S. (1991) The characterization and localization of the glutamate receptor subunit, GluR1, in the rat brain. *Journal of Neuroscience*, **11**, 2713-2724.

Rogers, D.C., Wright, P.W., Roberts, J.C., Reavill, C., Rothaul, A.L. & Hunter, A.J. (1992) Photothrombotic lesions of the frontal cortex impair the performance of the delayed non-matching to position task by rats. *Behavioural Brain Research*, **49**, 231-235.

Rose, K., Goldberg, M.P. & Choi, D.W. (1993) Cytotoxicity in murine cortical cell culture. In *In Vitro Biological Methods*, ed. Tyson, C.A. & Frazier, J..M. pp 46-60. San Diego: Academic Press.

Rothman, S. (1984) Synaptic release of excitatory amino acid neurotransmitter mediates anoxic neuronal death. *Journal of Neuroscience*, **4**, 1884-1891.

Rothman, S.M. (1985) The neurotoxicity of excitatory amino acids is produced by passive chloride influx. *Journal of Neuroscience*, **5**, 1483-1489.

Ruderman, N.B., Ross, P.S., Berger, M. & Goodman, M.N. (1974) Regulation of glucose and ketone-body metabolism in brain of anaesthetized rats. *Biochemical Journal*, **138**, 1-10.

Sacaan, A.I. & Schoepp, D.D. (1992) Activation of hippocampal metabotropic excitatory amino acid receptors leads to seizures and neuronal damage. *Neuroscience Letters*, **139**, 77-82.

Sakimura, K., Morita, T., Kushiya, E. & Mishina, M. (1992) Primary structure and expression of the gamma 2 subunit of the glutamate receptor channel selective for kainate. *Neuron*, **8**, 267-274.

Salt, T.E. & Eaton, S.A. (1994) The function of metabotropic excitatory amino acid receptors in synaptic transmission in the thalamus: studies with novel phenylglycine antagonists. *Neurochemistry International*, **24**, 451-458.

Salt, T.E. & Eaton, S.A. (1995) Distinct presynaptic metabotropic receptors for L-AP4 and CCG1 on GABAergic terminals: pharmacological evidence using novel α-methyl derivative mGluR antagonists, MAP4 and MCCG, in the rat thalamus *in vivo*. *Neuroscience*, **65**, 5-13.

Salt, T.E. & Eaton, S.A. (1996) Functions of ionotropic and metabotropic glutamate receptors in sensory transmission in the mammalian thalamus. *Progress in Neurobiology*, **48**, 55-72.

Sanfeliu, C., Hunt, A. & Patell, A.J. (1990) Exposure to N-methyl-D-aspartate increases release of arachidonic acid in primary cultures of rat hippocampal neurons and not in astrocytes. *Brain Research*, **526**, 241-248.

Savaki, H.E. Davidsen, L. Smith, C. & Sokoloff, L. (1980) Measurement of free glucose turnover in brain. *Journal of Neurochemistry*, **35**, 495-502.

Scanziani, M., Salin, P.A., Vogt, K.E., Malenka, R.C. & Nicoll, R.A. (1997) Use-dependent increases in glutamate concentration activate presynaptic metabotropic glutamate receptors. *Nature*, *385*,630-634.

Schaffhauser, H., Richards, J.G., Cartmell, J., Chaboz, S., Kemp, J.A., Klingelschmidt, A., Messer, J., Stadler, H., Woltering, T. & Mutel, V. (1998) *In vitro* binding characteristics of a new selective group II metabotropic glutamate receptor radioligand, [^{3}H]LY354740, in rat brain. *Molecular Pharmacology*, **53**, 228-233.

Schiffer, H.H., Swanson, G.T. & Heinemann, S.F. (1997) Rat GluR7 and a carboxy-terminal splice variant, GluR7b, are functional kainate receptor subunits with a low sensitivity to glutamate. *Neuron*, **19**, 1141-1146.

Schoepp, D.D., Johnson, B.G., True, R.A. & Monn, J.A. (1991) Comparison of (1S,3R)-1-aminocyclopentane-1,3-dicarboxylic acid (1S,3R-ACPD)- and 1R,3S-ACPD-stimulated brain phosphoinositide hydrolysis. *European Journal of Pharmacology*, **207**, 351-353.

Schoepp, D.D., Johnson, B.G., Salhoff, C.R., Valli, M.J., Desai, M.A., Burnett, J.P., Mayne, N.G. & Monn, J.A. (1995a) Selective inhibition of forskolin-stimulated cyclic AMP formation in rat hippocampus by a novel mGluR agonist, 2R,4R-4-aminopyrolidine-2,4-dicarboxylate. *Neuropharmacology*, **34**, 843-850.

Schoepp, D.D., Lodge, D., Bleakman, D., Leander, J.D., Tizzano, J.P., Wright, R.A., Palmer, A.J., Salhoff, C.R. & Ornstein, P.L. (1995b) *In vitro* and *in vivo* antagonism of AMPA receptor activation by (3S,4aR,6R,8aR)-6-[2[(1(2)H-tetrazole-5-yl)ethyl] decahydroisoquinoline-3-carboxylic acid. *Neuropharmacology*, **34**, 1159-1168.

Schoepp, D.D., Johnson, B.G., Wright, R.A., Salhoff, C.R., Mayne, N.G., Wu, S., Cockerham, S.L., Burnett, J.P., Belegaje, R., Bleakman, D. & Monn, J.A. (1997) LY354740 is a potent and highly selective group II metabotropic glutamate receptor agonist in cells expressing human glutamate receptors. *Neuropharmacology*, **36**, 1-11.

Schröder, U.H., Opitz, T., Jäger, T., Sabelhaus, C.F., Breder, J. & Reymann, K.G. (1999) Protective effect of group I metabotropic glutamate receptor activation against

hypoxic/hypoglycemic injury in rat hippocampal slices: timing and involvement of protein kinase C. *Neuropharmacology*, **38**, 209-216.

Schuier, F. Orzi, F. Suda, S. Kennedy, C. & Sokoloff, L. (1981) The lumped constant for the [^{14}C]deoxyglucose method in hyperglycemic rats. *Journal of Cerebral Blood Flow and Metabolism*, **1** (suppl), S63.

Schwartz, W.J., Smith, C.B., Davidsen, L., Savaki, H.E., Sokoloff, L., Mata, M., Fink, D.J. & Gainer, H. (1979) Metabolic mapping of functional activity in the hypothalamo-neurohypophyseal system of the rat. *Science*, **205**, 723-725.

Schweizer, M. & Richter, C. (1994) Nitric oxide potently and reversibly deenergizes mitochondria at low oxygen tension. *Biochemical and Biophysical Research Communications*, **204**, 169-175.

Seeburg, P.H. (1996) The role of RNA editing in controlling glutamate receptor channel properties. *Journal of Neurochemistry*, **66**, 1-5.

Sekiguchi, M., Fleck, M.W., Mayer, M.L., Takeo, J., Choba, Y., Yamashita, S. & Wada, K. (1997) A novel allosteric potentiator of AMPA receptors: 4-[2-phenylsulfonylamino)ethyl thio]-2,6-difluro-phenoxyacetamide. *Journal of Neuroscience*, **17**, 5760-5771.

Seren, M.S., Aldinio, C., Zanoni, R., Leon, A. & Nicoletti, F. (1989) Stimulation of inositol phospholipid hydrolysis by excitatory amino acids is enhanced in brain slices from vulnerable regions after transient global ischemia. *Journal of Neurochemistry*, **53**, 1700-1705.

Sharkey, J., Ritchie, I.M., Butcher, S.P. & Kelly, J.S. (1994) Differential effects of competitive (CGS19755) and non-competitive (MK-801) NMDA receptor antagonists upon local cerebral blood flow and local cerebral glucose utilisation in the rat. *Brain Research*, **651**, 27-36.

Sheardown, M.J., Nielsen, E.O., Hansen, A.J., Jacobsen, P. & Honoré, T. (1990) 2,3-dihydroxy-6-nitro-7-sulfamoyl-benzo(F)quinoxaline: a neuroprotectant for cerebral ischaemia. *Science*, **247**, 571-574.

Shiells, R.A. & Falk, G. (1992) The glutamate-receptor linked cGMP cascade of retinal on-bipolar cells is pertussis and cholera toxin-sensitive. *Proceedings of Royal Society of London Series B-Biological Sciences*, **247**, 17-20.

Shigemoto, R., Nakanishi, S. & Mizuno, N. (1992) Distribution of the mRNA for a metabotropic glutamate receptor (mGluR1) in the central nervous system: an *in situ* hybridization study in adult and developing rat. *Journal of Comparative Neurology*, **322**, 121-135.

Shigemoto, R., Kulik, A., Roberts, J.D.B., Ohishi, H., Nusser, Z., Kaneko, T. & Somogyi, P. (1996) Target-cell-specific concentration of a metabotropic glutamate receptor in the presynaptic active zone. *Nature*, **381**, 523-525.

Siesjö, B.K. (1978) In *Brain Energy Metabolism*. New York: Wiley.

Siesjö, B.K. (1981) Cell damage in the brain: a speculative synthesis. *Journal of Cerebral Blood Flow and Metabolism*, **1**, 155-185.

Siesjö, B.K., Kristián, T. & Katsura, K. (1994) The role of calcium in delayed post-ischemic brain damage. In *Cerebrovascular Diseases, Nineteenth Princeton Stroke Conference 1994*, ed. Moskowitz, M. & Caplan, L. pp 353-370. Boston: Butterworth-Heinemann.

Siman, R. & Noszek, J.C. (1988) Excitatory amino acids activate calpain I and induce structural protein breakdown *in vivo*. *Neuron*, **1**, 279-287.

Siman, R., Bozyczko, C.D., Savage, M.J. & Roberts, L.J. (1996) The calcium-activated protease calpain I and ischemia-induced neurodegeneration. *Advances in Neurology*, **71**, 167-174.

Sladeczek, F., Pin, J-P., Récasens, M., Bockaert, J. & Weiss, S. (1985) Glutamate stimulates inositol phosphate formation in striatal neurones. *Nature*, **317**, 717-719.

Sladeczek, F., Momiyama, A. & Takahashi, T. (1993) Presynaptic inhibitory action of a metabotropic glutamate receptor agonist on excitatory transmission in visual cortical neurons. *Proceedings of the Royal Society of London Series B-Biological Sciences*, **253**, 297-303.

Smith, S.E. & Meldrum, B.S. (1992) Cerebroprotective effect of a non-N-methyl-D-aspartate antagonist, GYKI 52466, after focal ischemia in the rat. *Stroke*, **23**, 861-864.

Smith, S.E. & Meldrum, B.S. (1995) Cerebroprotective effect of lamotrigine after focal ischaemia in rats. *Stroke*, **26**, 117-122.

Sokoloff, L. (1977) Relation between physiological function and energy metabolism in the central nervous system. *Journal of Neurochemistry*, **29**, 13-26.

Sokoloff, L., Reivich, M., Kennedy, C., Des Rosiers, M.H., Patlak, C.S., Pettigrew, K.D., Sakurada, O. & Shinohara, M. (1977) The [^{14}C]deoxyglucose method for the measurement of local cerebral glucose utilization: theory, procedure, and normal values in the conscious and anesthetized albino rat. *Journal of Neurochemistry*, **28**, 897-916.

Soloviev, M.M., Brierley, M.J., Shao, Z.Y., Mellor, I.R., Volkova, T.M., Kamboj, R., Ishimaru, H., Sudan, H., Harris, J., Foldes, R.L., Grishin, E.V., Usherwood, P.N.R. & Barnard, E.A. (1996) Functional expression of a recombinant unitary glutamate receptor from Xenopus, which contains N-methyl-D-aspartate (NMDA) and non-NMDA receptor subunits. *Journal of Biological Chemistry*, **271**, 32572-32579.

Sommer, B., Keinänen, K., Verdoorn, T.A., Wisden, W., Burnashev, N,. Herb, A., Köhler, M., Takagi, T., Sakmann, B. & Seeburg, P.E. (1990) Flip and flop: a cell-specific functional switch in glutamate-operated channels of the CNS. *Science*, **249**, 1580-1585.

Sommer, B., Köhler, M., Sprengel, R. & Seeburg, P.H. (1991) RNA editing in the brain controls a determinant of ion flow in glutamate-gated channels. *Cell*, **67**, 11-19.

Sommer, B., Burnashev, N., Verdoorn, T.A., Keinänen, K., Sakmann, B. & Seeburg, P.H. (1992) A glutamate receptor channel with high affinity for domoate and kainate. *EMBO Journal*, **11**, 1651-1656.

Spooner, R.I.W. (1994) The Atlantis platform: A new design and further developments of Buresova's on-demand platform for the water maze. Learning and Memory, 1,203-211.

Squire, L.R. (1992) Memory and the hippocampus: a synthesis from findings with rats, monkeys, and humans. *Psychological Review*, **99**, 195-231.

Stephenson, D.T., Rash, K. & Clemens, J.A. (1992) Amyloid precursor protein accumulates in regions of neurodegeneration following focal cerebral ischemia in the rat. *Brain Research*, **593**:128-135.

Stowell, R.E. (1941) Effect on tissue volume of various methods of fixation, dehydration, and embedding. *Stain Technology*, **16**, 67-83.

Strasser, U., Lobner, D., Behrens, M.M., Canzoniero, L.M. & Choi, D.W. (1998) Antagonists for group I mGluRs attenuate excitotoxic neuronal death in cortical cultures. *European Journal of Neuroscience*, **10**, 2848-2855.

Sucher, N.J., Wong, L.A. & Lipton, S.A. (1990) Redox modulation of NMDA receptor-mediated Ca^{2+} flux in mammalian central neurons. *Neuropharmacology and Neurotoxicology*, **1**, 29-32.

Sucher, N.J., Awobuluyi, M., Choi, Y.B. & Lipton, S.A. (1996) NMDA receptors: from genes to channels. *Trends in Pharmacological Sciences*, **17**, 348-355.

Suzdak, P.D. & Sheardown, M.J. (1993) Effect of the non-NMDA receptor antagonist, 2,3-dihydro-6-nitro-7-sulfamoylbenzo(f)quinoxaline, on local cerebral glucose uptake in the limbic forebrain. *Journal of Neurochemistry*, **61**, 1577-1580.

Suzuki, T., Sekikawa, T., Nemoto, T., Moriya, H. & Nakaya, H. (1995) Effects of nicorandil on the recovery of reflex potentials after spinal cord ischaemia in cats. *British Journal of Pharmacology*, **116**, 1815-1820.

Swanson, G.T., Kamboj, S.K. & Cull-Candy, S.G. (1997) Single-channel properties of recombinant AMPA receptors depend on RNA editing, splice variation, and subunit composition. *Journal of Neuroscience*, **17**, 58-69.

Swanson, R.A., Morton, M.T., Tsao-Wu, G., Savalos, R.A., Davidson, C. & Sharp, F.R. (1990) A semiautomated method for measuring brain infarct volume. *Journal of Cerebral blood flow and metabolism*, **10**, 290-293.

Takahashi, T., Forsythe, I.D., Tsujimoto, T., Barnes-Davies, M. & Onodera, K. (1996) Presynaptic calcium current modulation by a metabotropic glutamate receptor. *Science*, **274**, 594-597.

Tamura, A., Graham, D.I., McCulloch, J. & Teasdale, G.M. (1981) Focal cerebral ischemia in the rat. 1. Description of technique and early neuropathological consequences following middle cerebral artery occlusion. *Journal of Cerebral Blood Flow and Metabolism*, **1**,53-60.

Tanabe, Y., Masu, M., Ishii, T., Shigemoto, R. & Nakanishi, S. (1992) A family of metabotropic glutamate receptors. *Neuron*, **8**, 169-179.

Tanabe, Y., Nomura, A., Masu, M., Shigemoto, R., Mizuno, N. & Nakanishi, S. (1993) Signal transduction, pharmacological properties, and expression patterns of two rat metabotropic glutamate receptors mGluR3 and mGluR4. *Journal of Neuroscience*, **13**, 1372-1378.

Thompson, R.F. (1986) The neurobiology of learning and memory. *Science*, **233**, 941-947.

Thomsen, C. & Suzdak, P.D. (1993) Serine-O-phosphate has affinity for type IV, but not type I, metabotropic glutamate receptor. *NeuroReport*, **4**, 1099-1101.

Thomsen, C., Klitgaard, H., Sheardown, M., Jackson, H.C., Eskesen, K., Jacobsen, P., Treppendahl, S. & Suzdak, P.D. (1994) (S)-4-carboxy-3-hydroxyphenylglycine, an antagonist of metabotropic glutamate receptor (mGluR)1a and an agonist of mGluR2, protects against audiogenic seizures in DBA/2 mice. *Journal of Neurochemistry*, **62**, 2492-2495.

Thomsen, C., Bruno, V., Nicoletti, F., Marinozzi, M. & Pellicciari, R. (1996) (2S,1'S,2'S,3'R)-2-(2'-carboxy-3'-phenylcyclopropyl)glycine, a potent and selective antagonist of type 2 metabotropic glutamate receptors. *Molecular Pharmacology*, **50**, 6-9.

Toms, N.J., Jane, D.E., Kemp, M.C., Bedingfield, J.S. & Roberts, P.J. (1996) The effects of (RS)-α-cyclopropyl-4-phosphonphenylglycine ((RS)-CPPG), a potent and selective metabotropic glutamate receptor antagonist. *British Journal of Pharmacology*, **119**, 851-854.

Tóth, K. & McBain, C.J. (1998) Afferent-specific innervation of two distinct AMPA receptor subtypes on single hippocampal interneurons. *Nature Neuroscience*, **1**, 572-578.

Toulmond, S., Serrano, A., Benavides, J. & Scatton, B. (1993) Prevention of eliprodil (SL82.0715) of traumatic brain damage in the rat. Existence of a large (18 h) therapeutic window. *Brain Research*, **620**, 32-41.

Trussell, L.O. & Fischbach, G.D. (1989) Glutamate receptor desensitization and its role in synaptic transmission. *Neuron*, **3**, 209-218.

Trussell, L.O., Zhang, S. & Raman, I.M. (1993) Desenstization of AMPA receptors upon multiquantal neurotransmitter release. *Neuron*, **10**, 1185-1196.

Tsien, J.Z., Chen, D.F., Gerber, D., Tom, C., Mercer, E.H., Anderson, D.J., Mayford, M. Kandel, E.R. & Tonegawa, S. (1996a) Subregion- and cell type-restricted gene knockout in mouse brain. *Cell*, *87*, 1317-1326.

Tsien, J.Z., Huerta, P.T. & Tonegawa, S. (1996b) The essential role of hippocampal CA1 NMDA receptor-dependent synaptic plasticity in spatial memory. *Cell*, **87**, 1327-1338.

Tymianski, M. & Tator, C.H. (1996) Normal and abnormal calcium homeostasis in neurons: a basic for the pathophysiology of traumatic and ischemic central nervous system injury. *Neurosurgery*, **38**, 1176-1195.

Uchino, H., Elmér, E., Uchino, K., Lindvall, O. & Siesjö, B.K. (1995) Cyclosporin A dramatically ameliorates CA1 hippocampal damage following transient forebrain ischemia in the rat. *Acta Physiologica Scandinavica*, **155**, 469-471.

Uemura, Y., Kowall, N.W. & Beal, M.F. (1990) Selective sparing of NADPH-diaphoras-somatostatin-neuropeptide Y neurones in ischaemic gerbil striatum. *Annals of Neurology*, **27**, 620-625.

Unsicker, K., Flanders, K.C., Cissel, D.S., Lafyatis, R., & Sporn, M.B. (1991) Transforming growth factor beta isoforms in the adult rat central and peripheral nervous system. *Neuroscience*, **44**, 613-625.

Vanderklish, P., Neve, R., Bahr, B.A., Arai, A., Hennegriff, M., Larson, J. & Lynch, G. (1992) Translational suppression of a glutamate receptor subunit impairs long-term potentiation. *Synapse*, **12**, 333-337.

Vandergriff, J. & Rasmussen, K. (1999) The selective mGlu2/3 receptor agonist LY354740 attenuates morphine-withdrawal-induced activation of locus coeruleus neurons and behavioral signs of morphine withdrawal. *Neuropharmacology*, **38**, 217-222.

Vargha-Khadem, F., Gadian, D.G., Watkins, K.E., Connelly, A., Van Paesschen, W. & Mishkin, M. (1997) Differential effects of early hippocampal pathology on episodic and semantic memory. *Science*, **277**, 376-380.

Verity, M.A. (1993) Mechanisms of phospholipase A2 activation and neuronal injury. *Annals of the New York Academy of Sciences*, **679**, 110-120.

Vickers, J.C., Huntly, G.W., Edwards, A.M., Moran, T., Rogers, S.W., Heinemann, S.F. & Morrison, J.H. (1993) Quantitative localization of AMPA/kainate and kainate glutamate receptor subunit immunoreactivity in neurochemically identified subpopulations of neurons in the prefrontal cortex of the macaque monkey. *Journal of Neuroscience*, **13**, 2982-2992.

Vignes, M. & Collingridge, G.L. (1997) The synaptic activation of kainate receptors. *Nature*, **388**, 179-182.

Viklicky, L., Patneau, D.K. & Mayer, M.L. (1991) Modulation of excitatory neurotransmission by drugs that reduce desensitization at AMPA/kainate receptors. *Neuron*, **7**, 971-984.

Vivien, D., Bernaudin, M., Buisson, A., Divoux, D., MacKenzie, E.T. & Nouvelot, A. (1998) Evidence of type I and type II transforming growth factor-β receptors in central nervous tissues: changes induced by focal cerebral ischemia. *Journal of Neurochemistry*, **70**, 2296-2304.

Wada, K., Dechesne, C.J., Shimasaki, S., King, R.G., Kusano, K., Buonanno, A., Hampson, D.R., Banner, C., Wenthold, R.J. & Nakatani, Y. (1989) Sequence and expression of a frog brain complementary DNA encoding a kainate-binding protein. *Nature*, **357**, 684-689.

Wang, X., Yue, T.L., Barone, F.C., White, R.F., Gagnon, R.C. & Feurestein, G.Z. (1994) Concomitant cortical expression of TNF-α and IL-1β mRNAs follows early response gene expression in transient focal ischaemia. *Molecular and Chemical Neuropathology*, **23**, 103-114.

Wang, X.K., Yue, T.L., Young, P.R., Barone, F.C. & Feuerstein, G.Z. (1995) Expression of interleukin-6, c-fos, and zif268 mRNAs in rat ischaemic cortex. *Journal of Cerebral Blood Flow and Metabolism*, **15**, 166-171.

Watson, B.D. & Ginsberg, M.D. (1989) Ischemic injury in the brain. Role of oxygen radical-mediated processes. *Annals of the New York Academy of Sciences*, **559**, 269-281.

Wenthold, R.J., Trumpy, V.A., Zhu, W.S. & Petralia, R.S. (1994) Biochemical and assembly properties of GluR6 and KA-2, 2 members of the kainate receptor family, determined with subunit-specific antibodies. *Journal of Biological Chemistry*, **269**, 1332-1339.

Westbrook, G.L. (1994) Glutamate receptor update. *Current Opinion in Neurobiology*, **4**, 337-346.

Wiard, R.P., Dickerson, M.C., Beek, O., Norton, R. & Cooper, B.R. (1995) Neuroprotective properties of the novel antiepileptic lamotrigine in a gerbil model of global cerebral ischaemia. *Stroke*, **26**, 466-472.

Wießner, C., Gehrmann, J., Lindholm, D., Töpper, R., Kreutzberg, G.W. & Hossman, K.A. (1993) Expression of transforming growth factor-β1 and interleukin-1β mRNA in rat brain following transient forebrain ischaemia. *Acta Neuropathologica*, **86**, 439-446.

Wilsch, V.W., Pidoplichko, V.I., Opitz, T., Shinozaki, H. & Reymann, K.G. (1994) Metabotropic glutamate receptor agonist DCG-IV as NMDA receptor agonist in immature rat hippocampal neurons. *European Journal of Pharmacology*, **262**, 287-291.

Wilding, T.J. & Huettner, J.E. (1997) Activation and desensitization of hippocampal kainate receptors. *Journal of Neuroscience*, **17**, 2713-2721.

Winder, D.G. & Conn, P.J. (1996) A novel form of glial-neuronal communication mediated by coactivation of metabotropic glutamate receptors and β-adrenergic receptors in rat hippocampus. *Journal of Physiology*, **494**, 743-755.

Wo, Z.G. & Oswald, R.E. (1994) Transmembrane topology of two kainate receptor subunits revealed by N-glycosylation. *Proceedings of the National Academy of Sciences USA*, **91**, 7154-7158.

Wong, L.A. & Mayer, M.L. (1993) Differential modulation by cyclothiazide and concanavalin A of desensitisation at native AMPA- and kainate-preferring glutamate receptors. *Molecular Pharmacology*, **44**, 504-510

Wright, R.A. & Schoepp, D.D. (1996) Differentiation of group 2 and group 3 metabotropic glutamate receptor cAMP responses in the rat hippocampus. *European Journal of Neuroscience*, **7**, 1906-1913.

Wroblewski, F. & LaDue, J.S. (1955) Lactic dehydrogenase activity in blood. *Proceedings of the Society of Experimental Biology and Medicine*, **90**, 210.

Wu, S., Wright, R.A., Rockey, P.K., Burgett, S.G., Arnold, J.S., Rosteck Jr, P.R., Johnson, B.G., Schoepp, D.D. & Belagaje, R.M. (1998) Group III human metabotropic glutamate receptors 4, 7 and 8: molecular cloning, functional expression, and comparison of pharmacological properties in RGT cells. *Molecular Brain Research*, **53**, 88-97.

Yam, P.S., McCulloch, J. & Graham, D.I. (1998a) Amyloid precursor protein immunoreactivity following focal cerebral ischaemia in the rat; influence of MK-801 treatment. *Neuropathology and Applied Neurobiology*, **24**, 145.

Yam, P.S., Patterson, J., Graham, D.I., Takasago, T., Dewar, D. & McCulloch, J. (1998b) Topographical and quantitative assessment of white matter injury following a focal ischaemic lesion in the rat brain. *Brain Research Protocols*, **2**, 315-322.

Yam, P.S., Dunn, L., Graham, D.I. & McCulloch, J. (in preparation) Quantitative analysis of white matter injury using amyloid precursor protein following drug intervention in the cat.

Yamada, K.A. & Tang, C.M. (1993) Benzothiazides inhibit rapid glutamate receptor desensitization and enhance glutamatergic synaptic currents. *Journal of Neuroscience*, **13**, 3904-3915.

Yamori, Y., Horie, R., Handa, H., Sato, M. & Fukase, M. (1976) Pathological similarity of strokes in stroke-prone spontaneously hypertensive rats and humans. *Stroke*, **7**, 46-53.

Yokoi, M., Katsunori, K., Manabe, T., Takahashi, T., Sakaguchi, I., Katsuura, G., Shigemoto, R., Ohishi, H., Nomura, S., Nakamura, K., Nakao, K., Katsuki, M. & Nakanishi, S. (1996) Impairment of hippocampal mossy fiber LTD in mice lacking mGluR2. *Science*, **273**, 645-647.

Zhao, Q., Pahlmark, K., Smith, M.L. & Siesjö, B.K. (1994) Delayed treatment with the spin trap α-phenyl-N-tert-butyl nitrone (PBN) reduces infarct size following transient middle cerebral artery occlusion in rats. *Acta Physiologica Scandinavica*, **152**, 349-350

Zheng, F. & Gallagher, J.P. (1992) Metabotropic glutamate receptors are required for the induction of long-term potentiation. *Cell*, **9**, 163-172.

Zheng, F., Hasuo, H. & Gallagher, J.P. (1995) 1S, 3R-ACPD-preferring inward current in rat dorsolateral septal neurons is mediated by novel excitatory amino acid receptor. *Neuropharmacology*, **34**, 905-917.

Zoratti, M. & Szabó, I. (1995) The mitochondrial permeability transition. *Biochimica et Biophysica Acta*, **1241**, 139-176.

Zukin, R.S. & Bennett, M.V.J. (1995) Alternatively spliced isoforms of the NMDARI receptor subunit. *Trends in Neurosciences*, **18**, 306-313.

APPENDICES

Appendix 1

Sources of commonly used materials

ABC kit	Vector
Amyloid precursor protein A4 IgG, mouse	Boehringer Mannheim
Ammonium persulphate (APS)	Sigma
B27 supplement	GibcoBRL
Biotinylated secondary antibodies	Vector
Bio-Rad colour reagent	Bio-Rad Labs
Blotting paper	Inverclyde Biologicals
Bovine serum albumin (BSA)	Sigma
[^{14}C]2-deoxyglucose	Amersham Life Science
Collagenase	GibcoBRL
Cytosine arabinoside	Sigma
Diaminobenzidine (DAB kit)	Vector
DABCO	Sigma
Dulbecco's modified Eagle's medium	GibcoBRL
Dimethylsulphoxide (DMSO)	Sigma
DNase	Sigma
ECL reagent	Amersham Life Science
Euthatal	Rhone Merieux
Foetal calf serum	GibcoBRL
Fluorescein secondary antibody	Vector Laboratories
Gentamicin	GibcoBRL
Glial fibrillary acidic protein IgG, mouse	Sigma
Glial fibrillary acidic protein IgG, rabbit	Dako
Glucose (D)	Sigma
Glutamine	GibcoBRL
Glycerol	Sigma
Glycine	BDH
Halothane	Concord Pharmaceuticals
Hank's balanced salt solution	GibcoBRL
Heparin	Leo Laboratories
HEPES	PAA laboratories
IBMX	Sigma
Isopentane	Fisher Scientific
Lysis buffer	Calbiochem
mGluR2/3 antibody, rabbit	Chemicon International
Neurobasal medium	GibcoBRL
Normal goat/horse serum	Vector laboratories
Nystatin (10 000U/ml)	Gibco
Paraffin wax	Bayers
Paraformaldehyde	Sigma
PBS Dulbecco's Balanced salt solution (w/o bicarbonate)	Gibco
Pepsin	Sigma
PMSF	Sigma
Poly-D-lysine hydrobromide	Sigma
Poly-L-lysine	Sigma
Polyvinyl alcohol	Sigma
Prestained protein standards (broad range)	Bio-Rad
Prosieve-50	Flowgen

Polyvinyl difluoride (PVDF)	Boehringer Mannheim
Soy bean trypsin inhibitor	Sigma
Staurosporine	Sigma
TEMED	Sigma
Transforming Growth factor-β1 IgG, rabbit	Santa Cruz Biotechnologies
Transforming Growth factor-β2 IgG, rabbit	Santa Cruz Biotechnologies
Transforming Growth factor-β2 IgG, rabbit	Chemicon International
Tertiary-amyl-alcohol	Sigma
Texas red avidin	Vector Laboratories
Tribromoethanol	Aldrich
Triton X-100	Sigma
Trypan Blue	Sigma
Trypsin	GibcoBRL
Xylocaine antiseptic gel 2%	Astra Pharmaceuticals

Appendix 2

Stock solutions

Buffers
Lysis buffer (100ml)

50mM Hepes pH 7.5	1.192g
150mM NaCl	8.76g
1mM EDTA	37.22mg
2.5mM EGTA	95.1mg
1mM DDT	15.42mg
0.1% Tween-20	100μl
10% glycerol	10ml
0.1mM PMSF (125mM stock)	80μl
10μg/ml leupeptin (1mg/ml stock)	1ml
2μg/ml aprotinin (1mg/ml stock)	200μl
10mM β-glycerophosphate	216mg
1mM NaF (1M stock)	100μl
0.1mM sodium metavanadate (0.1M stock)	100μl

Prepare lysis buffer in distilled water, pH 8. Aliquot and store at -20°C.

Phosphate Buffer (PB)
Stock solutions   A. Sodium dihydrogen orthophosphate ($Na_2HPO_42H_2O$) 31.2 g/l
   B. Disodium hydrogen orthophosphate ($Na_2HPO_42H_2O$) 35.6 g/l
95ml of stock A. and 405ml of stock B. PB made up to 2l, with either distilled water or 0.9% saline to produce PBS.

Sample buffer for gel loading
5X sample buffer: 0.5M sucrose   43.78g
   15% SDS   37.5g
   312.5mM Tris 9.5g
   10mM EDTA 0.925g
Prepare 5X sample buffer in 225ml distilled water. Heat gently and adjust to pH7 with HCl. Final volume of 5X sample buffer should be adjusted to 250ml.

2X working sample buffer solution:	dH_2O	1.5ml
	β-mercaptoethanol	50μl
	0.1% Bromophenol blue	25μl
	5X stock sample buffer	1ml

20 mM Tris Buffered Saline (TBS), 140 mM NaCl pH 7.6
Stock solutions   A. 0.2 M Tris, 24.2g/l
   B. 0.2 M Hydrochloric acid
50ml of stock A and 38.4ml of stock B. Dilute 1:10 with distilled water, and add 882mg NaCl/100ml Tris.

10 mM Tris pH 8.0
   Using the same stock solutions for TBS above, add 50ml solution A to 26.8ml solution B and dilute 1:1 with distilled water. Dilute this 1:10 with dH_2O.

2X TBS

Add 116.9g NaCl to 40ml 2M Tris/HCl. Make up to 2l with distilled water, pH 7.5.

20mM TBS-T

To 250ml 2X TBS, add 250ml distilled water and 1 ml Tween 20. Mix thoroughly.

Other Solutions

Astrocyte culture media (100ml)

	20% FCS-DMEM	10% FCS-DMEM	5% FCS-DMEM
Heat inactivated foetal calf serum	20ml	10ml	5ml
2mM Glutamine (200 mM stock)	1ml	1ml	1ml
25μg/ml Gentamicin (10mg/ml stock)	250μl	250μl	250μl
DMEM (1000g/l glucose)	78.75ml	88.75ml	93.75ml

Discard one month after preparation.

Collagenase

2000 U/ml solution of collagenase was prepared in Ca^{2+}/Mg^{2+} free Dulbecco's Modified Eagles Medium (DMEM-CFMF). The solution was passed through a 0.45μm filter, aliquotted and stored at -20°C

Cortical neurone culture media

To Neurobasal medium, 10% FCS (heat inactivated, non-dialysed), 1% glutamine, 1% gentamicin and 1% nystatin were added. Media was filtered before use and kept for 1 week only.

100X Cytosine arabinoside

A 5μM working solution was prepared by diluting stock solution 1:100. Stock solution of cytosine arabinoside was prepared freshly in water to give a concentration of 0.5 mM

Heat-inactivated FCS

FCS was thawed and heated to approximately 60°C for at least 1 hour. Aliquot and store at -20°C

Gels

8% resolving gel:	deionised water	45.6ml
(volume for 2 gels)	Prosieve-50	12.8ml
	1.5M Tris pH 8.8	20ml
	10% SDS	800μl
	10% APS	800μl
	TEMED	40μl

5% stacking gel:	deionised water	18ml
(volume for 2 gels)	Prosieve-50	2.4ml
	1M Tris, pH 6.8	3.1ml
	10% SDS	240µl
	10% APS	240µl
	TEMED	25µl

Neurobasal-B27 medium

Medium was prepared by adding 1ml of B27 supplement and 0.5ml 2 mM glutamine to 48.5ml Neurobasal medium

4% paraformaldehyde containing 4% sucrose

In a fume hood, approximately 60ml PBS was heated to 56°C. To this, 4g paraformaldehyde was added and stirred. 4g sucrose was added and the volume made up to 100ml with PBS. Once dissolved, the solution was cooled and any residual cloudiness was removed by filtration. Store at 4°C. This fixative should be freshly prepared.

Polyvinyl alcohol (aqueous base) mounting media

To 40ml 0.2 M Tris-HCl, pH 8.5, 8g polyvinyl alcohol was added and heated to 50°-60°C with occasional stirring. After the solution had cooled, 20ml glycerol and 2.5% 1,4 diazoabicyclo[2,2,2]octane (DABCO) were added. This was centrifuged at 5000 rpm for 15 min, aliquotted and stored at -20°C.

Soybean trypsin inhibitor-DNase

0.52mg/ml soybean trypsin inhibitor, 0.04mg/ml bovine pancreas Dnase and 3.0mg/ml BSA were mixed and dissolved in DMEM. Stirring is necessary to aid solubilisation. The solution was filtered through 0.22µm and stored at 4°C.

0.25% Trypsin

2.5mg/ml trypsin (bovine pancreas) was dissolved in DMEM-CFMF. Store at 4°C after filtration. A 10X solution was also prepared

Appendix 3

Protocols for tissue processing and histology

4% paraformaldehyde fixative

In a fume hood, 4g/100ml PB paraformaldehyde was added to the appropriate volume of PB. The solution was heated to 56°C and mixed until the paraformaldehyde had totally dissolved. The solution was left to cool, filtered and stored at 4°C. Approximately 200ml of fixative is required per animal.

Transcardiac perfusion fixation with 4% paraformaldehyde

For transcardiac perfusion fixation, the rat was anaesthetised with 5% halothane in a perspex anaesthetic chamber until the rat was deeply anaesthetised (no righting reflex, and breathing is slow and deep). Once deeply anaesthetised, 1ml euthatal was injected i.p. and the animal transferred to a fume hood and placed into the deep tray. Using forceps and large scissors, the skin was cut from below the sternum and up towards the throat. Holding the breast bone in place with forceps, the muscle layer was cut in the same direction as the diaphragm. The cartilege between the ribs was cut upwards towards the lungs on both sides and the breast bone was clamped in place. With forceps the heart was gently held in place and a small cut was made into the left ventricle. A stainless steel catheter attached to a bottle of heparinised saline (50 U/ml saline) was passed into the heart, up into the aorta and secured with clamps. Saline was introduced and a small incision was made in the right atrium. The pressure of saline flow was maintained at ~ 100 mmHg, and saline introduction was continued until the fluid expelled became clear (usually ~ 150-200 ml). Saline was stopped and paraformaldehyde fixative introduced into the animal, maintaining the pressure ~100mmHg. After ~200-250mls fixative, the fix was discontinued. Animals were decapitated and heads were post-fixed in fresh 4% paraformaldehyde overnight at 4°C.

Processing of tissue for paraffin embedding

Following the 24 hour post-fix, the brain was removed carefully (the post-fix should not exceed 24hr as this may produce artefacts in immunostaining), washed under running water and placed in 50 mM phosphate buffer (PB; for no longer than 7 days) at 4°C. The brains were then cut into coronal blocks using a rodent brain matrix (ASI instruments Inc., distributed by Bilaney). Each block was placed into an embedding cassette (Surgipath Medical Industries Inc.), caudal side up. The cassettes were placed into a container containing fresh PB and the cassettes were processed for embedding.

The cassettes were placed into:
1. Running water   30 min
2. 70% ethanol   2 x 30 min
3. 90% ethanol   2 x 30 min
4. 100% ethanol   2 x 30 min
5. xylene   2 x 30 min
6. paraffin wax   60°C, 1 - $1\frac{1}{2}$ hr
7. paraffin wax   60°C, overnight

Stainless steel moulds were cleaned in xylene. Wax was poured into one of the moulds carefully and placed onto a hotplate. Taking a cassette from the paraffin wax, the processed tissue (again caudal face up) was placed into the mould. The mould was then removed from the hotplate, and allowed to cool slightly. Once the base of the inside of the mould appeared slightly opaque, the cassette (without the lid) was pressed in place over the mould. The paraffin was allowed to cool a little while longer, then the mould was topped up with more paraffin. This process was repeated with all the remaining tissue.

The moulds are cooled at room temperature for at least 4 hrs before removing the mould. The wax blocks are now ready for cutting in a microtome.

Haematoxylin and Eosin histochemistry
1. Remove wax from sections, incubate in histoclear 10 min.
2. Dehydrate in absolute ethanol, 2 x 5 min.
3. Transfer into methylated spirits quickly, 1 min.
4. Wash sections in water, 1 min.
5. Stain with haematoxylin, 2 min
6. Rinse in water.
7. Transfer to 1% HCl in methanol, 30 sec-1 min.
8. Rinse in water.
9. Transfer to Scots Tap Water Substitute, 2 min.
10. Rinse in water.
11. Stain with eosin (aqueous) for approximately 3 min.
12. Rinse well in water.
13. Dehydrate through ethanol (70% and 90%), 5 min each.
14. Transfer into absolute ethanol, 2 x 5 min.
15. Transfer into histoclear, 2 x 5 min.
16. Mount coverslips with DPX mountant.
17. Allow to dry for 24 hours.

Counterstaining with haematoxylin following immunohistochemistry
Following the production of the colour reaction with DAB, and the rinse with water, counterstaining with haematoxylin was carried out by following steps 5-9 above. The sections were then dehydrated and mounted by following steps 13-17 of the protocol.

Appendix 4

[^{14}C]2-DG measurements following LY379268: statistical considerations

Following densitometric measurement of brain regions treated with LY379268, it was noticed that the glucose utilisation in some brain regions displayed a more heterogeneous spread, giving rise to a greater variance in standard deviation (SD), particularly in the higher dose treatment groups. A requirement of the ANOVA with post tests, in this case Student's *t*-test, is a homogeneity in variance. That is, the SD from one sample should not be significantly different from the SD from another sample. It follows that when a comparison between groups is made and there is a marked change in the mean of the test groups, but a greater heterogeneity in variance, the more difficult it will be for the data to reach statistical significance. This may lead to an underestimation of 'significant' data. Out of interest, the data was analysed *post hoc* using independent Student's *t*-test, to compare the individual test groups with the vehicle controls to examine whether any significant changes arose. The findings are presented in table A4.1. It is clear that together with the original statistically significant reductions in glucose use, a number of additional regions demonstrate statistical significance using the alternative test. These regions all exhibited marked changes in glucose use following the respective dose of LY379268 (chapter 3, tables 3.3-3.7), but failed to reach statistical significance because of the greater variance in the data.

Table A4.1   Glucose use in animals treated with LY379268: *post hoc* comparison of data using an alternative statistical test.

REGION	LY379268 0.1mg/kg	LY379268 1.0mg/kg	LY379268 10mg/kg
Cerebellar white matter			*T=2.7, P<0.03*
Cochlear nucleus			*T=3.4, P<0.009* **P<0.01**
Cocus coeruleus	*T=4.4, P<0.004* **P<0.001**	*T=6.0, P<0.0006* **P<0.001**	*T=5.7, P<0.0007* **P<0.001**
Inferior colliculus			*T=2.5, P<0.04* **P<0.05**
Median raphe nucleus			*T=2.581, P<0.05*
Superficial layer of the superior colliculus		*T=5.9, P<0.0004* **P<0.001**	*T=7.3, P<0.0001* **P<0.001**
Hippocampus		*T=3.3, P<0.01* **P<0.05**	
Mammillary body			*T=4.8, P<0.009* **P<0.001**
Lateral habenular nucleus			*T=2.6, P<0.03* **P<0.05**
Amygdala		*T=2.5, P<0.04*	
Anteroventral thalamic nucleus			*T=4.6, P<0.002* **P<0.01**
Sensory motor cortex (IV)	*T=3.3, P<0.01*	*T=3.0, P<0.02*	
Sensory motor cortex (I/II)		*T=3.176, P<0.01*	
Sensory motor cortex (V/VI)		*T=2.6, P<0.03*	
Genu		*T=2.8, P<0.02* **P<0.05**	

Comparison of results obtained in chapter 3 using ANOVA followed by post tests (Student's *t*-test with Bonferroni correction factor of 3) with Student's unpaired t-test. **Values indicate the original P values obtained from ANOVA and post tests.**

Values indicate results obtained using independent Student's unpaired t-test, comparing between the vehicle control group and the individual treatment group.

Appendix 5

Limbic system manipulation with LY326325; hippocampal analyses

Table A5.1   **Glucose utilisation at 4 days (minipump active) after LY326325 or aCSF infusion in the stratum lacunosum moleculare of the hippocampus: left and right hemispheres considered separately.**

Hippocampus (mm)	4 Days			
	aCSF		LY326325	
	Left	Right	Left	Right
(bregma ≈ -2.3mm) 2.2	77[a]	68[a]		
2.0	69[a]	69[a]		
1.8	61 ± 9	65 ± 5	71[a]	63[a]
1.6	60 ± 3	59 ± 2	55 ± 3	57 ± 4
1.4	61 ± 2	58 ± 1	53 ± 1	52[a]
1.2	55 ± 1	56 ± 3	49 ± 3	51 ± 2
1.0	56 ± 2	54 ± 2	44 ± 3	46 ± 3
0.8	52 ± 3	49 ± 2	42 ± 4	41 ± 4
0.6	54 ± 3	50 ± 3	40 ± 1	40 ± 2
0.4	51 ± 5	47 ± 1	38 ± 2	41 ± 3
0.2	55 ± 1	52 ± 2	38 ± 2	41 ± 2
0 (INJECTION)	54 ± 3	49 ± 3	37 ± 3	44 ± 2
0.2	53 ± 4	49 ± 2	43 ± 3	44 ± 3
0.4	55 ± 6	52 ± 5	45 ± 5	46 ± 0.5
0.6	57 ± 4	58 ± 3	48 ± 3	49 ± 3
0.8	58 ± 5	57 ± 3	53 ± 3	56 ± 3
1.0	62 ± 3	60 ± 4	54 ± 4	57 ± 3
1.2	62 ± 3	62 ± 4	61 ± 4	64 ± 1
1.4	63 ± 3	63 ± 3	64 ± 2	63 ± 3
1.6	62 ± 3	60 ± 3	64 ± 2	66 ± 3
1.8	64 ± 1	62 ± 1	67 ± 2	66 ± 4
2.0	66 ± 4	66 ± 1	66 ± 4	66 ± 3
2.2	65 ± 2	66 ± 4	72[a]	68 ± 1
2.4			63 ± 3	65 ± 3
(bregma ≈ -7mm) 2.6			71[a]	77[a]
Number of animals	5	5	5	5

Data are presented as mean ± SEM (μmol/100g/min). The injection site '0' approximates to bregma = -4.52 mm (Paxinos & Watson, 1986).

[a]Densitometric analysis at this level only possible in one animal

Due to differences in the cut of the sections, densitometric readings carried out at the most rostral and caudal points of the hippocampus may only include a couple of the animals within each group.

Table A5.2 **Glucose utilisation at 11 days (minipump exhausted) after LY326325 or aCSF infusion in the stratum lacunosum moleculare of the hippocampus: left and right hemispheres considered separately.**

Hippocampus (mm)	11 Days			
	aCSF		LY326325	
	Left	Right	Left	Right
(bregma ≈ -2.3 mm) 2.2	54[a]	74[a]		
2.0	59[a]	67 ± 12	±	
1.8	56[a]	61 ± 3	78[a]	66[a]
1.6	62 ± 8	65 ± 4	76 ± 8	74 ± 8
1.4	61 ± 7	65 ± 6	70 ± 3	75 ± 5
1.2	60 ± 8	64 ± 4	70 ± 2	72 ± 2
1.0	61 ± 10	63 ± 6	66 ± 4	68 ± 4
0.8	58 ± 11	61 ± 6	64 ± 2	64 ± 2
0.6	54 ± 5	57 ± 3	63 ± 2	62 ± 2
0.4	59 ± 5	54 ± 2	58 ± 2	57 ± 3
0.2	55 ± 4	52 ± 3	59 ± 4	56 ± 3
0 (INJECTION)	55 ± 3	53 ± 2	56 ± 4	56 ± 4
0.2	61 ± 5	57 ± 5	56 ± 3	58 ± 1
0.4	61 ± 4	58 ± 3	61 ± 2	65 ± 3
0.6	63 ± 4	61 ± 3	62 ± 2	62 ± 2
0.8	66 ± 4	65 ± 4	66 ± 3	67 ± 4
1.0	66 ± 4	68 ± 4	67 ± 2	68 ± 4
1.2	66 ± 2	68 ± 3	70 ± 3	69 ± 3
1.4	68 ± 1	71 ± 2	71 ± 1	71 ± 3
1.6	70 ± 1	66 ± 2	69 ± 3	75 ± 2
1.8	66 ± 2	67 ± 1	72 ± 3	71 ± 2
2.0	70 ± 1	70 ± 4	71 ± 4	75 ± 4
2.2	68 ± 3	71 ± 4	75 ± 5	73 ± 6
2.4	71 ± 2	73[a]	78 ± 6	73 ± 5
(bregma ≈ -7 mm) 2.6	71[a]	73[a]	78 ± 4	67 ± 0.1
Number of animals	4	4	5	5

Data are presented as mean ± SEM (μmol/100g/min). The injection site '0' approximates to bregma=-4.52 mm (Paxinos & Watson, 1986).

[a]Densitometric analysis at this level only possible in one animal

Due to differences in the cut of the sections, densitometric readings carried out at the most rostral and caudal points of the hippocampus may only include a couple of the animals within each group.

A. 4 days: minipump active
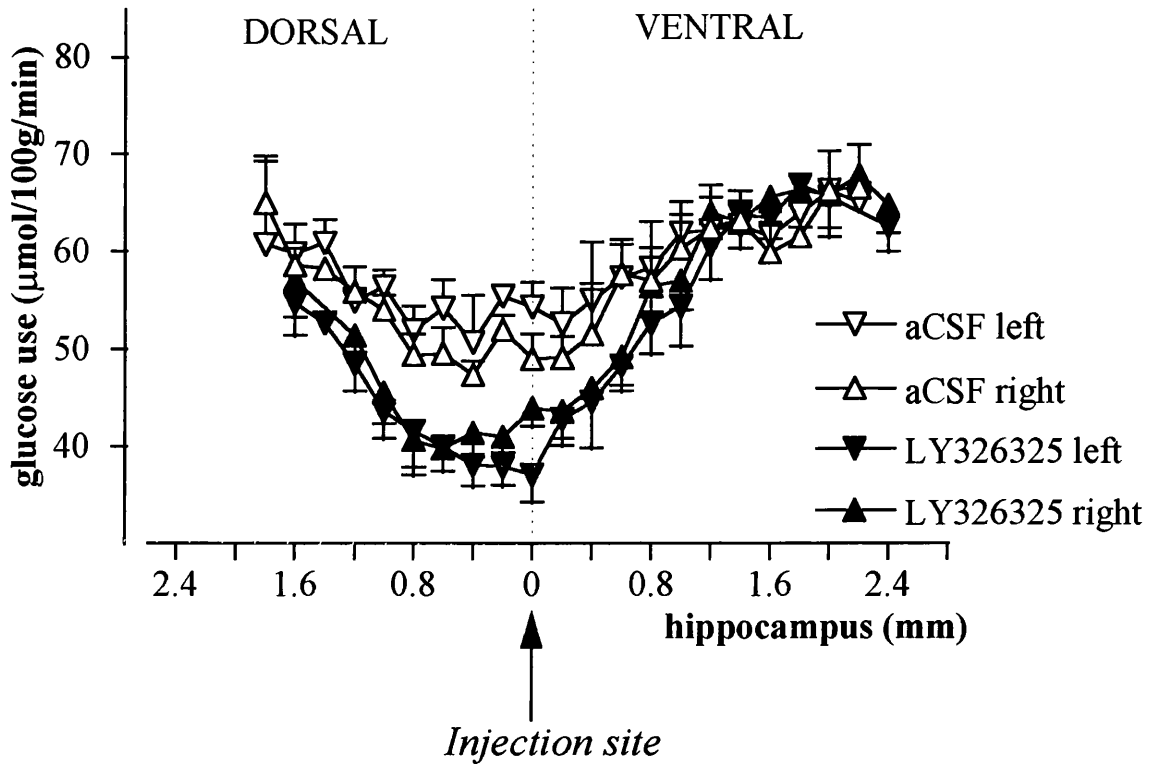
Figure A5.1a Extent of the reduction of glucose use in the stratum lacunosum moleculare of the hippocampus: 4 days (minipump active).

The data are presented as mean (left/right side) ± SEM. The dotted line represents the site of injection (chosen from H & E stained sections). All data points to the left of the dotted line represent glucose use in the hippocampus at distances rostral to the injection site, while data points to the right of the dotted line represent glucose use in the hippocampus at distances caudal to the injection site.

B.   11 days: minipump exhausted
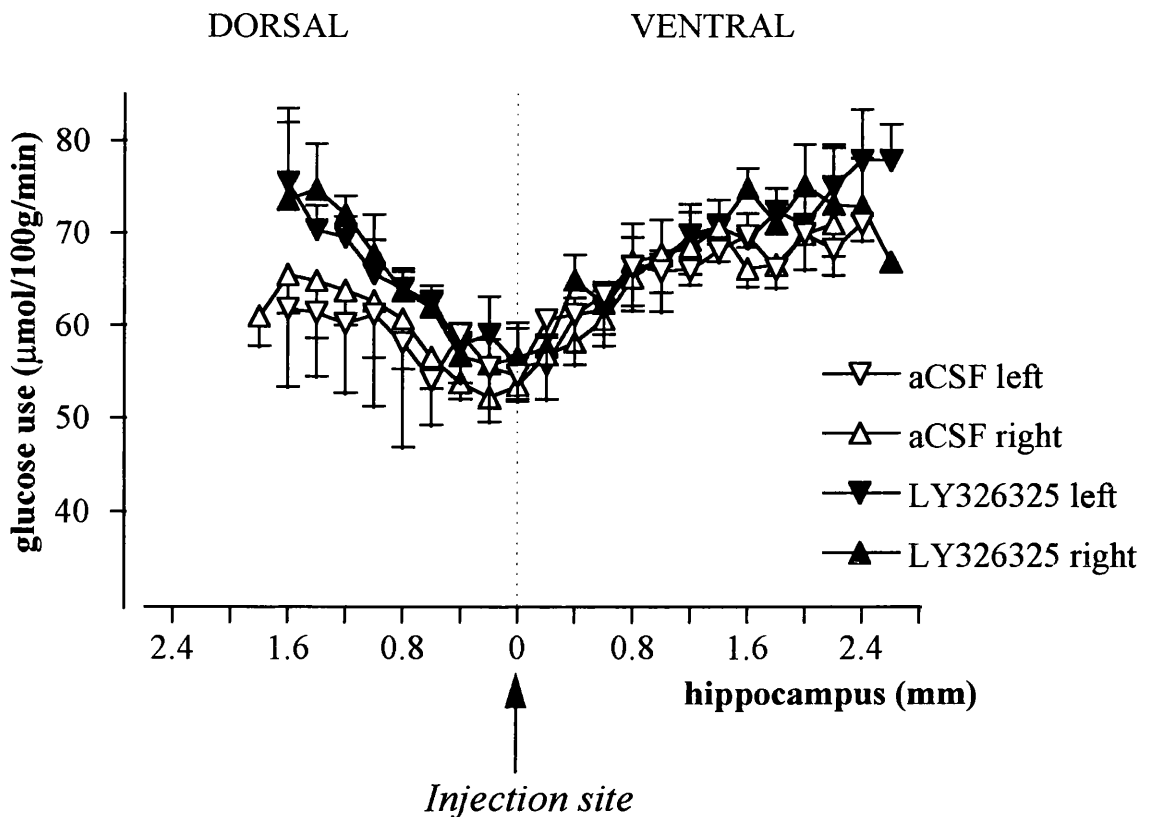
Figure A5.2b Extent of the reduction of glucose use in the stratum lacunosum moleculare of the hippocampus: 11 days (minipump exhausted).

The data are presented as mean ± SEM. The dotted line represents the site of injection (chosen from H & E stained sections). All data points to the left of the dotted line represent glucose use in the hippocampus at distances rostral to the injection site, while data points to the right of the dotted line represent glucose use in the hippocampus at distances caudal to the injection site.

Appendix 6

LY379268: Quantification of infarct size following 24 hour permanent MCA occlusion

The method of analysis used in chapter 5 for quantification of ischaemic damage after MCA occlusion is carried out directly from the histology sections (see methods 2.3). Therefore, to remain consistent with the previous study, and with a view to compare the two data sets, this same method was initially used to evaluate the changes in infarct size after intervention with LY379268. However, because of the negative result demonstrated with LY354740, a decision was made to investigate other outcome parameters, in this case, cellular changes using immunohistochemical markers. For this purpose, it was necessary to fix the tissue, as the cell architecture observed in cryostat sections normally taken for the quantification of ischaemic damage is very poor, and due to the thickness of cryostat sections, they contain multiple cell layers. The volumes of ischaemic damage are summarised in table A6.1.

Upon examining the data in more detail, it was noticed that there appeared to be an approximate 20% difference in the swelling volume between the vehicle treated and LY379268 treated group. In addition, the swelling volumes measured in this study were substantially lower that that normally expected following permanent occlusion of the MCA. Comparison with the LY354740 data (chapter 5, table 5.1) demonstrates that the volume of swelling has reduced markedly from approximately 100 mm^3 to less than 35 mm^3. Brain swelling is a consequence of the ischaemic insult, and is directly proportional to the volume of the lesion in animals (see chapter 5, figure 5.7). However, in this study, as figure A6.1 illustrates, there is no relationship whatsoever between the ischaemic lesion volume and swelling ($r^2=0$). From other plots carried out, figure A6.2 reveals there are no correlations between the volume of ischemic damage and the volume of the contralateral hemisphere. However, figure A6.3 suggests that there is a negative correlation between the volume of ipsilateral swelling and the volume of the contralateral hemisphere.

Shrinkage of tissue as a direct result of fixing is recognised (Stowell, 1941). One of the problems encountered in the fixation of tissue that has undergone an episode of trauma/insult, is the passage of water through the tissue. The fixation process requires all aqueous solutions present in the tissue to be substituted with paraffin wax. However, if tissue has undergone a traumatic episode, such as ischaemia, a proportion of cells in the tissue will be dead and will have lost its normal cell structure. As a result of this, water removal and replacement with wax will cause the tissue to shrink. Moreover, once cut, microtome sectioned tissue is placed over water to allow the tissue to flatten out and remove any creases or folds. Again, because the tissue has undergone damage, water entering the tissue
is not controlled as the cells have lost their normal architecture. The changes in the volume of swelling in this study can probably be directly attributed to the fixation process. In addition, figure A6.3 appears to suggest that there is less swelling present in tissue that exhibit a greater contralateral hemispheric volume. This could be an issue of time. It is possible that the longer the tissue has spent in the water bath before being picked up onto a slide results in a non uniform increase in the size of the tissue. That is, even if a section was hypothetically very swollen as a direct result of ischaemia, but spent a protracted time in water, any issue of swelling could not be measured. Figure A6.4 demonstrates the variability observed in the size of the tissue as a result of the fixation process.

Due to the distortion of the material, a decision was made to analyse the areas of ischaemic damage using an alternative approach. This method for measuring infarct size excludes the contribution of swelling (Osborne *et al.*, 1987). More specifically, this approach requires the delineation and transcription of the ischaemic damage onto scale

diagrams (4 times actual size) of the 8 pre-selected stereotaxic coronal levels of the brain drawn from the Atlas of König & Klippel (1963). A comparison between the volumes of ischaemic damage obtained by the direct histology method and the scale line diagram method is presented in table A6.2.

**Table A6.1** **LY379268 and the volume of ischaemic damage (mm3): direct histology method.**

| VOLUME (mm^3)	VEHICLE	LY379268 (10mg/kg)
Infarct	145 ± 13	135 ± 14
Swelling	34 ± 3	27 ± 4
% Infarct volume[a]	21 ± 2	19 ± 2
Number of animals	10[b]	10[b]

The data are presented as mean ± SEM.
[a]Swanson *et al.*, 1990. [b]One animal from each group only contained 7 of the 8 stereotaxic levels. For these animals, the volumes were still calculated, but taking into account the missing level.
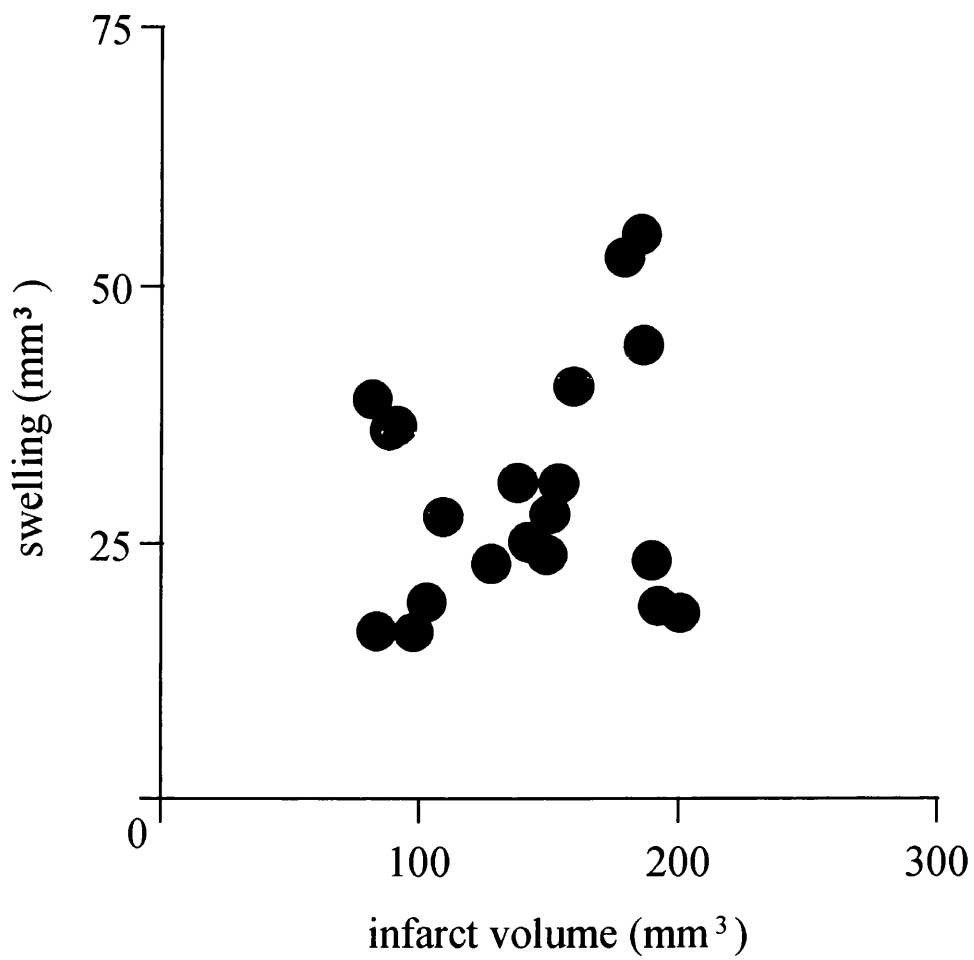
Figure A6.1   **The relationship between the volume of infarction (mm³) and the volume of ipsilateral hemispheric swelling (mm³) in vehicle and LY379268 treated animals**
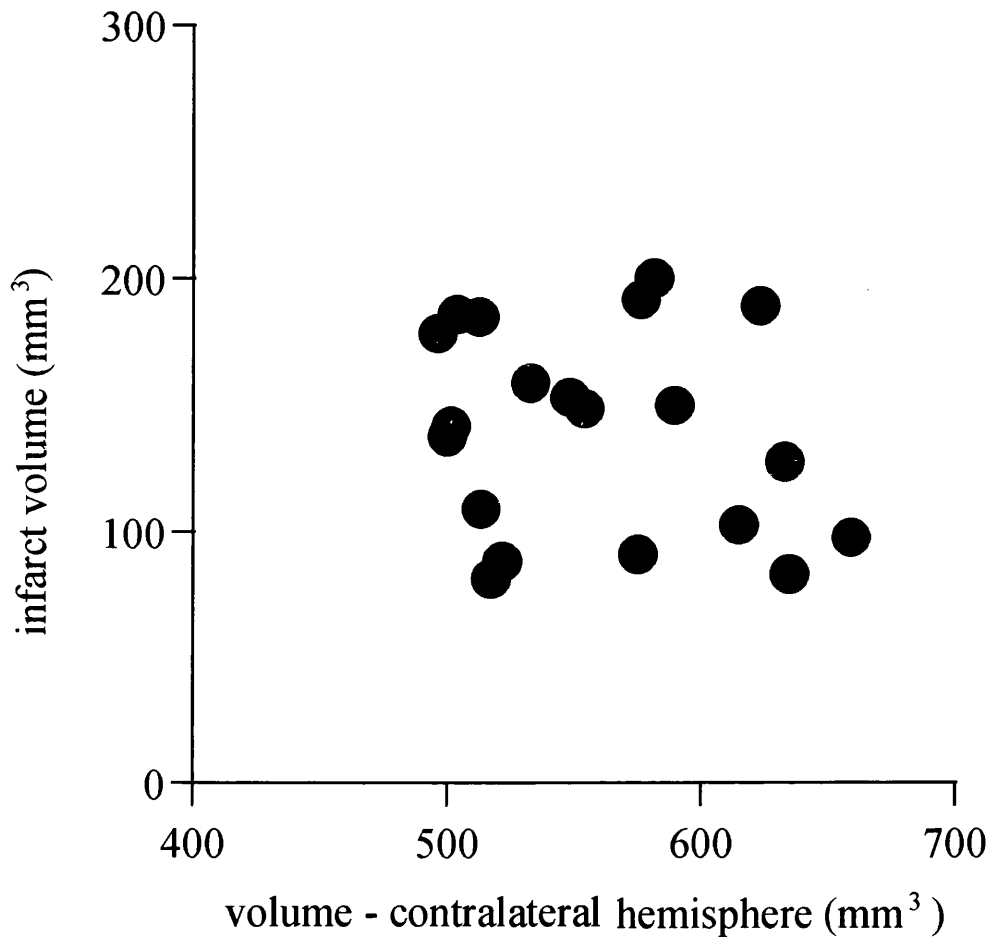
Figure A6.2 The relationship between the volume of infarction (mm^3) and the volume of the contralateral hemisphere (mm^3) in vehicle and LY379268 treated animals.
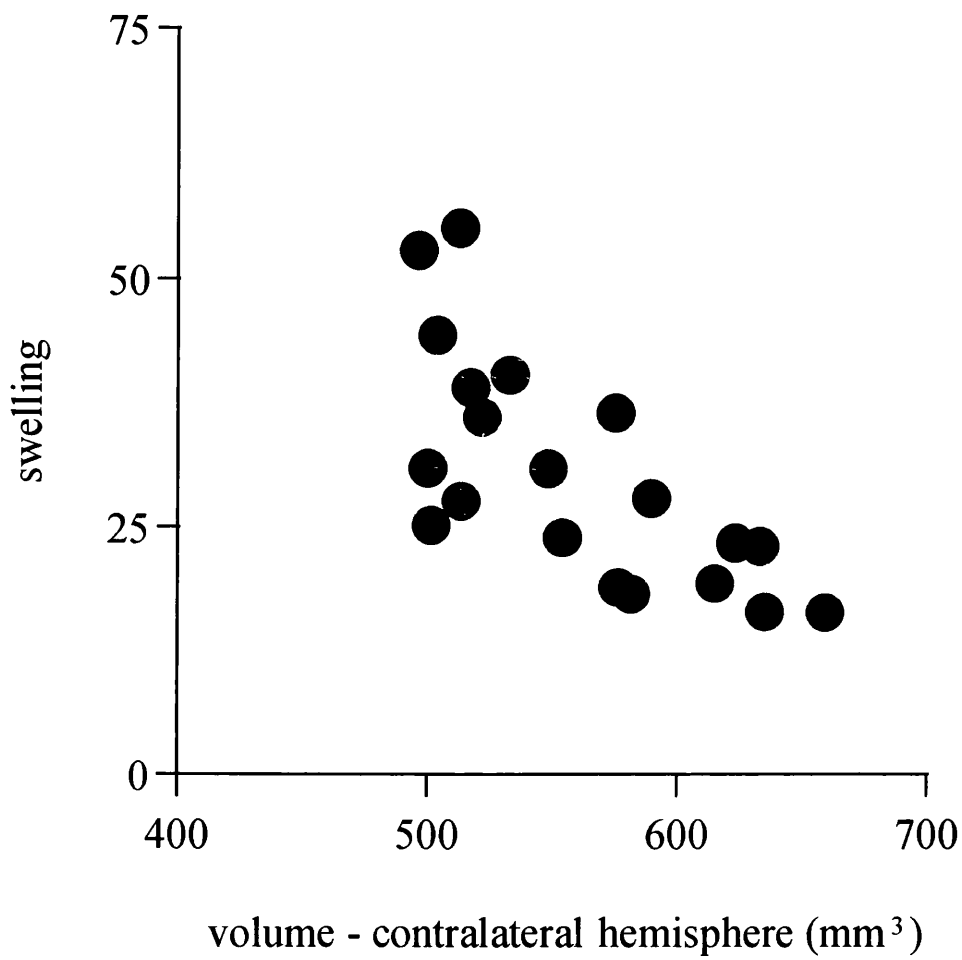
Figure A6.3 The relationship between the volume of ipsilateral hemispheric swelling (mm^3) and the volume of the contralateral hemisphere (mm^3) in vehicle and LY379268 treated animals.
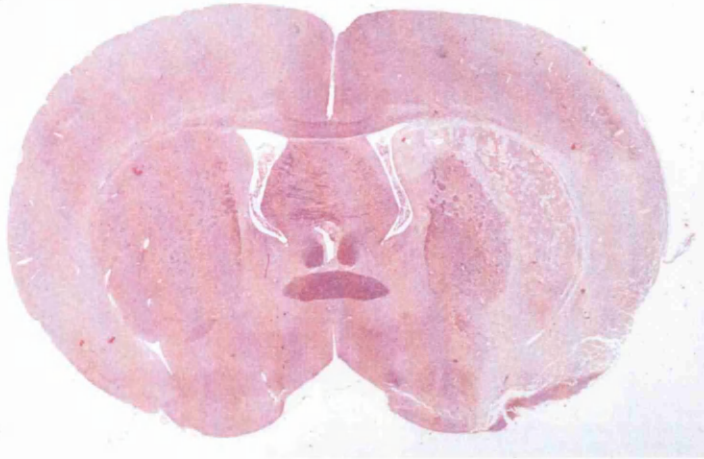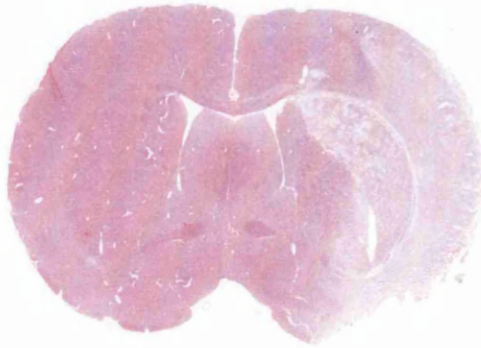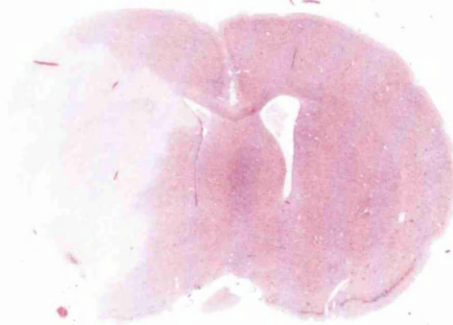
Figure A6.4   Artefacts resulting from the fixation and paraffin embedding process.

All the sections underwent the same fixation process a) + b) are sections obtained from the study described in chapter 6. c) is a representative example from a different study. Note the differences in the size of the tissue.

Table A6.2. Comparison of the volumes of ischaemic damage obtained using the direct histology method and the scale line diagram method which excludes the contribution of swelling.

ANIMAL	VOLUME OF ISCHAEMIC DAMAGE (mm3)	
Vehicle:	direct histology method	scale line diagram method
AM1	186.2	124.8
AM2	158.9	108.3
AM6	153.1	96.1
AM8	141.8*	n/a
AM9	81.5	72.4
AM10	91.0	54.9
AM11	109.0	95.0
AM12	148.8	111.8
AM13	178.4	115.3
AM19	200.2	125.8
LY379268:		
AM3	127.6	75.9
AM4	189.4	122.2
AM5	83.2	40.9
AM7	191.8	129.4
AM14	137.9	114.4
AM15	88.3	99.1
AM16	102.7*	n/a
AM17	150.1	115.2
AM18	97.8	55.1
AM20	184.9	123.1

* not all 8 levels present